OXIDATIVE OR NON–OXIDATIVE CONVERSION OF METHANE OR ETHANE INTO VALUE ADDED PRODUCTS

A
Thesis
Submitted to the.
University of Pune
For the degree of
Doctor of philosophy
In
Chemistry

By

KARTICK CHANDRA MONDAL

Chemical Engineering and Process Development Division

National Chemical Laboratory

Pune – 411 008, INDIA

December 2004

Dedicated

To
My Parents
And
My Sisters

"Experiments are the only means of knowledge at our disposal. The rest is poetry, imagination."

Max Planck

Acknowledgement

At the present moment let me in the beginning express my deepest sense of gratitude to my supervisor, Dr. Vasant R. Choudhary, for his invaluable guidance, meaningful teaching, constant support and advice throughout the course of this investigation. It is he, who introduced me to the world of catalysis, suggested my research problem and guided my sailing through the doctoral work. Working with him has at all times been a pleasant and stimulating experience for me and I shall be having long lasting gratitude and respect for him.

My sincere thanks are due to Dr. S. D. Sansare, Dr. S. G. Pataskar, Dr. A. M. Rajput, Dr. A. S. Mamman, Dr. A. G. Gaikwad, Dr. B. S. Uphade and Dr. S. A. R. Mulla for all the helpful discussion, encouragment and support. They not only extended their warm friendship, but they were always there whenever I needed them professionally.

I must then gratefully appreciate to help and cooperation of my lab-seniors Suman-da, Mantri-da and Subho-da. The help and cooperation received from Mr. V. L. Rajput and Mr. V. L. Chandekar is also duly acknowledged.

Association with colleagues Chanchal and Prabhas in all these years has been a really wonderful experience. The very wholeness of their warmth, support and encouragement has become a cherishing experience by now. Many thanks are due for my other lab-mates Joshi, Vijay, Jayant, Deepa, Rani, Kailash, Nilesh, Nitin and Mander.

The invaluable help and guidance received from Dr. Mandale for XPS, Dr. Sainkar for SEM, Dr. (Mrs) A. Mitra for XRD, Dr. Mirejkar for TPR, Mr. Bhujang for Drawing figures is also duly acknowledged.

The personnel from C.E. office and from the supporting groups like glass blowing and electrical sections had been very friendly and generous with their assistance.

My sincere gratitude goes also to Ramu-da, Kamu-da, Dadu, Debashish-da, Arindam-da, Denu-da, Prabal-da, Major, Nitul Sona (Bibhas-da) & Fuchka (Roopa), Angel (Debu-da), Babu-da, Ghota (Anirban-da), Soumitra (Bebun), Senapati-da, Saikat-da, Dilip-da, Samanta-da, Tarun-da, Anuradha-di, Chaitali, Sumit-da, Pradip (Gach) and Sugata. It was their love and cooperation, which has inspired me to do good work.

I would like to thank all my seniors and friends in NCL, Somnath-da, Sujata-di, Ananda-da, Laha-da, Sukhen-da, Annyt-da, Chitto-da, Raja-da, Bhowmik-da, Anamitra-da, Tikla-da, Dhanonjoy-da, Smriti-di, Nimu-da & Boudi, Amrita-di, Ambarish & Tanu, Rahaman,

Rita, Pallavi-di, Pradip (Candel), Chinmoy, Mukulesh, Bhaskar and all other friends in and around NCL. I am indebted to Swarup, Atanu, Kallol, Gurudeb, Mr. Mukherjee and all my University classmates for their cooperation.

I also catch hold of this golden opportunity to express my deepest respect for Prof. S. K. Bhowal, Dr. (Mrs.) Bhowal, Dr. S. Mukherjee, Prof. B. C. Roy, Prof. S. Lahiri, Shadhan-da and all my teachers who have not only taught me the basics of Chemistry, but also the basics of life and profession.

It gives me immense pleasure at this juncture to mention my parents and my elder sisters in this regard. It is their teachings, their ideals, their affection, their encouragement, their patience and their blessings, which have constituted a treasure for my life. I am sure this work could never been possible but for their enthusiasm and sacrifice. Words cannot express my feelings towards them. They were there by my side in all these years, and I am sure that they will be, through the best and worst of my times. Dedication of this thesis to them is just a very small token of love from my side. In all these years I have received love and affection from my relatives.

My sincere gratitude remains there for Dr. B. D. Kulkarni, Head, Chemical Engineering and Process Development Division, NCL and Dr. S. Sivram, Director, NCL, for allowing me to carry out this research work of mine at NCL and providing me with the infrastructure.

My thanks are due to the University Grant Commission, New Delhi for awarding me a Junior Research Fellowship.

Pune

December 2004 *(Kartick C. Mondal)*

Certificate as per Form “A”

Certified that the work incorporated in the thesis **“OXIDATIVE OR NON–OXIDATIVE CONVERSION OF METHANE OR ETHANE INTO VALUE ADDED PRODUCTS”** submitted by **Mr. Kartick Chandra Mondal** was carried out by the candidate under my supervision. Such material as has been obtained from other sources has been duly acknowledged in this thesis.

December 2004

(Dr. Vasant R. Choudhary)
Research supervisor

LIST OF CONTENTS

LIST OF TABLES

LIST OF FIGURES

SUMMARY AND CONCLUSIONS

Natural gas is an abundant resource in various part of the world. Methane is main constituent of natural gas, coal–bed gas and biogas. Methane is produced in huge quantities during oil production as associated gas and also produced in the petrochemical refining and petrochemical processes. It is also available in huge quantities as methane hydrate at sea beds. Since methane is available and produced mostly in remote places, its transportation is very costly or even impossible. Therefore, much of the natural gas associated with oil is flared causing not only a wastage of valuable energy under the present energy crisis but also global warming due to the release of very large quantity of CO_2 in the atmosphere. Even from the environmental consideration, the methane / natural gas produced in the remote places need to be converted into easily transportable and / or value added products involving either oxidative or non–oxidative activation of methane.

Syngas (a mixture of CO and H_2) is a versatile feedstock for methanol and ammonia syntheses and oxo-processes and also for a number of F.T. syntheses for the production of liquid fuels, olefins and oxygenates. Hence, the conversion of methane to value added products via its conversion to syngas is highly promising one, provided the syngas from methane is produced economically. Presently, syngas is produced by the steam reforming of methane or higher hydrocarbons. Because of its several limitations / drawbacks (high energy requirement, high H_2/CO ratio, low selectivity / yield for CO, high capital cost and low space-time-yield), the steam reforming process is uneconomical for its use in the methane conversion. Autothermal reforming of methane to syngas is also a well-established process but it also suffers from a number of serious drawbacks limiting its use in the syngas production. In the past 12 to 15 years, catalytic partial oxidation of methane to syngas has been extensively investigated. This process is mildly exothermic one and provides syngas with desirable H_2/CO ratio (about 2), required for the methanol and F.T. syntheses. However, it is highly hazardous in nature because of the simultaneously occurring highly exothermic combustion of methane to CO_2 and water. Although, this limitation could be partially overcome by carrying out the partial oxidation of methane simultaneously with the steam and / or CO_2 reforming of methane over the same catalyst, and thereby coupling the exothermic oxidative conversion and endothermic CO_2 and / or steam reforming reactions, the catalyst employed should have very high thermal stability (preferably upto 1500 ^oC). It is of great practical importance to develop a high

temperature stable catalyst having high activity and selectivity for the methane to syngas conversion reactions, involving the exothermic oxidative conversion reactions.

Because of the increasing importance of the CO_2 sequestration for avoiding global warming, CO_2 reforming of methane to syngas has been considered as an important process for the utilization of CO_2. Apart from the high-energy requirement, this process also suffers badly from a very rapid carbon deposition on the catalyst, particularly Ni-based catalysts. It is therefore of great practical importance to develop a non-noble metal-based catalyst, which allows only a little or no carbon formation in the CO_2 reforming reaction.

Methane is most inert amongst hydrocarbons and hence its activation at low temperature (< 600 ^oC) is very challenging. Earlier studies showed that at low temperatures, methane could be activated in the presence of higher hydrocarbons over bifuntional pentasil zeolite. Practically it would be more interesting if methane could be activated in the presence of methanol which itself can be produced from methane.

It is also interesting to investigate the conversion of ethane to ethylene (which is a keystone to petrochemical) in the pyrolysis of ethane in the presence of CO_2 with or without O_2 for utilizing CO_2 as an oxidizing agent.

The present work for Ph.D thesis is, therefore undertaken as a part of the comprehensive R & D programme in our lab for the conversion of methane / lower alkanes, with the following objectives:

- To develop high temperature (upto 1500 ^oC) stable catalyst for the partial oxidation of methane to syngas with or without simultaneously occurring steam and/ or CO_2 reforming reactions.
- To develop unsupported and supported non-noble metal containing catalyst having high activity with little or no coke formation in the CO_2 reforming of methane in the presence or absence of steam and / or O_2.
- To study low temperature activation of methane in the presence of methanol or other oxygenates over bifuntional pentasil zeolite catalysts.
- To study pyrolysis of ethane to ethylene in the presence of CO_2 with or without O_2.

The thesis has been divided into seven chapters, as follows-

CHAPTER I: INTRODUCTION–OBJECTIVE AND SCOPE

In this chapter, a general introduction including background and literature survey, covering the following catalytic and non-catalytic processes:

– methane–to–syngas conversion processes.

– non–oxidative activation of Methane for its conversion into value added products,

– non–catalytic oxidative dehydrogenation of ethane,

and also the objectives / scope of the Ph.D work have been covered

CHAPTER II: EXPERIMENTAL

In this chapter the experimental procedures for

- the preparation and / or modification for different catalysts used in the methane-to-syngas conversion reactions and non-oxidative activation of methane,
- the characterization of the catalysts by different surface and bulk analytical tools (viz, BET surface area, TPR, XRD, XPS, H_2 pulse study, SEM-EDAX), and
- the catalytic reactions and also non-catalytic ethane pyrolysis

have been described.

CHAPTER III: CO_2 REFORMING, SIMULTANEOUS CO_2 AND STEAM REFORMING AND OXY- CO_2 REFORMING OF METHANE TO SYNGAS OVER COBALT CONTAINING CATALYSTS

A number of nickel, cobalt or nobel metal containing catalysts (viz. $CoMgO_x$, $CoCaO_x$, $NiMgO_x$, CoO_x/Al_2O_3, CoO_x-ZrO_2, CoO_x-ThO_2, CoO_x-Y_2O_3, $CoLaO_x$, $CoSmO_x$, $CoCeO_x$, $CoEuO_x$, $CoYbO_x$, $CoNdO_x$, Rh/Al_2O_3, Ru/Al_2O_3) have been compared for their performance in the CO_2 reforming of methane to syngas at 850^{o}C (CO_2/CH_4=1.1 and GHSV=20,000 $cm^3g^{-1}h^{-1}$). The $NiMgO_x$, CoO_x–ZrO_2, CoO_x–Y_2O_3, $CoCeO_x$ and Rh or Ru/Al_2O_3 catalysts showed high activity and also high H_2 selectivity but also a high rate of carbon deposition on them during the reaction. However, almost no carbon formation was observed when the $CoNdO_x$ (Co/Nd = 0.1 – 4.0) was used as the catalyst in the CO_2 reforming. The performance of this catalyst (with Co/Nd=1.0) in the CO_2 reforming, in the Oxy–CO_2 (simultaneous partial oxidation and CO_2 reforming reactions, with CH_4/O_2= 2.2 to 2.9 and CH_4/CO_2= 2.6 to 7.3) and also in the simultaneous CO_2 and steam reforming (CO_2/H_2O= 0 to 2.5) of methane has been thoroughly evaluated at different temperatures (750 to 900 ^{o}C) and space velocities (10,000 –

40,000 $cm^3g^{-1}h^{-1}$). The catalyst showed high activity in these processes. Moreover, at all process conditions, almost no carbon formation over the catalyst was observed in these methane-to-syngas conversion processes. The TPR (by hydrogen) studies of the catalyst indicated the presence of both the free cobalt oxide and $NdCoO_3$ perovskite in the $CoNdO_x$ catalysts, depending upon the Co/Nd ratio.

CHAPTER IV: CO_2 REFORMING AND OXY-CO_2 REFORMING OF METHANE TO SYNGAS OVER COBALT CONTAINING CATALYSTS SUPPORTED ON DIFFERENT COMMERCIAL MACROPOROUS CATALYST CARRIERS

Different Co containing supported catalysts (viz. CoO/MgO/SZ-5205, CoO/ZrO_2/SA-5205, CoO/CeO_2/SA-5205, CoO/Y_2O_3/SA-5205, CoO/ThO_2/SA-5205, CoO/ZrO_2/SZ-5564, CoO/CeO_2/SZ-5564, CoO/Y_2O_3/SZ-5564, CoO/ThO_2/SZ-5564, CoO/Nd_2O_3/SA-5205, CoO/Nd_2O_3/SZ-5564, CoO/MgO/SZ-5564) have been evaluated for their performance in the CO_2 reforming reaction at 850 ^oC (CO_2/CH_4=1.1 and GHSV=20,000 $cm^3g^{-1}h^{-1}$). Among these catalysts, CoO/MgO/SA-5205 catalyst showed the best performance (high activity and H_2 selectivity). The performance of this catalyst has also been studied at different reaction temperatures (750 – 900 ^oC), space velocities (10,000 – 40000 $cm^3g^{-1}h^{-1}$) and CO_2/CH_4 ratios (0.5 – 2.0). The influence of the catalyst calcination temperature (900 ^oC and 1200 ^oC), Co loading (5 – 40 wt%) and different commercial supports on the performance of the supported CoO/MgO catalyst in the CO_2 reforming process has been studied. Detailed investigations on the temperature effect (700 – 900 ^oC), GHSV effect (23000 – 92000 $cm^3g^{-1}h^{-1}$) and feed gas ratio effect (CH_4/CO_2= 2.5 to 7.3 and CH_4/O_2= 2.1 to 2.9) for the Oxy–CO_2 reforming of methane over the CoO/MgO/SA-5205, CoO/CeO_2/SA-5205 and CoO/ZrO_2/SA-5205 catalysts have also been carried out. On these catalysts, only a little carbon deposition was observed during the CO_2 reforming but no carbon deposition was detected during the Oxy-CO_2 reforming.

CHAPTER V: HIGH TEMPERATURE STABLE SUPPORTED Ni–Co CATALYSTS USEFUL FOR HIGHLY EXOTHERMIC METHANE-TO-SYNGAS CONVERSION PROCESSES

In order to develop a high temperature stable catalyst for exothermic methane-to-syngas conversion processes, including the autothermal reforming of methane, a number of supported

different Ni-Co catalysts (viz. CoO-NiO/SZ-5564, CoO-NiO/ZrO_2/SZ-5564, ZrO_2/SZ-5564, CoO-NiO-MgO/SZ-5564, CoO-NiO/MgO/SZ-5564, CoO-NiO-ZrO_2/SZ-5564, CoO-NiO-MgO-CeO_2/SZ-5564, CoO-NiO-ZrO_2-CeO_2/SZ-5564) have been evaluated for their performance in the partial oxidation of methane (POM) to syngas at different temperatures (550 to 900 ^oC for CH_4/O_2=1.8 and GHSV= 62,000 $cm^3g^{-1}h^{-1}$). Among the catalysts, CoO–NiO–MgO/SZ-5564 (with or without CeO_2) catalyst, even when calcined at 1400 ^oC, showed high activity with high selectivity (for both H_2 and CO) at the high space velocity (62,000 $cm^3g^{-1}h^{-1}$). Effect of temperature (550 – 900 ^oC), space velocity (30000 – 120000 cm^3 g^{-1} h^{-1}) and presence of sulphur in the feed (7000 ppm) on the conversion and selectivity for this catalyst has also been studied. When the catalyst was subjected directly to oxy–acetylene flame for a short period (0.5 min) repeatedly or once for a much longer period (30 min), there was no significant change in its performance in the POM reaction. The performance of the catalyst (calcined at different temperatures or subjected to the oxyacetylene flame) in the POM, Oxy–CO_2 and Oxy–Steam reforming of methane at different process conditions have also been evaluated, the catalyst showed excellent performance in all these exothermic processes.

CHAPTER VI: LOW TEMPERATURE NON-OXIDATIVE ACTIVATION OF METHANE OVER BIFUNTIONAL PENTASIL ZEOLITES IN PRESENCE OF METHANOL OR OTHER OXYGENATES: SIMULTANEOUS CONVERSION OF METHANE AND METHANOL OR OTHER OXYGENATES INTO HIGHER HYDROCARBONS / GASOLINE

Non-oxidative methane activation in the presence of methanol and simultaneous conversion of methane and methanol to higher hydrocarbons / gasoline (at < 600 ^oC) over a number of bifunctional pentasil zeolites (viz. Ga, In, Mo, Zn, Tl, Fe or Pt modified ZSM–5 catalyst's (such as - H-GaAlMFI, H-GaMFI, Zn/H-ZSM5, Zn-Mo/H-ZSM5, Zn-In/H-ZSM5, Fe-Al/GaAlMFI, Zn/GaAlMFI, Zn-Tl/H-ZSM5, Zn-Ga/H-ZSM5, Pt/GaAlMFI) have been investigated. In the presence of methanol or other oxygenates (e.g. ethanol, acetone, etc.), methane was found to be activated and converted to higher hydrocarbons, depending upon the bifunctional zeolite catalyst and process conditions. The methane converted per mole of oxygenate was strongly influenced by the temperature, CH_4/oxygenate ratio in the feed and space velocity.

CHAPTER VII: NON–CATALYTIC PYROLYSIS OF ETHANE TO ETHYLENE IN THE PRESENCE OF CO_2 WITH OR WITHOUT O_2

Non–catalytic pyrolysis of ethane to ethylene in the presence of oxygen and / or CO_2 has been studied at different temperatures (750^oC – 900^oC), space velocities (1500 – 9000 h^{-1}), CO_2/C_2H_6 ratios (0 – 2.0) and O_2/C_2H_6 ratios (0 – 0.3). The influence of the process parameters on the ethane conversion and product (viz. ethylene, methane and higher hydrocarbons, CO, etc.) selectivity in the pyrolysis has been thoroughly investigated.

CHAPTER 1

GENERAL INTRODUCTION: LITERATURE SURVEY, OBJECTIVES AND SCOPE

CHAPTER 1

GENERAL INTRODUCTION: LITERATURE SURVEY, OBJECTIVES AND SCOPE

Natural gas is an abundant resource in various part of the world. Methane is main constituent of natural gas, coal–bed gas and biogas. Methane is produced in huge quantities during oil production as associated gas and also produced in the petrochemical refining and petrochemical processes. It is also available in huge quantities as methane hydrate at sea beds. Since methane is available and produced mostly in remote places, its transportation is very costly or even impossible. Therefore, much of the natural gas associated with oil is flared causing not only a wastage of valuable energy under the present energy crisis but also global warming due to the release of very large quantity of CO_2 in the atmosphere. Even from the environmental consideration, the methane / natural gas produced in the remote places need to be converted into easily transportable and / or value added products involving either oxidative or non–oxidative activation of methane.

Syngas (a mixture of CO and H_2) is a versatile feedstock for methanol and ammonia syntheses and oxo-processes and also for a number of F.T. syntheses for the production of liquid fuels, olefins and oxygenates. Hence, the conversion of methane to value added products via its conversion to syngas is highly promising one, provided the syngas from methane is produced economically. Presently, syngas is produced by the steam reforming of methane or higher hydrocarbons. Because of its several limitations / drawbacks (high energy requirement, high H_2/CO ratio, low selectivity / yield for CO, high capital cost and low space-time-yield), the steam reforming process is uneconomical for its use in the methane conversion. Autothermal reforming of methane to syngas is also a well-established process but it also suffers from a number of serious drawbacks limiting its use in the syngas production. In the past 12 to 15 years, catalytic partial oxidation of methane to syngas has been extensively investigated. This process is mildly exothermic one and provides syngas with desirable H_2/CO ratio (about 2), required for the methanol and F.T. syntheses. However, it is highly hazardous in nature because of the simultaneously occurring highly exothermic combustion of methane to CO_2 and water. Although, this limitation could be partially overcome by carrying out the partial oxidation of methane simultaneously with the endothermic steam and / or CO_2 reforming of

methane over the same catalyst, and thereby coupling the exothermic oxidative conversion and endothermic CO_2 and / or steam reforming reactions, the catalyst employed should have very high thermal stability (preferably upto 1500 ^oC). It is of great practical importance to develop a high temperature stable catalyst having high activity and selectivity for the methane to syngas conversion reactions, involving the exothermic oxidative conversion reactions.

Because of the increasing importance of the CO_2 sequestration for avoiding global warming, CO_2 reforming of methane to syngas has been considered as an important process for the utilization of CO_2. Apart from the high-energy requirement, this process also suffers badly from a very rapid carbon deposition on the catalyst, particularly Ni-based catalysts. It is therefore of great practical importance to develop a non-noble metal-based catalyst, which allows only a little or no carbon formation in the CO_2 reforming reaction.

Methane is most inert amongst hydrocarbons and hence its activation at low temperature (< 600 ^oC) is very challenging. Earlier studies showed that at low temperatures, methane could be activated in the presence of higher hydrocarbons over bifuntional pentasil zeolite. Practically it would be more interesting if methane could be activated in the presence of methanol which itself can be produced from methane.

It is also interesting to investigate the conversion of ethane to ethylene (which is a keystone to petrochemical) in the pyrolysis of ethane in the presence of CO_2 with or without O_2 for utilizing CO_2 as an oxidizing agent.

1.1. Conversion of Methane to Syngas – Literature Survey

Increased concern about world's dependence upon petroleum oil in the light of its fast depleting reserves has provoked increased interest in the efficient utilization of natural gas. Methane (a major constituent of natural gas) may be converted to synthesis gas. It is a mixture of carbon monoxide and hydrogen, a highly versatile feedstock used in methanol, Fischer-Tropsch synthesis processes, carbonylation, hydrogenation, hydroformylation and other industrially important reactions. The present section focuses on the industrial importance of synthesis gas and its diverse applications in synthesis of chemicals and liquid fuels and the literature on the conversion of methane to syngas.

Syngas, the technical jargon for mixtures of hydrogen and carbon oxides, is crucially important building block of the chemical industry and is widely used in a variety of processes. Currently, the production of H_2 and CO, synthesis gas, (syngas), is carried out by steam

reforming of methane [1,2], partial oxidation of fuel oil [3], coal gasification [4,5] and naphtha reforming [6]. Synthesis gas is widely used and can be converted into petrochemicals, higher alcohols and synthetic fuels. Hydrogen is used in ammonia synthesis and petroleum refining industries, while carbon monoxide is widely used in the production of plastics, paints, foams, pesticides and insecticides.

Common names of mixtures of CO and H_2 are derived from their origin such as: "water gas" ($CO + H_2O$) from steam gasification of coal and "crack gas" ($CO + 3H_2O$) from the steam reforming of methane, or from their application such as "methanol synthesis gas" ($CO + 2H_2$) for the manufacture of methanol and "oxo gas" ($CO + H_2$) for hydroformylation reactions. Another synthesis gas is ammonia synthesis gas ($N_2 + 3H_2$), which does not contain CO.

Recent focus of syngas conversion development is on catalyst to improve the economics of producing hydrocarbon and/or oxygenates liquid fuels, particularly those suitable for transportation.

The pathways of syngas conversion are:

Table 1.1. Syngas Stoichiometry Required for some Industrially Processes

Process	**H_2/CO ratio**	**$H_2/2(CO+3CO_2)$**	**Syngas production process**	**Feed stock**
Methanol	≥ 2.0	≥ 1.0	[a] [b] [c]	Natural gas
Methanol – higher alcohols	1.0 – 2.5	-	[b] [c] (removal of CO_2) [e] and/or H_2 in some cases	Natural gas Heavy residue Coal, Biomass
Glycol (direct – indirect synthesis	1.5 – 1.0	-	[d] [e] (or [b] with H_2 partially removed)	Heavy residue Coal, Biomass Natural gas
Hydro-carbonylation	1.0 2.0	(aldehyde) (alcohol)	[b] [e] [b] (or [c] with H_2 partially removal)	Heavy residue coal, Biomass Natural gas (Steam reforming and ATR)

Carbonylation (acetic acid, acetic anhydride)	0.0	(Pure CO)	[a] [b] [c] [d] [e] (selective CO extraction)	Natural gas Heavy residue Coal, Biomass
Oxo synthesis	1.0	-	[e]	Coal, Biomass

[a] Steam reforming [c] Steam reforming & Auto thermal reforming (ATR)

[b] Partial oxidation [d] Gasification [e] CO_2 reforming

1. Fuels and chemicals by direct synthesis (methanol, ammonia, gasoline, diesel fuel, olefins and methane.
2. Fuels and chemicals by indirect synthesis via methanol (acetic acid, acetic anhydride, gasoline diesel fuel, ethanol etc.)
3. Chemicals by secondary reactions of products obtained from direct or indirect synthesis (acid, alcohols, single cell protein etc.)

Thus a remarkable diversity of chemical / liquid fuels [7] can be synthesized from syngas.

There are several catalytic options available for the production of synthesis gas from natural gas/methane. In the present section, some important catalytic routes and the conventional technologies available for the generation of synthesis gas from natural gas / methane have been discussed briefly.

1.1.1. CO_2 Reforming of Methane to Syngas

Although technological practices should minimize environmental impact, this is not always economically feasible. During the past decade, for example, there has been increasing global concern over the rise of anthropogenic CO_2 emission into the Earth's atmosphere, estimated to be around 2×10^5 g of carbon per annum [8]. Although the precise CO_2 emission flux is uncertain, there are several difficult indicators which raise the possibility that anthropogenic greenhouse gas emissions are causing a global problem. They include a correlation of mean global temperature rise with atmospheric CH_4 and CO_2 concentrations [9], drastic changes in the annual temperature cycle of the Northern Hemisphere [10], and increasing volatility of global weather patterns [11]. Consequentially, there has been increased interest in a better understanding of CH_4 and CO_2 removal, disposal and utilization as well as the influence of these gases on the atmosphere. Today as well as historically, however, the

principal interest has been the study of the reaction between CO_2 and CH_4 to produce synthesis gas (i.e. $CO + H_2$), which can be used in chemical energy transmission systems [12–15] or utilized in the Fischer-Tropch reaction to produce liquids [16,17]. The latter approach would be especially useful at remote natural gas fields containing large amount of CO_2 and at petroleum fields where natural gas is now being flared because liquids can be transported less expansively than gasses. Reforming with CO_2, rather than H_2O, is attractive because it can be employed in areas where water is not available and it yields syngas with lower H_2/CO ratios, which is a preferable feedstock for the Ficher – Tropsch synthesis of long – chain hydrocarbons [18]. In other situations, a combination of CO_2 and steam reforming may be advantageous [19]. Indeed, a limited number of industrial processes are already in operation, which utilizes the $CO_2 – CH_4$ reforming reaction [20–23].

The CO_2 reforming of methane involves a highly endothermic reaction (Equation – 1). The thermodynamics and equilibrium characteristics of CO_2 reforming of methane are similar to the widely employed steam reforming of methane (Equation – 2) except that the former reaction produces synthesis gas with lower H_2/CO ratio,

$$CO_2 + CH_4 \rightarrow 2CO + 2H_2 \quad - 62.2 \text{ kcal.mol}^{-1} \qquad (1)$$

$$CH_4 + H_2O \rightarrow CO + 3H_2 \quad - 54.2 \text{ kcal.mol}^{-1} \qquad (2)$$

The CO_2 reforming of methane has been used in conjunction with steam reforming process and the coupled reactions are likely to be conducted under conditions where carbon formations via reactions,

$$CH_4 \rightarrow C + 2H_2 \qquad (3)$$

$$2CO \rightarrow C + CO_2 \qquad (4)$$

is thermodynamically feasible. Other reactions, which could also have an important influence on the overall product spectrum, are:

$$CO_2 + H_2 \rightarrow CO + H_2O \qquad (5)$$

$$C + H_2O \rightarrow CO + H_2 \qquad (6)$$

Thus, the CH_4/CO_2 reforming reaction (Eq. – 1) can be seen as consisting of reactions (3) and the reverse reaction (4). The carbon formed in reaction (3) should be rapidly consumed by the reverse of reaction (4) and, to a lesser extent, by the steam carbon gasification reaction (i.e. reaction 6). Reaction (6) can play a role in CO_2/CH_4 reforming because steam is almost always formed via the reverse water gas shift (RWGS) reaction (Eq. – 5). If the reaction (3) is faster

than the carbon removal rate(s), there will be a net build-up of carbon to pose serious problems and reactor blockages. Apart from reaction (3), reaction (4) and the reverse of reaction (6), both, which are favoured at low temperatures, are also potential sources of carbon. It may also be noted that reaction (5), which consumes product hydrogen, represents a disadvantage unless both reactions (5) and (6) are made to take place efficiently in tandem so that the overall stoichiometry of the CO_2/CH_4 reforming reaction is maintained.

Apparently, the role of suitable catalysts would be not only a speed up the overall reaction but also to adjust the appropriate elementary steps in a way, which prevents both net carbon deposition and water formation. It therefore is relevant to carry out literature survey on the catalysis of the CO_2 reforming of methane to know if carbon deposition (a problem of serious magnitude) and water formation can be prevented in suitable catalyst system.

In 1995, Ruckenstein and Hu [24] reported a highly efficient 16.7 wt% NiO-MgO solid solution catalyst for CO_2 reforming of methane, which was prepared by impregnation and was calcined at 800 ^oC for 15 hr. It exhibited almost 100% conversion of CO_2, > 91 % conversion of CH_4, > 95 % selectivities to CO and H_2, at 790 ^oC, atmospheric pressure and a very high space velocity of 60,000 $cm^3g^{-1}h^{-1}$, for a CH_4/CO_2 mol ratio of 1. The conversions of the reactants and the selectivity of the products remained unchanged during the entire time of the reaction employed (120 h). In contrast to MgO, the other alkaline – earth oxides, such as CaO, SrO and BaO, were found to be poor supports for NiO since they provided low activities, selectivities or stabilities. Although the reduced NiO/Al_2O_3 catalyst provided very high initial conversions (CH_4: 91 % and CO_2: 98 %) and selectivities (both CO and H_2: > 95 %), it had the fastest carbon deposition, which led to the complete plugging of the reactor after only 6 hr of reaction [25].

Choudhary et al. reported a number of catalysts for the CO_2 reforming of methane, viz. NiO-CaO [26], NiO-MgO or Ni-Co-MgO [27], NiO or $Ni_{1-x}Co_xO$/MgO/SA-5205 [28, 29] catalysts. But a very serious problem associated with the CO_2 reforming of methane is a rapid carbon deposition on the catalyst. In general, the rate of carbon deposition is very high for the Ni-based catalysts and relatively slower for the Co- and noble metal based catalysts. Choudhary et al. also reported that the addition of cobalt [27,29,30] to nickel catalyst has also been found to suppress the carbon formation in the CO_2 reforming.

In 1997, Fujimoto and coworkers [31–33] reported new results regarding the reforming of methane CO_2 over the $Ni_{0.03}Mg_{0.97}O$ solid solution catalyst, which was used in 1992 [34],

and its bimetallic catalysts which contained in addition small amounts of Pt, Pd or Rh (the atomic ratio of M / (Ni + Mg) was varied 0.007 and 0.032 %, where M = Pt, Pd or Rh) [31]. The $Ni_{0.03}Mg_{0.97}O$ solid solution catalyst provided a low CO yield (about 215 $\mu mol.g^{-1}_{cat.}sec^{-1}$; i.e. 38 %) at a space velocity of 44,800 $mLg^{-1}_{cat.}hr^{-1}$ even at 850 ^oC. However, the addition of a noble metal promoted both the activity and the stability at 500 ^oC. The optimum loading of a noble metal was obtained for an atomic ratio of M / (Ni + Mg) ≈ 0.021 %. Temperature programmed hydrogenation (TPH) of the carbonaceous species formed during the catalytic reaction indicated that the resistance of $Ni_{0.03}Mg_{0.97}O$ solid solution to carbon deposition was retained by the bimetallic catalysts as well.

J.Z.Luo et al. [35] investigated the carbon deposition and reaction pathways in CO_2/CH_4 reforming over $Li–La_2O_3/5A$ catalyst by means of XRD, insitu TG, Pulse experiments, Chemical trapping, TEM and EPR. The XRD results showed that due to the formation of perovskite–like La_2NiO_4 phase in $Ni–La_2O_3/5A$, the small–size (ca. 9 nm) Ni^o crystallites formed in H_2 reduction remained unsintered during 48 hr of on stream reaction at 800 ^oC. The accumulation of carbon on the active sites was the main reason for $Li–La_2O_3/5A$ deactivation. The deactivation of $^{13}CO_2$ and CO_2 in O_2 pulsing onto a sample pretreated with $^{13}CH_4/CO_2$ confirmed that the deposited carbon was from both CH_4 and CO_2.

In 2000, Wang et al. [36] studied the effects of promoters, such as alkali metal oxide (Na_2O), alkali–earth metal oxides (MgO, CaO) and rare - earth metal oxide (La_2O_3, CeO_2) on the catalytic activity and selectivity in terms of coking resistance. CaO -, La_2O_3 – and CeO_2 – promoted Ni/γ- Al_2O_3 catalysts exhibited higher stability; whereas MgO - and Na_2O - promoted catalysts demonstrated lower activity and significant deactivation. Metal oxide promoters (Na_2O, MgO, La_2O_3 and CeO_2) suppressed carbon deposition, primarily due to the enhanced basicity of the supports and highly reactive carbon species formed during the reaction. In contrast, CaO increased carbon deposition; however, it also promoted the carbon reactivity.

In 2001, L. Ji et al. [37] reported the influence of different catalyst preparation method for coke deposition. They had prepared three cobalt – based catalysts with the same cobalt content (10 wt%) by conventional impregnation of commercial γ- Al_2O_3 supported ($CoAl_{CO-IM}$), sol-gel-made γ-Al_2O_3 ($CoAl_{SG-IM}$) and direct sol-gel processing from organometallic compounds ($CoAl_{SG}$), respectively. At 750 ^oC, all three catalysts had shown the same catalytic activity. However $CoAl_{SG}$ catalyst showed relatively low catalytic activity at low reaction temperatures (550 – 650 ^oC) and high space velocity, due to the formation of $CoAl_2O_4$. It had

the best coking resistivity with average coking rate of 0.0025 gm (carbon) g $(cat)^{-1}h^{-1}$. Fast and heavy coke deposition occurred on $CoAl_{(CO\text{-}IM)}$ catalyst with an average coking rate of 0.11 gm (carbon) g $(cat)^{-1}h^{-1}$. The lifetime of $CoAl_{SG}$ catalyst was 24 times longer than that of $CoAl_{CO\text{-}IM}$ catalyst, under thermodynamically severe reaction conditions (CO_2/CH_4 = 0.88, 700 ^oC).

Seok et al. [38] reported that addition of Mn onto Ni/Al_2O_3 catalyst reduce coke formation. Catalyst prepared by co-precipitate method showed higher coke resistance and more stable activity compared to the catalyst prepared by impregnation method.

B.S.Liu et al. [39] reported that catalyst calcinations temperature played a very important role in carbon deposition on 9% La_2NiO_4/γ- Al_2O_3 (9NLA) catalyst system. The catalyst has been calcined at different temperatures (500 and 800 ^oC). It has been reported that with the rise in calcinations temperature coke formation decreased due to formation of stable $NiAlO_4$.

Very recently A. Effendi et al. [40] investigated with regards to carbon deposition on 4.5 wt% NiO/SiO_2 catalyst at 1023 K, 1 atm and a CH_4/CO_2 ratio of 1.0 employing micro–fluidized and fixed bed reactors. A higher catalytic activity (by 20%) has been observed in the initial stage (0.5 hr) of the fluidized–bed reforming which may be attributed to lesser deactivation of the catalyst compared to fixed–bed operation.

From the brief literature survey, it is evident that catalytic CO_2 reforming of methane study, though long been known, has not really been explored on the catalyst which showed high activity and selectivity without formation of carbon in the CO_2 reforming reaction. Some recent literatures have addressed the topic in some details on several aspects of this catalytic process like nature of the carbon filaments formed during the course of the reaction, effect of support, calcinations temperature and the different types of reactors on the carbon accumulation. But the issue of without carbon formation has rarely been discussed. It is, therefore, of great practical importance to develop a catalyst, which allow only little or no carbon formation in the CO_2 reforming. The earlier studies for CO_2 reforming of methane to CO and H_2 over different non-noble and noble metal catalysts (at atmospheric pressure under given reaction conditions) are summarized in Tables 1.2 and 1.3.

Table 1.2 Summary of Earlier Work on the CO_2 Reforming of Methane to Syngas over Non-Noble Metal Catalysts

Catalyst	Reaction condition			Remarks, if any	Author (s) Year	Ref
	Temp (^oC)	Feed (CH_4:CO_2:dil)	W/F, GHSV or contact time			
NiO-MgO solid solution	790	1.0: 1.0:0.0	60,000 $cm^3.g^{-1}.h^{-1}$	Investigated the activity of the catalyst and also compared the catalyst with other alkaline earth oxides (CaO, SrO &BaO). Catalyst showed stable activity during the time-on-stream (120 hr) study.	Ruckenstein et. al. (1995)	24
NiO-CaO	850	1.0	11,550 $cm^3.g^{-1}.h^{-1}$	The time-on stream activity/selectivity and pressure drop across the catalyst bed in CO_2 reforming of methane to syngas has been studied.	Choudhary & Rajput (1996)	26
NiO-MgO and NiO-CoO-MgO catalysts	850	1.0	13,500 $cm^3g^{-1}h^{-1}$	The influence of time-on-stream activity on the conversion and pressure drop across the reactor (which is the measure of filamental carbon deposition) has been studied.	Choudhary & Mamman (1998)	27
NiO/MgO/SA5205	700 - 900	1.0	10,000 – 1,00,000$cm^3g^{-1}h^{-1}$	Influence of temperature & space velocity has been investigated.	Choudhary et al. (1998)	28
$Ni_{0.03}Mg_{0.97}O$	500 & 850	CH_4/CO_2=1	44,800 $cm^3.g^{-1}h^{-1}$	Effect of small amount (0.007 – 0.032%) of noble metals (Pt, Pd or Rh) on the catalyst & the catalytic performance has been investigated. Addition of noble metal promoted both the activity and selectivity at 500^oC.	Fujimoto et. al. (1997)	31 – 33
Ni-La_2O_3/SA	800	-	-	Carbon deposition and reaction pathways over the catalyst have been studied by means of XRD, in situ TG, Pulse expts, Chem. trapping, TEM and EPR	J.Z.Luo et. al. (1999)	35
Na_2O, MgO, CaO, La_2O_3, CeO_2 metal oxide promoted Ni/γ-Al_2O_3	-	-	-	Effect of promoter on the activity and stability in terms of coking resistance and coke reactivity were studied. CaO, La_2O_3 and CeO_2 promoted catalyst exhibited higher stability where as MgO & Na_2O promoted catalyst showed low activity.	S.Wang et.al. (2000)	36
Co / γ-AL_2O_3	700	CH_4=19.8 CO_2=17.5 Bal Ar	4.0×10^4 $ml/h/g_{cat}$	Influence of different catalyst preparation method for coke deposition has been studied (Impregnation, sol-gel made and direct sol-gel). Coke registivity as follows: $CoAl_{SG} > CoAl_{SG-IM} > CoAl_{CO-IM}$	L.Ji et al. (2001)	37

Table 1.2 continued.

Catalyst	Reaction condition			Remarks, if any	Author (s) Year	Ref
	Temp (^oC)	Feed	W/F, GHSV or contact time			
Ni / MgO-Al_2O_3	650	CH_4/CO_2=1.0	Total flow 81.7 μmol/sec Catalyst 200 mg	Role of MnO has been discussed particularly in view of the deposition of unreactive carbon on the catalyst surface	S.H.Seok et. al. (2001)	38
9% La_2NiO_4 / χ-Al_2O_3 (9NLA)	700, reduced at 700 ^oC or 800 ^oC with H_2	-	4.8×10^4 $ml.g^{-1}.h^{-1}$	Carbon deposition and catalyst stability has been studied. Catalyst calcine at different temp (500 and 800). With the rise in calcination temp. Coke formation decrease due to formation of stable $NiAl_2O_4$	B.S.Liu et al (2003)	39
Ni / SiO_2	1027 K	CH_4/CO_2=1	-	Carbon deposition on catalyst employing micro-fluidized-bed & fixed-bed has been investigated. Lesser deactivation observed in fluidized bed reactor system.	A.Effendi et al. (2003)	40
17.0 wt% Ni/La_2O_3, CaO, γ-Al_2o_3 or Ni/(10wt%)/γ-Al_2o_3	750	1.0:1.0:3.0	-	Comparative study of methane over NiO/La_2O_3 and conventional Ni-based catalyst has been done.	Zhang et. al. (1996)	41
A series of Ni/Al_2O_3 catalysts	650 - 850	1.0	1.1×10^4 h^{-1}	The influence of promoters and catalyst prepn. Techniques for CO_2 reforming of CH_4 over these catalysts has been studied.	Chang et. al. (1996)	42
NiO/MgO/SA 5205	700 - 900	1.0	$1.0 - 9.5 \times 10^4$ $cm^3g^{-1}h^{-1}$	Influence of the reaction temperature and the space velocity on the conversion, H_2 selectivity and H_2/CO ratio in the process has been studied.	Choudhary et. al. (1998)	43
Ir supported on TiO_2, ZrO_2, Y_2O_3, Al_2O_3, La_2O_3, MgO & SiO_2	600	1.0	3.6×10 h^{-1}	The support activity order in the CO_2 reforming of methane was reported to be as follows: $TiO_2 \geq ZrO_2 \geq Y_2O_3 > La_2O_3 > SiO_2$	Nakagawa et. al. (1998)	44
Ni/ZrO_2	973 K	-	-	Carbon deposition on the catalyst during reaction has been studied. A relationship between the amount of coke deposited & the activity reveals that the carbon acts as a reaction intermediate & reacts with CO_2 to form CO	X.Li et. al. (1999)	45
Ni/γAl_2O_3	700	CO_2/CH_4=0.88		Influence of catalyst preparation (WI, sol-gel method & direct sol gel) methods on the performance of the catalyst has been studied. Coking resistivity: $Ni/\gamma Al_2O_{3(SG-IM)} > Ni/Al_2O_{3(SG)} > Ni/Al_2O_{3(CO-IM)}$	S.Tang et. al. (2000)	46
Supported Ni and Rh catalyst	-	-	-	Carbon deposited on the catalyst at high pressure has been studied by using SEM and TPO tech.	S.T. Srinivas et. al. (2000)	47

Table 1.2 continued

Catalyst	Reaction condition			Remarks, if any	Author (s) Year	Ref
	Temp (^oC)	Feed	W/F, GHSV or contact time			
$Ni/\gamma\text{-}Al_2O_3$	-	-	-	The carbon deposition & carbon elimination were investigated by means of TGA, XRD & TEM. Optimization of feed ratio (CO_2/CH_4=1.3) was also investigated.	Z.Xu et. al. (2001)	48
$NiO/CoO/Al_2O_3$	976 – 1033 K	CO_2/CH_4>2	-	Kinetics study has been studied in a packed bed reactor & mechanism was also proposed	C.E. Quincoces et.al (2001)	49
Fe, Co and Ni catalyst supported on Cerium oxide	1123 K	CO_2/CH_4=1	Total flow 100 ml/min (STP) Catalyst taken 500mg	Ni Catalyst gave highest activity with H_2/CO close to 1.0. No carbon deposition observed. Co catalyst showed almost same activity to that Ni. Fe catalyst showed a poor activity	K. Asami et al. (2003)	50

Table 1.3 Summary of Earlier Work on the CO_2 Reforming of Methane to Syngas over Noble Metal Catalysts

Catalyst	Reaction condition			Remarks, if any	Author (s) Year	Ref
	Temp (^oC)	Feed (CH_4:CO_2:dil)	W/F, GHSV or contact time			
Noble metal (Pt, Pd or Rh) dopped $Ni_{0.03}Mg_{0.97}O$	500 & 850	CH_4/CO_2=1	44,800 $cm^3.g^{-1}h^{-1}$	Effect of small amount (0.007 – 0.032%) of noble metals (Pt, Pd or Rh) on the catalyst & the catalytic performance has been investigated. Addition of noble metal promoted both the activity and selectivity at 500^oC.	Fujimoto et. al. (1997)	31 – 33
Thin Pd film (20μm) supported on outer surface of porous alumina cylinder	500	-	-	The methane conversion exceeded the equilibrium attaintable in the conventional system, since use of H_2 permeable membrane shifted the thermodynamic equilibrium towards right hand side.	Kikuchi et. al. (1997)	51
Pt/ZrO_2	800	-	-	Effect of promoter to the catalyst was investigated. The promoters have multiples effects- They stabilize the surface area for high temp operation, increase degree of CO_2 adsorption site near metal particle and reduce particle growth	S.M.Stagg et. al. (1998)	52
Pt/ZrO_2	-	-	-	The effect of the method of preparation & pretreatment on the dispersion & catalytic properties has been studied.	J.R.H.Ross et.al. (2000)	53
Pt promoted Co/Al_2O_3	600 – 800	-	-	The effect of calcinations temperature (1200^oC), content of Co & promoter, feed composition, pretreatment & reaction conditions on catalytic activity, anti-carbon deposition property & stability were studied.	C.J.Huang et.al. (2000)	54
Pt/Al_2O_3 & Pt/ZrO_2	875 – 1125 K	CH_4=25%, CO_2=25%, N_2=5%, Ar=45%	-	Relation between coke formation & deactivation has been investigated. Pt/ZrO_2 showed high catalytic stability with no carbon formation compared to Pt/Al_2O_3	K. Nagaoka et. al. (2001)	55
Pt, Rh, Ru, Pd (5% each)/Al_2O_3	773 – 1173K	CO_2CH_4=2.9	-	No deactivation was observed. The activity of the catalyst as Ru≈Rh>Pt≈Pd>Ir. Approx 0.1 mg/g/h carbon deposited on Ru or Ir catalyst	Thomas Suhartanto et. al. (2001)	56
$Pt/ZrO_2/AL_2O_3$ & Pt/ZrO_2	723–1073 K reduced in 10% H_2 at 773K – 1h	CH_4/CO_2=1.0	WHSV 960 h^{-1}	Catalytic activity studied with different ZrO_2 loading. 10% loading ZrO_2 exhibited excellent stability, due to strong Pt-Zr^{n+} interaction, under severe conditions.	M.M.V.M. Souza et.al. (2002)	57

Table 1.3 continued

Catalyst	Reaction condition			Remarks, if any	Author (s) Year	Ref
	Temp (^oC)	Feed (CH_4:CO_2:dil)	W/F, GHSV or contact time			
Rh/NaY or Rh/αAl_2O_3, Nb_2O_5, TiO_2	723 – 973K	$CH_4/CO_2/N_2$ =20/20/60	Total flow 100 ml/min Catalyst 0.05-0.2 mg	The conversion is strongly influenced by the method of preparation (ion-exchange & impregnation) and preliminary activation of the catalyst.	U.L. Portugal et. al. (2002)	58
$Ln_{1-x}Ca_xRu_{0.8}Ni_{0.2}O_3$ (Ln= La, Sm, Nd)	723 – 1123K	CH_4/CO_2=1 N_2 as diluent	WHSV 241/hg	A series of peronskite-like oxide was partially or totally substituted by Ca, Sr, Nd have been used to produce in situ nanoparticles of Ru (Ni). Here also calcium proportion and effect of lanthanides have been described.	M.R. Goldwasser et. al. (2003)	59
Ru, Rh, Ir, Pt, Pd, Au / $MgAlO_x$	800	-	F/W 370,909 & 92,727 $cm^3g^{-1}h^{-1}$	A simple and effective approach has been developed for the synthesis of precious metal catalysts supported on Mg-Al mixed oxide. The most efficient being that of Ruthenium.	A.I. Tsyganok et.al. (2003)	60
Ru based ceramic membrane reactor	400	CH_4/CO_2=1	140 ml/min	An Ru-based catalytic menbrane reactor used for dry reforming and its catalytic performance compared with tubular packed bed reactors. Results showed good catalytic activity.	L. Paturzo et.al. (2003)	61
Ti modified Ru/Zeolite	723 – 873 K	$CH_4/CO_2/N_2$ = 20/20/60 & CH_4/CO_2 =66/33	Total flow rate 100, 200, 300 ml/min Catalyst 0.2 g	Introduction of Ti into Ru/NaY zeolite by ion-exchange caused structural collapse of zeolite frame work. TEM data showed that Ti incorporated into Ru/USY was well distributed. The crytallinity of USY decreased after introduction of Ti by WI tech. Ti loading also studied.	S.M.Gheno et. al. (2003)	62
Rh & Pt-Re/γ-Al_2O_3	450 – 975	CO_2/CH_4=1	62000 h^{-1}	The loading of these catalysts onto wash coated α-Al_2O_3 & the advantages arising from the unique properties of the foams as catalyst supports has been studied. Pt-Re is an alternative catalyst for dry reforming gas also been described.	J.T. Richardson et. al. (2003)	63

1.1.2. Steam Reforming of Methane [SRM] to Syngas

Steam reforming is established process for converting methane or natural gas and other hydrocarbons into syngas [1,2]. It has been used for several decades since its first development in 1926 [64] and over the year's substantial improvement has been introduced. The traditional SRM process consists of feed gas preheating and pretreatment, reforming, high and low shift, CO_2 removal and methanation. Methane is reacted with steam on a Ni-based catalyst in a primary reformer to produce H_2 and CO at residence of several seconds. The catalytic reactions are as follows,

Main reaction

$CH_4 + H_2O \rightarrow CO + 3H_2$ - 54.2 kcal.mol^{-1}

Side reaction

$CO + H_2O \rightarrow CO_2 + H_2$ + 8.0 kcal.mol^{-1}

Reformed gas is formed at a ca. 1200 K and pressures of 5–30 bar. Excess of steam is introduced to avoid carbon deposition.

Today, steam reforming is a principal process for the production of H_2 and synthesis gas. More than 80% of world ammonia production is based on steam reforming. Though steam reforming is a well – established process, it suffers from the following disadvantages.

1. It is highly endothermic process and hence, energy requirements are very high.
2. H_2/CO ratio obtained in the product stream is very high (> 3) and therefore is unsuitable for methanol and Fisher – Tropsch synthesis.
3. The CO selectivity obtained is very poor because of the water gas reaction.
4. The catalyst undergoes deactivation very fast due to coke deposition on the surface of the catalyst, which results in the poor heat transfer from wall of the reactor.

The steam reforming of methane has been documented extensively in the literature.

The addition of magnesia provides a positive effect on the performance of the typical Ni – based steam-reforming catalysts by lowering the coking rate [65–67] and by enhancing the steam adsorption and the gasification of the deposited carbon, appears to be crucial in hindering coking [66-68]. Borowiecki examined the influenced of calcinations and reduction temperature in stabilizing a surface MgO rich phase, which by improving the capacity of the Ni/MgO catalyst for steam adsorption, ensures a higher gasification rate of the carbonaceous deposits [67]. In spite of this, the use of MgO as support in working catalysts was limited because of its

poor stability [69,70] and the negative effect of the formation of the solid solution on the NiO reducibility, and hence on the formation of highly active metal areas [69,70,71].

Fujimoto et al. [72] studied the steam reforming of methane for a low Steam/CH_4 ratio over a NiO-MgO solid solution catalyst. While a commercial Ni/Al_2O_3-MgO exhibited stability and activity for more than 40 h for a Steam/CH_4 ratio of 2.0, it lost its activity and the reactor became plugged due to the large amount of coke deposited (about 104 wt% - carbon/g_{cat} after 20 h) for a steam/CH_4 ratio of 1.0. In contrast, the $Ni_{0.03}Mg_{0.97}O$ solid solution catalyst exhibited excellent activity (90% methane conversion), which is close to the equilibrium conversion (95%) and the activity remained unchanged for over 70 h even for a Steam/Carbon ratio of 1.0. This indicates that coke formation and deactivation did not occur over the $Ni_{0.03}Mg_{0.97}O$ solid solution catalyst. They suggested that the suppression of coke formation over the catalyst was caused by very small nickel particles and by the carbonaceous species formed on the Ni metal particles as reaction intermediates.

Choudhary et al. [73] reported the catalytic steam and oxy-steam reforming of methane to syngas over $Co_xNi_{1-x}O$ supported on MgO precoated SA5205 catalyst carriers. The influence of the Co/Ni ratio of the catalyst on its performance in steam and oxy-steam reforming processes (at 800 and 850 ^oC) was studied. They had shown that the steam reforming process, the Co/Ni ratio influences strongly on the methane and steam conversion and CO selectivity and product H_2/CO ratio, particularly at lower temperature when the Co/Ni ratio is increased, the methane and H_2O conversion and CO selectivity are decreased markedly.

W. S. Dong et al.[74] reported the effect of Ni content on the Ni/Ce-ZrO_2 catalyst in the methane conversion reactions to syngas. Ni/Ce-ZrO_2 catalyst with 15% Ni-loading exhibits not only the highest catalytic activity and selectivity but also remarkable stability. From H_2 chemisorptions and TPR results they have concluded that Ni surface area and the chemical environment of nickel, as well as the properties of the Ce-ZrO_2 support, played very important roles in the catalytic activity and stability of the catalyst.

F. Gallucci et al. [75] reported the reaction of methane steam reforming in both a traditional reactor (TR) and a membrane reactor (MR). They investigated the enhancement of the methane conversion in an MR. The effect of various kinds of sweep gas (H_2, N_2, CO, air, O_2 and steam), as well as no sweep were analyzed as a function of temperature at different molar flow rates of the sweep gas used. The dependence of the methane conversion on increasing H_2O/CH_4 feed ratio was also studied.

Choudhary et al. [26] investigated the steam reforming, CO_2 reforming and simultaneous steam and CO_2 reforming of methane to CO and H_2 over NiO-CaO catalyst (without any prereduction treatment) at different temperatures (700–850 ^oC) and space velocities (5000 – 70,000 $cm^3g^{-1}h^{-1}$). The catalyst showed high activity / selectivity in both the steam and CO_2 reforming reactions and the simultaneous steam and CO_2 reforming. In the CO_2 reforming, the coke deposition on the catalyst is found to be very fast. However, in steam reforming, the coke deposition on the catalyst is drastically reduced. The high activity of the catalyst is due to some physical interactions between NiO and CaO, causing a change in the particle size or dispersion of NiO with a change in the Ni/Ca ratio.

In 1998, Choudhary and coworkers [28] reported steam reforming of methane over NiO/MgO/SA-5205 (prepared by depositing NiO or MgO precoated SA-5205 support) at different process conditions. The catalyst showed high activity and selectivity in the above methane-to-syngas conversion reaction at low contact times after its reduction by temperature programmed desorption of hydrogen. They have reported that the precoating of the support with MgO, before depositing NiO on it, a protective layer of a thermally stable $MgAl_2O_4$ (spinal), resulting from soild-solid reaction between MgO and Al_2O_3 (from support), is formed at the MgO-support interface. This is avoided the formation of catalytically inactive $NiAl_2O_4$ (spinal) phase, and hence avoided the consumption of nickel, the active component of the catalyst.

Very recently E. Ramirez-Cabrera et al. [76] investigated methane steam reforming and dry reforming over ceria and ceria doped with 1.4 and 5% Nb cation at 900 ^oC. The influence of the calcinations atmosphere on the Nb-doped ceria has also been studied. They have reported the inhibitory effect of H_2 and also a redox mechanism in which the rate is controlled by the slow reaction of a surface carbon species with oxygen in ceria and a more facile reaction between steam and the cerias to replenish the oxygen. They have also reported the Nb-doping slows down the rate of steam reforming, mainly as a consequence of strong segregation of Nb to the ceria surface. It has been also reported that Nb-doped ceria showed extremely resistant to carbon deposition in steam reforming conditions (Steam/methane < 1).

1.1.3. Partial Oxidation of Methane [POM] to Syngas

The conventional process for syngas ($CO + H_2$) production from methane, which is based on the steam reforming of methane (SRM), is highly endothermic and hence highly energy intensive process. Catalytic partial oxidation of methane to syngas offers the most viable alternative to the steam reforming. It is mildly exothermic reaction, which produces H_2 and CO with the desirable H_2/CO ratio of 2.0, suitable for various down stream processes such as Ficher – Tropsch and methanol synthesis processes. The reactions, which occur during the partial oxidation of methane to syngas, are given below.

Main reaction

$CH_4 + 0.5\ O_2 \rightarrow CO + 2H_2 + 8.5$ kcal.mol.$^{-1}$

Side reactions

$CH_4 + O_2 \rightarrow CO + 2H_2O + 124.1$ kcal.mol^{-1}

$CH_4 + 2\ O_2 \rightarrow CO_2 + 2\ H_2O + 191.8$ kcal.mol^{-1}

In the last 1 – 2 decades, extensive efforts have been made on the catalytic partial oxidation of methane (CPOM) to syngas over noble metal and non-noble metal containing catalysts, which is covered in a number of recent reviews [77] and Tables 1.4 and 1.5. The CPOM process operating at a very low contact time (about millisecond), is of great practical importance [78-82]. However, in this process a high methane conversion (> 90%) coupled with very high space velocity ($\geq$ 500,000 $cm^3g^{-1}h^{-1}$) leads to production of a large amount of heat in a small catalyst zone, even at very high selectivity (> 95 %) for CO and H_2, causing a large adiabatic temperature rise (which is difficult to control) and ultimately resulting in the deactivation of a thermally unstable catalyst. Choudhary et al. showed that a highly active / selective supported Ni-containing catalyst (prepared by depositing NiO on a MgO precoated low surface area macroporous silica-alumina) is thermally stable when calcined only up to about 1000 ^oC; at the higher calcination temperature (1200 ^oC), it is completely deactivated mostly because of the formation of catalytically inactive mixed metal oxides [83].

Since the methane combustion reactions ($CH_4 + 2O_2 \rightarrow CO_2 + 2H_2O + 191.8$ kcalmol^{-1} and $CH_4 + O_2 \rightarrow CO + 2H_2O + 124.1$ kcalmol^{-1}) are much more exothermic than the partial oxidation of methane to syngas ($CH_4 + 0.5O_2 \rightarrow CO + 2H_2 + 5.4$ kcalmol^{-1}), even a small loss in the selectivity due to catalyst deactivation is expected to make the CPOM process highly hazardous / out of control. It is therefore of great practical interest to overcome the major

limitation of the MATR and CPOM processes by developing a high temperature stable catalyst, showing desirable activity and selectivity in the methane-to-syngas conversion reactions and also having a high mechanical strength, even when the catalyst is subjected to a very high temperature (≥ 1200 ^{o}C) and thermal shocks. If such a high temperature stable catalyst having desirable activity / selectivity and also high mechanical strength is developed, it would also be useful for the autothermal reforming process, overcoming its major limitation about the requirement of the catalyst which is stable against fouling under the severe operating conditions (high temperature shocks) of the autothermal process.

Very recently T. Utaka et al. [84] investigated Ni/Al_2O_3, hexaaluminate-type $BaNi_xAl_{12-x}O_{19-\alpha}$ and perovskite-type $LaAl_{5/6}Ni_{1/6}O_3$ catalyst for partial oxidation of methane. The hexaaluminate-type $BaNiAl_{11}O_{19-\alpha}$ calcined at 1400 ^{o}C demonstrated more stable and higher activity than Ni/Al_2O_3 calcined at 1000 ^{o}C. They have also reported that the $BaNiAl_{11}O_{19-\alpha}$ catalyst reduced at 1000 ^{o}C was more active than the catalyst reduced at 800 ^{o}C. The results from XPS analysis revealed that the hexaaluminate-type catalysts calcined and reduced at higher temperature had Ni-rich surfaces and highly dispersed Ni species derived from hexaaluminate crystal, resulting in high activity for partial oxidation of methane. Apart from this there is no report on the use of high temperature (> 1200 ^{o}C) calcined catalyst for the POM.

1.1.4. Simultaneous CO_2 and Steam Reforming of Methane to Syngas

Release of large quantities of CO_2 in the atmosphere has created a large green house effect causing a global warming. Hence worldwide efforts are being mage for conversion of CO_2 to useful products. One of the ways of activating CO_2 is its reaction with methane to carbon monoxide and hydrogen, commonly known as CO_2 reforming of methane. In the last few years the research activities on the CO_2 reforming of methane have gained a lot of momentum.

In the simultaneous CO_2 and steam reforming reaction, following reactions occur during the process.

Main reaction

$CH_4 + H_2O \rightarrow CO + 3H_2$ - 54.2 kcal.mol^{-1}

$CH_4 + CO_2 \rightarrow 2CO + 2H_2$ - 62.2 kcal.mol^{-1}

Side reaction

No side reaction occurs during above process when the conversion of both water and CO_2 is positive.

Table 1.4 Summary of Earlier Work on the Oxidative Conversion of Methane to Syngas Over Non-Noble Metal

Catalyst	Reaction condition			Remarks, if any	Author (s) Year	Ref
	Temp (^oC)	Feed CH_4:O_2:dil	W/F, GHSV or contact time			
NiO/MgO & CoO/Mgo	300 - 700	2:1:0	5.0×10^5 $cm^3.g^{-1}.h^{-1}$	Activity of the catalysts investigated at a extremely high space velocity. Conversion was increased during the initial period of the reaction over NiO/MgO catalyst.	Choudhary et. al. (1992)	80
Ni/Yb_2O_3 (Ni/Yb = 0.1 – 4.0)	700	2:1:0	5.0×10^5 $cm^3.g^{-1}.h^{-1}$	Ni/Yb_2O_3 showed a high activity/selectivity at wide range of temperatures. The process follows a reaction path totally different from that of high temperature noncatalytic and catalytic process.	Choudhary et. al. (1992)	81
$NiO\text{-}LnO_x$ Ln=La, Ce, Pr, Nd, Sm, Eu, Gd, Tb, Dy, Er, Yb	535 - 560	2:1:0	5.0×10^5 $cm^3.g^{-1}.h^{-1}$	The pulse reaction of CH_4 on $NiO\text{-}Nd_2O_3$ (at 600^oC) showed involvement of lattice O_2 in the initial reaction & reveals the formation of C from CO on the catalyst reduced in the reaction.	Choudhary et. al. (1993)	82
NiO supported on different commercial low surface area porous catalyst carriers precoated with alkaline & rare earth oxides	700 & 800	1.8	5.2×10^5 $cm^3g^{-1}h^{-1}$	Influence of support (its composition & surface properties), method of NiO & MgO deposition, support precoating agent, loadings of NiO & MgO (as support precoating agent) & calcination temperature on the conversion and selectivity has been studied.	Choudhary et al. (1997)	83
Ni catalyst based on hexaaliminate or perovskite type	-	10% CH_4, 5% O_2 and N_2 balance	12000 or 120,000 l/kg/h	Ni/Al_2O_3, hexaaluminates-type $BaNi_xAl_{12-x}O_{19-x}$ and perovskite-type $LaAl_{5/6}Ni_{1/6}O_3$ were investigated for POM. Hexaaluminate type calcined at 1400^oC demonstrated more stable and higher activity than Ni/Al_2O_3 calcined at 1000^oC Hexaaluminate catalyst reduced at 1000^oC was more active than the catalyst reduced at 800^oC.	T. Utaka et. al. (2003)	84
Co-MgO (Co/Mg=0.1 – 10)	700	2:1:0	5.0×10^5 $cm^3.g^{-1}.h^{-1}$	It has been shown that POM at 700^oC and high space velocities used in the process do not involve the formation of CO_2 and H_2O, as initial products, followed by endothermic reactions of unconverted methane to CO & H_2.	Choudhary et. al. (1992)	85
$Ni\text{-}Yb_2O_3$	300 - 700	2:1:0	5.0×10^4 $cm^3.g^{-1}.h^{-1}$	The hot spots have been detected visually and with an optical pyrometer during the oxidation reactions.	Dissanayaka et. al. (1993)	86

Table 1.4 continued

Catalyst	Reaction condition			Remarks, if any	Author (s) Year	Ref
	Temp (^oC)	Feed CH_4:O_2:dil	W/F, GHSV or contact time			
NiO-CaO	500	1.5:1.0:0.0 – 2.5:1.0:0.0	$5.0 – 50 \times 10^4$ $cm^3.g^{-1}.h^{-1}$	The authors suggested that yield of syngas was found to deviate from the equilibrium values due to the temperature higher than actually measured one.	Theron et. al. (1994)	87
Strontium hydroxyapatite	600 - 900		0.9 $dm^3.h^{-1}$	The pretreatment of catalyst at 900^{o}C generate new active sites on its surface in the form of structural defects.	Matasumura et. al. (1994)	88
18.7 wt% Ni/Al_2O_3 (reduced & unreduced catalyst)	50 - 800	1.8:1.0:0.0	5.0×10^5 $cm^3.g^{-1}.h^{-1}$	It has been concluded that using an extremely high space velocities results in a much higher selectivity & productivity with a change in a reaction pathway.	Choudhary et. al. (1995)	89
Ni/Al_2O_3 in ceramic membrane	800	2:1:1	-	The performance of the membrane reactor has been compared with that of fixed bed reactor.	Santos et. al.(1995)	90
20 wt% Ni/La_2O_3	400 - 750	Pulse of 45 µl of CH_4 & O_2	3.0×10^5 $cm^3g^{-1}h^{-1}$	The transient response curve revealed that CO_2 generation is delayed in comparison to that of CO_2 hence that CO is primary product & CO_2 is subsequently generated on the catalyst during CH_4/O_2 pulses.	Ruckenstein et. al. (1996)	91
$LaNiO_x$	800	1.8:1.0:0.0	5.2×10^5 $cm^3.g^{-1}.h^{-1}$	$LaNiO_3$ perovskite has been reported to be transformed to Ni^o/La_2O_3 during its operation in the catalyst process.	Choudhary et. al. (1996)	92
NiO-MgO	790	$O_2/CO_2/CH_4$ = 14.5/26.9/58.6	90,000 $cm^3.g^{-1}.h^{-1}$	Combined reaction with O_2 & CO_2 carried out over NiO-MgO catalyst. Compared the activity of NiO/MgO catalyst with NiO/SiO_2 & NiO/Al_2O_3 catalyst. MgO supported catalyst showed higher activity.	Ruckenstein et. al. (1998)	93
NiO/MgO/SA5205	600 – 900	1.8:1.0:0.0 – 8.0:1.0:0.0	6000 – 510,000 $Cm^3.g^{-1}.h^{-1}$	Influence of space velocity, catalyst particle size (22 – 70 mesh) and catalyst dilution by inert solid particles on the performance at different temp has been investigated.	Choudhary et. al. (1999)	94
20% CeO_2/γ-Al_2O_3	700	CH_4/O_2=2	Contact time 0.26 s	The reaction between methane & lattice oxygen of cerium oxide has been investigated. The production of syngas is strongly promoted by Pt & Rh. The selectivity depends on degree of reduction of CeO_2	M. Fathi et. al. (2000)	95

Table 1.4 continued

Catalyst	Reaction condition			Remarks, if any	Author (s) Year	Ref
	Temp (^oC)	Feed CH_4:O_2:dil	W/F, GHSV or contact time			
NiO/γ-Al_2O_3	850	CH_4/O_2=2/1	1.8×10^5 l/Kg/h	Influence of preparation method (impregnation & sol-gel) on the activity of the catalyst has been studied. The effect of carbon deposition, the loss & sintering of Ni & the phase transformation of γ-Al_2O_3 were investigated. Only slow phase transformation (γ-Al_2O_3 to αAl_2O_3) affects the performance. Catalyst prep[d] by sol-gel method showed excellent ability to resistant Carbon.	Y. Zhang et. al. (2000)	96
Ni/Mg-Al oxide	1073K	$CH_4/O_2/N_2$ = 2/1/4	1.05×10^4 ml/g/h	Catalyst prepared by spc method from Mg-Al HT like precursors & compared with the same catalyst prepared by impregnation method. Both catalysts showed similar activity.	T. Shishido et. al. (2001)	97
Mg/Ga_2O_3, Zn/Ga_2O_3	-	CH_4/O_2/He= 23/2/5 ml/min	7200 h^{-1}	A combined experimental & theoretical approach to the study of CH_4 activation over oxide catalyst has been done. A comparison of the catalytic activity for both catalysts on their preparation method (dopping & ppt[d]) has been studied. β Ga_2O_3 doped with Mg & Zn showed broading similar activity. Ppt[d] Zn & Mg catalyst showed lower activity	C.A. Cooper et. al. (2001)	98
Ni/γ-Al_2O_3	600 – 800	CH_4/O_2=2	Total flow 300 – 1200 ml/min Catalyst 5 gm	POM has been investigated in a fluidized-bed reactor. Low rate of carbon deposition observed. Effect of temp & feed rate has been studied. With increasing temp there was an increase of activity but flow rate had little effect on the performance.	Y. Ji. et. al. (2001)	99
Spc-Ni/Mg-Al, spc-Ni/Ca-Al, spc-Ni/Sr-Al, imp-Ni/CaO, imp-Ni/Al_2O_3	773 – 1073K	$O_2/CH_4/N_2$= 20/40/80 (v/v)	42000 – 168,000 ml/h/g	The activities of the catalyst prepared by spc method were studied in relation to the structure of the catalysts & compared with those prepared by impregnation method. Spc Ni/Ca-Al showed good activity with highest sustainability against coke formation.	H. Morioka et. al (2001)	100

Table 1.4 continued

Catalyst	Reaction condition			Remarks, if any	Author (s) Year	Ref
	Temp (^oC)	Feed CH_4:O_2:dil	W/F, GHSV or contact time			
Ni/CeO_2 [CeO_2, Ce (4% La)O_x, 5% Ni-Ce(La)O_x, 20% Ni-Ce(La)O_x	600 – 700	CH_4/O_2 = 2/1	Contact time 0.06 – 0.54 g s/cm^3	POM was studied over catalyst with Ni content 5 – 20 wt%. Au catalyst showed similar activity ≥ 550^{o}C. Contact time effect were absent over 5% Ni-Ce (La)O_x catalyst. This catalyst showed excellent resistance carbon deposition.	T. Zhu et. al. (2001)	101
CoO/ MgO, CaO, SrO or BaO	850	CH_4/O_2 = 2/1	720,000 ml/g/hr	POM was investigated over alkaline earth metal oxide supported Co catalysts. MgO proved to be suitable support. Reaction behavior significantly influenced by calcinations temp & Co loading.	H.Y.Wang et. al. (2001)	102
Ni added Strontium Phosphate	673K, 1023K, 1073K	CH_4/O_2=2	Total flow 100 cm^3(NTP)/min Catalyst 0.1 g	It was found that Ni-added Strontium phosphate exhibited high activity and selectivity in the reaction. From XRD it has been observed that the catalytically active species is metallic Nickel. This metallic Ni considered to come from Ni-substituted or phosphate under reducing environment giving highly disperse Ni metal particle.	S.J. Lee et.al. (2002)	103
Spc-Ni/$SrTiO_3$, $CaTiO_3$, $BaTiO_3$	1073K to 773K	$CH_4/O_2/N_2$ = 10/5/20 ml/min	10/5/20	Structure of catalyst, effect of space velocity & effect of temp were investigated. The order of crystal growth as spc-$Ni_{0.2}/CaTiO_3$ > spc-$Ni_{0.2}/BatiO_3$ > spc-$Ni_{0.2}/SrTiO_3$. According to TEM result Ni dispersion in the order of spc-Ni/$SrTiO_3$> spc-Ni/$BaTiO_3$> spc-Ni/$CaTiO_3$. Activity result coincided well with Ni-dispersion order.	K. Takehira et. al. (2002)	104
Ni/θ-Al_2O_3	923 – 1073K	CH_4/O_2 = 2	-	Pulse reaction has been studied over both fresh & partially reduces catalyst of CH_4 activation. Fresh catalyst showed high activity.	Z.W.Li et. al. (2002)	105
Ni modified hexaaluminate $BaNi_yAl_{12-y}O_{19-\delta}$	500 - 950	CH_4/O_2=2	F/W= 1.2 × 10^4 ml/g/hr	A series of Ni-modified hexaaluminates (Y = 0.3, 0.6, 0.9, 1.0) were prepared and catalytic properties were investigated by using XRD, XPS, TPR & TG. Reduce Ni-hexaaluminates exhibited excellent activity & stability. No loss of Ni observed & carbon deposition negligible.	W. Chu et. al. (2002)	106

Table 1.4 continued

Catalyst	Reaction condition			Remarks, if any	Author (s) Year	Ref
	Temp (^oC)	Feed CH_4:O_2:dil	W/F, GHSV or contact time			
LiLaNiO/γAl_2O_3	-	-	-	The POM was investigated in a tubular $Ba_{0.5}Sr_{0.5}Co_{0.8}Fe_{0.2}O_{3-\delta}$ membrane reactor as a function of temp, airflow rate in the shell side and methane concentration in the tube side. Mechanism of POM in membrane reactor was discussed.	H. Wang et. al. (2003)	107

Table 1.5 Summary of Earlier Work on the Oxidative Conversion of Methane to Syngas over Noble Metals

Catalyst	Reaction condition			Remarks, if any	Author (s) Year	Ref
	Temp (^oC)	Feed CH_4:O_2:dil	W/F, GHSV or contact time			
Pt & Pt-Rh coated monoliths	1100	19-23 % CH_4 in air	$1 \times 10^{-4} - 10^{-2}$	-	Hickman et al. (1992)	78 (b)
10 wt% Pt or Rh/Al_2O_3	850 - 1250	1.8	1.0×10^6 h^{-1}	Rhodium catalyst has been reported to be superior to Pt. This has been explained by the known chemistry & kinetics of reactants, intermediates, & products on these surfaces.	Hickman et al. (1993)	78 (a)
Noble metal addition to Ni/Al_2O_3	800	CH_4/O_2 = 2.0	5.6 ($\pm$ 0.2) $\times 10^5$	The beneficial effects (viz. drastic decrease in reaction start temperature, increase in catalytic activity and CO selectivity) of noble metal addition to Ni/Al_2O_3 catalyst for oxidative methane-to-syngas conversion have been investigated.	Choudhary et al. (1995)	89
Pt & Rh/alumina foam monoliths	327 - 1227	-	-	An elementary-step model (19 steps) has been developed using rate parameters from the literature. The consistency of the model and the experimental results strongly suggest that H_2 & CO are primary products of POM to syngas via a Pyrolysis mechanism and at high temperatures.	Hickman & Schmidt (1993)	108
4.0 wt% Pt/Al_2O_3	900 - 1100	1.8	1.0×10^6 h^{-1}	The metal films on the ceramic monoliths are preferred to metal gauzes, which become too brittle in excess of hydrocarbon. The variation is selectivity and conversion on different metals is key in designing useful reactor systems.	Schmidt et al. (1994)	109
0.5 wt% Pt/Al_2O_3	800	2.0:1.0:0.0	4.0×10^3 h^{-1}	The authors have suggested that fluidized beds offer viable energy-efficient alternative reactor configurations for syngas production by the catalytic oxidation of methane to syngas.	Schmidt et. al. (1994)	110
Pt/10 wt% Rh gauze catalyst	200 – 1050	2.0:1.0:10.0	1.5 to 5.0 $\times 10^{-4}$ sec	The products with compositions far from equilibrium were obtained.	Hofstad et. al. (1997)	111
Ru supported on SiO_2, γ-Al_2O_3, YSZ or TiO_2	550 – 750	-	-	Isotopic labeling expts. Demonstrated that direct partial oxidation route is responsible for the high CO & H_2 selectivity at low CH_4 conversion observed over the Ru/TiO_2 catalysts.	Boucouvalas et. al. (1997)	112

Table 1.5 continued

Catalyst	Reaction condition			Remarks, if any	Author (s) Year	Ref
	Temp (^oC)	Feed CH_4:O_2:dil	W/F, GHSV or contact time			
Pt (1.0 wt%) & Pd (1.0 wt%) containing alkaline earth & rare earth oxide catalysts.	700 & 800	-	$5.6 (\pm 0.2) \times 10^5$	Pt containing alkaline earth & rare earth oxide catalysts showed higher activity than Pd – containing catalysts. The alkaline earth & rare earth oxides are basic in nature & therefore act not only as support for dispersing the noble metals but also play significant role in deciding the activity & selectivity of the Pt- & Pd containing catalysts.	Choudhary et al. (1998)	113
1.0 wt% Pt/CeO_2 & CeO_2	400 – 800	-	-	Authors suggested that the synthesis gas was directly formed from CH_4.	Otsuka et. al. (1997)	114
CeO_2 or Pt black/CeO_2	-	-	-	The addition of Pt black accelerated the formation rates of H_2 & CO & decreased the activation energy for their production.	Otsuka et. al. (1998)	115
5.0 wt% It/TiO_2	600		5.0 s	The active species of Ir/TiO_2 was found to be Ir^o by XPS.	Nakagawa et. al. (1998)	116
Rh sponge diluted with SiC or Al_2O_3 & 0.3 wt% Rh/Al_2O_3	400 – 850	-	-	The reaction has been studied using the temporal-analysis-of products setup on different Rh catalysts.	Hofstad et. al. (1998)	117
Ru, Pd, Pt, Ni, Rh supported on γ-Al_2O_3, Pt, Rh/MgO, or ZrO_2 & Rh powder.	-	-	-	The study reveals that in POM to synthesis gas, CO_2 is primary product.	Baerns et. al. (1998)	118
Ru/TiO_2	973 – 1073K	$CH_4/O_2/N_2$= 6/3/91 (v/v)	Total flow 400 – 1000 cm^3/min(STP) Catalyst 10 – 30 mg	The effect of modification of the support on the Ox.State of Ru & the catalytic performance of the catalyst has been studied. Using XPS & FTIR tech. Ox. State of Ru depends on reaction temp & supporting material. Doping of W^{6+} favored oxygen adsorption on Ru, resulting lower activity. In contrast Ca^{2+} doped TiO_2 exists mainly metallic form & promotes activity.	C. Elmasides et. al. (2001)	119

Table 1.5 continued

Catalyst	Reaction condition			Remarks, if any	Author (s) Year	Ref
	Temp (^oC)	Feed CH_4:O_2:dil	W/F, GHSV or contact time			
Pt/CeO_2 & Pt/Al_2O_3	400, 500, 600	CH_4/O_2=1.7 to 2.3	Total flow 110 – 120 ml/min	POM & redox properties have been investigated. At low temp Pt/CeO_2 gave higher conversion & selectivity, due to redox reaction near the interface of Pt/CeO_2. At higher temp promotion effect became less important & both catalyst showed activity.	P. Pantu et al. (2001)	120
Rh-coated spheres	-	-	4×10^5 , 1.8×10^6 h^{-1}	The effect of GHSV using different support geometries has been studied. Catalyst showed superior activity than Rh-coated monoliths. Activity decreases with increasing space velocity for Rh-coated monolith. But Rh-coated sphere showed stable activity even at high GHSV. Sphere size effect also studied.	K.L. Hohn et.al. (2001)	121
Rh, Ru/SiO_2	-	CH_4/O_2Ar = /1/45	-	The concentration of oxygen species over SiO_2 supported different noble metal catalysts & its relationship with the mechanism has been studied. Direct oxidation to syngas is dominated by Rh/SiO_2 catalyst while combustion-reforming mechanism is feasible over Ru/SiO_2 catalyst.	Wei Zheng Wang et. al. (2001)	122
Pt/CeO_2	500 – 900	$CH_4/O_2/N_2$= 2/1/3.8	80000 h^{-1}	Fuel cell developers are investigating the generating of H_2 from light HC. Effect of Pt loading (0.5 – 2%), effect of temp, GHSV (40000 – 120000 h^{-1}) has been investigated. 2% Pt containing catalyst showed no carbon deposition.	L. Pino et. al. (2002)	123
Ni, Rh and Rh/Ni containing catalyst	750 and 500	CH_4/O_2/He= 2/1/4	Residence time 12 ms	Rh-Ni synergy in the catalytic POM & also surface phenomena and catalyst stability studied. The presence of Rh % Ni in the same catalyst allows an increase of CPO activity in O_2 reach conditions.	F.Basile et. al. (2002)	124
$Pt/\gamma\text{-}Al_2O_3$	500 or 700	CH_4/O_2/He= 2/1/20	-	The deactivation of a Pt/Al_2O_3 catalyst used in an industrial plant for the POM to syngas was investigated. Promoted modifications to the catalyst, inducing sintering phenomena and, therefore, deactivation effects.	S. Albertazzi et. al. (2003)	125

Table 1.5 continued

Catalyst	Reaction condition			Remarks, if any	Author (s) Year	Ref
	Temp (^oC)	Feed CH_4:O_2:dil	W/F, GHSV or contact time			
Ru nanoparticles	350 – 650	CH_4/O_2=1.8	60,000 h^{-1}	POM over Ru nanoparticles supported on Al_2O_3 studied. Evaluation of chemical state & morphology has been done with TEM, H_2 chemisorption, XRD, TPR,TPO. Result showed that mechanism of POM related to the morphology & chemical state of the supported Ru nanoparticles.	I Balint et. al. (2003)	126
Rh catalyst (Rh/Al/Mg 5/24/71)	750	CH_4/O_2/He= 2/1/4, 2/1/20 & 2/1/2 v/v	Residence time 24 ms to 7.2 ms and from 9 to 1 ms	Preparation & characterization of a stable Rh catalyst has been studied. Catalyst obtained via a hydrotalcite type precursor. Structure of material & Rh position were thoroughly studied at each step of preparation. Dispersion of Rh before & after the reaction evaluated by HRTEM study.	F. Basile et. al. (2003)	127
Pt/Ce-ZrO_2	673K & 1073K	CH_4/O_2=2/1	520 h^{-1}	The mechanism of POM was studied on Pt/Al_2O_3, Pt/ZrO_2 & Pt/Ce-ZrO_2 catalysts. The reducibility & O_2 transfer capacity evaluated by TPR and OSC tech. Effect of support also investigated. Pt/Ce-ZrO_2 showed higher activity and stability.	L.V.Mattos et.al. (2003)	128

In the last several years, few studies on the simultaneous CO_2 and steam reforming of methane to syngas have been carried out. The brief account of the work reported in the literature is given below.

Solymosi and coworker [129] studied the CO_2 reforming, steam and simultaneous steam and CO_2 reforming of methane at 427 – 500 ^oC and at 850 ^oC on supported Ir catalysts in a fixed- bed continuous-flow reactor. In addition, the dissociation of CO_2, the low temperature interaction of CO_2 with methane and the effects of supports has been also examined. The dissociation of CO_2, detected by IR spectroscopy, is greatly promoted by the presence of methane. The reaction between CO_2 and methane occurred rapidly above 400 ^oC to give CO and H_2 with ratio 1.0 – 3.7. The highest specific activity was measured for Ir/TiO_2. In the presence of water, H_2 was dominant reaction products due to the water gas shift reaction. Using a stoichiometric gas mixture, carbon deposition was very limited in all the three reactions. Kinetic parameters of the reaction were detected and a possible reaction mechanism has been proposed.

Choudhary and coworker [26] investigated steam reforming, CO_2 reforming and simultaneous steam and CO_2 reforming of methane to CO and H_2 over NiO-CaO catalyst (without any prereduction treatment) at different temperatures (700–850 ^oC) and space velocities (5000 – 70,000 $cm^3g^{-1}h^{-1}$). The catalyst showed high activity / selectivity in both the steam and CO_2 reforming reactions and the simultaneous steam and CO_2 reforming. In the CO_2 reforming, the coke deposition on the catalyst is found to be very fast. However, when the CO_2 reforming is carried out simultaneous with the steam reforming, the coke deposition on the catalyst is drastically reduced. By the simultaneous CO_2 and steam reforming (at $\geq$ 800 ^oC and space velocity of about 20,000 – 30,000 $cm^3g^{-1}h^{-1}$), methane can be converted almost completely to syngas with 100% selectivity for both CO and H_2.

In 1998, Choudhary et al. [28] investigated the steam reforming, CO_2 reforming and simultaneous steam and CO_2 reforming reactions of methane for its conversion into syngas over NiO/MgO/SA-5205 at different process conditions. It showed high activity and selectivity in the methane-to-syngas conversion reactions at low contact times. The H_2/CO product ratio in the simultaneous methane conversion reactions showed a strong dependence on the feed composition; such dependence is increase by increasing the concentration of steam relative to that of CO_2 in the feed.

Recently, Choudhary and coworkers [130] investigated the conversion of methane to CO and H_2 by CO_2 reforming, steam reforming and by both the reactions occurring simultaneously over Co_xNiO_{1-x} (X = 0.0 – 0.5) supported on commercial macro porous silica-alumina catalyst carrier (SA5205, obtained from M/S Norton Co. USA) precoated with MgO at different temperatures (700 – 900 ^oC) and contact times (0.025 – 0.29 s at STP). With the increasing Co/Ni ratio of the catalyst, its surface area has decreased and its degree of reduction in TPR (by H_2) from 100 to 900 ^oC has increased. The influence of Co/Ni ratio of the catalyst and feed ratios (H_2O/CH_4 = 0.4 – 4.0 and CO_2/CH_4 = 0.3 – 1.2) on the conversion and selectivity or H_2/CO product ratio has also been thoroughly investigated. With the increase of the Co/Ni ratio, the methane conversion and CO selectivity in the steam reforming has been decreased, the carbon deposition on the catalyst during the CO_2 reforming has been reduced drastically and the conversion of methane and CO, H_2 selectivity and H_2/CO ratio in the CO_2 reforming is passed through a maximum and also the conversion, particularly of methane, in the simultaneous steam and CO_2 reforming is passed through a maximum, at the CO/Ni ratio of about 0.17. The supported catalyst with Co/Ni ratio of 0.17 showed high methane conversion activity (CH_4 conversion > 95%) and 100% selectivity for both CO and H_2 with H_2/CO ratio varying from 1.2 – 2.2 in the simultaneous steam and CO_2 reforming processes at high space velocity (24,740 $cm^3g^{-1}h^{-1}$). The H_2/CO ratio can be controlled by manipulating the H_2O/CO_2 ratio in the feed, it has increased with increasing the H_2O/CO_2 ratio and vice-versa.

1.1.5. Oxy – Steam and / or CO_2 Reforming of Methane to Syngas

The conversion of methane to value added products via its conversion to syngas is highly promising one, provided the syngas from methane is produced economically. Presently, syngas is produced by the steam reforming of methane or higher hydrocarbons. Because of its several limitations / drawbacks (high energy requirement, high H_2/CO ratio, low selectivity / yield for CO, high capital cost and low space-time-yield), the steam reforming process is uneconomical for its use in the methane conversion. Catalytic partial oxidation of methane to syngas has been extensively investigated (Table 1.4 & 1.5). This process is mildly exothermic one and provides syngas with desirable H_2/CO ratio (about 2), required for the methanol and F.T. syntheses. However, it is highly hazardous in nature because of the simultaneously occurring highly exothermic combustion of methane to CO_2 and water. Although, this limitation could be partially overcome by carrying out the partial oxidation of methane

simultaneously with the steam and / or CO_2 reforming of methane, and thereby coupling the exothermic oxidative conversion and endothermic CO_2 and / or steam reforming reactions. The following important reactions occur during the oxy – steam reforming of methane – to – syngas conversion reaction.

Main reaction

$CH_4 + 0.5\ O_2 \rightarrow CO + 2\ H_2 \quad + 8.5\ kcal.mol^{-1}$

$CH_4 + H_2O \rightarrow CO + 3\ H_2O \quad - 54.2\ kcal.mol^{-1}$

Side reaction

$CO + H_2O \rightarrow CO_2 + H_2 \quad + 8.0\ kcal.mol^{-1}$

The work on the oxy – steam reforming of methane to syngas over different catalysts is summarized in Table 1.6.

Following important reactions take place during the Oxy – CO_2 reforming of methane to syngas conversion process.

Main reaction

$CH_4 + 0.5\ O_2 \rightarrow CO + 2\ H_2 \quad + 8.5\ kcal.mol^{-1}$

$CH_4 + CO_2 \rightarrow 2\ CO + 2\ H_2 \quad + 62.2\ kcal.mol^{-1}$

Side reaction

$CO_2 + H_2 \rightarrow CO + H_2O \quad - 8.0\ kcal.mol^{-1}$

The summary of the work done on the oxy – CO_2 reforming of methane to syngas at 1 atmospheric pressure is presented in Table 1.7.

1.2. Non Oxidative Activation of Methane – Literature Survey

Over the past several years, considerable time and effort have been invested in the study of methane activation [78,138 – 153]. The main goal of these efforts has been to develop effective process for the efficient and environmentally benign utilization of natural gas. Activation of methane represents an intensely challenging problem. A plethora of investigations has addressed the issue of methane conversion over the past three decades and a number of excellent reviews can be found in the literature [154 – 161]. Conversion of methane to hydrocarbons can be effected via an indirect or a direct route as observed. The indirect route involves the production of hydrocarbons via intermediates formed from the reaction of methane

Table 1.6 Summary of Earlier Work on the Oxy- Steam Reforming of Methane to Syngas

Catalyst	Reaction condition			Remarks, if any	Author (s) Year	Ref
	Temp (^oC)	Feed Composition	W/F, GHSV or contact time			
NiO.CoO.MgO	700 & 800	CH_4/O_2 = 1.8 – 3.8 & CH_4/H_2O = 1.5	9500 $cm^3g^{-1}h^{-1}$	The study revealed that conversion of methane, CO selectivity and H_2/CO ratio are decreased but that of water & the value of ΔH_r are increased markedly.	Choudhary et. al. (1998)	27
NiO/MgO/SA5205	800 & 850	CH_4/O_2 = 2.4 CH_4/H_2O = 1.9 – 10.4	4.7×10^4 $cm^3g^{-1}h^{-1}$	The results reveal that the oxidative conversion of methane to syngas reaction occurs simultaneously with steam reforming and WGS reactions.	Choudhary et. al. (1998)	28
Co_xNi_{1-x}/MgO/SA 5205 (Co/Ni = 0.17)	800 & 850	$CH_4/(O_2 + 0.5 H_2O)$ = 1.8	4.7×10^4 $cm^3g^{-1}h^{-1}$	The effect of reaction temperature, space velocity and CH_4/O_2 feed ratio on the conversion, selectivity and H_2/CO ratio and the net heat of reaction in the process has been studied.	Choudhary et. al. (2001)	30
Ni/Ce-ZrO_2	-	-	-	The effect of Ni content on the catalyst has been investigated in the oxy-reforming, steam reforming &oxy-steam reforming of methane. 15% Ni loading exhibited excellent activity and stability.	W.-S. Dong et. al. (2001)	74
NiO/MgO solid solution	700 & 800	CH_4/O_2 = 1.8 – 3.8 & CH_4/H_2O = 1.44	4.9×10^4 $cm^3g^{-1}h^{-1}$	The effect of CH_4/O_2 ratio in the feed on the conversion, selectivity and H_2/CO ratio and the net heat of reaction in the process has been studied.	Choudhary et. al. (2000)	131
NiO-CaO (Ni/Ca = 3.0)	700 - 850	CH_4/O_2 = 1.8 – 6.0 & CH_4/H_2O = 1.6 – 10.0	16×10^3 – 1090×10^3 h^{-1}	By coupling of the exothermic oxidative conversion and the endothermic steam reforming of methane over the same catalyst, almost all the limitations of these two individual processes are eliminated.	Choudhary et. al. (1994)	132
Ni/Ce-ZrO_2	750	CH_4/O_2 = 0.0 – 0.5 CH_4/H_2O = 1	-	Catalyst exhibited high catalytic activity in steam reforming as well as oxy-steam reforming of CH_4. The high catalytic stability may be due to synergistic effect of Ce.	H.-S. Roh et. al. (2001)	133

Table 1.7. Summary of Earlier Work on the Oxy- CO_2 Reforming of Methane to Syngas

Catalyst	Reaction condition			Remarks, if any	Author (s) Year	Ref
	Temp (^oC)	Feed Composition	W/F, GHSV or contact time			
NiO.CoO.MgO	800	CH_4/O_2 = 2.5 CH_4/CO_2 = 3.4	4.5×10^4 $cm^3g^{-1}h^{-1}$	The Oxy-CO_2 reforming reaction over this catalyst, the exothermic & endothermic reactions are coupled making this reaction highly energy efficient & non hazardous or safe to operate.	Choudhary et. al.(1998)	27
NiO/MgO/SA5205	750 - 850	CH_4/O_2 = 2.0 – 3.0 CH_4/CO_2 = 2.6 – 9.4	4.58×10^4 $cm^3g^{-1}h^{-1}$	The H_2 selectivity is lower than 100% because of the reverse shift reaction occurring simultaneously with the oxidative conversion & CO_2 reforming of methane to syngas.	Choudhary et. al. (1998)	28
Ni/ALPO-5	750 - 900	CH_4/O_2 = 2.1, CH_4/CO_2 = 10.0	4.7×10^5 $cm^3g^{-1}h^{-1}$	The NiO/ALPO-5 catalyst under operating conditions is in the form of $NiO/AlPO_4$ (tridymite). The former is transformed into the later during the short initial reaction period at high temperature.	Choudhary et. al. (1997)	43
1.0 wt% Ir/Al_2O_3	777	$CH_4:O_2:CO_2$ = 4.0:1.0:9.0	2.0×10^4 h^{-1}	The study revealed that the POM & endothermic CO_2 reforming reaction can be carried out simultaneously thus introducing the possibility of tuning the thermodynamics of the process.	Ascroft et. al. (1991)	134
NiO-CaO (Ni/Ca = 3.0)	700 - 900	CH_4/O_2 = 2.1 CH_4/CO_2 = 8.0	$10.0 – 50.0 \times 10^3$ $cm^3g^{-1}h^{-1}$	The coupling of endothermic & exothermic reactions of methane with CO_2 & O_2, respectively, over NiO-CaO catalyst results in its high conversion, selectivity & high productivity without catalytic deactivation for a long period in an energy efficient & safe manner.	Choudhary et. al. (1995)	135
$Pt/CoAl_2O_4/Al_2O_3$	1023K	$CH_4:CO_2:O_2$ = 1.0:0.4:0.3	24,000 h^{-1}	$Pt/CoAl_2O_4/Al_2O_3$, $Pt/CoO_x/Al_2O_3$, $CoAl_2O_4/Al_2O_3$ & CoO_x/Al_2O_3 catalysts were studied for Oxy-CO_2 reforming. $Pt/CoAl_2O_4/Al_2O_3$ catalyst showed higher activity. XRD results indicate that Pt species were well dispersed.	L. Mo et. al. (2003)	136
Co/MgO, Co/CaO, Co/SiO_2	-	CH_4/CO_2O_2 = 4/2/1	105,000 $mlg^{-1}h^{-1}$	Co/MgO catalyst showed highest activity & stability. The effect of reaction temperature, space velocity (420000, 210000, 105000, 52500 $cm^3.g^{-1}.h^{-1}$) and O_2/CO_2 ratio (0, 0.5, 1.0, 4.0, ∞) in the feed gases also investigated over Co/MgO catalyst.	Ruckenstein et. al. (2001)	137
Pt/Al_2O_3, Pt/ZrO_2 & $Pt/10\%ZrO_2/Al_2O_3$	450 - 900	-	600,000 $cm^3g^{-1}h^{-1}$	$Pt/10\%ZrO_2/Al_2O_3$ catalyst was found to be most active and stable for combined Oxy-CO_2 reforming. The addition of O_2 to feed increased CH_4 conversion.	M.M.V.M. Souza et. al. (2003)	138

with steam, oxygen, HCl etc. [154] whereas the direct route involves coupling of methane in the presence of oxygen (oxidative coupling of methane) or non-oxidative coupling (high temperature coupling and low temperature two step methane homologation) (Fig. 1.1). Hydrocarbon production via synthesis gas (produced by the steam reforming process) is uneconomical.

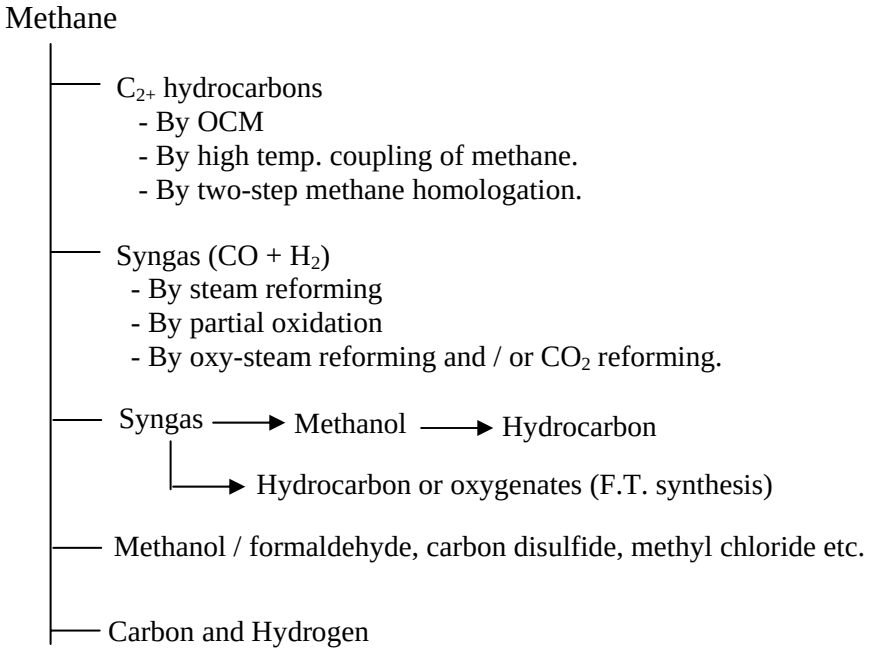

Figure 1.1: Different routes for methane conversion

In the last few years, few studies on the nonoxidative activation of methane to higher hydrocarbon have been carried out. The brief account of the work reported in the literature is given below.

Wang et al. [162] pioneered the nonoxidative dehydrogenative methane aromatization reaction on ZSM-5 based catalysts. HZSM-5 catalysts showed a 1.4 % conversion of methane with 100% selectivity to benzene at 973 K. The conversion of methane was greatly enhanced (without any detrimental effect of benzene selectivity) by loading the zeolite with Mo or Zn cations. Mo / HZSM-5 exhibited the best activity: 7.2 % and 4.4 % for the SiO_2/Al_2O_3 ratios of 50 and 25, respectively. The catalyst was found to be stable without any loss in activity and selectivity under the reaction conditions employed for the study.

Solymosi and coworker investigated various aspects related to the methane aromatization process [163 – 168]. Studies pertaining to MoO_3 on various support oxides [169]

showed s common tend: initial induction period (varied with the support) followed by a maximum in conversion was observed on MoO_3/SiO_2 (but was less than that on MoO_3/ZSM5 [170]) and the least on MoO_3/MgO.

Meriaudeau et al. carried out methane and ethylene aromatization over Mo/HZSM-5 and HZSM-5 [171]. Surprisingly, the results indicated that ethylene aromatization was more facile on Mo/HZSM-5 than on HZSM-5. This led the authors to express concern about ethylene being the key intermediates in methane aromatization. The authors suggested acetylene as being the intermediate in methane aromatization.

Zhang et al. [172] compared the effect of different molecular sieves support on the catalytic performance of Mo-based catalysts and found that the zeolite structure exerted a significant influence on the catalytic activity. Zeolites possessing two-dimensional pore diameters (such as ZSM-5, ZSM-8 and ZSM-11) in the vicinity of the dynamic diameters of a benzene molecule (0.6 nm) were suggested to be excellent supports for methane aromatization.

Addition of Fe and Co to the Mo/HZSM-5 catalyst resulted in a significant enhancement in the conversion of methane to benzene and naphthalene [173]. Similarly, introduction of Cu (by ion-exchange method) into Mo/HZSM-5 improved both the activity as well benzene selectivity for the methane dehydro-aromatization process [174]. In contrast, addition of phosphorous and lithium to Mo/HZSM-5 reduced the catalytic acidity and activity [170].

Choudhary et al. achieved high methane aromatization activity on H-galloaluminate ZSM-5 type zeolite by co-feeding methane with higher alkenes and alkanes [175]. A mechanism involving hydrogen transfer was invoked for describing the methane activation mechanism.

Y. Xu et al. [176] discussed the direct conversion of methane into hydrogen and valuable product under nonoxidative conditions over Mo/HZSM-5 catalyst in general, while the bifuntionality of Mo/HZSM-5 catalysts and the role of carbonaceous deposits formed were reviewed in more detailed.

O. A. Anuziata et al. [177] reported the catalytic conversion of methane into higher hydrocarbon using n-pentane as co-reactant over Zn/HZSM-11 zeolite. The aromatics yield was very high, achieving values of over 40 mol % at 500^oC and w/f = 30 $ghmol^{-1}$ with a C1/(C1 + C5) molar fraction (XC1) = 0.30. Contact time and time-on-stream effects on the products distribution were also analyzed in detail in order to obtain information about the evolution of

different species. They have reported 30 mol % methane conversions without CO_x reaction products.

T. Baba and coworkers [178,179] studied the catalytic conversion of methane to higher hydrocarbon over HZSM-5 loaded with silver cation. The effects of reaction parameters, such as reaction temperature, were examined. The maximum conversion of methane was 13.2 mol % at 673K. They have also investigated the reaction mechanism with ^{13}C labeling experiment.

Even from the environmental consideration, for avoiding the methane flaring the methane produced in the remote places needs to be converted into easily transportable energy sources like liquid hydrocarbon fuels at the methane production sites. Most important approach to transform methane into liquid hydrocarbons is to follow the well-established and already commercially proven route [181]: methane $\rightarrow$ syngas $\rightarrow$ methanol $\rightarrow$ gasoline, based on Mobil's MTG (methanol–to–gasoline) process [180 - 182]. In 1985, Mobil had successfully operated a commercial plant in New Zealand for the methane-to-gasoline conversion. However, the commercial unit could not be operated economically due to unfavorable process economics [182,183]. The cost of syngas production step (by steam reforming) is about twice the cost of methanol–to–gasoline production step [181]. The methane–to–gasoline process would get back its life and could be practiced economically provided an appreciable part of the methane is converted to gasoline without a need for its conversion to syngas and consequently to methanol. We have accomplished this very difficult goal by activating methane non–oxidatively and converting it simultaneously with methanol to gasoline range hydrocarbons. We have shown here that the methane converted can be comparable to or even more than the methanol converted in this novel process, depending upon the process conditions.

1.3. Non – Catalytic Pyrolysis of Ethane to Ethylene in the Presence of CO_2 with or without O_2

Ethylene, which is the keystone of petrochemical industry, is produced from ethane, an ethane-propane mixture or naphtha by thermal (non catalytic) cracking in the presence of steam [184]. However the thermal cracking process is highly endothermic and hence consumes a lot of external energy and produces a large amount of coke. The extensive coke deposits on the inner walls of the tubular cracking reactor cause serious problems such as reduced heat transfer

from the reactor walls. This in turn requires a higher wall temperatures (up to 1100 ^{o}C), which increases the energy demands and reduces the life of the reactor tubes. The reactor must therefore be shut down so the coke can be removed. In order to overcome these problems, studies have been made throughout the world by many workers in the area of heterogeneous catalytic oxidative dehydrogenation of ethane to ethylene [185 - 194]. Choudhary et al. have suggested earlier to carry out ethane and propane thermal cracking reactions in the presence of limited oxygen [195 - 197]. By carrying out the thermal cracking of ethane, propane or $C_2 - C_4$ hydrocarbons from natural gas in the presence of steam and limited oxygen, not only the energy requirement is drastically reduced but also the coke formation is eliminated or drastically reduced and also the hydrocarbon conversion much above 70 % could be obtained. Also in the presence of oxygen, the thermal cracking of ethane/propane is enhanced because of the change in the hydrocarbon activation mechanism and hence the oxy cracking process could be carried out at a much lower temperature and/or contact time than that required for achieving the same conversion in the thermal cracking process.

Carbon dioxide (a green house gas) can also act as a mild oxidant. Utilization of carbon dioxide in catalytic methane partial oxidation reactions, such as catalytic CO_2 reforming of methane [198] and oxidative coupling of methane [199], and also in the catalytic oxidative dehydrogenation of ethane [200,201 – 206] or propane [207] has been reported earlier. It is also interesting to use CO_2, as an oxidant, instead of oxygen or even in the presence of limited oxygen in the non-catalytic (thermal) hydrocarbon cracking processes for the production of ethylene and other olefins. The present investigation was undertaken for this purpose.

1.4. Objective and Scope of the Present Work

The work for the present Ph.D. thesis was undertaken as a part of the comprehensive research program in our laboratory for the development of highly active, selective and productive catalysts and the underlying processes for the conversion of methane / lower alkanes, with the following objectives:

1) To evaluate the performance of the following catalysts and develop high temperature (upto 1500 ^{o}C) stable supported non-noble metal catalysts for the partial oxidation of methane to syngas with or without simultaneously occurring steam and/ or CO_2 reforming reactions.

CoO-NiO (Co/Ni=0.2)/SZ-5564

CoO-NiO (Co/Ni=0.2)-MgO (7 wt %)/SZ-5564

CoO-NiO (Co/Ni=0.2)-MgO (7 wt %)-CeO_2 (Ce/Mg= 0.1 & 1.0)/SZ-5564

CoO-NiO (Co/Ni=0.2)/MgO (7 wt %)/SZ-5564

CoO-NiO (Co/Ni=0.2)/ZrO_2 (7 wt %)/SZ-5564

CoO-NiO (Co/Ni=0.2)-ZrO_2 (7 wt %)-CeO_2 (Ce/Zr=0.1 & 1.0)/SZ-5564

2. To study unsupported and supported non-noble metal containing following catalysts having high activity with little or no coke formation in the CO_2 reforming of methane in the presence or absence of steam and / or O_2.

   CoO-Nd_2O_3 (Co/Nd=0.1 to 4.0)

   CoO-MgO (Co/Mg=1.0)

   CoO (5 to 30 wt %)/MgO (5 wt %)/SA-52505

   CoO (20 wt %)/ZrO_2 (20 wt %)/SA-5205

   CoO (20 wt %)/CeO_2 (20 wt %)/SA5205

3. To study low temperature activation of methane in the presence of methanol or other oxygenates over bifuntional pentasil zeolite catalysts, such as

   H-GaAlMFI

   Mo (2 to 4 wt %)-Zn (4 to 0 wt %)/H-ZSM-5

4. To study pyrolysis of ethane to ethylene in the presence of CO_2 with or without O_2.

References

1. B. Elvers, S. Hawkins, M. Ravenscroft, J. F. Rouniavilla, and G. Schulz, Eds. (1989) in Ulmann's Encyclopaedia of Industrial Chemistry, Vol. A 12, 5th Revised Ed. (VCH, Weinheim) pp. 169.
2. (a) Encyclopedia of Chemical Technology, Vol. 12 (Eds.: RE Kirk, D. F. Othmer), 3rd ed., Willy Interscience, New York.
3. K. Weissermel, and H-J. Arpe, Handbook of industrial Chemistry, translated by C.R.lindley, 2nd revised extended edition, VCH, New Tork, (1993).
4. A. H. Pelofsky, In Partial Oxidation in Heavy Oil Gasification (Pelofsky, a. H., Ed.), Marcel Dekker, New York, (1997) pp. 48.
5. J. E. Frank, Coal Technology, In Riegel's Handbook of Industrial Chemistry 8th Edition (J. A. Kent, Ed.), Van Nostrand Reinhold Company, Cincinnati, (1983).
6. J. G. Speight, The Chemistry and Technology of Coal, Marcell Dekker, New York, (1983).
7. J. C. W. Kuo, Gassification and Indirect Liquidification in The Science and technology of Coal and Coal Utilization (B. R. Cooper, and W. A. Ellingson, Eds.) Plenum Publishing Corp., New York, (1984).
8. D. Dyrssen and D. R. Turner, in Carbon Dioxide Chemistry: Environmental Issues (J. Paul and C.-M. Pradier, eds.), Athenaeum Press, Cambridge, (1994) p. 317.
9. R. A. Houghton and G. M. Woodwell, Scientific Am., 206 (1989) 36.
10. D. Schneider, Scientific Am., 272 (1995) 13.
11. B. Hileman, Chem. Eng. News, 28 (April 14) (1997).
12. T. A. Chubb, Sol. Energy, 24 (1980) 341.
13. J. H. McCrary, G. E. McCrary, T. A. Chubb, J. J. Nemecek, and D. E. Simmons, Sol. Energy, 29 (1982) 141.
14. J. D. Fish and D. C. Hawn, J. Sol. Energy Eng., 109 (1987) 215.
15. J. H. Edwards, K. T. Do, A. H. Maitra, S. Schuck, and W. Stein, Sol. Eng., 1 (1995) 389.
16. J. R. H. Ross, A. N. J. Van Keulen, M. E. S. Hegarty, and K. Seshan, Catal. Today, 30 (1996) 193.
17. M. A. Vannice, Catal. Rev. – Sci. Eng., 14 (1976) 153.
18. A. M. Gadalla and B. Bower, Chem. Eng. Sci., 43 (1988) 3049

19. J. R. Rostrup-Nielsen, J.-H. Bak Hansen, and L. M. Aparicio, Sekiya Gak-Kaikhi 40 (1997) 366.
20. H. J. Töpfer, Gas Wasserfach, 117 (1976) 412.
21. S. Teuner, Hydrocarbon Process., 64 (1985) 106.
22. S. Teuner, Hydrocarbon Process., 66 (1987) 52.
23. N. R. Udengaard, J.- H. B. Hansen, D. C. Hanson, and J. A. Stal, Oil Gas J., 90 (1992) 62.
24. E. Ruckenstein, Y. H. Hu, Appl. Catal. A 133 (1995) 149.
25. E. Ruckenstein, Y. H. Hu, J. Catal., 161 (1996) 55.
26. V. R. Choudhary, A. M. Rajput, Ind. Eng. Chem. Res., 35 (1996) 3934.
27. V. R. Choudhary, A. S. Mamman, J. Chem. Technol. Biotech., 73 (1998) 345.
28. V. R. Choudhary, B. S. Uphade, A. S. Mamman, Appl Catal. A, 168 (1998) 33.
29. V. R. Choudhary, B. S. Uphade, A. S. Mamman, R. E. Babcock, ACS Symp. Ser., 809 (2002) 224.
30. V. R. Choudhary, A. S. Mamman, B. S. Uphade, Prepr.-Am. Chem. Soc. Div. Pet. Chem. 46 (2001).
31. Y. Chen, K. Tomishige, K. Yokoyama, K. Fujimoto, Appl. Catal. A 165 (1997) 335.
32. K. Tomishige, O. Yamazaki, Y. Chen, K. Yokoyama, X. Li, K. Fujimoto, Catal. Today, 45 (1998) 35.
33. K. Tomishige, Y. Himeno, Y. Matsuo, Y. Yoshinaga, K. Fujimoto, Ind. Eng. Chem. Res. 39 (2000) 1891.
34. O. Yamazaki, T. Nozaki, K. Omata, K. Fujimoto, Chem. Lett., (1992) 1953.
35. J. Z. Luo, L. Z. Gao, C. F. Ng, C. T. Au, Catal. Lett., 62 (1999) 153.
36. S. Wang, G. Q. Lu, J. Chem. Technol. Biotechnol., 75 (2000) 589.
37. L. Ji, S. Tang, H. C. Zeng, J. Lin and K. L. Tan, Appl. Catal. A 207 (2001) 247.
38. S.-H. Seok, S. H. Choi, E. D. Park, S. H. Han and J. S. Lee, J. Catal., 209 (2002) 6.
39. B. S. Liu, C. T. Au, Appl. Catal. A: 244 (2003) 181.
40. A. Effendi, K. Hellgardt, Z.-G. Zhang, T. Yoshida, Cat. Comm., 4 (2003) 203.
41. Z. Zhang., X. E. Verykios, S. M. Macdonald, S. Affrosman, J. Phys. Chem., 100 (1996) 744.
42. Z. Chang, Q. Wu, J. Li, Q. Zhu., Catal. Today, 30 (1996) 147.
43. V. R. Choudhary, B. S. Uphade, A. S. Mamman, Microporous and Mesoporous Materials, 23 (1998) 61.

44. K. Nakagawa, K. Ankai, N. Matasui, K. Ikenaga, T. Suzuki, Y. Teng, Y. Kobayashi, M. Haruta, Catal. Lett., 51 (1998) 163.
45. X. Li, J. S. Chang, E. K. Lee, S. E. Park, React. Kinet. Catal. Lett., 67 (1999) 383.
46. S. Tang, L. Ji, J. Lin, H. C. Zeng, K. L. Tan, K. Li, J. Catal., 194 (2000) 424.
47. S. T. Srinivas, C. Song, W. Pan, L. Sun, Div. Pet. Chem., 45 (2000) 348.
48. Z. Xu, L. Chang, J. Zhang, Chihua Xuebao, 22 (2001) 16.
49. C. E. Quincoces, V. S. P. De, M. G. Gonzalez, Stud. Surf. Sci. Catal., 130 D (2000) 3681.
50. K. Asami, X. Li, K. Fujimoto, Y. Koyama, A. Sakurama, N. Kometani, Y. Yonezawa, Catal. Today, 84 (2003) 27.
51. E. Kikuchi, Y. Chen, Stud. Surf. Sci. Catal., Natural Gas Conversion, 107 (1997) 547.
52. S. M. Stagg, D. E. Resasco, Stud. Surf. Sci. Catal. 119 (NGC V) (1998) 813.
53. J. R. H. Ross, A. N. J. Van Keulen, A. M. Oconnor, M. E. S. Hegarty, Div. Pet. Chem., 45 (2000) 157.
54. C. J. Huang, D. J. Wang, G. X. Qi, J. H. Fei, Z. Y. Hou, X. M. Zheng, Shiyou Huagong, 29 (2000) 323.
55. K. Nagaoka, K. Seshan, K. I. Aika, J. A. Lercher, J. Catal., 197 (2001) 34.
56. T. Suhartanto, P. E. A. York, A. Hanif, H. Al – Megren, L. H. M. Green, Catalysis Letters, 71 (2001) 49.
57. M. M. V. M. Souza, D. A. G. Aranda, M. Schmal, Ind. Eng. Chem. Res., 41 (2002) 4681.
58. U. L. Portugal, A. C. S. F. Santos, S. Damyanova, C. M. P. Marques, J. M. C. Bueno, J. Mol. Catal. A, 184 (2002) 311.
59. M. R. Golgwasser, M. E. Rivas, E. Pietri, M. J. Perez-Zurita, M. L. Cubeiro, L. Gingembre, L. Leclercq, G. Leclercq, Appl. Catal. A, 255 (2003) 45.
60. A. I. Tsyganok, M. Inaba, T. Tsmoda, S. Hamakawa, K. Suzuki, T. Hayakawa, Cat. Comm., 4 (2003) 493.
61. L. Paturzo, F. Gallucci, A. Basile, G. Vitulli, P. Pertici, Catal. Today, 82 (2003) 57.
62. S. M. Gheno, S. Damyanova, B. A. Riguetto, C. M. P. Marques, C. A. P. Leite, J. M. C. Bueno, J. Mol. Catal. A, 198 (2003) 263.
63. J. T. Richardson, M. Garrait, J. K. Hung, Appl. Catal. A, 255 (2003) 69.
64. C. N. Satterfield, Heterogeneous Catalysis in Industrial Practice McGraw-Hill, New York, (1991) 333.

65. J. R. Rostrup-Nielsen, Symposium on the Science of Catalysis and its Application in Industry, FPDIL, Sindri, February 22 – 24 (1979) Paper No. 39.
66. J. R. Rostrup-Nielsen, J. Catal., 33 (1974) 184.
67. T. Borowiecki, Appl. Catal., 10 (1984) 273.
68. T. Borowiecki, React. Kinet. Catal. Lett., 33 (1987) 429.
69. A. Parmaliana, F. Arena, S. Coluccia, L Marchese, G. Marta, A. L. Chuvilin, J. Catal., 141 (1993) 34.
70. T. E. Holt, A. D. Logan, S. Chakraborti, A. k. Datye, Appl. Catal. A, 34 (1987) 199.
71. S. Narayanan, G. J. Sreekanth, Chem. Soc., Faraday Trans. I, 85 (1989) 3785.
72. O. Yamazaki, K. Tomishige, K. Fujimoto, Appl. Catal. A, 136 (1996) 49.
73. V. R. Choudhary, A. S. Mamman, B. S. Uphade, AIChE Journal, 47 (2001) 1632.
74. W.-S. Dong, H.-S. Roh, K.-W. Jun, S.-E. Park, Y.-S. Oh, Appl. Catal. A, 226 (2002) 63.
75. F. Gallucci, L. Paturzo, A. Kama, A. Basile, Ind. Eng. Chem. Res., 43 (2004) 928.
76. E. Ramirez-Cabrera, N. Laosiripojana, A. Atkinson, D. Chadwick, Catalysis Today, 78 (2003) 433.
77. (a) S. S. Bhardwaj and L. D. Schmidt, Fuel Processing Technol., 42 (1995) 109; (b) M. A. Pena, J. P. Gomez and J. L. G. Fierro, Appl. Catal., 144 (1996) 7; (c) S. C. Tsang, J. B. Claridge and M. L. H. Green, Catalysis Today, 23 (1995) 3; (d) Y. H. Hu and E. Reckenstein, Catalysis Reviews, 44 (2002) 423.
78. (a) D. A. Hickman, L. D. Schmidt, Science, 259 (1993) 343; (b) D. A. Hickman, E. A. Haupfear and L. D. Schimdt, J. Catal., 138 (1992) 267.
79. V. R. Choudhary, A. M. Rajput and V. H. Rane, Catal. Lett., 16 (1992) 269.
80. V. R. Choudhary, A. S. Mamman, S. D. Sansare, Angew. Chem. Int. Ed. Engl., 31 (1992) 1189.
81. V. R. Choudhary, A. M. Rajput, V. H. rane, J. Phys. Chem., 96 (1992) 8686.
82. V. R. Choudhary, V. H. Rane, A. M. Rajput, Catal. Lett., 22 (1993) 289.
83. V. R. Choudhary and A. S. Mamman, J. Catal., 172 (1997) 172.
84. T. Utaka, S. Abdulaziz Al – Drces, J. Veda, Y. Iwasa, T. Takeguchi, R. Kikuchi, K. Eguchi, Appl. Catal. A, 247 (2003) 125.
85. V. R. Choudhary, S. D. Sansare, A. S. Mamman, Appl. Catal. A, 90 (1992) L1.
86. D. Dissanayake, M. P. Rosynek, J. H. Lunsford, J. Phys. Chem., 97 (1993) 3644.
87. J. N. Theron, J. C. Q. Feltcher, C. T. O. Cnnor, Catal. Today, 21 (1994) 489.

88. Y. Matsumura, S. M. Sugiyama, H. Hayashi, M. Sigemota, K. Saitoh, J. B. Moffat, J. Mol. Catal., 92 (1994) 81.
89. V. R. Choudahary, B. Prabhakar, A. M. Rajput, J. Catal., 157 (1995) 752.
90. A. Santos, J. Coronas, M. Menendez, J. Santamaria, Catal. Lett., 30 (1995) 189.
91. Y. H. Hu, E. Ruckenstein, J. Catal., 158 (1996) 260.
92. V. R. Choudhary, B. S. Uphade, A. Belhekar, J. Catal., 163 (1996) 312.
93. E. Ruckenstein, Y. H. Hu, Ind. Eng. Chem. Res., 37 (1998) 1744.
94. V. R. Choudhary, A. S. Mamman, Fuel Process Technol, 60 (1999) 203.
95. M. Fathi, F. Bjorgum, T. Viig, O. A. Rokstad, Catal. Today, 63 (2000) 489.
96. Y. Zhang, G. Xiong, S. Sheng, W. Yang, Catal. Today, 63 (2000) 517.
97. T. Shishido, M. Sukenobu, H. Morioka, M. Kondo, Y. Wang, K. Takaki, K. Takehira, Appl. Catal. A, 223 (2001) 35.
98. C. A. Cooper, C. R. Hammond, G. J. Hutchings, S. H. Taylor, D. J. Willock, K. Tabata, Catal. Today, 71 (2001) 3.
99. Y. Ji, W. Li, H. Xu, Y. Chen, Appl. Catal. A, 213 (2001) 25.
100. H. Morioka, Y. Shimizu, M. Sukenobu, K. Ito, E. Tanabe, T. Shishido, K. Takehira, Appl. Catal. A, 215 (2001) 11.
101. T. Zhu, M. Flytzani – Stephanopoulos, Appl. Catal. A, 208 (2001) 403.
102. H. Y. Wang, E. Ruckenstein, J. Catal., 199 (2001) 309.
103. S. J. Lee, J. H. Jun, S. H. Lee, K. J. Yoon, T. H. Lim, S. W. Nam, S. A. Hong, Appl. Catal. A, 230 (2002) 61.
104. K. Takehira, T. Shishido, M. Kondo, J. Catal., 207 (2002) 307.
105. Z. W. Liu, K. W. Jun, H. S. Roh, S. C. Baek, S. E. Park, J. Mol. Catal. A, 189 (2002) 283.
106. W. Chu, W. Yang, L. Lin, Appl. Catal. A, 235 (2002) 39.
107. H. Wang, Y. Cong, W. Yang, Catalysis Today, 82 (2003) 157.
108. D. A. Hickman and L. D. Schmidt, AIChE J., 39 (1993) 1164.
109. L. D. Schmidt, S. S. Bhardwaj, J. Catal., 146 (1994) 11.
110. L. D. Schmidt, M. Huff., Catal. Today, 21 (1994) 113.
111. K. H. Hofstad, T. Sperel, O. A. Roksad, A. Holmen, Catal. Lett., 47 (1997) 97.
112. J. Boucouvalas, A. M. Efstathiou, Z. L. Zhang, X. E. Verykios, Stud, Surf. Sci. Catal., 107 (Natural Gas Conversion IV) (1997) 435.
113. V. R. Choudhary, H. Prabhakar, A. M. Rajput and A. S. Mamman, Fuel, 77 (1998) 1477.

114. K. Otsuka, E. Sunada, T. Ushiyama, I. Yamanaka, Stud. Surf. Sci. Catal., 107 (Natural Gas Conversion IV) (1997) 531.
115. K. Otsuka, Y. Wang, E. Sunada, I. Yamanaka, J. Catal., 175 (1998) 152.
116. K. Nakagawa, N. Ikenaga, T. Suzuki, T. Kobayashi, M. Haruta, Appl. Catal. A, 169 (1998) 281.
117. H. K. Heitnes, J. H. B. J. Hoebink, A. Holmen, G. B. Marin, Catal. Today, 40 (1998) 157.
118. M. Baerns, O. V. Buyevaskaya, L. Mleczko, D. Wolf, Stud. Surf. Sci. Catal., 107 (Natural Gas Conversion IV) (1997) 421.
119. C. Elmasides, D. I. Kondarides, S. G. Neophytides, X. E. Verykios, J. Catal., 198 (2001) 195.
120. P. Pantu, G. R. Gavalas, Appl. Catal. A, 223 (2001) 253.
121. K. L. Hohn, L. D. Schmidt, Appl. Catal. A, 211 (2001) 53.
122. W. Z. Weng, Q. G. Yan, C. R. Luo, Y. Y. Liao, H. L. Wan, Catal. Lett., 74 (2001) 37.
123. L. Pino, V. Recupero, S. Beninati, A. K. Shukla, M. S. Hegde, P. Bera, Appl. Catal. A, 225 (2002) 63.
124. F. Basila, G. Fornasani, F. Trifiro, A. Vaccani, Catal. Today, 77 (2002) 215.
125. S. Albertazzi, P. Arpentinier, F. Basile, P. Del Gallo, G. Fornasari, D. Cray, A. Vaccani, Appl. Catal. A, 247 (2003) 1.
126. I. Balint, A. Miyazaki, K. I. Aika, J. Catal., 220 (2003) 74.
127. F. Basile, G. Fornasari, M. Gazzano, A. Kiennemann, A. Vaccani, J. Catal., 217 (2003) 245.
128. L. V. Mattos, E. R. DeOliveria, P. D. Resende, F. B. Noronna, F. B. Passos, Catal. Today, 77 (2002) 245.
129. A. Erdohelyi, K. Fodor, F. Solymosi, Stu. Surf. Sci. Catal., 107 (Natural Gas Conversion IV) (1997) 525.
130. V. R. Choudhary, A. S. Mamman, B. S. Uphade, R. E. Babcock, Am. Chem. Soc., Div. Pet. Chem., 45 (2000) 164.
131. V. R. Choudhary, A. S. Mamman, Appl. Energy, 66 (2000) 161.
132. V. R. Choudhary, A. M. Rajput, B. Prabhakar, In., Bhasin, M. M., Slocum, D. W., (Eds.), Methane & Alkane Chemistry, Pro. Am. Chem. Soc. Symp., 207th Annul Meeting, San Diego, CA March (1994) 13018, Plenum Publishing Corporation, New York (1995) P. 305.

133. H. S. Roh, K. W. Jun, W. S. Dong, S. E. Park, Y. S. Baek, Catal. Lett., 74 (2001) 31.
134. A. T. Ashcoft, A. K. Cheetham, M. L. H. Green, P. D. F. Vernon, Nature, 352 (1991) 225.
135. V. R. Choudhary, A. M. Rajput, B. Prabhakar, Catal. Lett., 32 (1995) 391.
136. L. Mo, J. Fei, C. Huang, X. Zheng, J. Mol. Catal. A, 193 (2003) 177.
137. E. Ruckenstein, H. Y. Wang, Catalysis Letters, 73 (2001) 99.
138. M. M. V. M. Souza, M. Schmal, Appl. Catal. A, 255 (2003) 83.
139. T. Ito, J. H. Lunsford, Nature, 314 (1985) 721.
140. A. T. Ashcroft, A. K. Cheetham, J. S. Foord, M. L. H. Green, C. P. Grey, A. J. Murrell, P. D. F. Vernon, Nature, 344 (1990) 319.
141. R. A. Periana, D. J. Taube, S. Gamble, H. Taube, T. Satoh, H. Fujii, Science, 280 (1998) 560.
142. F. Solymosi, G. Kutsan, A. Erdohelyi, Catal. Lett., 11 (1991) 149.
143. M. C. Wu, C. M. Truong, K. Coulter, D. W. Goodman, J. Catal., 140 (1993) 344.
144. R. A. Periana, D. J. Taube, E. R. Evitt, D. G. Loffler, P. R. Wentrcek, G. Voss, T. Masuda, Science, 259 (1993) 340.
145. V. R. Choudhary, A. M. Rajput, B. Prahakar, Catal. Lett., 15 (1992) 363.
146. M. G. Poirier, A. R. Sanger, K. J. Smith, Can. J. Chem. Eng., 69 (1991) 1027.
147. N. Yamagata, K. Tanaka, S. Sasaki, S. Okazaki, Chem. Lett., (1987) 81.
148. S. S. Bharadwaj, L. D. Schmidt, J. Catal., 146 (1994) 11.
149. S. Kasztelan, J. B. Moffat, J. Chem. Soc. – Chem. Commun., (1987) 1663.
150. M. Sigl, M. C. J. Bradford, H. Knozinger, M. A. Vannice, Top. Catal., 8 (1999) 211.
151. S. Rezgui, A. Liang, T. K. Cheung, B. C. Gates, Catal. Lett. 53 (1998) 1.
152. K. D. Campbell, H. Zhang, J. H. Lunsford, J. Phys. Chem., 92 (1998) 750.
153. P. Pereira, S. H. Lee, G. A. Somorjai, H. Heinemann, Catal. Lett., 6 (1990) 255.
154. J. R. Anderson, Appl. Catal., 47 (1989) 177.
155. J. H. Lunsford, Catal. Today, 63 (2000) 165.
156. G. Renesme, J. Saint-Just, Y. Muller, Catal. Today, 13 (1992) 371.
157. N. D. Parkyns, C. I. Warburton, J. D. Wilson, Catal. Today, 18 (1993) 385.
158. J. R. RostrupNielsen, Catal. Today, 21 (1994) 257.
159. R. H. Crabtree, Nat. Gas Conversion II, 81 (1994) 85.
160. L. Guczi, R. A. Vansanten, K. V. Sarma, Catal. Rev. – Sci. Eng., 38 (1996) 249.
161. H. D. Gesser, N. R. Hunter, Catal. Today, 42 (1998) 183.

162. L. S. Wang, L. X. Tao, M. S. Xie, G. F. Xu, J. S. Huang, Y. D. Xu, Catal. Lett. 21 (1993) 35.
163. F. Solymosi, A. Erdohelyi, A. Szoke, Catal. Lett., 32 (1995) 4353.
164. F. Solymosi, A. Szoke, J. Cserenyi, Catal. Lett., 39 (1996) 157.
165. A. Szoke, F. Solymosi, Appl. Catal. A, 142 (1996) 361.
166. F. Solymosi, J. Cserenyi, A. Szoke, J. Catal., 165 (1997) 150.
167. F. Solymosi, L. Bugyi, A. Oszko, I. Horvath, J. Catal., 185 (1999) 160.
168. F. Solymosi, L. Bugyi, A. Oszko, J. Catal. Lett., 57 (1999) 103.
169. M. C. Iliuta, I. Iliuta, B. P. A. Grandjean, F. Larachi, Ind. Eng. Chem. Res., 42 (2003) 3203.
170. L. Y. Chen, L. W. Lin, Z. S. Xu, X. S. Li, T. Zhang, J. Catal., 157 (1995) 190.
171. P. Meriaudeau, V. T. T. Ha, L. V. Tiep, Catal. Lett., 64 (2000) 49.
172. C. L. Zhang, S. A. Li, Y. Yuan, W. X. Zhang, T. H. Wu, L. W. Lin, Catal. Lett., 56 (1998) 207.
173. S. T. Liu, Q. Dong, R. Ohnishi, M. Ichikawa, Chem. Comm, (1997) 1455.
174. S. Li, C. L. Zhang, Q. B. Kan, D. Y. Wang, T. H. Wu, L. W. Lin, Appl. Catal. A, 187 (1999) 199.
175. V. R. Choudhary, A. k. Kinage, T. V. Choudhary, Science, 275 (1997) 1286.
176. Y. Xu, X. Bao, L. Lin, J. Catal., 216 (2003) 386.
177. O. A. Anunziata, G. V. Gonzalez Mercado, L. B. Pierella, Catalysis Letters, 87 (2003) 167.
178. T. Baba, Y. Abe, Appl. Catal. A, 250 (2003) 265.
179. T. Baba, H. Sawada, Phys. Chem. Chem. Phys., 4 (2002) 3919.
180. S. L. Meisel, J. P. McCullough, C. H. Lechthaler, P. B. Weizs, Chemtech 89 (Feb. 1976).
181. C. D. Chang, et al. Ind. Eng. Chem. Process Des. Dev. 17 (1978) 255.
182. J. Haggin, Chem Eng.News 22 (June 22, 1987).
183. J. Haggin, Chem. Eng. News. 22 (June 01, 1987).
184. L. Kniel, O. Winter, K. Stork, In Ethylene: Key stone of petrochemical Industry, Dekker, New York (1980).
185. A. Argent, P. Harris, J. Chem. Soc. Chem. Comm., (1986) 1058.
186. R. Burch, E. M. Crabb, Appl. Catal. A, 97 (1993) 49.
187. O. Desponds, R. I. Keiski, G. A. Somorjai, Catal. Lett., 19 (1993) 17.

188. M. Huff, L. D. Schmidt, J. Phy. Chem., 97 (1993) 11815.
189. E. M. Kennedy, N. W. Cant, Appl. Catal., 75 (1991) 321.
190. E. Morales, J. H. Lunsford, J. Catal., 118 (1989) 255.
191. H. M. Swaan, A. Toebes, K. Seshan, J. G. van Ommen, J. R. H. Ross, Catal. Today, 13 (1992) 629.
192. M. Zhang, J. Liu, R. Lan, L. Ji, X. Chen, J. Chem. Soc. Chem. Comm., (1993) 1480.
193. A. Erdohelyi, F. J. Solymosi, J. Catal., 123 (1990) 31.
194. V. R. Choudhary, A. M. Rajput, J. Chem. Soc. Farad. Trans., 91 (1995) 843.
195. V. R. Choudhary, S. A. R. Mulla, and A. M. Rajput, I & EC Res., 36 (1997) 2075.
196. V. R. Choudhary, S. A. R. Mulla, AIChEJ, 43 (1997) 1545.
197. V. R. Choudhary, V. H. Rane, and A. M. Rajput, AIChE J., 44 (1998) 2293.
198. M. C. Bradford, and M. A. Vannice, Catal. Rev.-Sci. Eng., 41 (1999) 1.
199. T. Nishiyama, and K. Aika, J. Catal., 122 (1990) 346.
200. K. Nakagawa, M. Okamura, N. Ikenaga, T. Suzuki and T. Kobayashi, Chem. Comm., (1998) 1025.
201. S. Wang, K. Murata, T. Hayakawa, S. Hamakawa, and K. Suzuki, Chem. Lett., 569 (1999)
202. S. Wang, K. Murata, T. Hayakawa, S. Hamakawa, and K. Suzuki, Catal. Lett., 63 (1999) 59.
203. S. Wang, K. Murata, T. Hayakawa, S. Hamakawa, and K. Suzuki, React. Kinet. Catal. Lett., 68 (1999) 265.
204. S. Wang, K. Murata, T. Hayakawa, S. Hamakawa, and K. Suzuki, Appl. Catal., 196 (2000) 1.
205. X. Longya, L. Liwu, W. Qingxia, Y. Li, W. Debao, and L. Weichen, Natural Gas Conversion V, 119 (1998) 605.
206. F. Solymosi, and R. Nemeth, Catal. Lett., 62 (1999) 197.
207. I. Takahara, and M. Saito, Chem. Lett., 973 (1996).

CHAPTER 2

EXPERIMENTAL

CHAPTER 2

EXPERIMENTAL

This chapter has been divided into three sections: Catalyst Preparation, Catalyst Characterization and Catalytic Reactions. In the first section, the preparation of different catalysts used for different catalytic reactions is discussed. In the second section, the techniques used to characterize the catalysts are described, and in the last section, the experimental set–ups and procedures for various catalytic reactions are described with diagrams.

2.1. Catalyst Preparation

In this section, the preparation procedures for different catalysts used for various catalytic reactions have been described.

2.1.1. Preparation of Catalysts used for Catalytic Methane to Syngas Conversion Reactions

2.1.1.1. CoO – Nd_2O_3

The CoO – Nd_2O_3 catalyst with different Co/Nd mole ratios (0.1, 1.0, 2.0, 4.0) were prepared from thick paste of thoroughly mixed, finely ground cobalt nitrate (GR Loba), neodymium nitrate (Sigma Aldrich), and deionized water, which was dried and heated in air at 600 ^{o}C for 4 h. The treated solid was powdered, pressed without a binding agent, crushed to particles of 22 – 30 mesh, and calcined in air at 900 ^{o}C for 4 h.

2.1.1.2. Co – containing alkaline and rare earth oxide catalysts

The Co containing alkaline earth oxides (viz. MgO or CaO) or rare earth oxide (viz. La_2O_3, Sm_2O_3, CeO_2, Eu_2O_3, Yb_2O_3, ThO_2, ZrO_2) catalysts were prepared by mixing thoroughly finely ground high purity cobalt nitrate and required alkaline or rare earth nitrate(s) [with required mole ratio(s)], along with deionized water just sufficient to form a thick paste, drying and decomposing the mass at 600 ^{o}C for 4 h, powdering, pressing and crushing to 22 – 30 mesh particles and calcining in air at 900 ^{o}C for 4 h. The catalysts after calcinations are stored in a desiccator over NaOH pellets. In the Co – containing mixed alkaline or rare earth oxides, the concentration of alkaline earth or rare earth oxides was equimolar.

2.1.1.3. CoO/MgO/SA-5205

Supported cobalt catalysts with different cobalt loadings [CoO (5, 10, 20 or 30 wt %)/MgO (5 wt%)/SA-5205] used in this investigation was developed in our laboratory for the CO_2 reforming, steam reforming, simultaneous oxy-CO_2 and oxy-steam reforming of methane to syngas at extremely short contact times. It has high thermal and hydrothermal stability and also has high mechanical strength. It was prepared by depositing cobalt nitrate from its aqueous solution on 22 – 30 mesh size particles of commercial catalyst carrier – SA-5205 [sintered low surface area macro porous silica-alumina support, obtained from Norton Co., USA] precoated with MgO, using an incipient wetness impregnation technique followed by drying and decomposing (or calcining) in air at 900 ^oC for 4 h. The catalyst carrier was precoated with MgO by impregnating the carrier with Mg-nitrate, drying and decomposing as above. The support (SA-5205) consists mainly of alumina (86.1 wt%) and silica (11.8 wt%) and its surface area, porosity, pore volume and average pore size are < 0.01 m^2g^{-1}, 54 %, 0.35 cm^3g^{-1} and 200 μm, respectively.

2.1.1.4. CoO/ZrO_2/SA-5205

Supported cobalt catalyst, CoO (20 wt %)/ZrO_2 (20 wt%)/SA-5205, was developed in our laboratory for the CO_2 reforming, steam reforming, simultaneous oxy-CO_2 and oxy-steam reforming of methane to syngas at extremely short contact times. It was prepared by depositing cobalt nitrate from its aqueous solution on 22 – 30 mesh size particles of commercial catalyst carrier – SA-5205 precoated with ZrO_2, using an incipient wetness impregnation technique followed by drying and decomposing (or calcining) in air at 900 ^oC for 4 h. The catalyst carrier was precoated with ZrO_2 by impregnating the carrier with zirconyl nitrate, drying and decomposing as above.

2.1.1.5. CoO-NiO/MgO/SZ-5564

Supported CoO-NiO (loading = 12 – 13 wt %, Co/Ni = 0.2) / MgO (7 wt%) / SZ-5564 catalyst used in this investigation was developed in our laboratory for the partial oxidation of methane, steam reforming of methane, simultaneous oxy-CO_2 and oxy-steam reforming of methane to syngas at extremely short contact times. It has high thermal and hydrothermal stability and also has high mechanical strength. It was prepared by depositing mixed nitrates of Co and Ni with Co/Ni mole ratio 0.2 from their aqueous solution on 22 – 30 mesh size particles

of commercial catalyst carrier, SZ-5564 [sintered low surface area macro porous stable zirconia support, obtained from M/S Norton Co., USA] precoated with MgO, using an incipient wetness impregnating technique, followed by drying and decomposing (or calcining) in air first at 900 ^{o}C for 4 h and then 1400 ^{o}C for 4 h. The catalyst carrier was precoated with MgO by impregnating the carrier with Mg-nitrate, drying and decomposing as above. The catalyst support (SZ-5564) consists mainly of zirconia-haffnia (94.1 % ZrO_2-HfO_2) and its surface area, porosity and pore volume are ≅ 0.1 m^2g^{-1}, 45 % and 0.15 cm^3g^{-1}, respectively.

2.1.1.6. CoO-NiO-MgO/SZ-5564

Supported CoO-NiO-MgO/SZ-5564 was prepared by depositing mixed nitrates of Co, Ni and Mg with the Co/Ni and Mg/Ni mole ratio of 0.2 and 1.2, respectively, from their aqueous solution on 22 – 30 mesh size particles of commercial catalyst carrier, SZ – 5564, using an incipient wetness impregnating technique, followed by drying and decomposing (or calcining) in air first at 900 ^{o}C for 4 h and then 1400 ^{o}C for 4 h.

2.1.2. Preparation of Zeolite Catalysts used for Low Temperature Non – Oxidative Activation of Methane over Bifuntional Pentasil Zeolites in Presence of Methanol or other Oxygenates.

2.1.2.1. H-ZSM-5

H-ZSM-5 samples with different Si/Al ratios were prepared and characterized earlier [1]. They were prepared by hydrothermal crystallization from a gel (P^H = 11 – 12) consisting of Na-trisilicate, aluminum nitrate, TPA Br, sulfuric acid and deionized water in a stainless steel autoclave at 180 ^{o}C for 96 h, washing, drying and calcining the resulting zeolite crystals at 550 ^{o}C in static air for 15 h to remove the occluded organic template, exchanging with 1 M ammonium nitrate at 80 ^{o}C for 4 times and drying and again calcining the zeolite under static air at 550 ^{o}C for 4 h to convert their NH_4-from to H-form.

2.1.2.2. H-GaMFI and H-GaAlMFI

The H-GaMFI and H-GaAlMFI zeolite catalysts were prepared and characterized earlier [2–4]. These were prepared by hydrothermal crystallization from a gel (P^H = 9-10) consisting of Na-trisilicate, gallium nitrate, with or without aluminum nitrate, TPA Br, sulfuric acid and deionized water in a stainless steel autoclave at 180 ^{o}C for 96 h, washing, drying and calcining the resulting zeolite catalysts at 550 ^{o}C in static air for 15 h to remove the occluded

organic template, exchanging with 1 M ammonium nitrate at 80 ^{o}C for 4 times and drying and again calcining the zeolite under static air at 550 ^{o}C for 4 h to convert their NH_4-form to H-form.

2.1.2.3. Mo – Zn/H-ZSM-5

Supported Mo (2 wt%)-Zn (2 wt%)/H-ZSM-5 catalyst was prepared by impregnating required quantity of ammonium hepta molybdate and zinc nitrate from their aqueous solution on H-ZSM-5 as follows. Aqueous solution of ammonium hepta molybdate and zinc nitrate and the required quantity of H-ZSM-5 were taken in a glass container and stirred at 30 ^{o}C for 4 h using a magnetic stirrer followed by drying on a water bath while the mixture continuously stirring, pressing, crushing to 22 – 30 mesh size particles and then calcining in air at 550 ^{o}C for 4 h.

2.2. Catalyst Characterization

2.2.1. Surface Area

The surface area of the catalysts was measured by the single point BET method by measuring the adsorption of nitrogen at liquid nitrogen temperature and at the N_2 concentration of 30 mol% (balance helium), using a Monosorb Surface Area Analyzer (Quantachrome Corp., USA) based on dynamic adsorption / desorption technique. Before the measurement, the catalyst was pretreated in situ in the sample cell at 300 ^{o}C for 1 hr in the flow of a mixture of helium and nitrogen (at a flow of 30 ml min^{-1}) to remove the traces of moisture and also the analyzer was calibrated by injecting a known amount of air.

The surface area was calculated from the observed desorption counts instead of the adsorption ones, as follows:

$$\textit{Surface area } (m^2.g^{-1}) = (\textit{Desorption counts} \times 2.84) \div (\textit{Wt. of catalysts in gram} \times \textit{counts for1 } cm^3 \textit{ of air})$$

[2.84 m^2 area = 1 cm^3 of N_2 or air; counts are expressed in terms of surface area, m^2]

2.2.2. X-Ray Diffraction (XRD)

The XRD analysis of the catalysts was done by using a Holland Philips, PW / 1730 X-ray generator with the CuKα radiation scintillation counter.

2.2.3. X-ray Photoelectron Spectroscopy (XPS)

Surface chemical analysis of the catalysts was carried out by X-ray photoelectron spectroscopy (XPS) using a VG Scientific ESCA-3 MK II electron spectrometer. C_{1s} (with

binding energy = 284.6 eV) was used as an internal standard. The electron binding energies (with the accuracy of 0.2 eV) were determined from the observed electron kinetic energies using the relation:

Binding energy (B. E.) = hν - kinetic energy (K. E.)

The X-ray radiation (hν) used in the XPS was MgKα (1253.6 eV).

The atom ratio of two elements (say, A and B) on the catalyst surface was determined from the XPS peaks as follows:

A/B atom ratio = [(peak area of A / photo ionization cross section of A) ÷ (peak area of B / photo ionization cross section of B)].

2.2.4. Temperature Programmed Reduction (TPR)

The schematic diagram of the experimental set-up used for the measurement of temperature-programmed reduction (TPR) with H_2 of the catalyst is shown in Fig. 2.4. The temperature-programmed reduction of the unreduced catalysts was carried out in a quartz reactor (I. D. 4.5 mm), packed with 150 mg catalyst in a flow (40 $cm^3.min^{-1}$) of H_2-Ar mixture (5 mol% H_2) from 35 °C to 1100 °C at a linear heating rate of 10 $^oCmin^{-1}$, using a Micromeritics Autochem 2910 instrument. The hydrogen consumed in the TPR was measured quantitatively by TCD.

2.2.5. Catalyst Reduction by H_2 Pulse Reaction

The experimental set-up used to study H_2 pulse reaction over the catalysts is shown in Figure 2.3. The H_2 pulse reaction over the catalysts was carried out in a quartz pulse micro reactor (containing 0.1g catalyst) connected to a gas chromatograph [5] (with a porapak-Q column and thermal conductivity detector) by injecting a pulse of pure H_2 (0.2 cm^3) in the reactor, using Ar as the carrier gas, at different temperatures (200 – 900 ^oC) or injecting at 900 ^oC a number of H_2 pulses, one after another, at an interval of time of 10 min or 1 h and determining the conversion of H_2 in each pulse experiment.

2.2.6. Measurement of Acidity

The acidity of the catalysts was determined by the GC adsorption/desorption methods, using pyridine as an acid probe. Gas chromatographic adsorption/desorption data were collected using a Perkin-Elmer Sigma 300 GC fitted with a flame ionization detector. Nitrogen,

passed over catalysts to remove traces of moisture, was used as the carrier gas. The flow rate was about 40 cm^3 (NTP) min^{-1} in all the experimental set up is shown in Figure 2.1.

The catalyst column was prepared by packing about 0.5 g of the adsorbent particles (particle size: 0.3 – 0.4 mm) in a stainless steel tube (length = 5.5 cm, i.d. = 1.5 mm and o.d. = 3.0 mm). In order to minimize the dead volume, one end of the column was directly connected to the detector and the other end to the injector through a 40 cm long stainless steel capillary (about 1.5 mm o.d. and 0.7 mm i.d.), which acted as a preheater. The

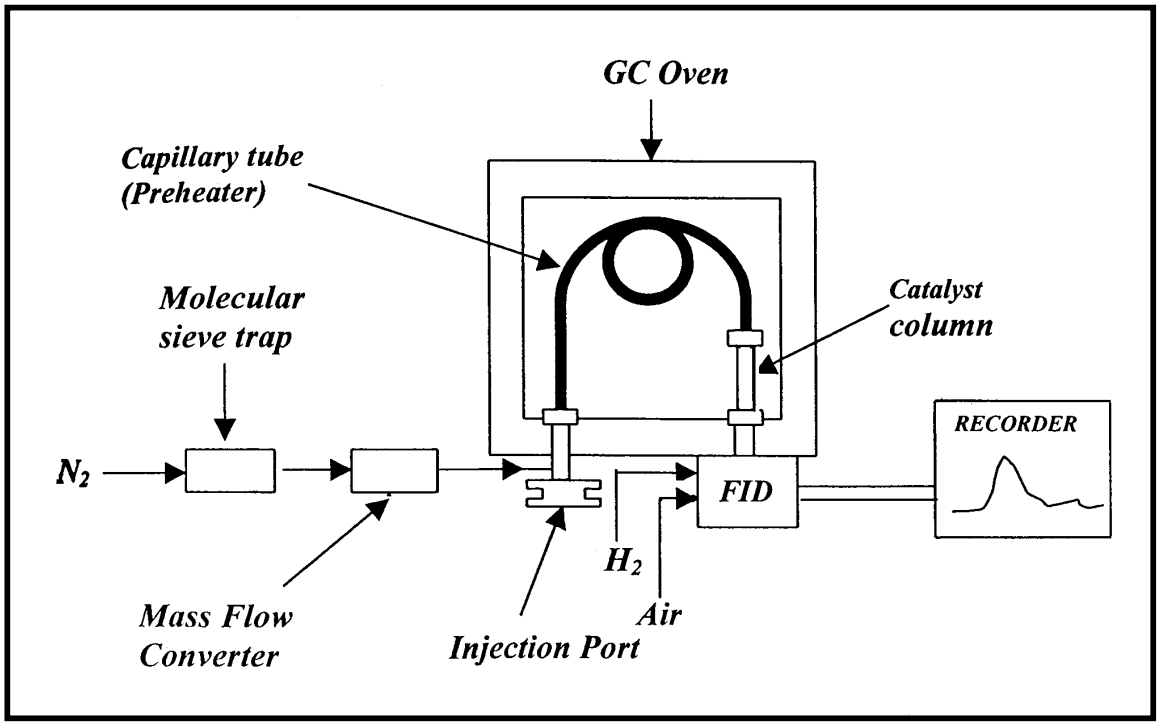

Figure 2.1: Experimental set-up for acidity measurement

catalyst was calcined in situ by heating rate of 20 ^oC min^{-1} and further at 400 ^oC for 1 h. The chemisorptions of pyridine in the catalyst was measured by the GC pulse method [6] based on TPD under chromatographic conditions, as follows.

The initial temperature chosen for the TPD was 80 ^oC. The catalyst was pretreated in situ in a flow of N_2 (carrier gas) for 1 h. After the pretreatment of the catalyst, the GC oven temperature was brought down to 80 ^oC and a known amount of pyridine was injected into the catalyst column. After allowing redistribution of the adsorbed species in the column, the TPD was started at a linear heating rate of 20 ^oC min^{-1} in the flow of nitrogen. The final temperature chosen for the TPD (or the temperature at which the irreversible adsorption of the adsorbate was to be measured) was 400 ^oC. After the final temperature was reached, the desorption of the reversibly adsorbed species was allowed to continue for a further period of 60 min isothermally

at that temperature. At the end of the TPD, the catalyst retained only the adsorbate irreversibly adsorbed at 400 ^{o}C.

After recording the first TPD chromatogram, the GC oven temperature was reduced to 80 ^{o}C and the procedure was repeated to obtained the second TPD chromatogram by injecting the same amount of pyridine.

The amount of pyridine irreversibly adsorbed was calculated from the expression:

$q_i = (A^* / s)/M$

where A* is the difference between the areas of the two chromatograms obtained by the superimposition of the two chromatograms and cutting and weighing, s is the detector sensitivity (areamol^{-1}) and M is the mass of the catalyst. The irreversibly adsorption (or chemisorption) in the present study is defined as the amount of adsorbate retained by the presaturated catalyst after it was swept with pure nitrogen at the temperature of chemisortion for 1 h.

2.3. Catalytic Reactions

2.3.1. Oxidative Conversion of Methane to Syngas

The experimental set-up and quartz reactor used for the partial oxidation of methane to syngas are shown in Figs. 2.5 and 2.2, respectively.

The oxidative methane-to-syngas conversion over the catalyst (0.2 g) was carried out in a continuous flow microreactor (Fig. 2.2) made up of quartz at 1 atm using a feed consisting of pure methane and oxygen with CH_4/O_2 ratio of about 1.8 and at different space velocities (30000 – 120000 cm^3.g^{-1}.h^{-1}) and at different temperatures (550 – 900 ^{o}C). The reaction temperature was measured with Chromel-Alumel thermocouple located in catalyst bed. The water from the reaction product was separated by condensing at 0 ^{o}C. The feed and product were analyzed by an on-line GC equipped with TCD using Spherocarb column at the following GC operating conditions:

Detector temperature	:	100 ^{o}C
Injector temperature	:	100 ^{o}C
Oven temperature	:	45 ^{o}C
Current	:	132 mA
He carrier gas flow rate	:	35 cm^3.min^{-1}

The response factor and retention time of the product gases were obtained by injecting the high purity individual gases into the column before carrying out the methane-to-syngas conversion reaction.

The methane conversion, CO-selectivity, H_2-selectivity, GHSV (gas hourly space velocity) and CO-productivity are defined / calculated as follows:

$$\text{Conversion, \%} = \frac{\text{(Methane in feed – Methane in product)}}{\text{Methane in feed}} \times 100$$

$$\text{Selectivity, \%} = \frac{\text{Conversion of methane to a particular product}}{\text{Conversion of methane}} \times 100$$

$$\text{GHSV } (cm^3g^{-1}h^{-1}) = \frac{\text{Total flow rate of feed gases (at } ^oC \text{ and 1 atm) } (cm^3h^{-1})}{\text{Wt. of catalyst (g)}}$$

$$\text{CO productivity } (molg^{-1}h^{-1}) = \frac{\text{GHSV} \times \text{MF of } CH_4 \times \text{FC of } CH_4 \times \text{FS for CO}}{22400}$$

Where, FC = Fractional conversion

MF = Mole fraction

FS = Fractional selectivity

2.3.2. CO_2 Reforming of Methane to Syngas

The experimental set-up and quartz reactor used for the CO_2 reforming of methane to syngas are shown in Figs. 2.5 and 2.2, respectively.

The CO_2 reforming reaction over the catalysts was carried out at atmospheric pressure by passing continuously a gaseous feed containing pure methane and carbon dioxide (CO_2/CH_4 mole ratio = 1.1) over the catalyst (0.3 g) packed in a quartz tubular reactor (i.d.=9 mm), provided with a thermocouple in the catalyst bed, at different GHSVs (gas hourly space velocity, measured at ^oC and 1 atm pressure) and temperatures. After attaining the reaction steady state, the reaction products were analyzed by an on-line gas chromatograph with thermal conductivity detector using a Spherocarb column. The carbon deposited on the catalyst during the reaction for a period of 15 ± 2h was determined by oxidizing it to CO_2 in a flow of air (60 cm^3min^{-1}) for a period of 2h at 800 ^oC and measuring quantitatively the amount of CO_2

produced by absorbing it in barium hydroxide solution forming barium carbonate, which was then estimated gravimetrically.

2.3.3. Simultaneous Oxidative Conversion and Steam and/or CO_2 Reforming of Methane

The experimental setup and quartz reactor used for the oxy-CO_2 reforming, oxy-steam reforming, and CO_2-steam reforming of methane-to-syngas are same as that used for the CO_2 reforming of methane.

The catalytic oxy-CO_2 reforming, oxy-steam reforming, and CO_2-steam reforming of methane-to-syngas reactions over the catalysts were carried out at atmospheric pressure in a continuous flow reactor (i.d. 9 mm) packed with 0.3 g catalyst and provided with a chromel-alumel thermocouple located in the center of the catalyst bed. The feed was a mixture of pure methane (> 99.95%), O_2 (99.9%), CO_2 (99.99%) and/or steam. Water was added to the feed using a SAGE syringe pump and a specially designed evaporator. Before carrying out the reaction, the catalyst was heated insitu at 900 ^oC in a flow (50 cm^3min^{-1}) of moisture-free nitrogen for 1 h. The catalytic reactions were carried out at different temperatures, gas hourly space velocities (GHSV), (measured at 0 ^oC at 1 atm) and relative concentrations of methane, O_2, CO_2, or steam in the feed. The product gases (after condensation of the water from them at 0^oC) were analyzed by an on-line gas chromatography with TCD, using a Spherocarb column and He as a carrier gas. The C, H, and O balances across the reactor were within 2–6%. All experiments with larger error in the material balances were rejected.

2.3.4. Simultaneous Conversion of Methane and Methanol or other Oxygenates into Higher Hydrocarbons / Gasoline

The experimental setup and quartz reactor used for the simultaneous conversion of methane and methanol or other oxygenates reaction are shown in Figs. 2.6 and 2.2, respectively.

The simultaneous methane and methanol reaction over the catalyst were carried out at atmospheric pressure in a continuous flow reactor packed with 5.0 g catalyst and provided with a chromel-alumel thermocouple located in the center of the catalyst bed. The feed was a mixture of methanol or other oxygenates vapour, pure methane (> 99.95%), and nitrogen in a quartz reactor. Methanol was added to the feed using a SAGE syringe pump and a specially designed evaporator. The reaction products, unconverted methane and methanol and N_2 were analyzed by an on-line GC (gas chromatograph) with SE-30 and poropak-Q columns, using

thermal conductivity and flame ionization detectors connected in series. The methane conversion using nitrogen as an internal standard, was determined as follows:

$$\text{Conversion of Methane (\%)} = \frac{(CH_4/N_2)_{\text{Feed}} - (CH_4/N_2)_{\text{Products}}}{CH_4/N_2)_{\text{Feed}}} \times 100$$

Hydrogen produced during the reaction has been analyzed by injecting the gaseous products [collected in a constant pressure gas collector (7)] in the GC, using thermal conductivity detector.

2.3.5. Non–Catalytic Pyrolysis of Ethane to Ethylene in the Presence of CO_2 with or without O_2

The quartz reactor and experimental setup used for the non-catalytic pyrolysis of ethane to ethylene reactions are shown in Figs. 2.7 and 2.8, respectively.

The thermal cracking of ethane in the presence of CO_2 was carried out at different process conditions (viz. temperature = 750 – 900 ^oC; CO_2 / ethane = 0 – 2.0 and GHSV = 1500 – 9000 h^{-1}) with or without oxygen (O_2 / ethane = 0 – 0.3). All the ratios of feed components are mole ratios. GHSV is defined as the volume of gaseous feed (measured at 0^oC and 1 atm pressure) passed through a unit volume of the reactor per hour. The inlet and outlet temperatures of the reactor were measured by Chromel-Alumel thermocouples similar to that described earlier [8]. The maximum difference in the reactor inlet and outlet temperatures was 7^oC. The reactions were carried out by a procedure similar to that described earlier [9]. After the removal of water (formed particularly in the oxy-CO_2 ethane cracking) by condensation at 0^oC, the feed and products were analyzed by an on-line gas chromatograph with a thermal conductivity detector (TCD) and flame ionization detector (FID), using Poropak-Q and Spherocarb columns. The water condensed from the products was weighed.

The formation of O-containing products other than CO, CO_2, and H_2O was not observed. The experimental runs with the error in C, H, and O mass balances less than 6 % were considered; the runs with higher errors were discarded. Product distribution data are provided for the product stream without CO_2 and water. Product selectivity reported in this investigation is based on the conversion of carbon from ethane to a particular product. It is described as follows:

Product selectivity = 100 × [Moles of the product formed per hour × number of C in the Product] ÷ [2 × Mole of ethane converted per hour]

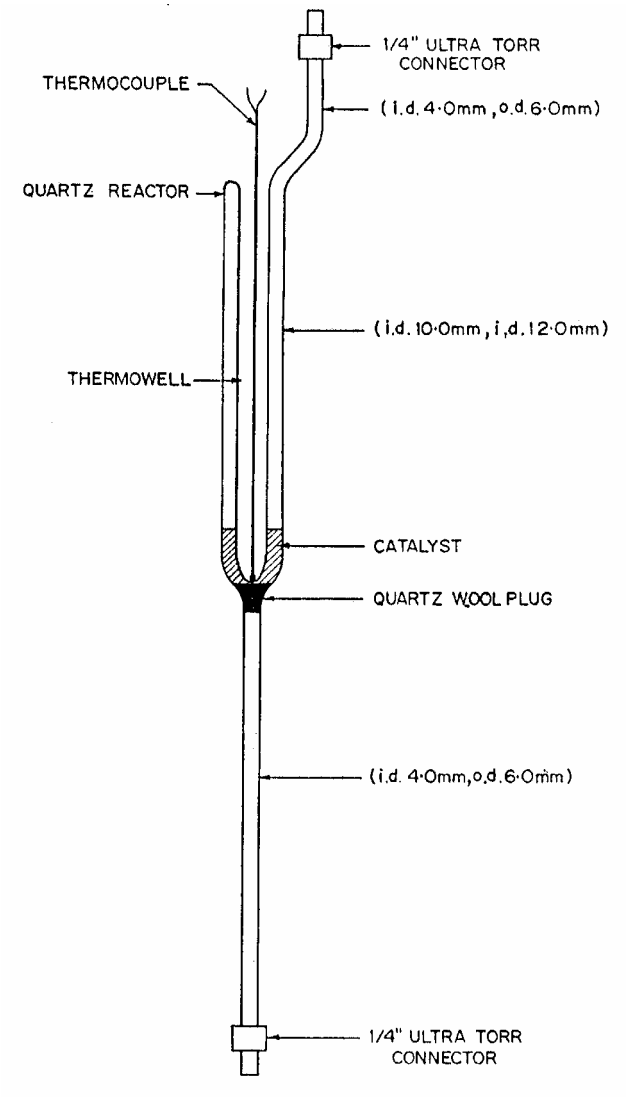

Figure 2.2 Quartz reactor used in different catalytic process

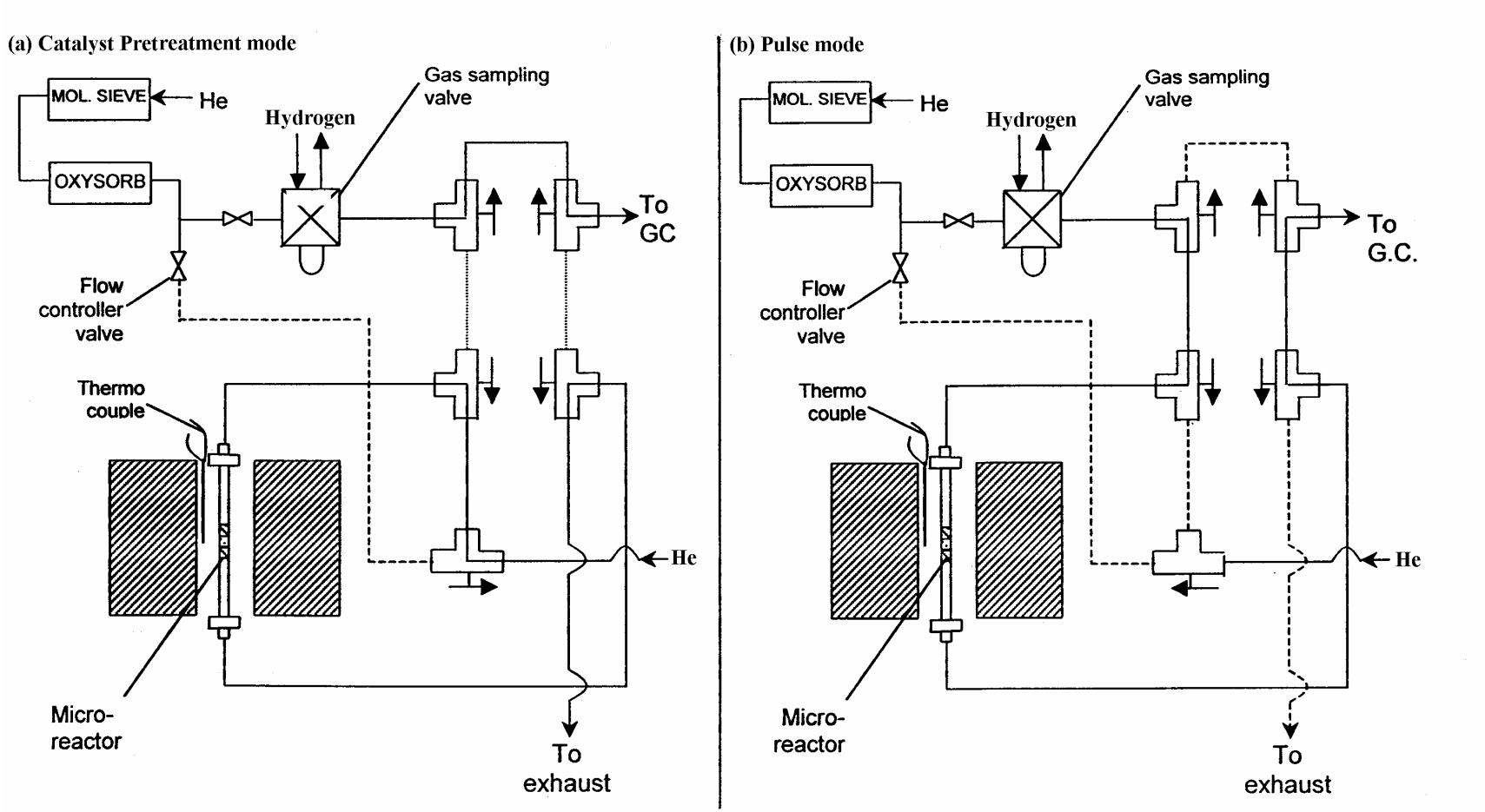

Figure 2.3 Experimental set-up for (a) insitu pretreatment of catalyst and (b) H_2 pulse reaction on the catalyst in pulse micro reactor [FCV = flow control valve; GSV = gas sampling valve; BV = three-way ball valve.

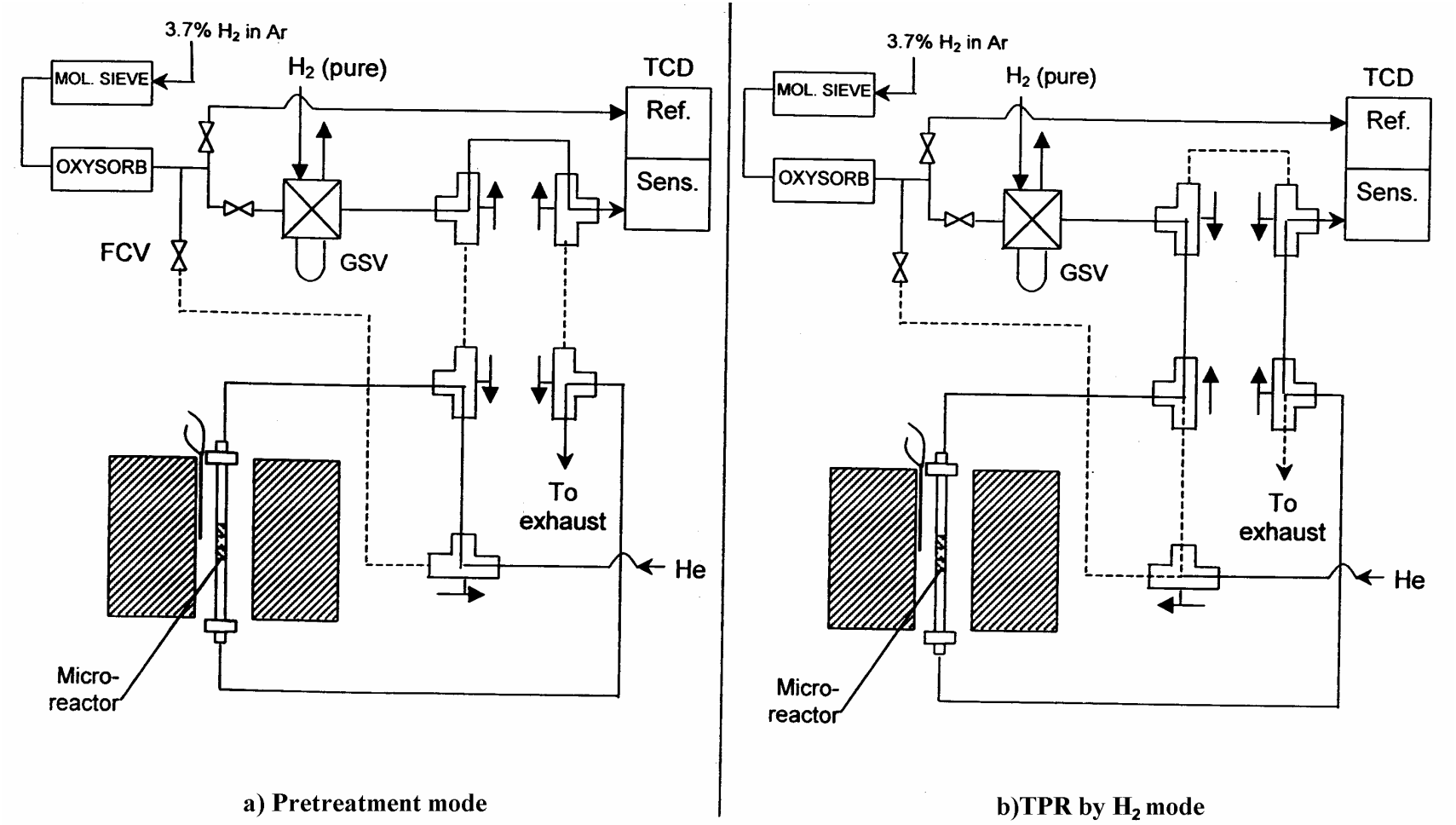

Figure 2.4 Experimental set-up for temperature programmed reduction (TPR) by H_2 (a) insitu pretreatment of catalyst and (b) TPR by H_2 [FCV = flow control valve; GSV = gas sampling valve; BV = three-way ball valve.

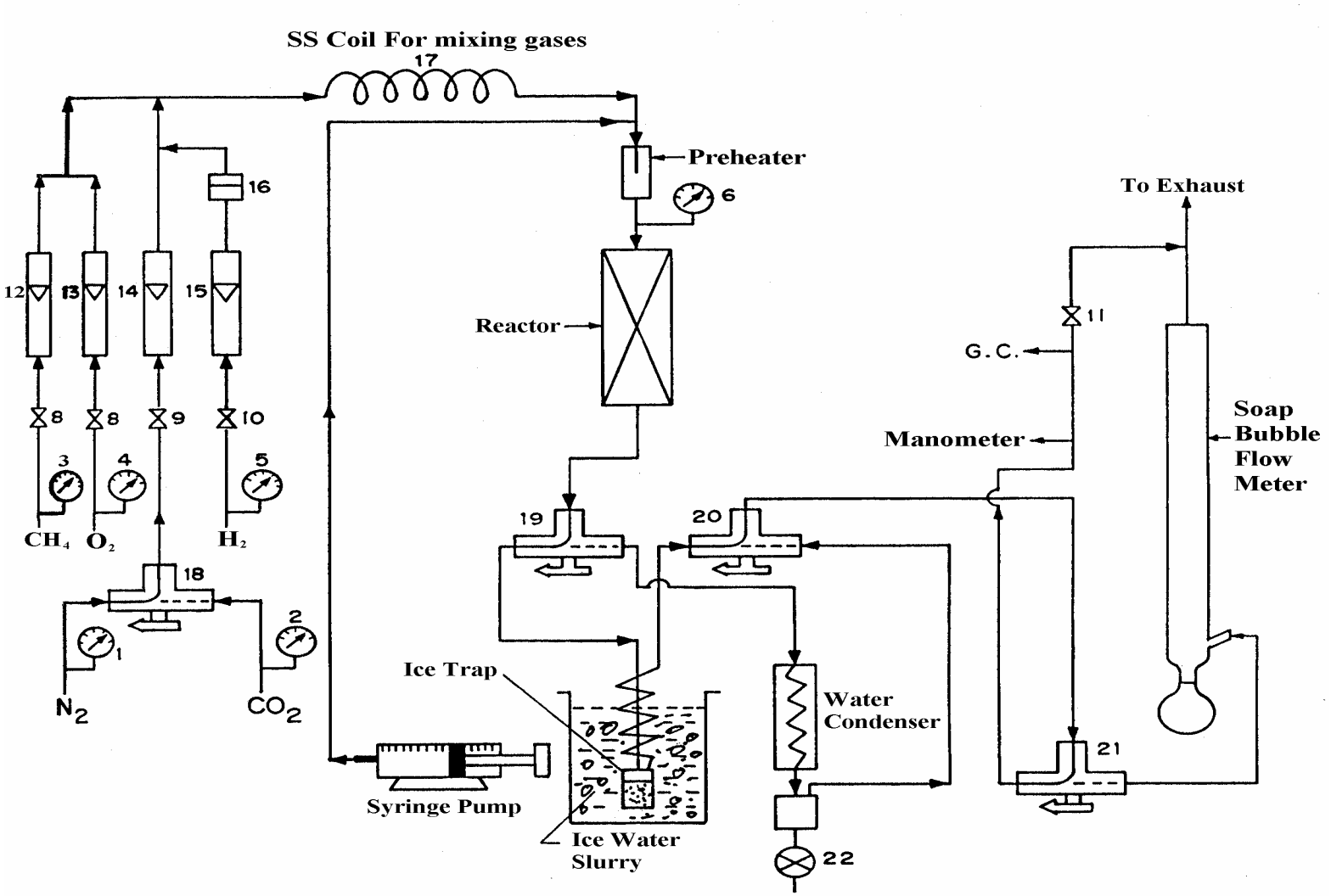

Figure 2.5 Experimental Setup for Evaluation of Catalyst Performance in Oxidative Conversion of Methane, CO_2 Reforming, Oxy – CO_2 Reforming, Oxy – Steam Reforming, CO_2 – Steam Reforming and Steam Reforming of Methane to Syngas.

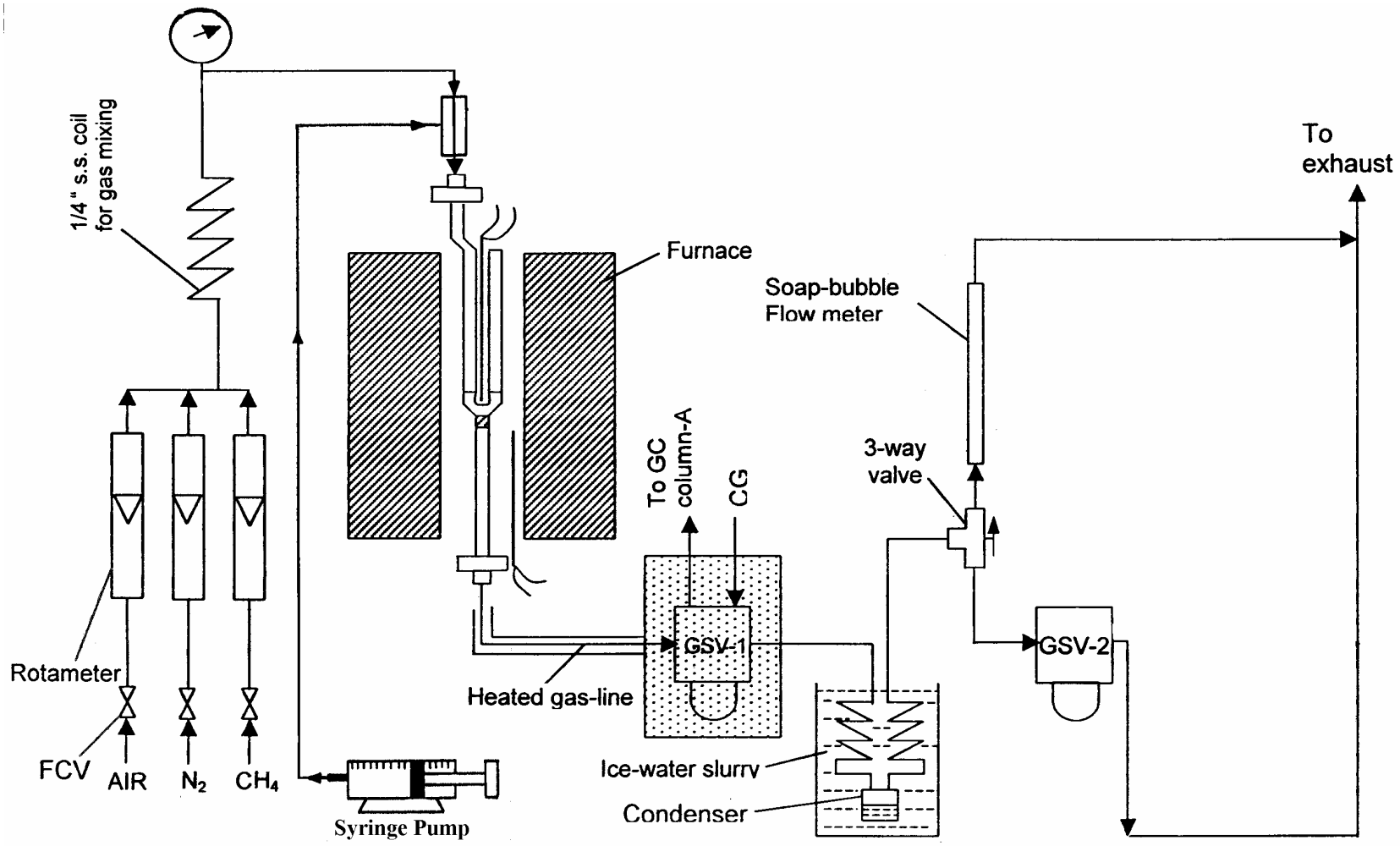

Figure 2.6 Experimental set – up for simultaneous conversion of methane and oxygenates [GSV 1 = heated gas sampling valve, GSV 2 = gas sampling valve, Column A = Porapak P; CG = carrier gas, FCV = flow control valve].

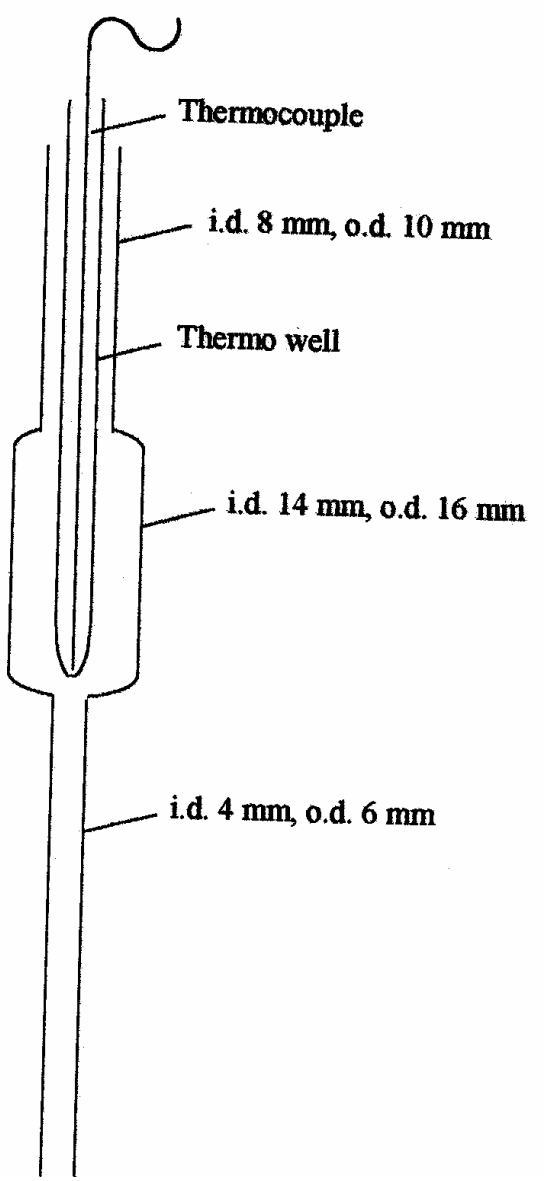

Figure 2.7 Quartz reactor used in non-catalytic ethane pyrolysis reaction

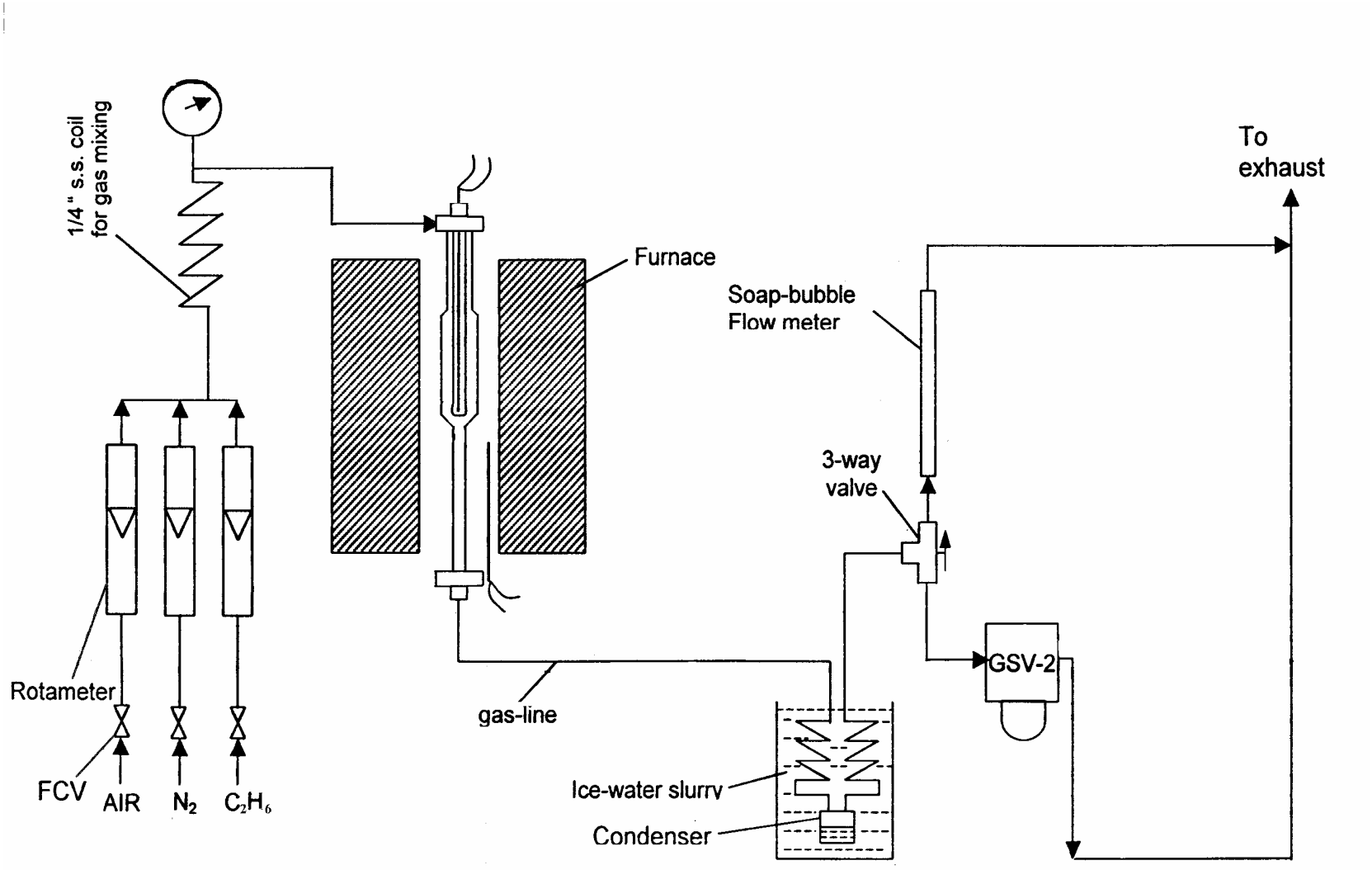

Figure 2.8 Experimental set – up for non-catalytic ethane pyrolysis reaction [GSV 2 = gas sampling valve, FCV = flow control valve].

References

1. V. R. Choudhary, V. S. Nayak, Appl. Catal., A: 4 (1982) 333.
2. V. R. Choudhary, A. K. Kinage, C. Sivadinarayana, P. Devadas, S. D. Sansare, M. Guisnet, J. Catal., 158 (1996) 34.
3. V. R. Choudhary, A. K. Kinage, C. Sivadinarayana, M. Guisnet, J. Catal., 158 (1996) 23.
4. V. R. Choudhary and V. H. Rane, J. Catal., 135 (1992) 310.
5. V. R. Choudhary, A. K. Kinage, T. V. Choudhary, Appl. Catal. A: Gen., 162 (1997) 239.
6. V. R. Choudhary and V. S. Nayak, Appl. Catal., 4 (1982) 31.
7. V. R. Choudhary, M. G. Parande and P. H. Brahme, Ind. Eng. Chem. Fundam., 21 (1982) 472.
8. V. R. Choudhary, V. H. Rane and A. M. Rajput, AIChE J., 44, (1998) 2293.
9. V. R. Choudhary, S. T. Choudhari, and A. M. Rajput, AIChE J., 37 (1991) 915.

CHAPTER 3

CO_2 REFORMING, SIMULTANEOUS CO_2 AND STEAM REFORMING AND OXY- CO_2 REFORMING OF METHANE TO SYNGAS OVER COBALT CONTAINING CATALYSTS

CHAPTER 3

CO_2 REFORMING, SIMULTANEOUS CO_2 AND STEAM REFORMING AND OXY-CO_2 REFORMING OF METHANE TO SYNGAS OVER COBALT CONTAINING CATALYSTS

3.1. Earlier Work / Background and Objective of the Present Work

Carbon dioxide is a green house gas. The present global warming has been attributed to a large increase in the CO_2 concentration in the atmosphere [1,2]. Environmental concerns over the increasing CO_2 concentration have recently driven the interest of CO_2 conversion particularly for the production of syngas by CO_2 reforming (commonly called as dry reforming) of methane [2-4]. Since, the last few years, the research activities on the CO_2 reforming have gained a lot of momentum. Recent studies showed use of a number of catalysts for the CO_2 reforming of methane, viz. NiO-CaO [5], NiO-MgO [6,7], NiO-CoO-MgO [7], NiO or $Ni_{1-x}Co_xO$/MgO/SA-5205 [8,9], Ni/ZrO_2 [10], Ni or Co/Al_2O_3 [11], Co/MgO [12] and supported Pt [13], Rh [14] and Ru or Ir [15] catalysts. Methane reforming with carbon dioxide is thought to consist of similar elementary reaction steps as in methane reforming with steam [16], but the absence of water and the high C/H ratio in the reactant feed favours, thermodynamically, coke formation during CO_2/CH_4 reforming [17]. In general, the rate of carbon deposition is very high for the Ni-based catalysts and relatively slower for Co- and noble metal based catalysts. Carbon formation in the CO_2 reforming results mainly by carbon monoxide disproportionation ($2CO \rightarrow CO_2 + C$) and/or methane decomposition ($CH_4 \rightarrow C + 2H_2$) reactions. Options to reduce the coke build up include the increase of the H/C or O/C content of the feed by (i) the addition of water (CO_2 plus steam reforming) [16,18,19], (ii) the addition of oxygen (CO_2 reforming plus partial oxidation) [16,19], or (iii) the use of catalysts which minimize the rate of coking. Addition of cobalt [7,9,20] or alkali metal oxide [21] to nickel catalyst has also been found to suppress the carbon formation in the CO_2 reforming. However, in spite of all these efforts, the rapid coking of catalyst remained as a major problem in the CO_2 reforming process. It is, therefore, of great practical importance to develop a catalyst, which does not allow carbon formation in the CO_2 reforming.

3.2. Experimental

The preparation procedure of different Ni-, Co-, and noble metal containing catalysts used for this purpose has been discussed earlier (section 2.1.1.1 & 2.1.1.2). In short the Rh (5.0 wt%)/Al_2O_3 and Ru (5.0 wt%)/Al_2O_3 catalysts were obtained from Lancaster (England). The Ni or Co containing mixed metal oxide catalysts (Table 3.1) were prepared by mixing nickel or cobalt nitrate with corresponding metal oxide in the required mole ratio in the presence of deionized water such that a thick paste was formed, drying the paste and then calcining it at 900 ^oC for 4h and crushing the catalyst mass to 22 - 30 mesh size particles.

The $CoNdO_x$ (Co/Nd=0.1 - 4.0) catalysts were characterized by X-ray diffraction and temperature programmed reduction in a flow of 5.0 mol% H_2 in Ar at a linear heating rate of 10 $^oC\ min^{-1}$ from 100 ^{o} to 800 ^oC, using a thermal conductivity detector. The catalyst in its active form (i.e. after the reaction) was also characterized by X–ray photoelectron spectroscopy.

The experimental procedure for the CO_2 reforming with or without simultaneous steam reforming or partial oxidation of methane to syngas reactions over the catalysts, have already discussed (section 2.3.2 & 2.3.3 and Fig. 2.5). The reactions were carried out at atmospheric pressure by passing continuously, a gaseous feed containing pure methane and carbon dioxide (CO_2/CH_4 mole ratio = 1.1) and/or steam or oxygen over the catalyst (0.3 g) packed in a quartz tubular reactor (Fig. 2.2), provided with a thermocouple in the catalyst bed, at different GHSVs (gas hourly space velocity, measured at ^oC and 1 atm pressure) and temperatures. The reactor effluent gases were cooled to about 2 ^oC using a coiled condenser immersed in the ice-water slurry to remove the water from the product gases. After attending the reaction steady state, the reaction products were analyzed by a gas chromatograph with thermal conductivity detector using Spherocarb column. The carbon deposited on the catalyst during the reaction for a period of 15 ± 2h was determined by oxidizing it to CO_2 in a flow of air (60 $cm^3\ min^{-1}$) for a period of 2h at 800 ^oC and measuring quantitatively the amount of CO_2 produced by absorbing it in barium hydroxide solution forming barium carbonate, which was then estimated gravimetrically.

The C, H, and O balance across the reactor was within 2 – 6 %. All experiments with larger error in the material balances were rejected. The H_2 and CO selectivity reported in this chapter is based on the methane conversion alone.

A fresh catalyst was used for the different reactions (viz. CO_2 reforming, simultaneous steam and CO_2 reforming, oxy-CO_2 reforming). No catalyst deactivation was observed during the course of these reactions. This was confirmed by repeating the first run, which was carried out after a reaction period of 30 min at the end of the experiments for each of the methane-to-syngas conversion reactions. We observed no significant changes in the conversion or selectivity.

3.3. Results and Discussions

3.3.1. Catalyst Characterization

The $CoNdO_x$ (Co/Nd = 0.1 – 4.0) catalysts were characterized for their surface, bulk properties and degree of reduction. The results of catalyst characterization are presented in Table 3.1 and Figs. 3.1 & 3.2.

The different crystalline phases (individual metal oxide phases and perovskite-type $NdCoO_3$ phase) present in the catalyst were strongly influenced by the Co/Nd ratio (Table 3.1). The catalyst with Co/Nd ratio of ≥ 1 showed the presence of perovskite-type mixed metal oxide ($NdCoO_3$) as a major crystalline phase, with the minor (or very small) crystalline phases like Nd_2O_3, CoO, Co_3O_4 and/or Co_2O_3. The reduction of $NdCoO_3$ during the initial period of the CO_2 reforming process (Fig. 3.3) is expected to produce finely dispersed metallic cobalt on the Nd_2O_3 support, as in case of the reduction of Ni- or Co- containing perovskite-type mixed metal oxides [20].

The TPR of the $CoNdO_x$ catalysts (Fig. 3.1) indicates that the catalyst reduction occurs in two distinct steps, as shown by the two distinct TPR peaks. It is interesting to note that the degree of reduction in step-I is increased, and that in step–II is consequently decreased with increasing the Co/Nd ratio (Table 3.1). The cobalt containing compounds present in the catalyst are reduced during the TPR, leading to the formation of metallic cobalt dispersed on Nd_2O_3, by the following stoichiometric reactions:

$$CoO_x + xH2 \longrightarrow Co^o + xH2O \uparrow \quad (1)$$

and

$$2NdCoO_3 + 3H_2 \longrightarrow 2Co^o + Nd_2O_3 + 3H2O \uparrow \quad (2)$$

The above two reactions may occur in more than one steps, as follows:

$$Co_2O_3 \xrightarrow{H_2} Co_3O_4 + CoO \xrightarrow{H_2} Co^o \quad (3)$$

$$NdCoO_3 \xrightarrow{H_2} Nd_2O_3 + CoO \xrightarrow{H_2} Co^o + Nd_2O_3 \quad (4)$$

A comparison of the TPR peaks for the $CoNdO_x$ catalysts reveals that, in the first step of the TPR, the cobalt in higher oxidation state [Co (III)] is reduced to lower oxidation state [Co (II)] in the first step and the reduction [Co (II) $\rightarrow$ Co (0)] is completed in the second step.

Table 3.1: Surface and bulk properties and degree of reduction for the $CoNdO_x$ catalysts with different Co/Nd ratios

Co/Nd mol ratio	Surface area ($m^2.g^{-1}$)	XRD phases	Degree of reduction (%) (temperature range)	
			Step-I	Step-II
0.1	7.3	Nd_2O_3, Co_3O_4 & Co_2O_3 (major), and $NdCoO_3$[a] (trace)	20.0 (300 ^{o} – 460 ^{o}C)	80.0 (460 ^{o} – 600 ^{o}C)
1.0	23.7	$NdCoO_3$[a] (Major) & CoO, Co_3O_4, and Nd_2O_3 (very small)	39.6 (300 ^{o} – 490 ^{o}C)	60.4 (490 ^{o} – 610 ^{o}C)
2.0	1.0	$NdCoO_3$[a] (major) & CoO, Co_2O_3 and Nd_2O_3	61.0 (300 ^{o} – 530 ^{o}C)	39.0 (530 ^{o} – 610 ^{o}C)
4.0	0.9	$NdCoO_3$[a] (major) & CoO, Co_2O_3, Co_3O_4 and Nd_2O_3	82.6 (290 ^{o} – 510 ^{o}C)	17.4 (510 ^{o} – 605 ^{o}C)

[a] perovskite-type mixed metal oxide

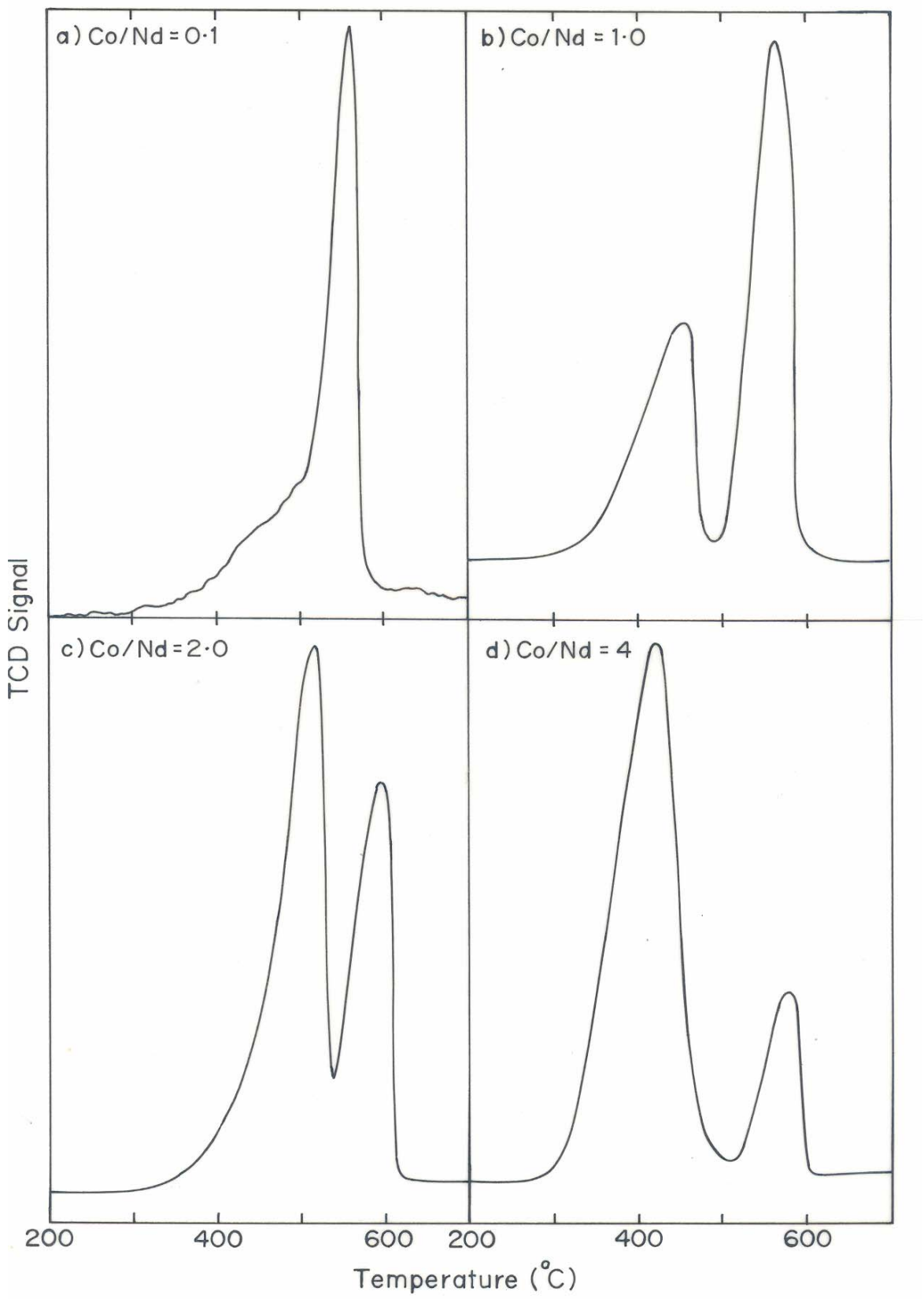

Figure 3.1 TPR peaks for the CoNdOx catalyst with different Co/Nd mole ratio.

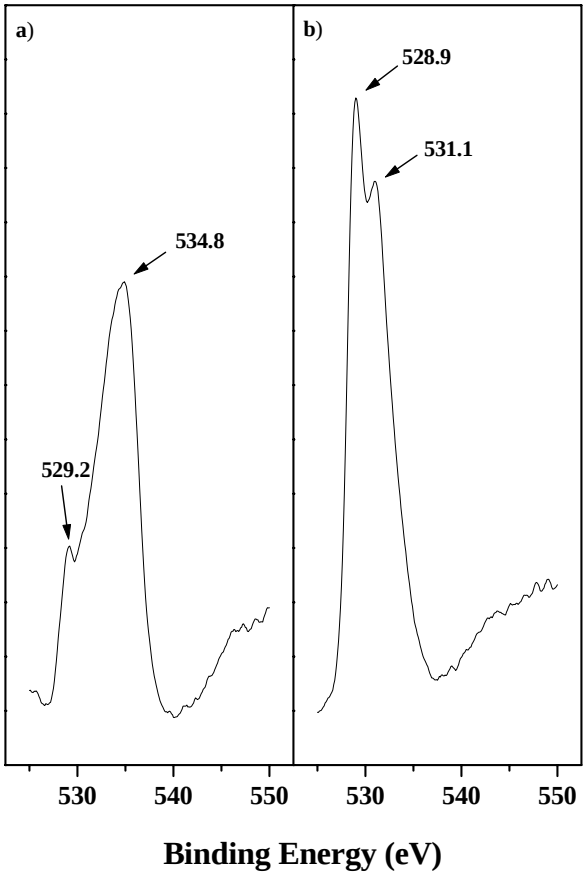

Figure 3.2 O (1s) XPS spectra of the $CoNdO_x$ (Co/Nd = 1.0) catalyst (a) before and (b) after its use in the CO_2 reforming reaction.

The support Nd_2O_3 is basic in nature. XPS analysis of the $CoNdO_x$ (Co/Nd = 1.0) catalyst before the CO_2 reforming reaction showed two XPS peaks for O (1s) : a small peak for binding energy (BE) of 529.2 eV and a much larger peak for BE of 534.8 eV (Fig. 3.2.). However, after the reaction, the XPS peak at lower BE (528.9 eV) is increased very markedly, while that at higher BE shifted to lower energy (531.1 eV), indicating an increase in the basicity and / or large changes in the electronic properties of the catalyst, which are expected to result from the interaction of metallic cobalt (formed during the reaction) with the support. The metallic cobalt-support (Nd_2O_3) interactions seem to be responsible for the observed inhibition to the carbon formation on the catalyst during the CO_2 reforming process.

3.3.2. *CO_2 Reforming over Different Catalysts: Comparison of the Catalysts*

A number of important nickel, cobalt or noble metal containing catalysts have been evaluated for their performance in the CO_2 reforming and the results are presented in Table 3.2. The $NiMgO_x$, CoO_x-ZrO_2, CoO_x-Y_2O_3, $CoCeO_x$ and Rh or Ru/Al_2O_3 catalysts showed high activity (methane conversion > 90%) and also high H_2-selectivity (>94%) but with high rate of carbon deposition on them during the reaction. However, no carbon formation was observed in the reaction when the $CoNdO_x$ (Co/Nd = 1.0) was used as the CO_2 reforming catalyst. Moreover, this catalyst also showed not only high activity (methane conversion = 92.3%) with high H_2 selectivity (95.5%) at a high space velocity (20,000 $cm^3g^{-1}h^{-1}$) but also high stability against the catalyst deactivation in the process (Fig. 3.3.). All these qualities make this catalyst practically very promising for the CO_2 reforming process. During the initial CO_2 reforming period (up to 6h), the $CoNdO_x$ catalyst is reduced, first by the methane from the feed and then by the H_2 and CO produced in the reforming of methane over the partially reduced catalyst. Consequently, both the activity and H_2 selectivity in the reforming over the catalyst are increased with the time in the initial short reaction period (upto about 6 h) and then remained constant for the further period. After the initial reaction period, there was no change in the methane conversion and H_2 selectivity, when the reaction was carried out for 60h (Fig. 3.3). However, when the catalyst was prereduced by hydrogen (5 % H_2/N_2 mixture), there was no effect of time on the conversion and selectivity in the initial reaction period. The catalyst in its active form is essentially a highly dispersed metallic cobalt on Nd_2O_3.

3.3.3. CO_2 Reforming over $CoNdO_x$ with Different Co/Nd Ratios

Result showing the activity of $CoNdO_x$ catalyst, strongly influenced by the Co/Nd ratio, is shown in Fig. 3.4. A Co/Nd ratio of 1.0 has been found to be the optimum ratio for the catalyst for its best performance. However, for all these $CoNdO_x$ catalysts, there was no carbon formation in the CO_2 reforming. With this ratio, the catalyst is mainly in the form of a perovskite-type mixed metal oxide ($NdCoO_3$).

Table 3.2: Results of the CO_2 reforming of methane over different Ni, Co or noble metal containing catalysts at 850 ^oC [feed: a mixture of CH_4 and CO_2 (47.5 mol % CH_4), GHSV = 20,000 $cm^3\ g^{-1}\ h^{-1}$ and time-on-stream = 15 ± 2h]

Catalyst	CH_4 Conversion (%)	H_2 Selectivity (%)	H_2/CO ratio	Rate of carbon deposition[b] x 10^3 [$g(C)g^{-1}$ $(cat)h^{-1}$]	TOF [c] ($mmolg^{-1}h^{-1}$)
$CoMgO_x$ (Co/Mg = 1.0) [a]	No reaction	-	-	-	-
$CoCaO_x$ (Co/Ca = 1.0) [a]	< 5	-	-	-	< 21
$NiMgO_x$ (Ni/Mg = 1.0)	98.0	97.9	0.94	1.83	413.1
CoO_x/Al_2O_3 (Co/Al = 1.0)	77.3	94.7	0.86	1.01	325.9
CoO_x-ZrO_2 (Co/Zr = 1.0)	98.1	93.5	0.95	0.48	413.5
CoO_x-ThO_2 (Co/Th = 1.0)	84.3	94.7	0.86	0.15	355.4
CoO_x-Y_2O_3 (Co/Y = 1.0)	93.0	93.8	0.92	0.61	392.0
$CoLaO_x$ (Co/La = 1.0)	26.0	55.5	0.38	1.53	109.6
$CoSmO_x$ (Co/Sm = 1.0)	34.2	60.5	0.45	1.12	144.2
$CoCeO_x$ (Co/Ce = 1.0)	94.1	99.8	0.91	0.35	396.7
$CoEuO_x$ (Co/Eu = 1.0)	13.0	51.7	0.35	0.12	54.8
$CoYbO_x$ (Co/Yb = 1.0)	30.5	60.1	0.45	0.51	128.6
$CoNdO_x$ (Co/Nd = 1.0)	92.3	95.5	0.91	0.00	389.1
Rh (5 wt%)/Al_2O_3	97.7	94.0	0.94	0.25	411.9
Ru (5 wt%)/Al_2O_3	97.8	97.9	0.96	0.57	412.3

[a] With or without reduction by H_2 at 800 ^{o} or 900 ^oC for 1h. [b] Mass of carbon deposited per unit mass of the catalyst per hour. [c]Turn over frequency, defined as the amount of methane converted per unit mass of catalyst per hour

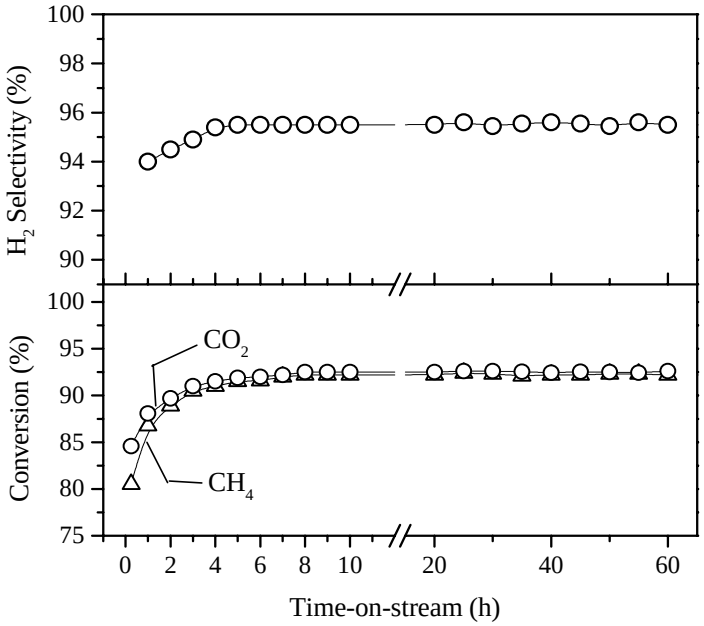

Figure 3.3. Time-on-stream activity and selectivity of the $CoNdO_x$ (Co/Nd = 1.0) catalyst in the CO_2 reforming of methane at 850 ^oC (CO_2/CH_4 mole ratio in feed = 1.1, GHSV = 20,000 $cm^3g^{-1}h^{-1}$)

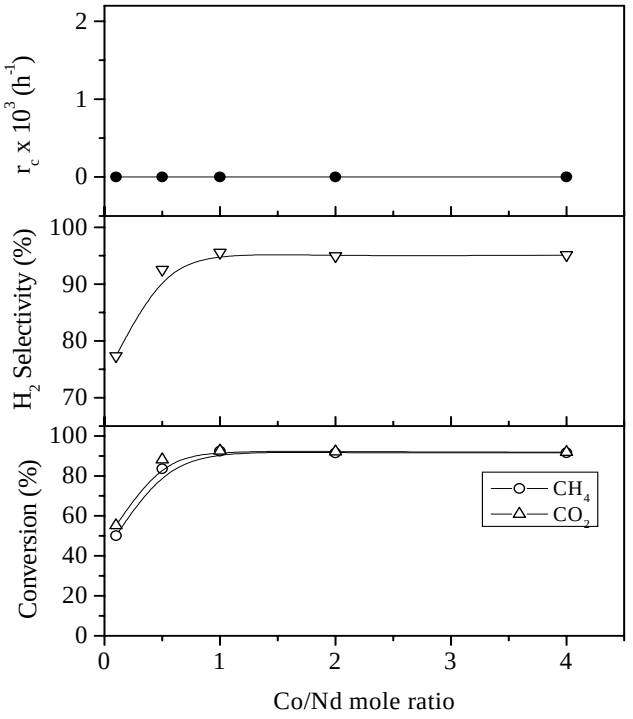

Figure 3.4. Influence of Co/Nd ratio on the performance (conversion, H_2 selectivity and rate of carbon deposition, r_c) of $CoNdO_x$ catalyst in the CO_2 reforming at 850 ^oC (CO_2/CH_4 = 1.1, GHSV = 20,000 $cm^3g^{-1}h^{-1}$, time-on-stream = 15 ± 2h)

3.3.4. CO_2 Reforming over $CoNdO_x$ (Co/Nd = 1.0): Influence of Process Variables

3.3.4.1. Effect of temperature and space velocity

Results in Figure 3.5 showed the influence of reaction temperature and space velocity on the conversion, H_2 selectivity and H_2/CO product ratio in the CO_2 reforming of methane over $CoNdO_x$ (Co/Nd = 1.0) catalyst. The conversion of both CH_4 and CO_2 is increased by increasing the temperature and decreased exponantionally with increasing the space velocity. The H_2 selectivity and H_2/CO ratio are increased with increasing the temperature, but decreased by increasing the space velocity. The facts that the conversion of CO_2 is higher than that of methane and that the H_2/CO ratio is less than 1.0 indicate occurrence of reverse water-gas shift reaction,

$$CO_2 + H_2 \rightarrow CO + H_2O \qquad (5)$$
$$(\Delta H_r = + 8.0 \text{ kcalmol}^{-1})$$

simultaneously with the CO_2 reforming reaction (Eq. 6), depending upon the process conditions. The thermodynamic feasibility of the reaction (Eq. 5) is increased with increasing the temperature. Unexpectedly the H_2 selectivity is higher at the higher temperature. This is because of the lower CO_2 concentration available for the reverse shift reaction at the higher temperatures.

3.3.5. Simultaneous Steam and CO_2 Reforming Reactions over $CoNdO_x$ (Co/Nd = 1.0): Influence of CO_2/H_2O Ratio in feed

Results showing the influence of CO_2/H_2O ratio (at 850 ^oC) on the conversion and H_2/CO product ratio in the simultaneous steam and CO_2 reforming of methane over $CoNdO_x$ (Co/Nd = 1.0) catalyst are presented in Figure 3.6. In this process, both the CO_2 and H_2O are converted simultaneously by their reaction with methane, as follows:

$$CH_4 + CO_2 \rightarrow 2CO + 2H_2 \qquad (6)$$
$$(\Delta H_r = + 62.2 \text{ kcalmol}^{-1} \text{ at } 850\ ^oC)$$
$$CH_4 + H_2O \rightarrow CO + 3H_2 \qquad (7)$$
$$(\Delta H_r = + 54.13 \text{ kcalmol}^{-1} \text{ at } 850\ ^oC)$$

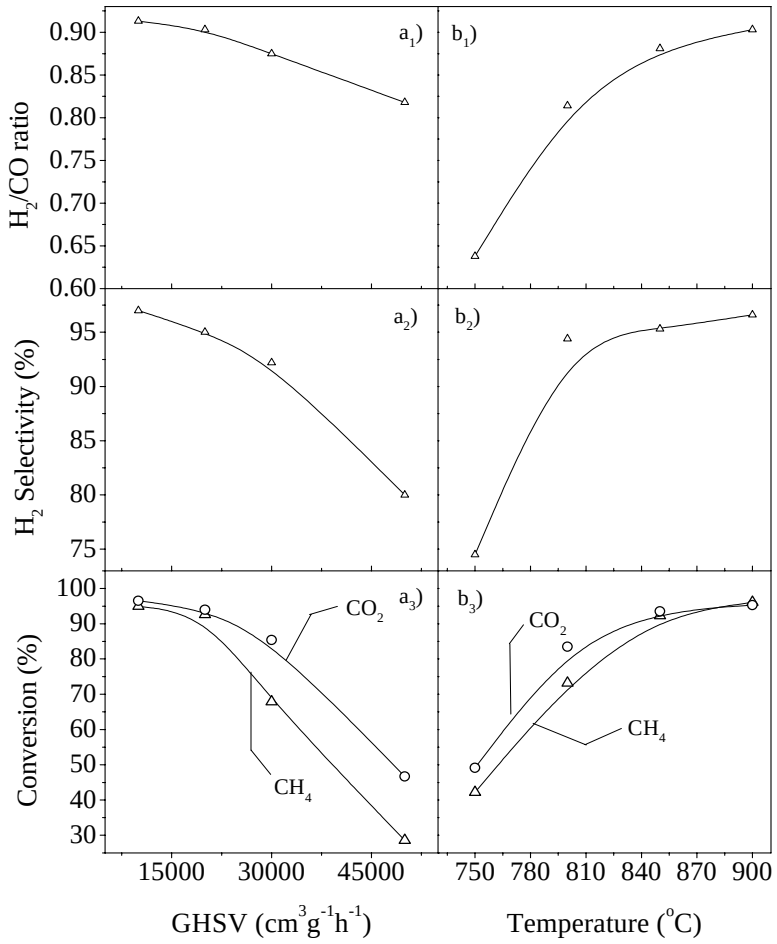

Figure 3.5. Performance of the $CoNdO_x$ (Co/Nd = 1.0) catalyst in the CO_2 reforming at different GHSVs and temperatures (CO_2/CH_4 = 1.1. For a_1, a_2, and a_3, temperature = 850 ^oC. For b_1, b_2, and b_3, GHSV = 20,000 $cm^3g^{-1}h^{-1}$)

Hence, as long as the conversion of both CO_2 and H_2O is ≥ 0, the formation of H_2 and CO is controlled only by Eqs. 6 and 7. Under this situation, the selectivity (based on methane) for both H_2 and CO is always 100% and it is also not dependent upon the process conditions (eg. temperature, pressure, space velocity). The H_2/CO ratio, however, depends strongly on the relative concentration of CO_2 and H_2O in the feed (Figure 3.6)**.** The increase in the CO_2/H_2O ratio from 0 to 2.4 has slightly affected the methane conversion but did cause a large decrease in the H_2/CO ratio (from 3.69 to 1.59). The conversion of methane even at the high space velocity (20,000 $cm^3g^{-1}h^{-1}$) is high (≈ 83 %).

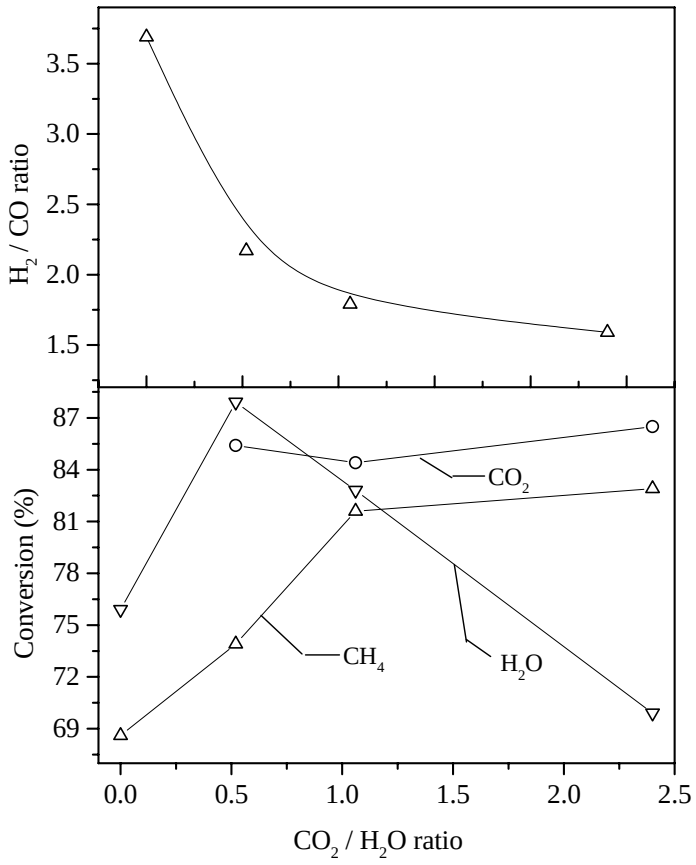

Figure 3.6. Effect of CO_2/H_2O ratio on the simultaneous steam and CO_2 reforming of methane to syngas over the $CoNdO_x$ (Co/Nd = 1.0) catalyst at 850 ^oC. (Reaction condition: $(H_2O + CO_2)/CH_4 = 1.06 \pm 0.03$; GHSV=20,000 $cm^3g^{-1}h^{-1}$)

In steam reforming over the $CoNdO_x$ (Co/Nd = 1.0) catalyst (at 850 ^oC and at a H_2O/CH_4 ratio of 1.09), the observed higher H_2/CO ratio (> 3.0 for CO_2/H_2O =0) indicates that a water gas shift reaction

$$CO + H_2O \rightarrow CO_2 + H_2 \qquad (8)$$

(ΔH_r = - 8.08 $kcalmol^{-1}$ at 850 ^oC)

occurs to an appreciable extent simultaneously with the steam reforming.

3.3.6. Oxy-CO_2 Reforming of Methane over $CoNdO_x$ (Co/Nd = 1.0): Influence of Process Parameters

3.3.6.1. Effect of temperature

The effect of temperature on the conversion, selectivity and H_2/CO product ratio and net heat of reactions (ΔH_r) involved in the oxy-CO_2 reforming process is shown in Figure 3.7. The conversion of O_2 in all cases was 100%. The CO selectivity (based on methane) is 100 %, as the conversion of CO_2 is positive. The net heat of reaction (ΔH_r) is estimated by subtracting the heat of formation (at the process temperature) of the components in the feed from that of the components in the product stream.

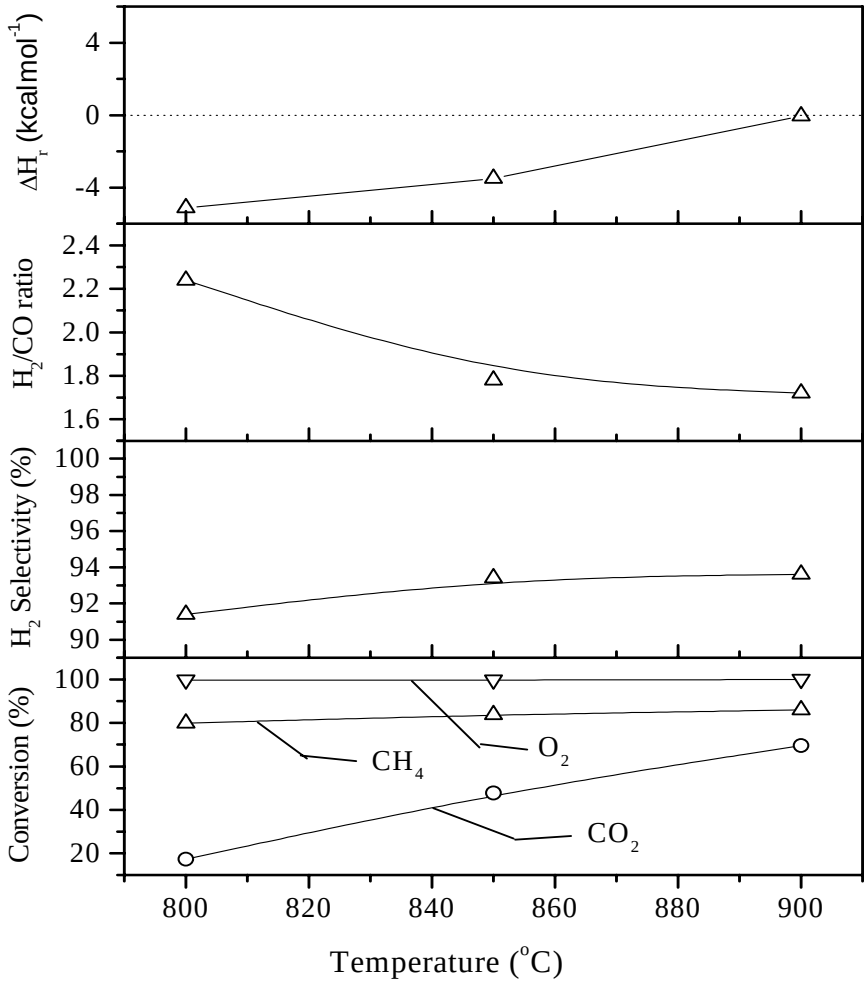

Figure 3.7. Effect of temperature on the performance of $CoNdO_x$ (Co/Nd = 1.0) catalyst in the Oxy-CO_2 reforming of methane. (O_2/CH_4 = 0.45 & CO_2/CH_4 = 0.14; $CH_4/(O_2 + 0.5CO_2)$ = 1.87; GHSV = 46,000 $cm^3g^{-1}h^{-1}$, ΔH_r = the net heat of reaction).

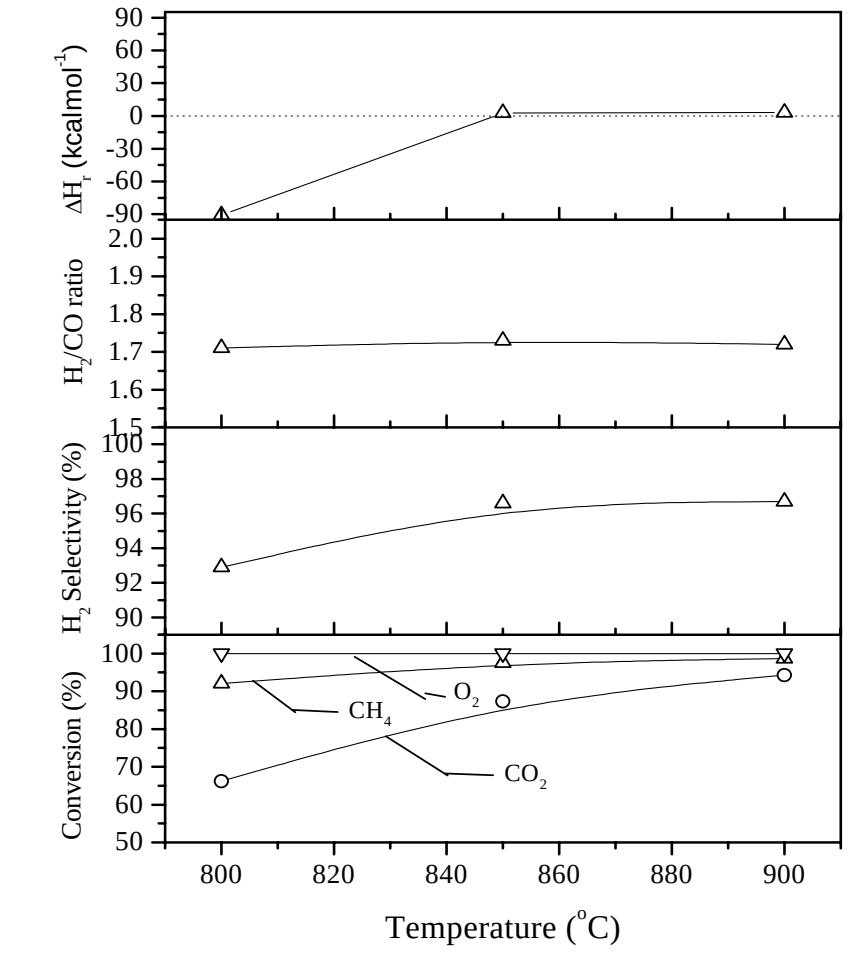

Figure 3.8. Effect of temperature on the performance of $CoNdO_x$ (Co/Nd = 1.0) catalyst in the Oxy-CO_2 reforming of methane. (O_2/CH_4 = 0.45 & CO_2/CH_4 = 0.14; $CH_4/(O_2 + 0.5CO_2)$ = 1.87; GHSV = 10,000 $cm^3g^{-1}h^{-1}$)

The results (Figure 3.7) show that, with the increase of temperature (from 800 – 900°C) in the oxy-CO_2 reforming of methane, (a) the conversion of methane and CO_2 is increased, the increase being larger in the CO_2 conversion, (b) the selectivity for H_2 is increased but to a small extent, (c) the H_2/CO ratio is decreased, whereas at lower space velocity (10,000 $cm^3g^{-1}h^{-1}$) there was little or no change in H_2/CO ratio (Figure 3.8), (d) the net heat of reaction (ΔH_r) is increased indicating a decrease in process exothermicity or an increase in the process endothermicity.

In the oxy-CO_2 reforming process, both the exothermic conversion of methane

$$CH_4 + 0.5\ O_2 \rightarrow CO + 2\ H_2 \qquad (9)$$

$(\Delta H_r = -\ 5.4\ kcalmol^{-1})$

and the endothermic CO_2 reforming of methane (Eq. 6) occur simultaneously, along with a side reverse water gas shift reaction,

$$CO_2 + H_2 \rightarrow CO + H_2O \qquad (10)$$

$(\Delta H_r = +\ 8.0\ kcalmol^{-1})$

The H_2 selectivity is lower than 100 % because of the reverse water gas shift (Eq. 10). The increase in the H_2 selectivity with increasing the temperature indicates that the reverse water gas shift reaction occurs to a small extent at the higher temperatures. However, the CO_2 reforming reaction is favoured more and more at the higher temperature. The observed decrease in the H_2/CO product ratio and increase in the value of ΔH_r (or increase in the process endothermicity) with increasing temperature are the result of a higher methane conversion by the CO_2 reforming. Thus, the reaction temperature is an important process variable for controlling the process exothermicity or endothermicity; the process can be made mildly exothermic, thermo neutral or mildly endothermic by manipulating the reaction temperature.

3.3.6.2 Effect of O_2/CH_4 ratio in feed

Results showing the influence of O_2/CH_4 ratio in the feed on the methane conversion, H_2 selectivity, H_2/CO ratio and net heat produced in the oxy-CO_2 reforming process are presented in Figure 3.9. There was no significant effect of the O_2/CH_4 ratio on the conversion of O_2. The CH_4 conversion, however, shows a small increase with increasing the O_2/CH_4 ratio. The net heat of reaction is decreased whereas the H_2 selectivity and H_2/CO ratio are increased markedly with increasing the O_2/CH_4 ratio. The $CoNdO_x$ (Co/Nd = 1.0) catalyst showed > 85 % CH_4 conversion and about 95 % H_2 selectivity at 900 ^oC for an O_2/CH_4 ratio of 0.45.

The H_2 selectivity is below 100% because of the reverse shift reaction (Eq. 10) occurring simultaneously with the oxidative conversion and CO_2 reforming of methane to syngas.

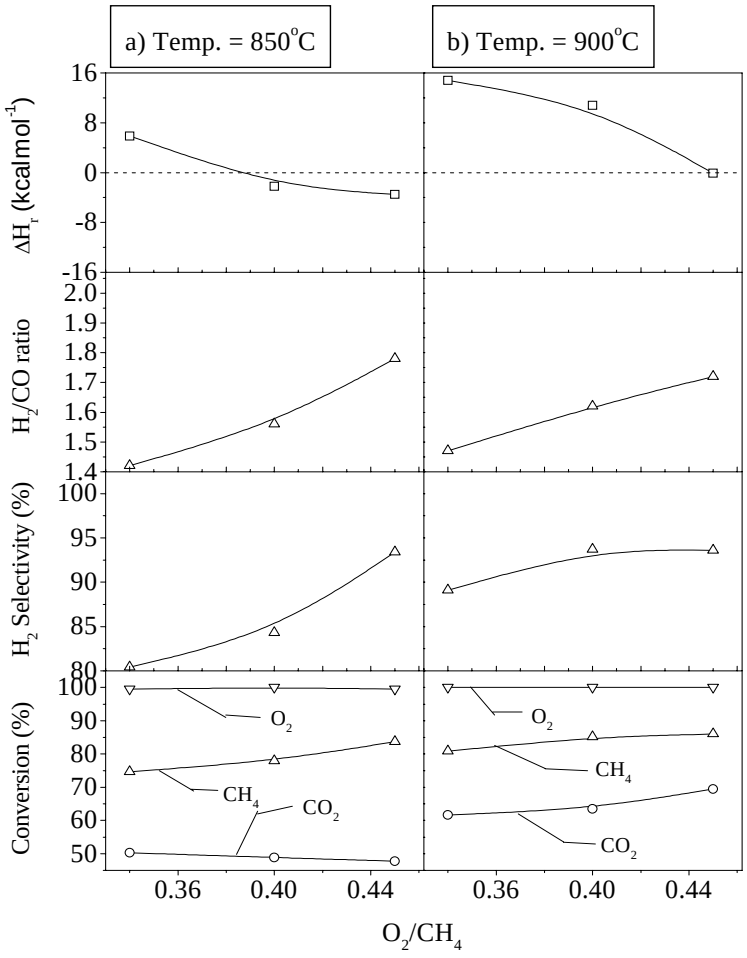

Figure 3.9. Effect of O_2/CH_4 ratio on the performance of $CoNdO_x$ (Co/Nd = 1.0) in the Oxy-CO_2 reforming of methane at a) 850 ^oC and b) 900 ^oC ($CH_4/(O_2 + 0.5CO_2)$ = 1.87; GHSV = 46,000 $cm^3g^{-1}h^{-1}$).

3.3.6.3 Effect of space velocity

Results in Figure 3.10 show a strong influence of space velocity on the process performance in the oxy-CO_2 reforming of methane over $CoNdO_x$ (Co/Nd = 1.0) catalyst at two different temperatures (850 ^oC and 900 ^oC). The conversion of both CH_4 and CO_2 is decreased almost exponentially with increasing the space velocity. The conversion of O_2 is nearly 100 %. But there is only a small effect of space velocity on the H_2 selectivity and H_2/CO ratio. The net heat produced in this process is, however, decreased markedly with increasing the space velocity.

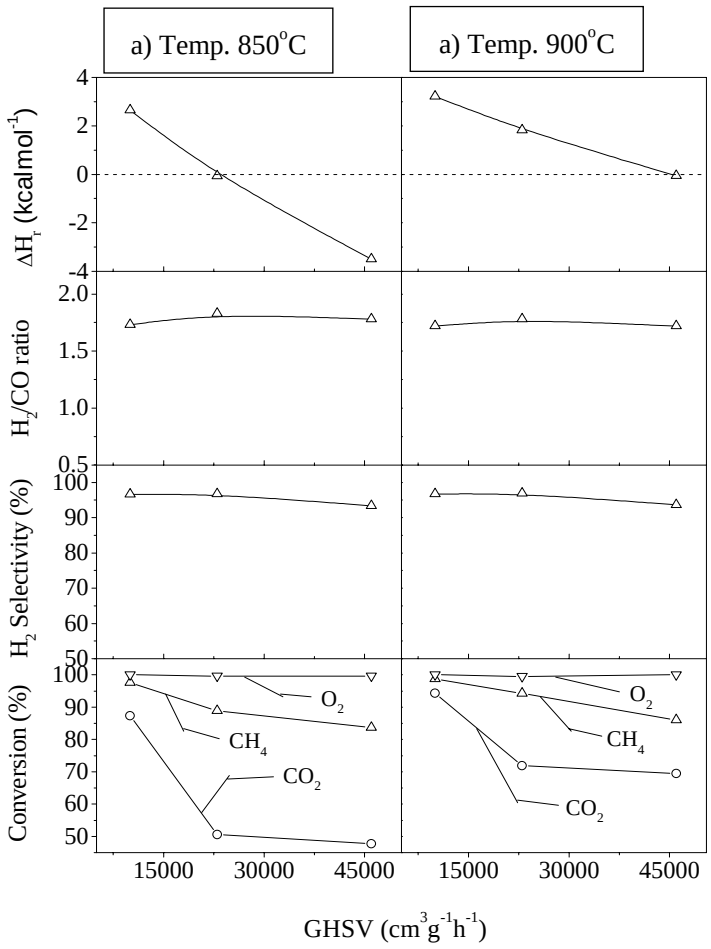

Figure 3.10. Effect of space velocity on the performance of $CoNdO_x$ (Co/Nd = 1.0) in the Oxy-CO_2 reforming of methane at a) 850 ^oC and b) 900 ^oC (O_2/CH_4 = 0.45 & CO_2/CH_4 = 0.14; $CH_4/(O_2 + 0.5CO_2)$ = 1.87).

3.4 Conclusions

From the studies on the CO_2 reforming, steam reforming, simultaneous steam and CO_2 reforming and oxy-CO_2 reforming reactions of methane for its conversion to syngas over the $CoNdO_x$ catalyst, following important conclusions have been drawn.

1. Among the different catalysts, the $CoNdO_x$ (Co/Nd = 1) is a highly promising catalyst for carbon–free CO_2 reforming of methane to syngas; the catalyst shows high activity, high selectivity and excellent stability against carbon formation during the process. No carbon formation was observed on the $CoNdO_x$ catalyst during the CO_2 reforming process at all the process conditions studies.

2. For the $CoNdO_x$ catalyst, the optimum Co/Nd ratio for its best performance is found to be 1; with this ratio, the catalyst is in the form of a perovskite-type mixed metal oxide ($NdCoO_3$).
3. The $CoNdO_x$ catalyst in its active form consists of metallic cobalt dispersed on Nd_2O_3. The catalyst is reduced and converted into its active form during the initial short period of the CO_2 reforming process.
4. The high resistance towards carbon formation for the $CoNdO_x$ catalyst is attributed to the strong interaction of metallic cobalt with Nd_2O_3 support, leading to an increase in the basicity of the support and/or a change in the electronic properties of the metallic cobalt finely dispersed on the support.
5. Methane can be converted to syngas with H_2/CO ratio close to 2.0 with 100 % selectivity for both H_2 and CO by manipulating the CO_2/H_2O ratio in the simultaneous steam and CO_2 reforming process over the $CoNdO_x$ (Co/Nd = 1) catalyst.
6. $CoNdO_x$ (Co/Nd = 1.0) is a highly promising catalyst for the oxy-CO_2 reforming of methane to syngas. The H_2/CO ratio and the net heat produced in this process can be controlled by manipulating the O_2/CH_4 ratio in the feed and / or reaction temperature.

References

[1] a) B. Hileman, Chem. Eng. News, May 3 (1999) 37 b) C. Song, ACS Symposium Ser., 809 (2002) 2.

[2] M. C. J. Bradford, M. A. Vannice, Catal. Rev.- Sci. Eng., 41 (1999) 1.

[3] J. H. Edwards, A. M. Maitra, Fuel Processing Technol., 42 (1995) 269.

[4] K. Seshan, J. A. Lercher, Spec. Publ.- R. Soc. Chem., 153 (1994) 16.

[5] V. R. Choudhary, A. M. Rajput, Ind. Eng. Chem. Res., 35 (1996) 3934.

[6] a) J. R. Rostrup-Nielsen, J. H. Bak-Hansen, J. Catal., 144 (1993) 38. b) E. Ruckenstein, Y. H. Hu, Appl. Catal. A: Gen., 133 (1995) 149 c) V. R. Choudhary, A. S. Mamman, Appl. Ener*gy*, 66 (2000) 161. d) B – Q. Xu, J. M. Wei, H – Y. Wang, K – Q. Sun, Q – M. Zhu, Catal. Today, 68 (2001) 217.

[7] V. R. Choudhary, A. S. Mamman, J. Chem. Technol. Biotechnol., 73 (1998) 345.

[8] V. R. Choudhary, B. S. Uphade, A. S. Mamman, Appl. Catal. A: Gen., 168 (1998) 33.

[9] V. R. Choudhary, B. S. Uphade, A. S. Mamman, R. E. Babcock, ACS Symp. Ser., 809 (2002) 224.

[10] J – M. Wei, B – Q. Xu, J –L. Li, Z – X. Cheng Q – M. Zhu, ACS Symp. Ser., 809 (2002) 197.

[11] a) E. Ruckenstein, Y. H. Hu, J. Catal., 162, 1996, 230 – 238. b) Z ‑ X. Cheng, X.‑ G. Zhao, J – L. Li, Q – M. Zhu, Appl. Catal. A: Gen., 205 (2001) 31. c) T. Osaki, H. Masuda, T. Horiuchi, T. Mori, Catal. Lett. 34 (1995) 59. d) H – Y. Wang, E. Ruckenstein, Catal. Lett., 75 (2001) 13. e) L. Ji, S. Tang, J. Lin, K.L. Tan, Appl. Catal. A: Gen., 207 (2001) 247.

[12] E. Ruckenstein, H. Y. Wang, Catal. Lett., 70 (2000) 15. Appl. Catal. A: Gen., 204 (2000) 257, b) H.Y. Wang, E. Ruckenstein, Appl. Catal., 209 (2001) 207.

[13] a) F. Solymosi, G. Kutsan, A. Erdohelyi, Catal. Lett., 11 (1991) 149. b) Y. Z. Chen, B – J. Liaw, C – F. Kao, J – C Kuo, Appl. Catal. A: Gen., 217 (2001) 23. c) Y. Z. Chen, B – J. Liaw, W – H. Lai, Appl. Catal. A: Gen., 230 (2002) 73, d) K. Nagaoka, K. Seshan, K – I. Aika, J. A. Lercher, J. Catal., 197 (2001) 34.

[14] a) J. T. Richardson, S. A. Paripatydar, Appl. Catal., 61 (1990) 293. b) A. Erdohelyi, J. Cserenyi, F. Solymosi, J. Catal., 141 (1993) 287. c) J. Nakamura, A. Aikawa, K. Sato, T. Uchijima, Catal. Lett., 25 (1994) 265. d) H. Y. Wang, E. Ruckenstein, Appl. Catal. A: Gen., 204 (2000) 143. e) S. T. Srimat, C. Song, ACS Symp. Ser., 809 (2002) 289.

[15] J. S. H. Q. Perera, J. W. Couves, G. Sanker, J. M. Thomas, Catal. Lett., 11 (1991) 219.

[16] I. M. Bodrov, L. Q. Apel'baum, Kinet. Katal., 8 (1967) 379.

[17] N. R. Udengaard, J. H. Bak Hansen, D. C. Hanson, J. A. Stal, Oil Gas J., 90 (1992) 62.

[18] D. Qin, J. Lapszewicz, Catal. Today, 21 (1994) 551.

[19] E. Riensche, H. Fedder, Stud. Surf. Catal., 21 (1994) 551.

[20] V. R. Choudhary, A. S. Mamman, B. S. Uphade, Prepr.- Am. Chem. Soc. Div.Fuel Chem., 46 (2001) 104.

[21] a) T. Horiuchi, K. Sakuma, T. Fukui, Y. Kubo, T. Osaki, T. Mori, Appl. Catal. A: 144 (1996) 111. b) T. Osaki, T. Mori, J. Catal. 204 (2001) 89.

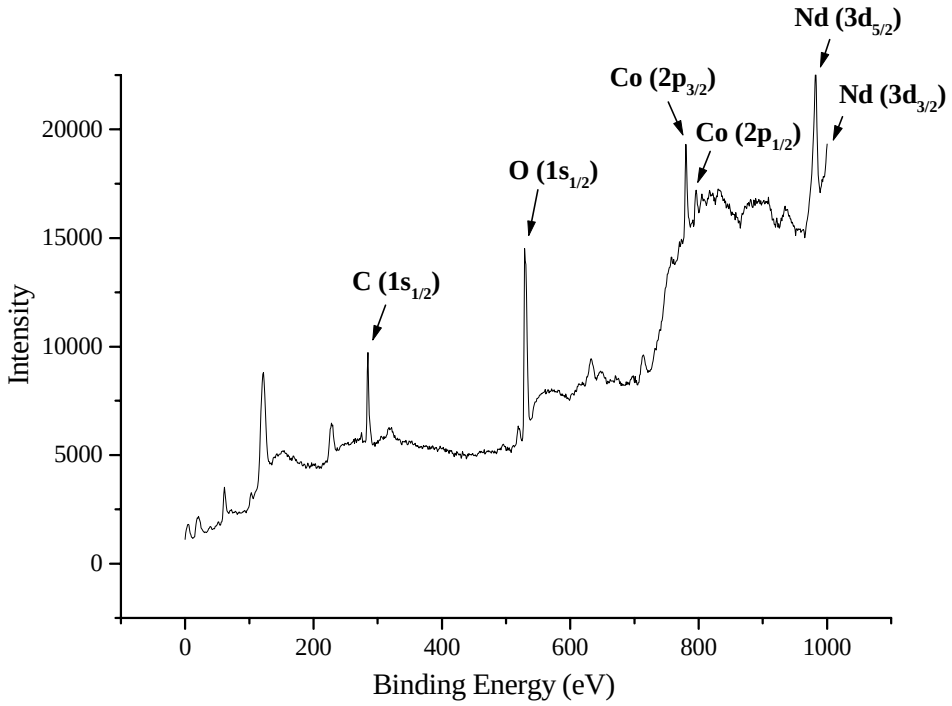

Appendix 3.1. XPS spectra of $CoNdO_x$ (Co/Nd=1.0) catalysts before CO_2 reforming reaction at 850 ^oC

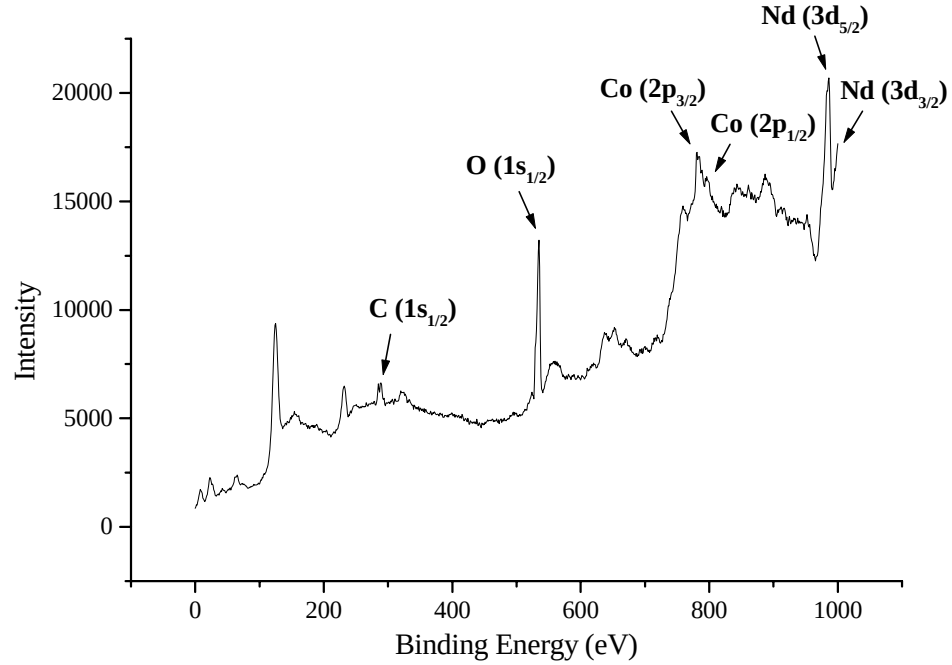

Appendix 3.2. XPS spectra of $CoNdO_x$ (Co/Nd=1.0) catalysts after CO_2 reforming reaction at 850 ^oC

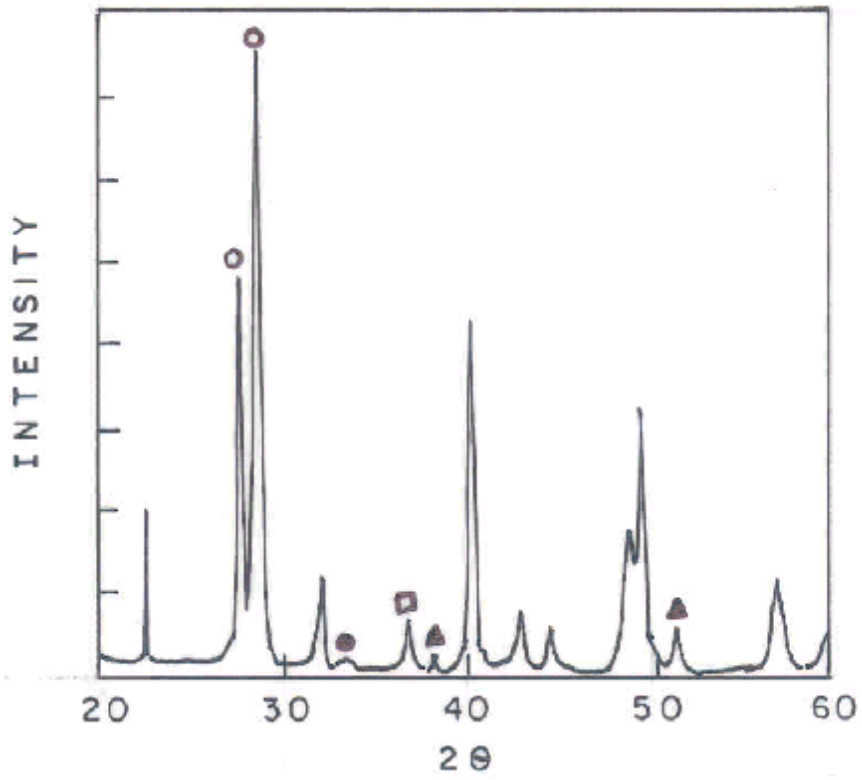

Appendix 3.3. XRD spectra for $2\theta = 20 - 60^{o}$ of the $CoNdO_x$ (Co/Nd = 0.1) catalyst before the CO_2 reforming reaction. [Symbol used here for the identification of different phases; O → Nd_2O_3; ● → $NdCoO_3$ perovskite type; □ → Co_3O_4; ▲ → Co_2O_3]

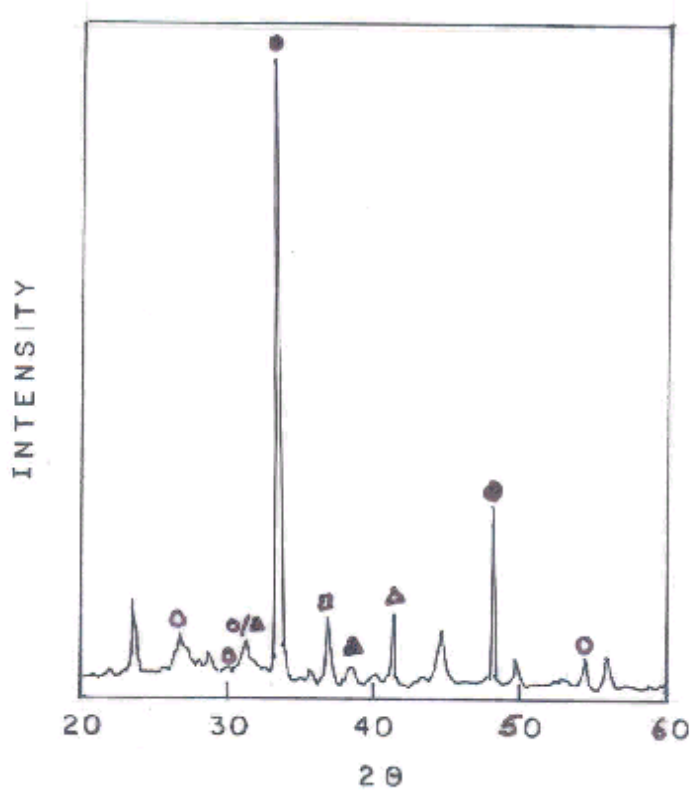

Appendix 3.4. XRD spectra for 2θ = 20 – 60 ^{o} of the $CoNdO_x$ (Co/Nd = 0.1) catalyst before the CO_2 reforming reaction. [Symbol used here for the identification of different phases; O → Nd_2O_3; ● → $NdCoO_3$ perovskite type; □ → Co_3O_4; ▲ → Co_2O_3; Δ → CoO]

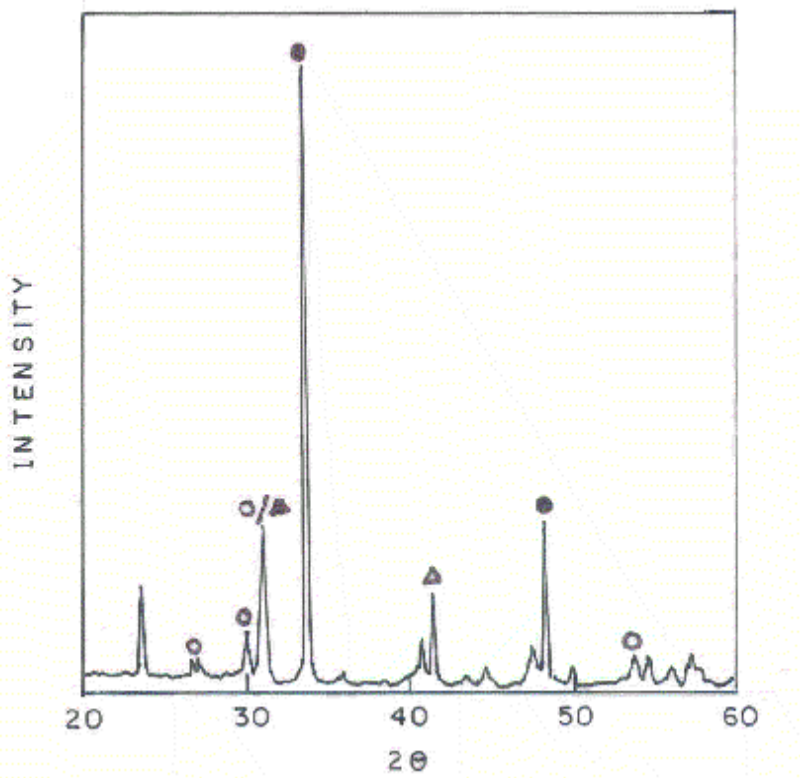

Appendix 3.5. XRD spectra for 2θ = 20 – 60 ^{o} of the $CoNdO_x$ (Co/Nd = 2.0) catalyst before the CO_2 reforming reaction. [Symbol used here for the identification of different phases; O → Nd_2O_3; ● → $NdCoO_3$ perovskite type; ▲ → Co_2O_3; Δ → CoO]

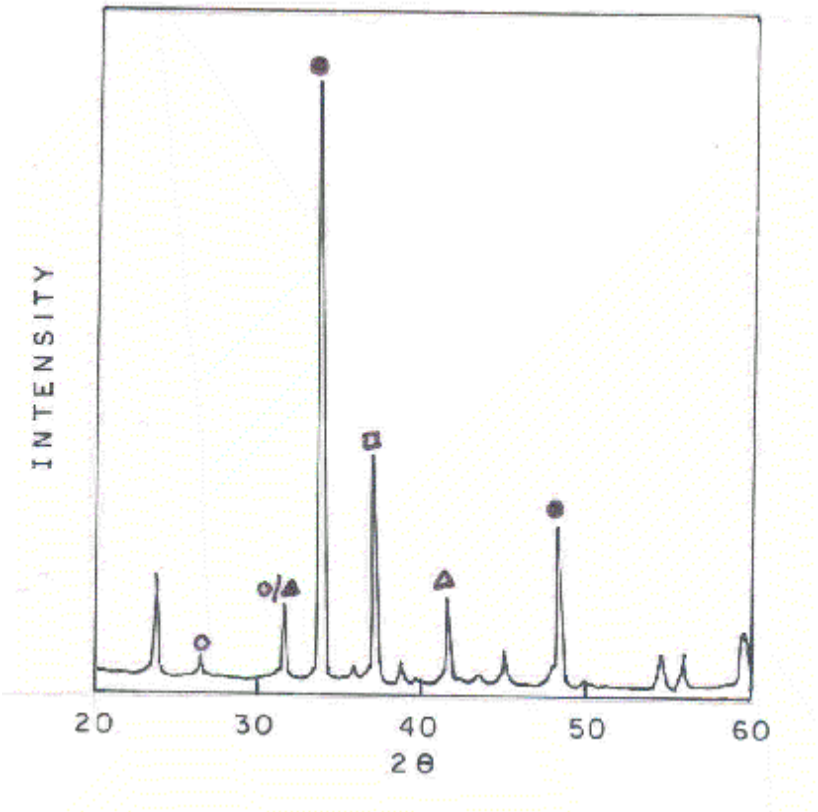

Appendix 3.6. XRD spectra for 2θ = 20 – 60 ^{o} of the $CoNdO_x$ (Co/Nd = 4.0) catalyst before the CO_2 reforming reaction. [Symbol used here for the identification of different phases; O → Nd_2O_3; ● → $NdCoO_3$ perovskite type; ▲ → Co_2O_3; Δ → CoO; □ → Co_3O_4]

CHAPTER 4

CO_2 REFORMING AND OXY-CO_2 REFORMING OF METHANE TO SYNGAS OVER COBALT SUPPORTED ON DIFFERENT COMMERCIAL MACROPOROUS CATALYST CARRIERS PRECOATED WITH DIFFERENT METAL OXIDES

CHAPTER 4

CO_2 REFORMING AND OXY-CO_2 REFORMING OF METHANE TO SYNGAS OVER COBALT SUPPORTED ON DIFFERENT COMMERCIAL MACROPOROUS CATALYST CARRIERS PRECOATED WITH DIFFERENT METAL OXIDES

4.1. Earlier Work / Background and Objective of the Present Work

Conversion of methane to CO and H_2 (i.e. syngas, which is a versatile feed stock for ammonia, methanol and Fischer-Tropsch synthesis processes and several other carbonylation and hydrogenation or reduction processes) in an energy efficient and safe manner by the coupling of the exothermic (partial oxidation with O_2) and endothermic (steam and/or CO_2 reforming) reactions of methane [1–3] is a process of great practical importance. A few studies have been reported on oxy-CO_2 reforming of methane over supported Rh [4], NiO-CaO, Ni/ALPO-5 [3–5], Pt/$CoAl_2O_4$/Al_2O_3 [7-9] catalysts, and CO_2 reforming of methane over NiO-CaO, Ni/ALPO-5 and $LaNiO_3$ catalysts [1,5,6]. Recently, extensive studies have been reported on the CO_2 reforming of methane over supported Pt group metals [10-13], NiO-alkaline earth oxide [12], Ca-promoted Ni/α-Al_2O_3 [14], NiO and NiO-MgO [17], Ni / γ-Al_2O_3 [15], Co / γ-Al_2O_3 [16], Co / MgO, CaO, SrO or BaO [18] catalysts.

In our earlier studies [19], NiO-MgO catalyst showed high activity and selectivity in the partial oxidation of methane to syngas at extremely low contact times ($\approx$ 1 ms). Supported nickel catalysts prepared using silica- and/or alumina- and/or silica- containing commercial low surface area sintered macroporous catalyst carriers, precoated with MgO, CaO or rare earth oxides, show much higher activity, selectivity and productivity in the methane-to-syngas conversion process than the catalysts prepared using the catalyst carriers without any precoating [20]. It is, therefore, interesting to study CO_2 reforming and oxy-CO_2 reforming of methane to syngas over cobalt deposited over different commercial low surface area macroporous supports precoated with different metal oxides (viz. MgO, ZrO_2, CeO_2 & ThO_2) for developing a better catalyst for these processes.

4.2. Experimental

The preparation procedure of different supported Co - containing catalysts used in this investigation has been discussed earlier (Section 2.1.1.3. & 2.1.1.4.). In short, the catalysts

were prepared by depositing cobalt nitrate from its aqueous solution on 22-30 mesh size particles of different commercial macroporous catalyst carriers [obtained from Norton, USA] precoated with different metal oxides, using an incipient wetness impregnation technique, followed by drying and calcining in air at 900 ^{o}C for 4 h.

All the catalysts were characterized by X-ray diffraction, using CuKα radiation source, and also by temperature programmed reduction (TPR) in a flow of 5.0 mol% H_2 in Ar at a linear heating rate of 10 ^{o}C min^{-1} from 40 ^{o} to 1100 ^{o}C, using a thermal conductivity detector. The catalyst was also characterized by X–ray photoelectron spectroscopy.

The experimental procedure for the CO_2 reforming with or without simultaneous partial oxidation of methane to syngas reactions over the catalysts, has already been described (Section 2.3.2 & 2.3.3 and Fig. 2.5). The reactions were carried out at atmospheric pressure by passing continuously a gaseous feed containing pure methane and carbon dioxide (CO_2/CH_4 mole ratio = 1.1) and/or oxygen over the catalyst (0.3 g) packed in a quartz tubular reactor (Fig. 2.2), provided with a thermocouple in the catalyst bed, at different GHSVs (gas hourly space velocity, measured at 0 ^{o}C and 1 atm pressure) and temperatures. The reactor effluent gases were cooled to about 2 ^{o}C using a coiled condenser immersed in the ice-water slurry to remove the water from the product gases. After attending the reaction steady state, the reaction products were analyzed by a gas chromatograph with thermal conductivity detector using Spherocarb column. The carbon deposited on the catalyst during the reaction for a period of 15 ± 2h was determined by oxidizing it to CO_2 in a flow of air (60 cm^3/min) for a period of 2h at 800 ^{o}C and measuring quantitatively the amount of CO_2 produced by absorbing it in barium hydroxide solution forming barium carbonate, which was then estimated gravimetrically.

The C, H, and O balance errors across the reactor was within 2 – 6 %. All experiments with larger errors in the material balance were rejected. The H_2 and CO selectivities reported in this chapter are based on the methane converted in the reactions.

4.3. Results and Discussions

4.3.1. CO_2 Reforming of Methane to Syngas over Cobalt Deposited on Low Surface Area Macroporous inert Silica-Alumina (SA-5205) and Zirconia (SZ-5564) Supports Precoated with MgO, ZrO_2, CeO_2, ThO_2 or Y_2O_3

4.3.1.1. Time-on-stream (TOS) activity of cobalt deposited on SA-5205 support precoated with MgO, ZrO_2, CeO_2, ThO_2 or Y_2O_3 catalysts

The time-dependent conversion of CH_4 and selectivity of H_2 for the different Co - containing catalysts are presented in Fig. 4.1 and Table 4.1. The CoO/ZrO_2/SA-5205, CoO/CeO_2/SA-5205, CoO/Y_2O_3/SA-5205 and CoO/ThO_2/SA-5205 catalysts showed high activity (methane conversion > 80 %) and also high H_2 selectivity (> 92 %) with no carbon deposition on them during the CO_2 reforming process. A very little carbon formation was observed (Table 4.1) in the reaction, when the CoO/MgO/SA-5205 was used as the CO_2 reforming catalyst. However, this catalyst showed not only high activity (methane conversion > 98 %) with high H_2 selectivity (> 93 %) at a high space velocity (20,000 $cm^3g^{-1}h^{-1}$) but also high stability against the catalyst deactivation in the process (Fig. 4.1). Both the methane conversion and selectivity for H_2 are increased to a small extent in the initial short period of about 1 h and thereafter remained almost constant in the CO_2 reforming process over CoO/MgO/SA-5205 catalyst. However, for the ThO_2 containing catalyst, the catalytic activity passed through a maximum with the TOS, indicating activation (during initial period) & deactivation (at the higher period) of the catalyst.

4.3.1.2. Time-on-stream (TOS) activity of cobalt deposited on SZ-5564 support precoated with MgO, ZrO_2, CeO_2, ThO_2 or Y_2O_3 catalysts

In general, the SZ-5564 supported catalysts show lower activity (Fig. 4.2 & Table 4.1) than the SA-5205 supported catalysts. Both the methane conversion activity and selectivity for H_2 are increased to a large extent in the initial short period of about 3 h and thereafter remained almost constant in the reaction, when the CoO/MgO/SZ-5564 was used as the CO_2 reforming catalyst. During the initial CO_2 reforming period (up to 3 h), the catalyst is reduced, first by the methane from the feed and then by the H_2 and CO produced in the reforming of methane over the partially reduced catalyst. Consequently, both the activity and H_2 selectivity in the reforming over the catalyst are increased with the time in the initial short period (up to about 3 h) and then remained constant for the further period.

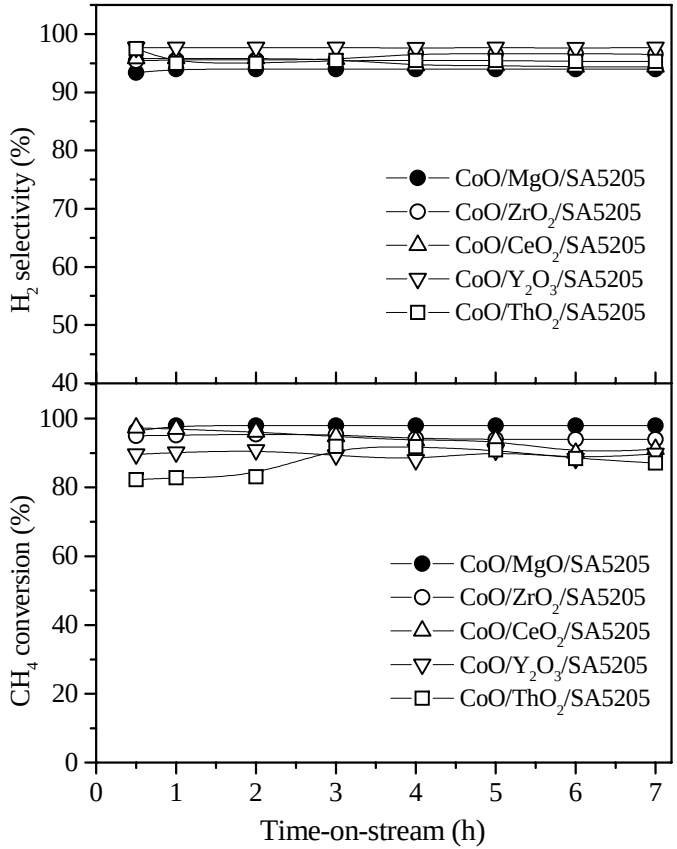

Figure 4.1 Time-on-stream activity/selectivity of the CoO_x containing catalysts supported on SA-5205 for the CO_2 reforming reaction at 850 ^oC [GHSV=20000 $cm^3g^{-1}h^{-1}$, CO_2/CH_4=1.1]

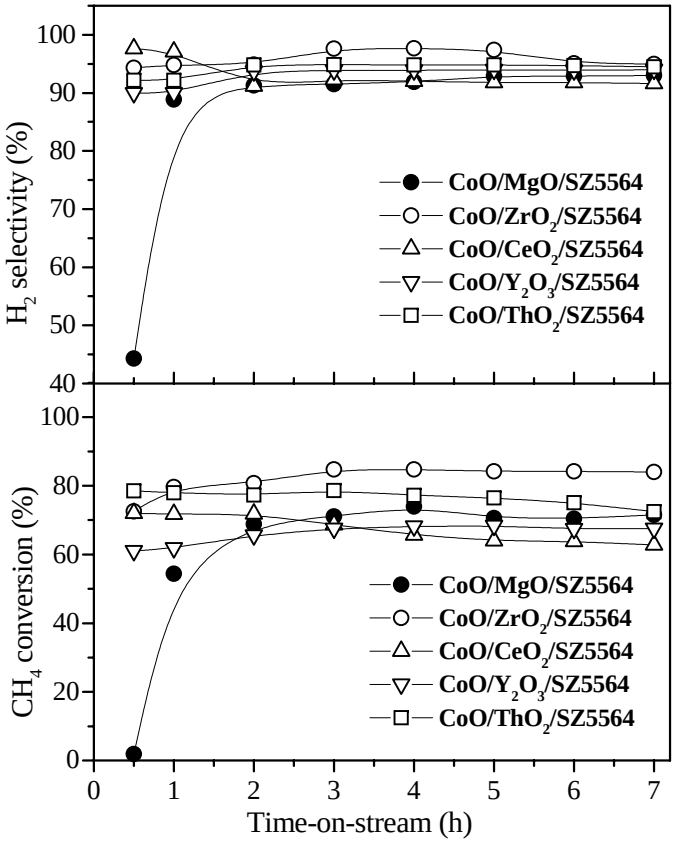

Figure 4.2 Time-on-stream activity/selectivity of the CoO_x containing catalysts supported on SZ-5564 for the CO_2 reforming reaction at 850 ^oC [GHSV= 20000 $cm^3g^{-1}h^{-1}$, CO_2/CH_4 = 1.1]

Table 4.1 Carbon deposited on the supported catalysts.

Catalyst	Time-on-stream (h)	CH_4 conversion (%)	H_2 selectivity (%)	Rate of carbon deposited ($g^{-1}_{(carbon)}\, g^{-1}_{(catalyst)} h^{-1}$)
CoO/MgO/SA-5205	7	99.0	93.9	0.0001592
CoO/ZrO_2/SA-5205	6	93.9	96.6	No carbon
CoO/CeO_2/SA-5205	7	91.3	94.5	No carbon
CoO/Y_2O_3/SA-5205	7	89.6	97.8	No carbon
CoO/ThO_2/SA-5205	7	91.0	95.3	No carbon
CoO/MgO/SZ-5564	7	71.5	93.0	0.0002432
CoO/ZrO_2/SA-5564	7	84.2	95.1	No carbon
CoO/CeO_2/SZ-5564	7	63.8	91.8	No carbon
CoO/Y_2O_3/SZ-5564	7	67.5	94.0	No carbon
CoO/ThO_2/SZ-5564	6	72.5	94.5	0.001023

4.3.2. CO_2 Reforming of Methane to Syngas over Co-containing Catalyst Supported on Different Commercial Catalyst Carriers Precoated with MgO: Influence of support, CoO loading and process conditions.

4.3.2.1. Catalyst characterization

The Co-containing catalysts (with different Co loadings) supported on SA-5205 precoated with MgO (precalcined at 900 ^oC) were characterized for their surface and bulk properties. The results of catalyst characterization are presented in Tables 4.2 and 4.3 and Figs. 4.3 – 4.8.

The XRD (Fig. 3) studies were carried out to determine the crystalline phases present in these catalysts. The different crystalline phases present in the catalyst are strongly influenced by the Co loading (Table 4.2). The XRD analysis showed no presence of a separate CoO phase, indicating a formation of a solid solution [(Co, Mg) O] between CoO and MgO in the supported catalyst. However, a minor phase $MgAl_2O_4$, resulting from a solid-solid reaction between MgO and Al_2O_3 (from the support) at the MgO-support interface, was observed. The

formation of this phase (which consumes most of the alumina from the support surface) between the active catalyst mass (i.e. CoO-MgO solid solution) and the support is essential

Table 4.2 Surface and bulk properties of the Co-containing catalysts (with different Co-loadings) supported on SA-5205 precoated with MgO (precalcined at 900 ^{o}C)

Co loading (%)	XRD phases
5	Al_2SiO_5 (sillimanite), $MgAl_2O_4$, $MgAl_2O_4$ (Spinel), (Co, Mg) O (solid solution, major), $MgCo_2O_4$ (minor), Co_2O_3 (minor), α - Al_2O_3 (major)
10	Al_2SiO_5 (sillimanite), $MgAl_2O_4$ (major), $MgAl_2O_4$ (Spinel), (Co, Mg) O (solid solution, major), $MgCo_2O_4$ (minor), Co_2O_3 (minor), α - Al_2O_3
20	Al_2SiO_5 (sillimanite), $MgAl_2O_4$, $MgAl_2O_4$ (Spinel), (Co, Mg) O (solid solution, major), $MgCo_2O_4$ (major), Co_2O_3 (minor), α - Al_2O_3
30	Al_2SiO_5 (sillimanite), $MgAl_2O_4$, $MgAl_2O_4$ (Spinel), (Co, Mg) O (solid solution, major), $MgCo_2O_4$ (major), Co_2O_3, α - Al_2O_3

for avoiding the formation of catalytically inactive $CoAl_2O_4$ (spinel) phase, which is difficult to reduce. With increasing Co-loading, the intensities of Co_2O_3 and $MgCo_2O_4$ phases increase. The formation of Co_3O_4 phase is not observed in all the catalysts with different Co-loading. The catalyst with 20 % cobalt loading showed the presence of $MgCo_2O_4$ mixed metal oxide and [(Co, Mg) O] solid solution as the major crystalline phases, with the minor (or very small)

crystalline phases like Co_2O_3, and $MgAl_2O_4$ (spinel). The reduction of $MgCo_2O_4$ during the initial period of the CO_2 reforming process (Fig.4.1) is expected to produce finely dispersed metallic cobalt on the support, as in case of the reduction of Ni- or Co- containing mixed metal oxides [21].

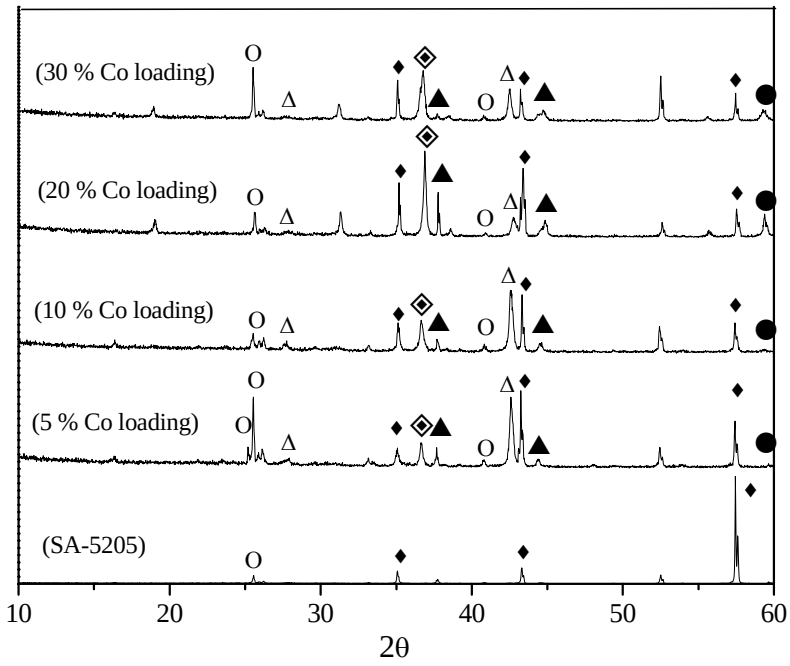

Figure 4.3 XRD spectra of the SA-5205 catalyst carrier and the Co-containing catalysts (with different Co loadings) supported on SA-5205 precoated with MgO (precalcined at 900 ^oC) before their use in CO_2 reforming reaction. [Symbol used here for identifying of different phases; O → Al_2SiO_5; • → $MgCo_2O_4$; ◈ → (Co, Mg) O solid solution; ▲ → $MgAl_2O_4$ (spinel); Δ → $MgAl_2O_4$; □ → Co_2O_3; and ♦ → α-Al_2O_3]

The formation of different crystalline phases with rise in the temperature from 40 ^{o} to 1200 ^oC were studied (Fig. 4.4) by performing insitu X-ray diffraction analyses, using Bruker XRD diffractometer equipped with a Cu tube (Cu Kα radiation), a monochromator, an automatic variable divergent slit and 1.0 mm receiver slit. Samples were analyzed in θ-2θ coupled mode with 0.01-degree step size and 2 s/step sampling time. It is observed that CoO (produced from the decomposition of Co $(NO_3)_2$) either diffuse into the MgO matrix to form a solid solution (2θ = 42.8 degree) at temperature >750^oC or was oxidized to Co_2O_3 (2θ = 31.0 degree) at low temperature (500^oC); the later reacted either with CoO to form Co_3O_4 (2θ = 31.0 and 53 degree,

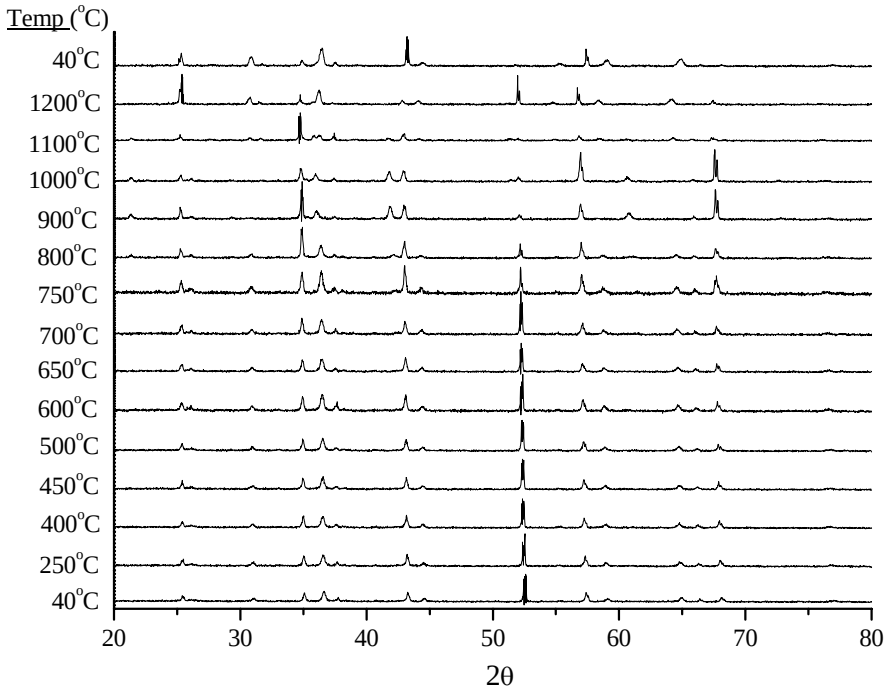

Figure 4.4 In situ XRD of the CoO (20%)/MgO (5 %)/SA-5205 catalyst (calcined at 400 °C) at different temperatures

respectively) or with MgO to generate $MgCo_2O_4$ (around 2θ = 59 degree). With increasing the temperature upto 800 °C, Co_3O_4 and $MgCo_2O_4$ partially decomposed because they are unstable at higher temperature [24]. At the higher temperature (> 900 °C), the Co_3O_4 phase was no longer present. That is why Co_3O_4 phase has disappeared at 900 °C but again at higher temperature one peak is observed at the same 2θ range (2θ = 31 degree), which is due to the formation of Co_2O_3 phase. There are also some interesting phase changes shown by the XRD peak around 2θ = 25.5 degree at 1200 °C temperature due to the formation of Al_2SiO_5 (sillimanite), which is formed at higher temperature. There are some other phase changes shown by the XRD peak around 2θ = 42.5 degree initiating at 800 °C, prominent at 900 and 1000 °C but disappearing at or after 1100 °C. This peak is due to the formation of $MgAl_2O_4$ crystalline phase. The XRD peak around 2θ = 43 ° is also reduced with increasing the temperature from 800 °C to 1200 °C but after cooling the catalyst (at 40 °C), it becomes highly prominent.

XPS spectra for C 1s, O 1s and Co $2p_{3/2}$ of the fresh and used (after the time-on- stream activity run for the CO_2 reforming of methane at 850°C for 7 h) catalyst (with 20 % cobalt loading) are presented in Figs. 4.5 – 4.7, and the binding energy data and the surface atomic

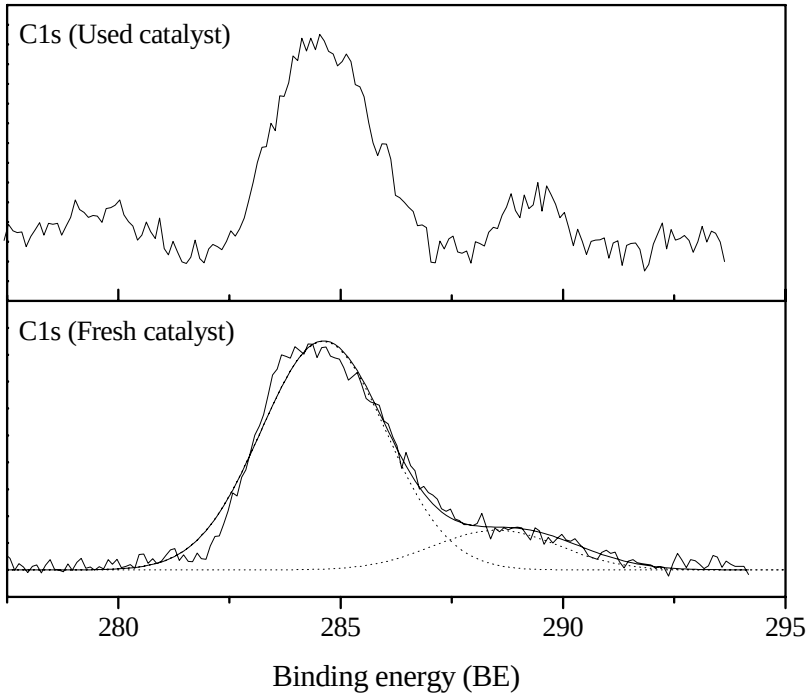

Figure 4.5 C 1s XPS spectra of CoO (20%)/MgO (5 %)/SA-5205 catalyst before and after its use in the CO_2 reforming reaction at 850 ^oC

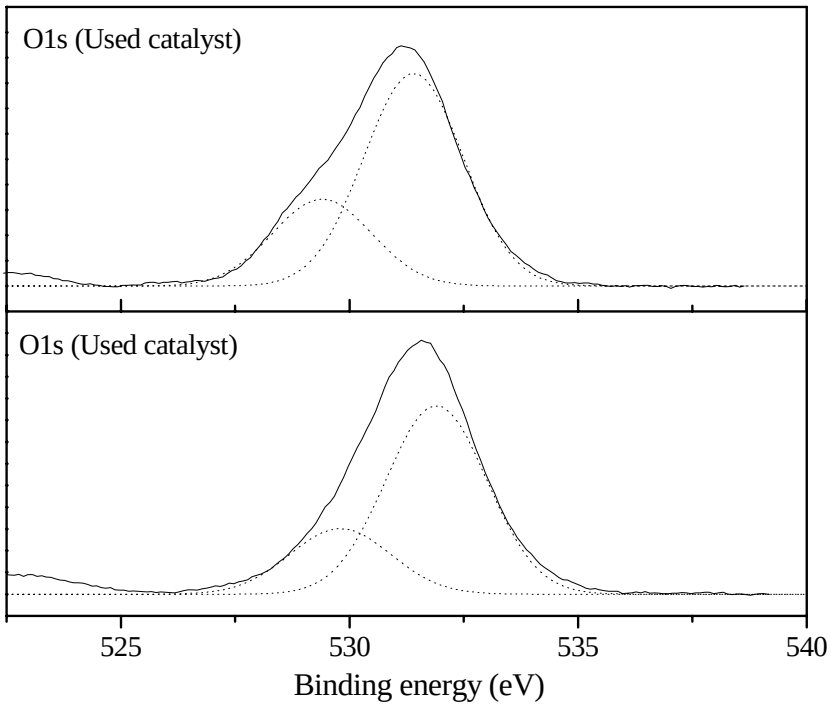

Figure 4.6 O 1s XPS spectra of CoO (20%)/MgO (5 %)/SA-5205 catalyst before and after its use in the CO_2 reforming reaction at 850 ^oC

concentrations of different elements are given in Table 4.3. The C 1s peak at the higher binding energy (about 289 eV) (Fig. 4.5) indicates the presence of surface carbonate (CO_3^{2-}) species in both the fresh and used catalysts. The surface carbonate species are expected to be formed by the interaction of CO_2 from atmosphere (for the fresh catalyst) or from the feed/reaction products with the catalyst. However, the C 1s peak at the lower binding energy (279.3 eV), observed for the used catalyst (Fig. 4.5), may be due to partially hydrogenated carbonaceous species. The XPS analysis of the O 1s of the fresh and used catalysts showed two XPS peaks – a small peak for BE (binding energy) of 529.2 eV and a much larger peak for BE of 531.7 eV (Fig. 4.6). However, after the reaction, the XPS peak at lower BE (529.4 eV) is increased markedly, indicating an increase in the basicity and / or large changes in the electronic properties of the catalyst, which are expected to result from the interaction of metallic cobalt (formed during the reaction) with the support. Also the area ratio of the two peaks for both the catalysts change significantly from 0.19 for the fresh catalyst to 0.42 for the used catalyst.

Table 4.3 XPS data for CoO (20 %)/MgO (5 %)/SA-5205 (calcined at 900 ^oC) catalyst before and after its use in the CO_2 reforming reaction.

Catalyst	Binding energy (eV)				Surface atomic concentration (%)		
	C 1s	O 1s	Co $2p_{3/2}$	Mg 2p	Co	Mg	O
Fresh	284.6 288.5	529.2 531.7	780.7	49.7	3.58	22.1	74.3
Used	279.3 284.6 289.6	529.4 531.5	778.8 780.7	49.3	3.31	26.6	70.1

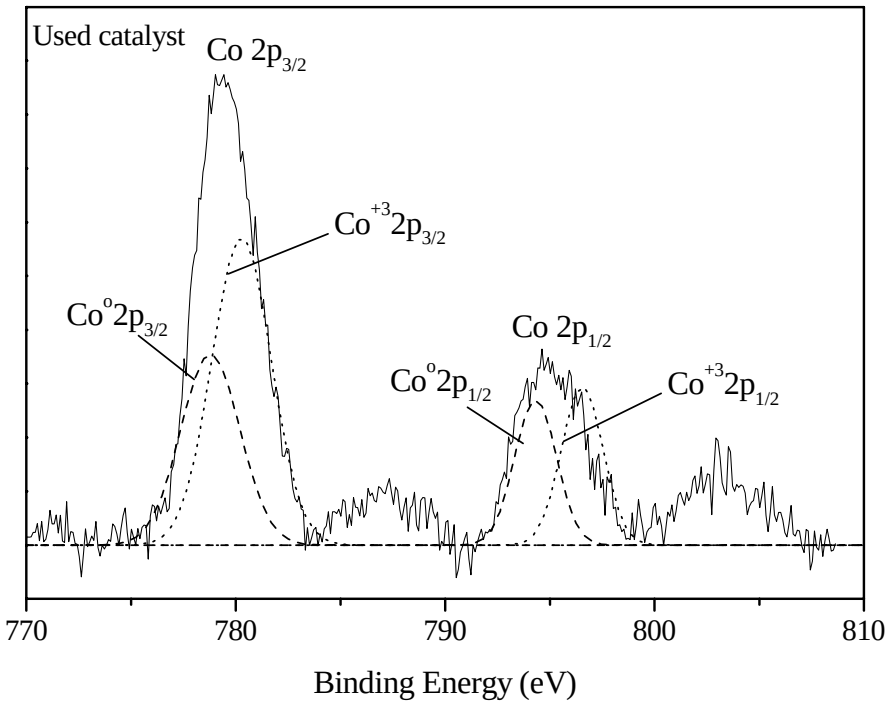

Figure 4.7 Co $2p_{3/2}$ XPS spectra of CoO (20%)/MgO (5 %)/SA-5205 catalyst after use in the CO_2 reforming reaction at 850 ^oC

The XPS spectra for Co $2p_{3/2}$ (Fig. 4.7) show the presence of Co^{3+} (BE around 780.7 eV) on the surface of both the fresh and used catalysts. However, a small concentration of surface Co^o (BE = 778.8 eV) is observed for the used catalyst. The observed binding energy of Co $2p_{3/2}$ for the fresh and used catalysts shifted towards higher energy side by about 0.7 eV is attributed to probable strong interactions of the metallic Co with the support. The metallic cobalt-support interactions seem to be responsible for the observed a very little carbon formation on the catalyst during the CO_2 reforming process. However, only a small change in the binding energies for O 1s and Mg (2p) is observed. It is also interesting to note that the surface concentration of cobalt in the used catalyst is decreased slightly, which may be caused by the coke deposition (Table 4.3).

The above results reveal that the cobalt oxide in the catalyst is atleast partly reduced during the reforming reaction. Hence, it is interesting to study the catalyst reduction. The TPR of the catalyst with the different Co loadings has been carried out by H_2 (5 % H_2 in Ar) from 40 ^oC to 1100 ^oC at a linear heating rate of 20 $^oCmin^{-1}$. The TPR curves of all the catalysts with different Co loadings indicate that the catalyst reduction occurs in three distinct steps, as shown

by the three distinct TPR peaks. The higher temperature TPR peak (above 800 ^{o}C) indicates the reduction of (Co, Mg) O solid solution. A comparison of the TPR peaks for the CoO/MgO/SA-5205 catalysts reveal that, the cobalt in higher oxidation state [Co (III)] is reduced to lower oxidation state [Co (II)] in the first step and the reduction Co (II) to Co (0) occurs in the second step.

$$Co_2O_3 \xrightarrow{H_2} Co_3O_4 + CoO \xrightarrow{H_2} Co^{o}$$

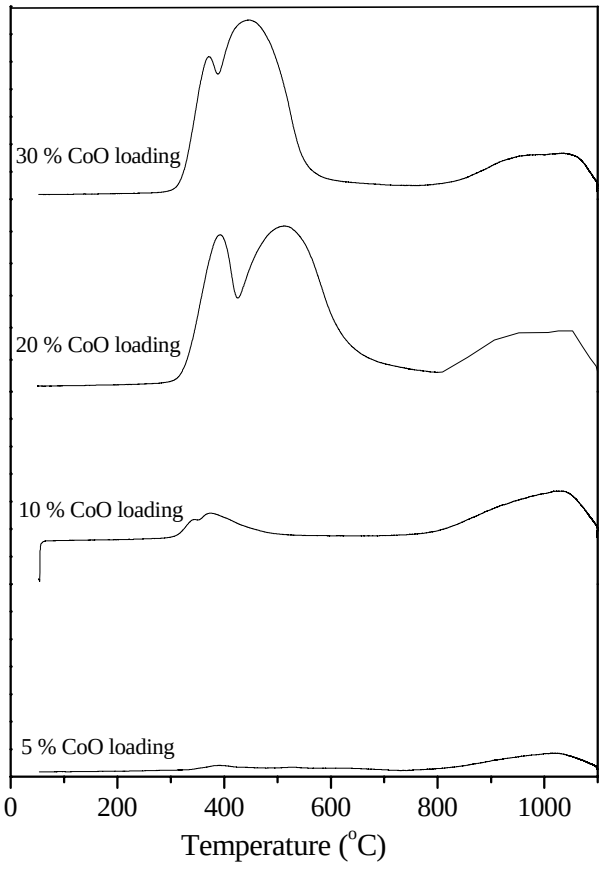

Figure 4.8 TPR profile of CoO/MgO/SA-5205 catalyst (calcined at 900 ^{o}C) with different cobalt loading

4.3.2.2. Influence of support on catalyst performance

The commercial catalyst carriers used for the supported Co-containing catalysts (Fig. 4.9) precoated with MgO are sintered low surface area, porous supports composed of refractory compounds, such as Al_2O_3, SiO_2, SiC, ZrO_2 and HfO_2, etc. They have different chemical compositions and surface properties (viz., surface area, pore volume, and porosity), as described in Appendix 4.1. The performances of the cobalt catalyst deposited on the different supports precoated with MgO, along with the rate of carbon deposition on them are presented in Fig. 4.9.

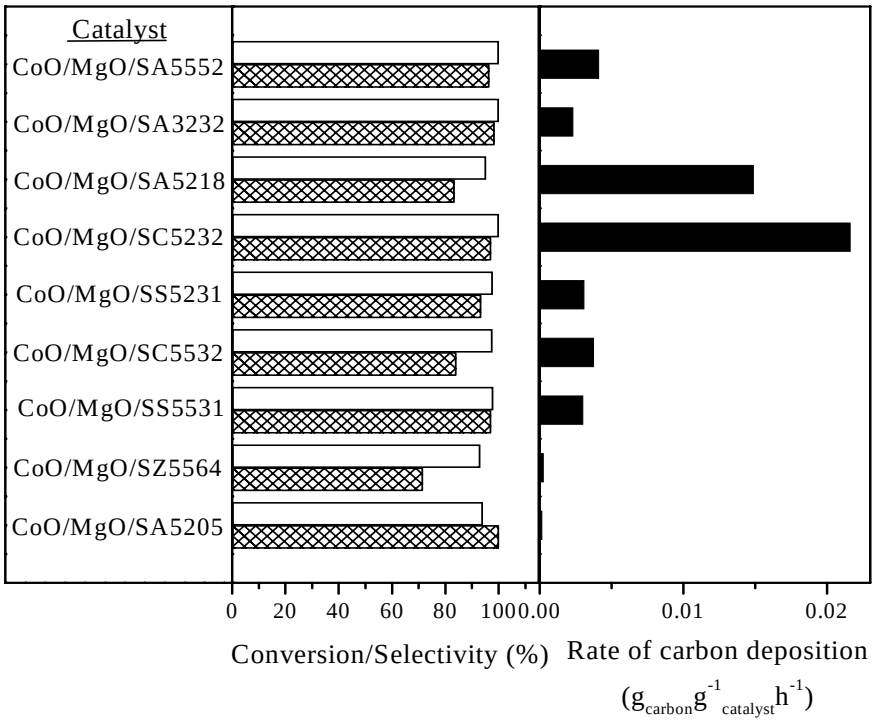

Figure 4.9 Influence of support on the performance and carbon deposition on the catalyst in the CO_2 reforming reaction at 850 ^oC. [Reaction condition: GHSV = 20,000 $cm^3g^{-1}h^{-1}$, CO_2/CH_4 = 1.1] Open bars represent for selectivity of H_2 and solid bars represent for the conversion of CH_4 (CoO and MgO loadings on support = 20 and 5.0 wt %, respectively)

The comparison clearly shows a strong influence of the catalyst support on the performance of CoO/MgO catalyst. The Co-containing catalyst supported on SS-5531, SC-5532, SS-5231, SC-5232, SA-5218, SA-3232 and SA-5552 commercial supports precoated with MgO showed high activity (methane conversion > 83 %) and also high H_2 selectivity (>

95 %) but with high rate of carbon deposition on them during the reaction. However, a very little carbon formation in the reaction was observed when the CoO supported on SA-5205 precoated with MgO was used as the CO_2 reforming catalyst. Moreover, this catalyst also showed not only high activity (methane conversion = 99 %) with high H_2 selectivity (93.9 %) at a high space velocity (20,000 $cm^3g^{-1}h^{-1}$) but also high stability against the catalyst deactivation in the process. All these qualities make this catalyst practically very promising for the CO_2 reforming process. It may be noted that the CoO-MgO catalyst (without the support) calcined at 900 ^oC showed almost no activity in the CO_2 reforming under identical conditions (Chapter 3).

The time dependent conversion of CH_4 and selectivity of H_2 for the two Co - containing catalysts supported on SA-5205 and SS-5531 precoated with MgO (5 wt%) are presented in Fig. 4.10. Both the methane conversion and selectivity for H_2 are increased to a small extent in

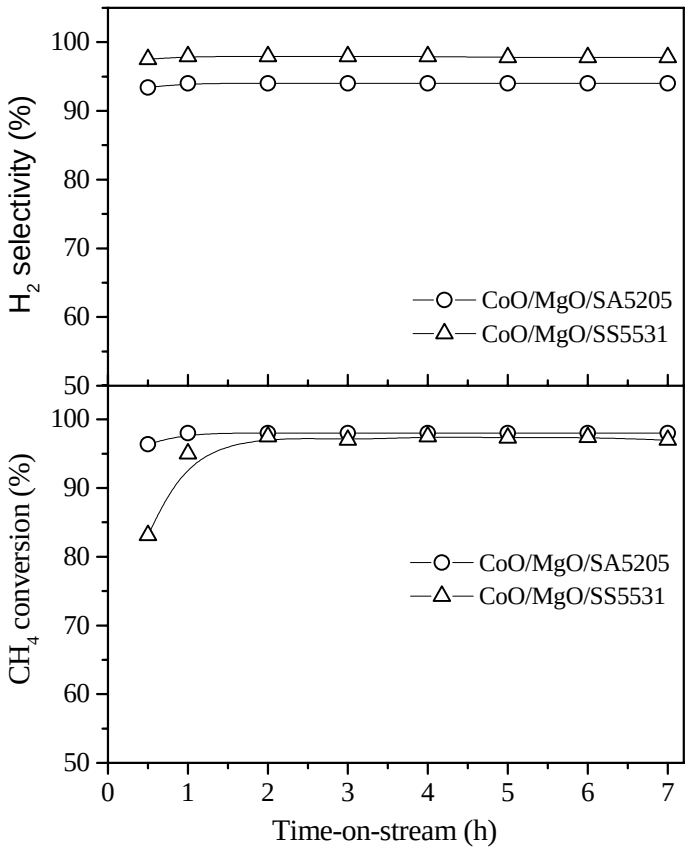

Figure 4.10 Time-on-stream activity / selectivity of the Co-containing catalysts supported on SA-5205 or SS-5531 precoated with MgO [Reaction temperature = 850 ^oC, GHSV = 20,000 $cm^3g^{-1}h^{-1}$, CO_2/CH_4 = 1.1]

the initial short period of about 1 h and thereafter remained almost constant in the CO_2 reforming over both the catalysts. This is because of the fact that, during the initial short period, the cobalt oxide from the catalyst is reduced first by methane and then by the reforming products (CO and H_2).

4.3.2.3. Influence of Co-loading in CoO/MgO/SA-5205 catalyst on its performance

Results showing the influence of Co-loading on the MgO (5 wt%)/SA-5205, on the catalyst performance in the CO_2 reforming of methane to syngas conversion are presented in Fig. 4.11. The CO_2 reforming reaction was carried out over both the prereduced and unreduced catalysts with different Co-loadings.

The CH_4 conversion and H_2 selectivity are increased markedly with increasing the Co-loading from 5 – 20 wt% for the catalyst without its prereduction by H_2. However, at the higher Co-loading (30 wt%), there was no further change in the CH_4 conversion and H_2 selectivity.

When the catalyst was reduced in the presence of 50 % H_2 in N_2 at 900^oC for 1 h before the reaction, the CH_4 conversion over the catalysts with low cobalt loading (5 or 10 wt %) is increased remarkably. However, no change in the CH_4 conversion was observed for the catalysts with the higher cobalt loading (20 and 30 wt%). The H_2 selectivity was almost constant for the prereduced catalysts. The catalyst in its active form is essentially a highly dispersed metallic cobalt on the support surface.

4.3.2.4. *Effect of catalyst prereduction by H_2 on time-on-stream activity / selectivity of CoO/MgO/SA-5205 catalyst*

Results showing the time-on-stream activity and selectivity of the CoO/MgO/SA-5205 catalyst in the CO_2 reforming of methane to syngas at 850 ^oC are presented in Fig. 4.12. Both the methane conversion and H_2 selectivity for the unreduced catalyst with high Co-loadings (20 and 30 wt%) showed high methane conversion activity (> 98%) and high H_2 selectivity (> 93 %) without any catalyst deactivation. However, a very low activity was observed for the catalysts with the lower Co-loading (5 and 10 wt%).

However, when the catalysts were prereduced by hydrogen (5 % H_2/N_2 mixture) at 900 ^oC, both the methane conversion and H_2 selectivity for the catalysts with the lower Co-loading (5 & 10 wt%) increased markedly. However, a little or no effect of the prereduction was observed for the catalysts with high cobalt loading (≥ 20 wt%).

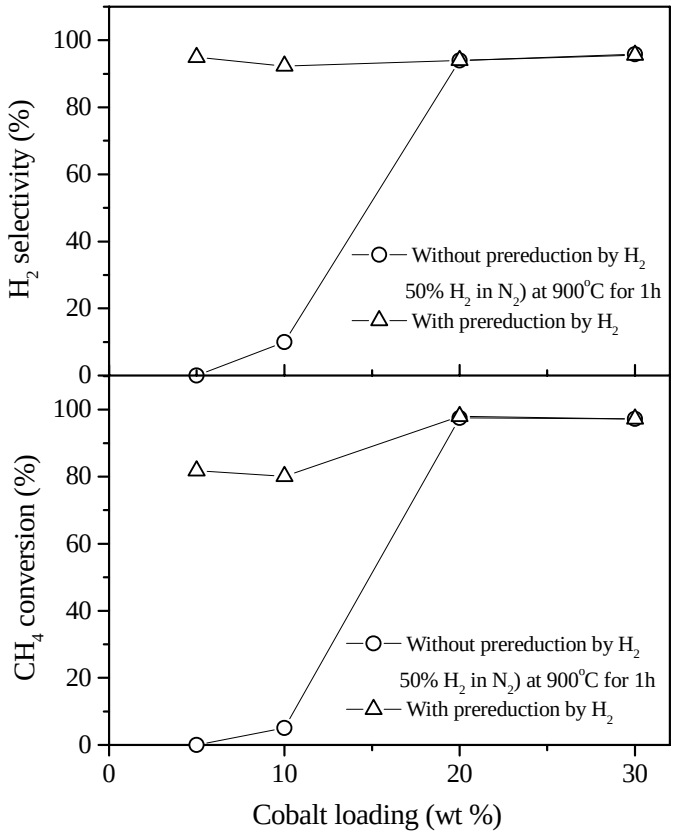

Figure 4.11 Effect of Co-loading in CoO/MgO/SA-5205 catalyst in its performance in the CO_2 reforming reaction at 850 ^oC [Reaction condition: GHSV = 20,000 $cm^3g^{-1}h^{-1}$; CO_2/CH_4 = 1.1]

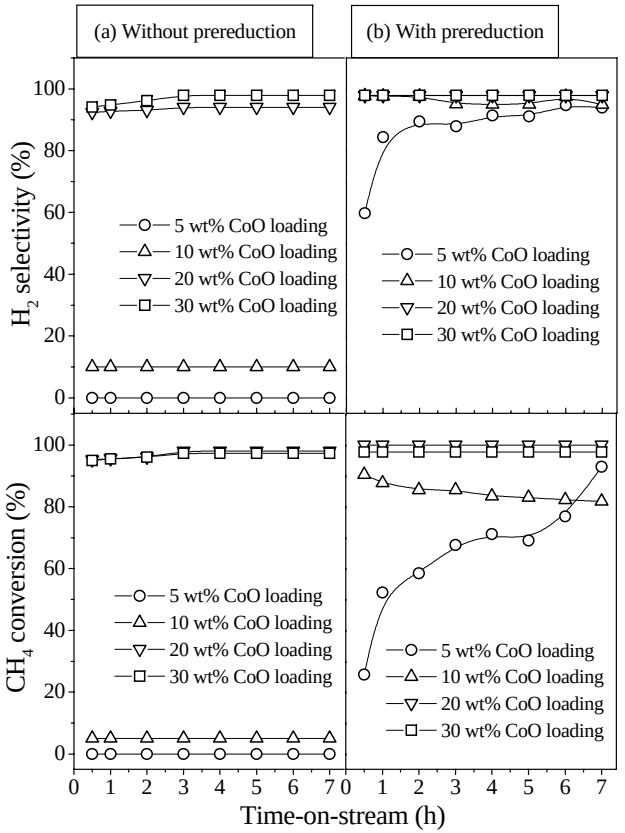

Figure 4.12 Effect of prereduction by H_2 on time-on-stream activity/selectivity in the CO_2 reforming for CoO/MgO/SA-5205 catalyst with different Co-loading at 850 ^oC[GHSV=20000 $cm^3g^{-1}h^{-1}$; CO_2/CH_4 = 1.1; reduction done by 50 % H_2 in N_2 at 900 ^oC]

4.3.2.5 Effect of reaction temperature and space velocity on performance of CoO/MgO/SA-5205 catalyst.

Results in Fig. 4.13 show the influence of reaction temperature and space velocity on the conversion and H_2 selectivity in the CO_2 reforming process over the CoO/MgO/SA-5205 catalyst. The conversion of both CH_4 and CO_2 is increased by increasing the temperature and decreased with increasing the space velocity; the increase and decrease are pronounced at the lower temperatures and higher space velocities, respectively. The H_2 selectivity is increased with increasing the temperature, but decreased by increasing the space velocity.

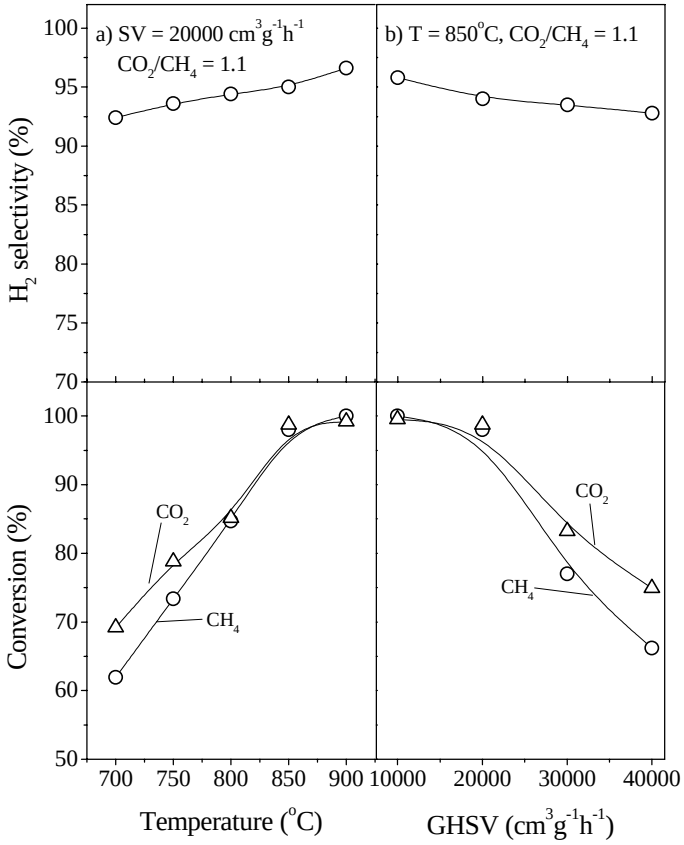

Figure 4.13 Influence of reaction temperature (a) and space velocity (b) on the conversion and H_2 selectivity in the CO_2 reforming of methane to syngas over the CoO/MgO/SA-5205 catalyst.

The fact that the conversion of CO_2 is higher than that of methane indicates an occurrence of the reverse water-gas shift reaction (reaction 1) simultaneously with the CO_2 reforming reaction (reaction 2) depending upon the process conditions.

$CO_2 + H_2 \rightarrow CO + H_2O$ (1)

($\Delta H_r = + 8.0$ kcalmol^{-1})

$CH_4 + CO_2 \rightarrow 2CO + 2H_2$ (2)

($\Delta H_r = + 62.2$ kcalmol^{-1})

It is interesting to note that, although the thermodynamic feasibility of the reverse water gas shift reaction (reaction 1) is increased with increasing the temperature, unexpectedly the H_2 selectivity is higher at the higher temperature. This is expected mostly because of the lower CO_2 concentration available for the reverse shift reaction at the higher temperatures.

4.3.3. Simultaneous CO_2 Reforming and Partial Oxidation of Methane to Syngas over CoO/MgO/SA-5205 Catalyst

4.3.3.1. Influence of reaction parameters (reaction temperature, O_2/CH_4 mole ratio and space velocity)

Results showing the influence of temperature and O_2/CH_4 ratio in the feed on the conversion, selectivity, and H_2/CO product ratio and also on the net heat of reaction (ΔH_r) in the process are presented in Figs 4.14 and 4.15, respectively. The net heat of reaction (ΔH_r) for the overall process is estimated by subtracting the heat of formation (at the process temperature) of the components in the feed from that of the components in the product stream.

When reaction temperature is increased, the conversion of CH_4 and CO_2, H_2 selectivity and net heat of reaction (ΔH_r) or process endothermicity are increased and the H_2/CO product ratio is decreased (Fig. 4.14). Whereas, with the increase in the O_2/CH_4 ratio (Fig. 4.15), while keeping $CH_4/(O_2 + 0.5CO_2)$ feed ratio constant, following effects on the process performance are observed:

i) The conversion of methane is increased to a small extent but that of O_2 is decreased with increasing the O_2/CH_4 ratio, whereas that of CO_2 is passed through a maximum.

ii) The H_2 selectivity is increased to a small extent and consequently the H_2/CO ratio is also increased.

iii) The process endothermicity is decreased.

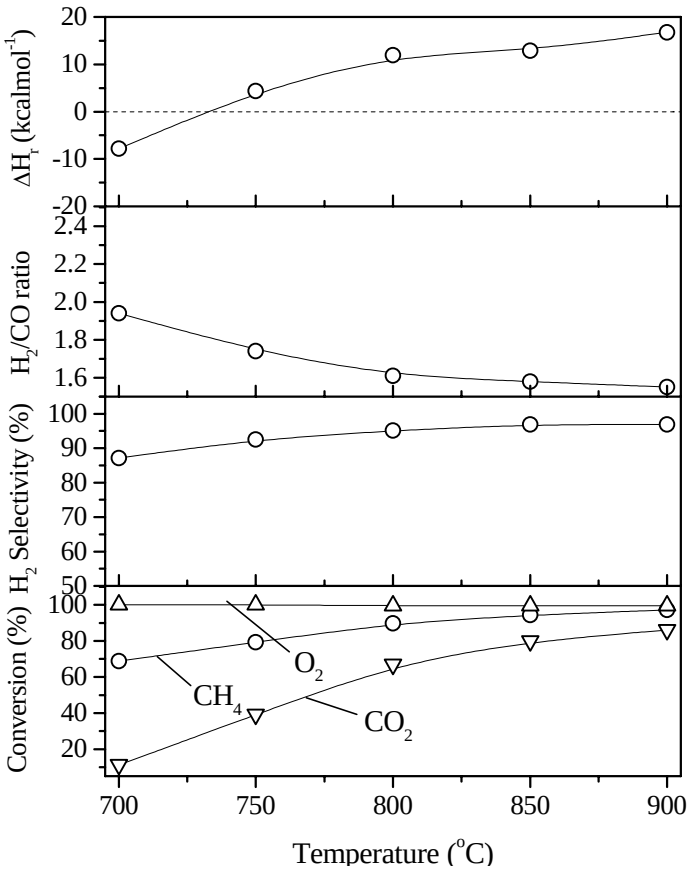

Figure 4.14 Effect of temperature on the performance of the CoO/MgO/SA-5205 in the Oxy-CO_2 reforming of methane. (O_2/CH_4 = 0.40; $CH_4/(O_2 + 0.5CO_2)$ = 1.87; GHSV = 46,000 $cm^3g^{-1}h^{-1}$). ΔH_r = the net heat of reaction)**.**

The above observations indicate the occurrence of endothermic CO_2 reforming of methane (reaction 2) simultaneously with the exothermic oxidative conversion of methane to CO and H_2,

$$CH_4 + 0.5O_2 \rightarrow CO + 2H_2,\ \Delta H_r = -5.4\ kcalmol^{-1} \qquad (3)$$

over the catalyst. The observed H_2 selectivity lower than 100% is because of the side reverse water gas reaction (reaction 1).

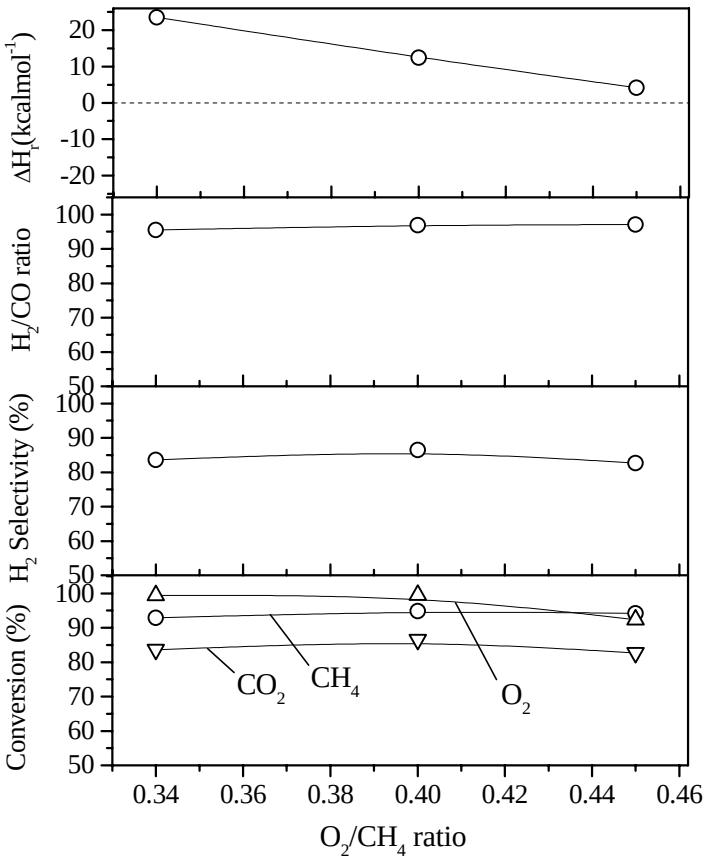

Figure 4.15 Effect of O_2/CH_4 ratio on the performance of the CoO/MgO/SA-5205 in the Oxy-CO_2 reforming of methane at 850 ^oC ($CH_4/(O_2 + 0.5CO_2)$ = 1.87; GHSV = 46,000 $cm^3g^{-1}h^{-1}$).

The conversion of CO_2 at the low temperature (Fig. 4.14) indicates that there is CO_2 formation in the process due to the combustion of methane,

$$CH_4 + 2O_2 \rightarrow CO_2 + 2H_2O, \ \Delta H_r = -191.8 \text{ kcalmol}^{-1} \qquad (4)$$

making the process more exothermic. Because of the coupling of the exothermic and endothermic reactions (reactions 2 and 3), the heat produced or absorbed in the process (or process exothermicity or endothermicity) can be controlled by manipulating the process parameters (viz. reaction temperatures or O_2/CH_4 feed ratio). Thus, by manipulating the reaction temperature and / or O_2/CH_4 ratio, the process can be made mildly exothermic, thermo neutral or mildly endothermic.

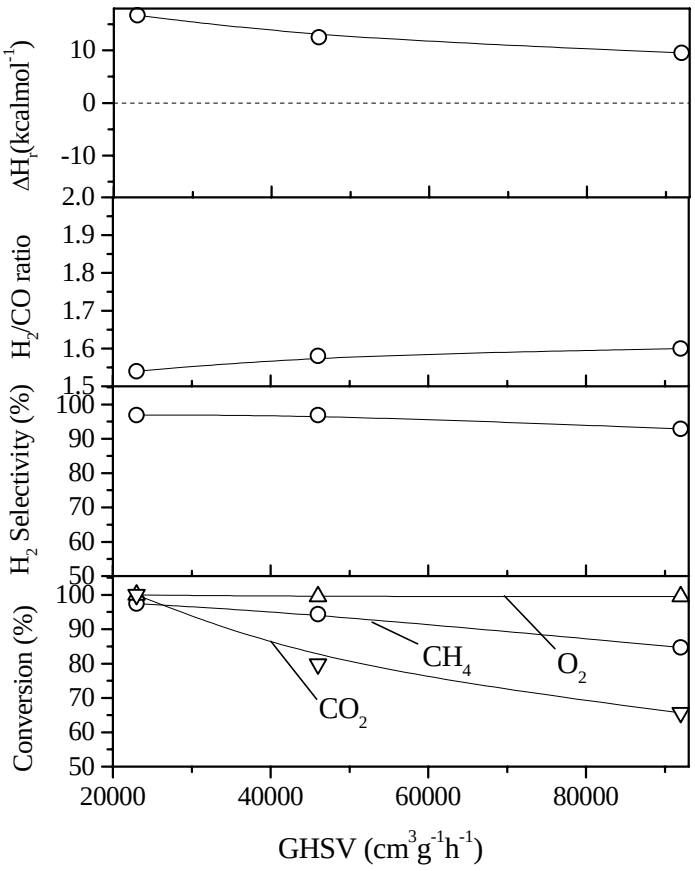

Figure 4.16 Effect of space velocity on the performance of the CoO (20 wt%)/MgO (5 wt%)/SA-5205 catalyst in the Oxy-CO_2 reforming of methane at 850 ^oC (O_2/CH_4 = 0.40 & CO_2/CH_4 = 0.14; $CH_4/(O_2 + 0.5CO_2)$ = 1.87).

Figure 4.16 shows the effect of space velocity on the conversion, selectivity, H_2/CO ratio and also on the net heat of reaction (ΔH_r) in the process at 850 ^oC. The effect of space velocity on the conversion of O_2 is small. The conversion of CH_4 and CO_2 and the H_2 selectivity and also the net heat produced in this process (ΔH_r) are decreased with increasing the space velocity.

In the oxy-CO_2 reforming process, as long as the conversion of CO_2 is greater than or equal to zero, the selectivity for CO is always 100%.

4.3.4. CO_2 Reforming and Oxy-CO_2 Reforming of Methane to Syngas CoO/ZrO_2 (or CeO_2)/SA-5205 Catalyst.

4.3.4.1 Catalyst characterization.

The Co-containing catalyst supported on SA-5205 precoated with ZrO_2 or CeO_2 (CoO/ZrO_2/SA-5205 and CoO/CeO_2/SA-5205) were characterized for their crystalline phases and degree of reduction by TPR are presented in Table 4.4 and Figs. 4.17 – 4.18.

The XRD data were collected to determine the crystal phases of these catalysts (Fig. 4.17). The XRD analysis showed the presence of a separate CoO phase for both the catalysts, indicating no formation of a solid solution between CoO and ZrO_2 for the CoO/ZrO_2/SA-5205. However, a minor phase of $CeAlO_3$ is observed for the CoO/CeO_2/SA-5205. A minor phase of $CoAl_2O_4$, resulting from a solid-solid reaction between CoO and Al_2O_3 (from the support) at the CoO-support interface, was observed for both the catalysts. The different crystalline phases present in the catalysts are given in Table 4.4.

Table 4.4 Crystalline phases and degree of reduction of the CoO/ZrO_2 (or CeO_2)/SA-5205 catalysts

Catalyst	XRD phases	Degree of reduction (%)
CoO (20%)/ZrO_2 (20%)/SA-5205	Co_2O_3 (major), CoO (minor), $CoAl_2O_4$, ZrO_2 (cubic), Al_2SiO_5, α-Al_2O_3	96.3
CoO (20%)/CeO_2 (20%)/SA-5205	CoO (major), Co_2O_3 (minor), CeO_2, $CoAl_2O_4$, $CeAlO_3$, Al_2SiO_5, α-Al_2O_3	70.0

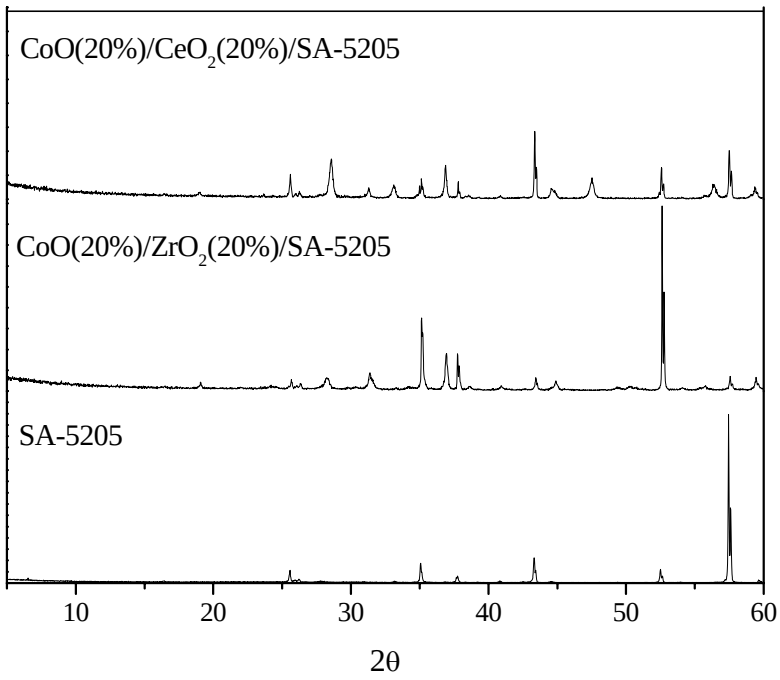

Figure 4.17 XRD spectra of SA-5205 support and cobalt-containing catalysts supported on SA-5205 precoated with ZrO_2 or CeO_2 before their use in oxy-CO_2 reforming of methane.

The TPR of the catalysts was carried out by H_2 (5 % H_2 in Ar) from 40 ^oC to 1100 ^oC at a linear heating rate of 20 $^oC.min^{-1}$. The degree of CoO reduction is determined from the concentration of CoO in the catalyst and the amount of H_2 consumed in the TPR, assuming the reaction stoichiometry ($CoO + H_2 \rightarrow Co^0 + H_2O$). TPR curve of the CoO/ZrO_2/SA-5205 catalyst (Fig. 4.18) shows only one distinct peak (peak maximum temperature = 430 ^oC), which is attributed to the reduction of free CoO species. The degree of CoO reduction (Table 4.4) for this catalyst is very high (96.3 %). This also indicates the presence of free CoO species in the catalyst.

The TPR curve for the CoO/CeO_2/SA-5205 catalyst shows two distinct peaks. One (peak maximum at 410 ^oC) is attributed to the reduction of relatively free CoO species. The second small peak appeared at higher temperature (Peak maximum at 800 ^oC), may be attributed to the reduction of CeO_2 to Ce_2O_3 in the catalyst. The observed lower degree of

reduction of the catalyst (70 %) may be due to the presence of difficult to reduce $CoAl_2O_4$ in the catalyst in appreciable amounts.

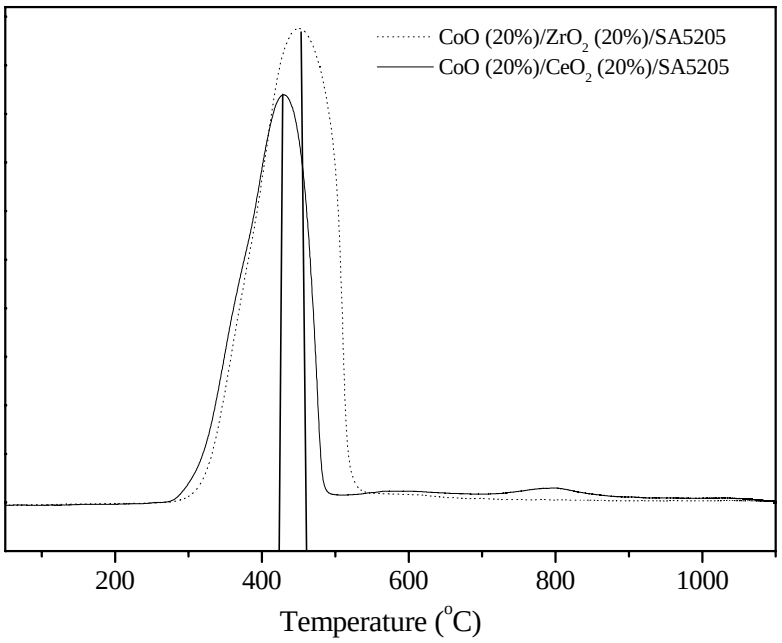

Figure 4.18 TPR patterns of the Co-containing catalyst supported on SA-5205 precoated with ZrO_2 or CeO_2

4.3.4.2. CO_2 reforming of methane: Influence of reaction temperature

Results in Figs. 4.19 and 4.20 show the influence of reaction temperature on the conversion, H_2 selectivity and H_2/CO product ratio in the CO_2 reforming of methane over the CoO/ZrO_2 (or CeO_2)/SA-5205 catalysts. The conversion of both CH_4 and CO_2 are increased by increasing the temperature. The H_2 selectivity and H_2/CO ratio are also increased with increasing the temperature for both the catalysts. The fact that the conversion of CO_2 is higher than that of methane and also the H_2/CO ratio is less than 1.0 indicates occurrence of the reverse water-gas shift reaction (reaction 1), simultaneously with the CO_2 reforming reaction (reaction 2), depending upon the process conditions.

4.3.4.3. Oxy-CO_2 reforming of methane: Influence of process parameters

The effect of temperature on the conversion, selectivity and H_2/CO product ratio and net heat of reactions (ΔH_r) in the oxy-CO_2 reforming process over both the catalysts is shown in Figs. 4.21 and 4.22. The conversion of O_2 for both the catalysts was 100%. The CO selectivity (based on methane) is 100 %, as the conversion of CO_2 is positive.

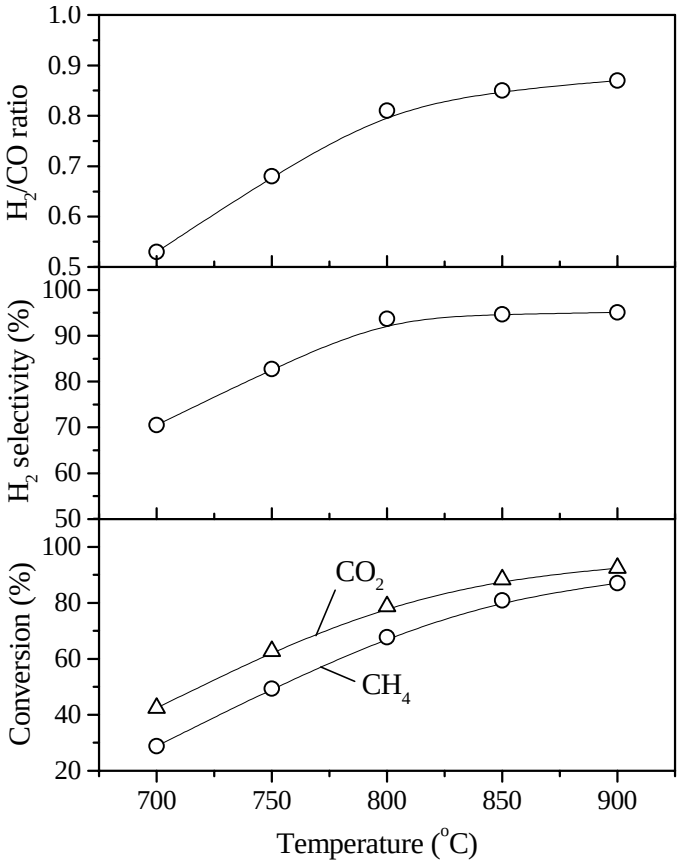

Figure 4.19 Effect of temperature on the performance of the CoO (20%)/ZrO_2 (20%)/SA-5205 catalyst in the CO_2 reforming of methane. [Reaction condition: GHSV=20,000 $cm^3g^{-1}h^{-1}$; CO_2/CH_4 = 1.1]

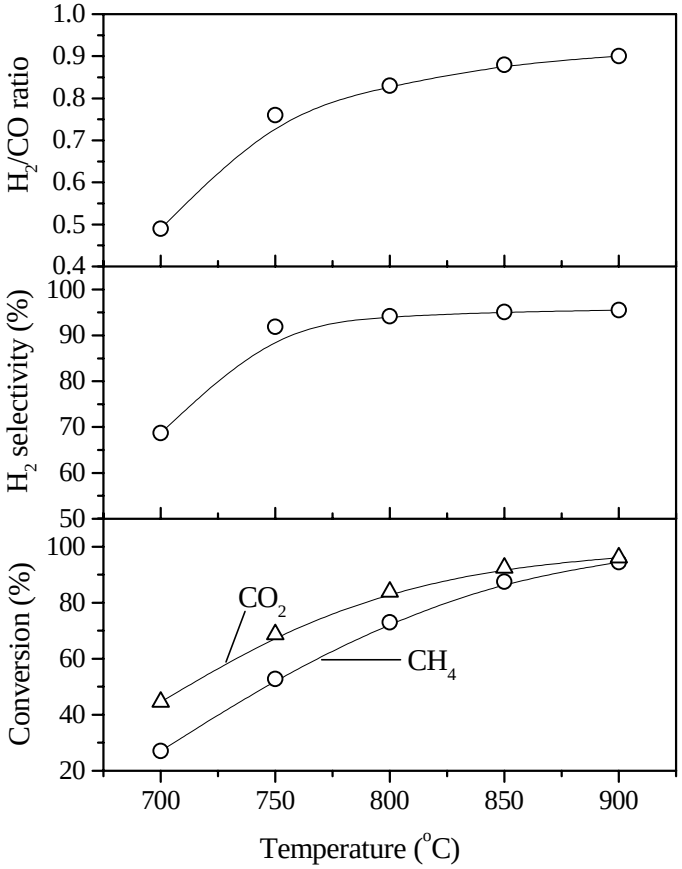

Figure 4.20 Effect of temperature on the performance of the CoO (20%)/ZrO_2 (20%)/SA-5205 catalyst in the CO_2 reforming of methane. [Reaction condition: GHSV=20,000 $cm^3g^{-1}h^{-1}$; CO_2/CH_4 = 1.1]

The results show that, with the increase of temperature (from 700 to 900 ^{o}C) in the oxy-CO_2 reforming of methane, (a) the conversion of methane and CO_2 is increased, (b) the selectivity for H_2 is increased, (c) the H_2/CO ratio is also decreased, (d) the net heat of reaction (ΔH_r) is increased indicating a decrease in process exothermicity or an increase in the process endothermicity.

The H_2 selectivity is lower than 100 % because of the reverse water gas shift (reaction 1). The increase in the H_2 selectivity with increasing the temperature indicates that the reverse water gas shift reaction occurs to a small extent at the higher temperatures. However, the CO_2 reforming reaction is favoured more and more at the higher temperature. The observed decrease in the H_2/CO product ratio and increase in the value of ΔH_r (or increase in the process endothermicity) with increasing temperature are the result of a higher methane conversion by the CO_2 reforming. Thus, the reaction temperature is an important process variable for controlling the process exothermicity or endothermicity; the process can be made mildly exothermic, thermo neutral or mildly endothermic by manipulating the reaction temperature.

Results showing the influence of O_2/CH_4 ratio in the feed on the methane conversion, H_2 selectivity, H_2/CO ratio and net heat produced in the oxy-CO_2 reforming process over both the catalysts are presented in Figs. 4.23 and 4.24, respectively. There was little or no change in the conversion of CH_4 and O_2 with increasing the O_2/CH_4 ratio. However, conversion of CO_2 is decreased markedly with increasing the O_2/CH_4 ratio. The H_2 selectivity, H_2/CO ratio and net heat produced in the process are increased. Both catalysts showed > 80 % CH_4 conversion and > 90 % of H_2 selectivity at O_2/CH_4 ratio of 0.40. The H_2 selectivity is lower than 100 % because of the reverse water gas shift reaction (reaction 1) occurring simultaneously with the oxidative conversion and CO_2 reforming of methane to syngas.

Results in Figs. 4.25 and 4.26 show that the influence of space velocity on the process performance in oxy-CO_2 reforming of methane over both the catalysts at 850 ^{o}C. The effect of space velocity on the conversion of O_2 and CH_4 is small but the effect on the CO_2 conversion, H_2 selectivity and H_2/CO ratio is appreciable, particularly at the higher space velocities. The net heat of reaction (ΔH_r) in this process is decreased markedly.

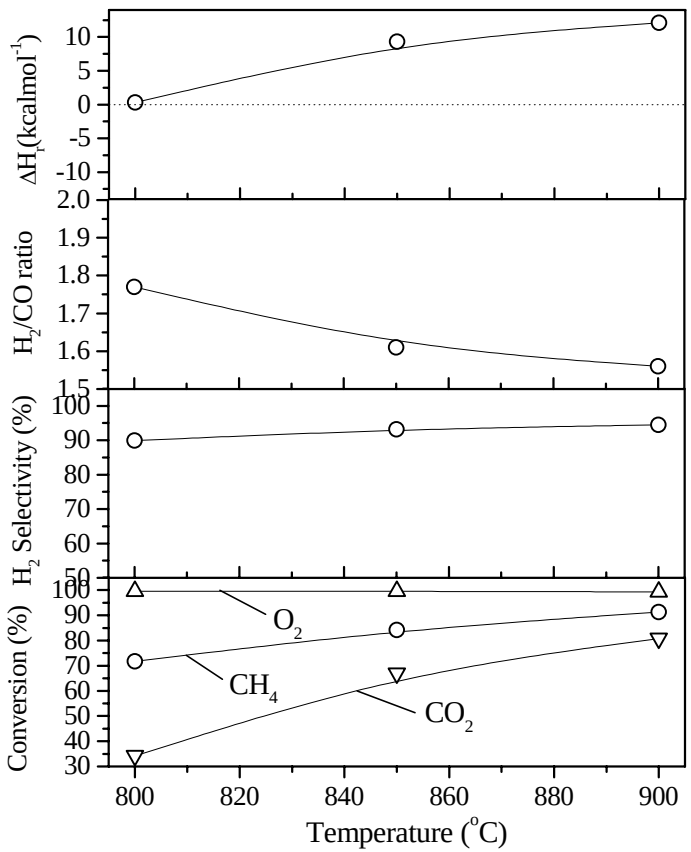

Figure 4.21 Effect of temperature on the performance of the $CoO(20\%)/ZrO_2(20\%)/SA\text{-}5205$ catalyst in the Oxy-CO_2 reforming of methane [O_2/CH_4=0.40, GHSV=46,000 $cm^3g^{-1}h^{-1}$, $CH_4/(O_2+0.5CO_2)$=1.87]

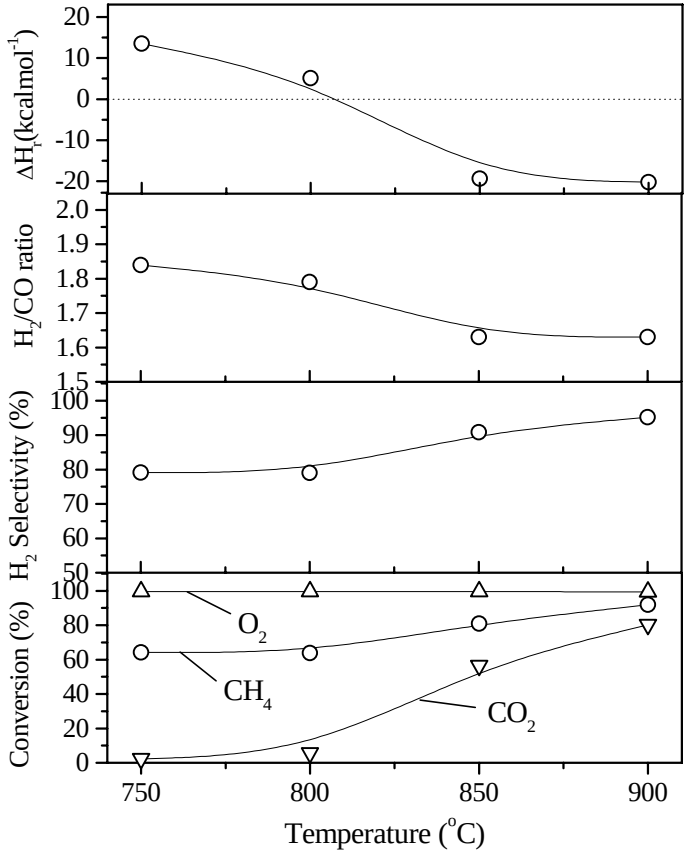

Figure 4.22 Effect of temperature on the performance of the $CoO(20\%)/CeO_2(20\%)/SA\text{-}5205$ catalyst in the Oxy-CO_2 reforming of methane [O_2/CH_4=0.40, GHSV=46,000 $cm^3g^{-1}h^{-1}$, $CH_4/(O_2+0.5CO_2)$=1.87]

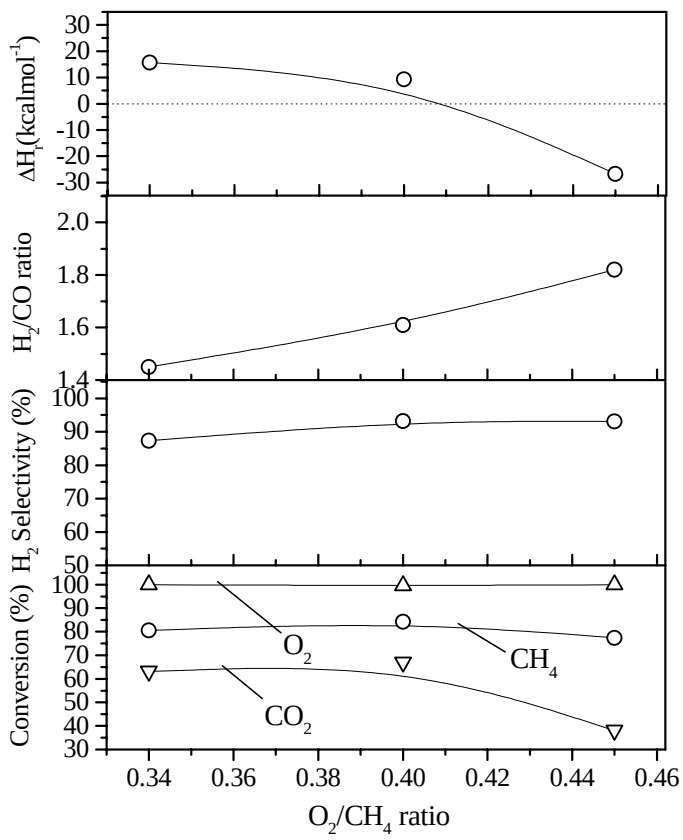

Figure 4.23 Effect of O_2/CH_4 ratio on the performance of the CoO (20%)/ZrO_2 (20%)/SA-5205 catalyst in the Oxy-CO_2 reforming of methane at 850 ^oC [GHSV=46,000 $cm^3g^{-1}h^{-1}$, $CH_4/(O_2+0.5CO_2)$=1.87]

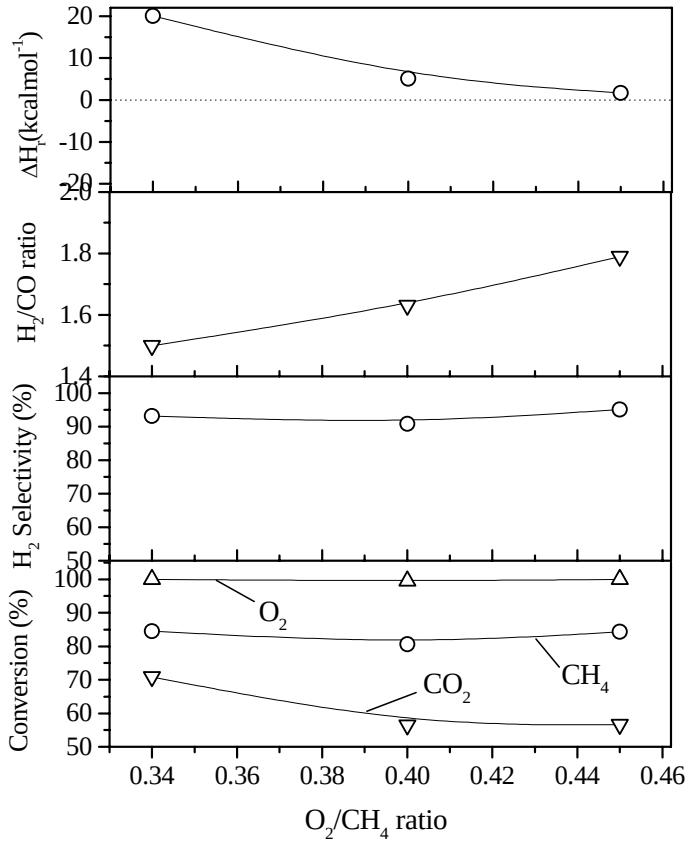

Figure 4.24 Effect of O_2/CH_4 ratio on the performance of the CoO (20%)/CeO_2 (20%)/SA-5205 catalyst in the Oxy-CO_2 reforming of methane at 850 ^oC [GHSV=46,000 $cm^3g^{-1}h^{-1}$, $CH_4/(O_2+0.5CO_2)$=1.87]

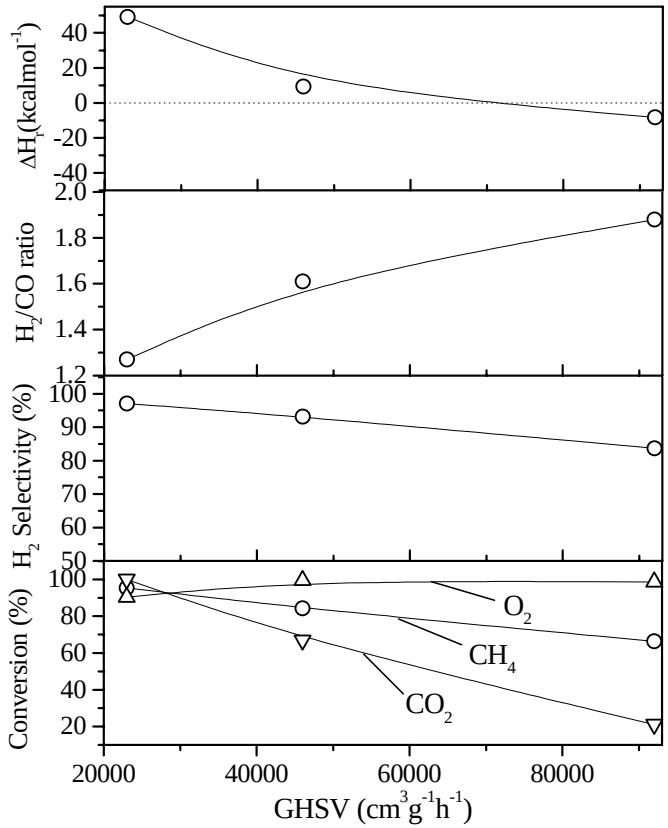

Figure 4.25 Effect of GHSV on the performance of the $CoO(20\%)/ZrO_2(20\%)/SA\text{-}5205$ catalyst in the oxy-CO_2 reforming of methane at 850 ^oC [O_2/CH_4=0.40, $CH_4/(O_2+0.5CO_2)$ = 1.87]

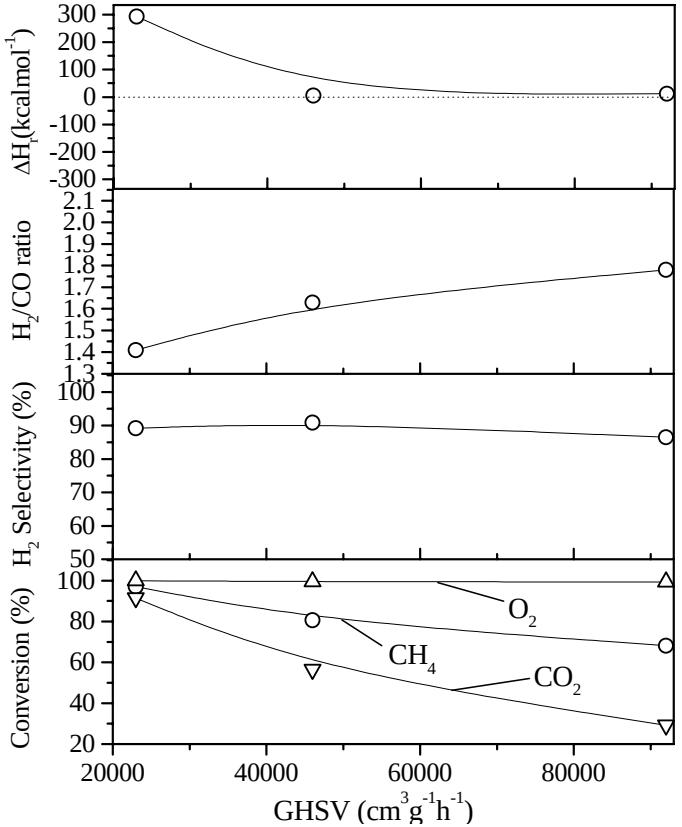

Figure 4.26 Effect of GHSV on the performance of the $CoO(20\%)/CeO_2(20\%)/SA\text{-}5205$ catalyst in the oxy-CO_2 reforming of methane at 850 ^oC [O_2/CH_4=0.40, $CH_4/(O_2+0.5CO_2)$ = 1.87]

4.4. Conclusions

From the studies on the CO_2 reforming and oxy-CO_2 reforming reactions of methane for its conversion to syngas over the cobalt containing catalysts supported on different commercial macroporous catalyst carriers precoated with different metal oxides, following important conclusions have been drawn.

1. Among the different catalysts, the CoO/MgO (5%)/SA-5205 catalyst with 20 wt% cobalt loading is a highly promising catalyst for the CO_2 reforming and oxy-CO_2 reforming of methane to syngas; the catalyst shows high activity, high selectivity for H_2 and also excellent stability against carbon formation during the CO_2 reforming process.
2. The CoO/MgO/SA-5205 catalyst in its active form consists of metallic cobalt dispersed on the support. The catalyst is reduced atleast partially and converted into its active form during the initial short period of the CO_2 reforming process.
3. Very little carbon formation on the CoO/MgO/SA-5205 catalyst in the CO_2 reforming was attributed to the strong interaction of metallic cobalt with support, leading to an increase in the basicity of the support and/or a change in the electronic properties of the metallic cobalt finely dispersed on the support.
4. The CoO and MgO in the catalyst exists in the form of their solid solution.
5. CoO/ZrO_2 and CoO/CeO_2 catalysts supported on SA-5205 also showed good activity and selectivity in the CO_2 and oxy-CO_2 reforming of methane to syngas.
6. By changing the O_2/CH_4 ratio of the feed gases one could control the product H_2/CO ratio between 1 and 2 in Oxy-CO_2 reforming process.
7. The reaction temperature and O_2/CH_4 ratio are important process variable for controlling the process exothermicity or endothermicity in the oxy-CO_2 reforming of methane; the process could be made mildly exothermic, thermo neutral or mildly endothermic by manipulating the reaction temperature and / or O_2/CH_4 ratio.

References

1. V. R. Choudhary, A. M. Rajput, B. Prabhakar, Angew. Chem. Int. Ed. Engl. 33 (1994) 2104.
2. V. R. Choudhary, A. M. Rajput, B. Prabhakar, Catal. Lett., 32 (1995) 391.

3. V. R. Choudhary, A. M. Rajput, B. Prabhakar, in; <. M. Bhasin, D. W. Slocum (Eds.), Methane and Alkane Conversion Chemistry, Proc. Am. Chem. Soc. Symp., 207th Annual Meeting, San Diego, CA, March (1994) 13018, Plenum Publishing Corporationm, New York (1995) p. 305.
4. A. T. Ashcroft, A. K. Cheetham, M. L. H. Green, P. D. F. Veron, Nature, 352 (1991) 225.
5. V. R. Choudhary, B. S. Uphade, A. S. Mamman, Mesopor. and Micropor. Mater., 23 (1998) 61.
6. V. R. Choudhary, B. S. Uphade, A. A. Belhekar, J. Catal., 163 (1996) 312.
7. A. L. Larentis, N. S. de. Ressende, V. M. M. Salim, J. C. Pinto, Appl. Catal. A: Gen., 215 (2001) 211.
8. L. Mo, J. Fei, C. Huang, X. Zheng, J. Mol. Catal. A, 193 (2003) 177.
9. M. M. V. M. Souza, M. Schmal, Appl. Catal. A, 255 (2003) 83.
10. T. Suhartanto, P. E. A. York, A. Hanif, H. Al – Megren, L. H. M. Green, Catalysis Letters, 71 (2001) 49.
11. U. L. Portugal, A. C. S. F. Santos, S. Damyanova, C. M. P. Marques, J. M. C. Bueno, J. Mol. Catal. A, 184 (2002) 311.
12. A. I. Tsyganok, M. Inaba, T. Tsmoda, S. Hamakawa, K. Suzuki, T. Hayakawa, Cat. Comm., 4 (2003) 493.
13. J. T. Richardson, M. Garrait, J. K. Hung, Appl. Catal. A, 255 (2003) 69.
14. Z. Hou, O. Yokota, T. Tanaka, T. Yashima, Appl. Catal. A: Gen., 253 (2003) 381.
15. H. K. Song, J-W. Choi, S. H. Yue, H. Lee, B-K. Na, Catalysis Today, 80 (2004) 27.
16. E. Ruckenstein, H. Y. Wang, J. Catal., 205 (2002) 289.
17. D. J. Moon, J. W. Ryu, Catalysis Today, 87 (2003) 255.
18. E. Ruckenstein, H. Y. Wang, Appl. Catal. A: Gen., 204 (2000) 257.
19. V. R. Choudhary, A. S. Mamman, S. D. Sansare, Angew. Chem. Int. Ed. Engl. 31 (1992) 1189.
20. V. R. Choudhary, B. S. Uphade, A. S. Mamman, Catal. Lett., 32 (1995) 387.
21. D. Qin, J. Lapszewicz, Catal. Today, 21 (1994) 551.
22. V. R. Choudhary, A. M. Rajput, Ind. Eng. Chem. Res., 35 (1996) 3934.
23. V. R. Choudhary, B. S. Uphade, A. S. Mamman, J. Catal., 172 (1997) 281.
24. H. Y. Wang, E. Ruckenstein, Appl. Catal. A: Gen., 209 (2001) 207.

Appendix 4.1. Composition and physical properties of the commercial macroporous supports

Support	Main components (wt %)				Surface area (m^2g^{-1})	Pore volume (cm^3g^{-1})	Porosity (%)
	Al_2O_3	SiO_2	SiC	HfO_2+ ZrO_2			
SA-5552	93.1	5.6	-	-	0.33	0.39	59
SA-5205	86.1	11.8	-	-	<0.05	0.35	54
SA-5218	86.1	12.0	-	-	<0.05	0.20	40
SC-5532	4.7	28.5	65.8	-	0.15	0.23	45
SS-5231	4.1	95.0	-	-	0.22	0.25	35
SZ-5564	0.4	1.6	-	94.1	0.10	0.15	45

CHAPTER 5

HIGH TEMPERATURE STABLE SUPPORTED Ni–Co CATALYSTS USEFUL FOR HIGHLY EXOTHERMIC METHANE-TO-SYNGAS CONVERSION PROCESSES

CHAPTER 5

HIGH TEMPERATURE STABLE SUPPORTED Ni-Co CATALYSTS USEFUL FOR HIGHLY EXOTHERMIC METHANE-TO-SYNGAS CONVERSION PROCESSES

5.1 Earlier Work / Background and Objective of the Present Work

Because of the increasing oil and energy costs, an effective utilization of methane (a main constituent of natural gas, the world reserves of which are almost equivalent to that of oil) by its conversion into value added products, such as hydrogen, petroleum products and petrochemicals, is a challenge for 21st century [1]. Technically, the most feasible route for the methane conversion is based on syngas (a mixture of H_2 and CO) as an intermediate product. However, the syngas-based routes are not at all economically feasible if syngas is produced from the presently practiced methane steam reforming (MSR) process [2]. This is mainly because of the high-energy consumption in the MSR process and also due to its high capital and operating costs to obtain desirable H_2/CO product ratio (1.5 – 2.0).

Methane autothermal reforming (MATR), which is also a well established process, is carried out in two separate reaction zones-in the first zone, a part of the methane from feed is combusted in a flame or catalytic burner, producing a hot (about 1400 ^{o}C) product stream and, in the second zone, the unconverted methane from the product stream is reformed to syngas by the methane combustion products (steam and CO_2) over a steam reforming catalyst [3]. Although the MATR process requires no external energy, yet its use is limited, mainly because of the catalyst fouling [deactivation (by sintering and formation of inactive mixed metal oxides) and degradation / disintegration] resulting from the high temperature (about 1400 ^{o}C) treatment and thermal shocks, particularly during the process start-up and close-down periods, received by the catalyst.

In the last 1 – 2 decades, extensive efforts have been made on the catalytic partial oxidation of methane (CPOM) to syngas, which is covered in a number of recent reviews [4]. The CPOM process operating at a very low contact time (about millisecond), is of great practical importance [5, 6]. However, in this process a high methane conversion (> 90%) coupled with very high space velocity (≥ 500,000 $cm^3g^{-1}h^{-1}$) leads to production of a large amount of heat in a small catalyst zone, even at very high selectivity (> 95 %) for CO and H_2, causing a large adiabatic temperature rise (which is difficult to control) and ultimately resulting

in the deactivation of a thermally unstable catalyst. Our earlier studies showed that a highly active / selective supported Ni-containing catalyst (prepared by depositing NiO on a MgO precoated low surface area macroporous silica-alumina) is thermally stable when calcined only up to about 1000 ^{o}C; at the higher calcination temperature (1200 ^{o}C), it is completely deactivated mostly because of the formation of catalytically inactive mixed metal oxides [7].

Since the methane combustion reactions ($CH_4 + 2\ O_2 \rightarrow CO_2 + 2H_2O$ - 191.8 kcal.mol^{-1} and $CH_4 + O_2 \rightarrow CO + 2H_2O$ - 124.1 kcal.mol^{-1}) are much more exothermic than the partial oxidation of methane to syngas ($CH_4 + 0.5O_2 \rightarrow CO + 2H_2$ - 5.4 kcal.mol^{-1}), even a small loss in the selectivity due to catalyst deactivation is expected to make the CPOM process highly hazardous / out of control. It is therefore of great practical interest to overcome the major limitation of the MATR and CPOM processes by developing a high temperature stable catalyst, showing desirable activity and selectivity in the methane-to-syngas conversion reactions and also having a high mechanical strength, even when the catalyst is subjected to a very high temperature (≥ 1200 ^{o}C) and thermal shocks. This has been accomplished in this investigation. We report here that a $NiCoMgCeO_x$ deposited on a low surface area macroporous zirconia-hafnia catalyst carrier, even when calcined at 1400^{o}C and subjected to oxy-acetylene flame (about 2000^{o}C) or subjected to a number of high temperature (about 2000^{o}C) thermal shocks, shows high catalytic activity, selectivity and stability in the CPOM, steam reforming, CO_2 reforming, oxy-steam and oxy-CO_2 reforming reactions, without loosing its mechanical strength. These highly desirable qualities are of great practical importance for using the catalyst in the MATR process and also in the high temperature CPOM process.

5.2 Experimental

The supported Ni-, Co- containing catalysts (Table 5.1) were prepared by impregnating respective metal nitrates from their mixed aqueous solution on a commercial low surface area (≅ 0.1 m^2g^{-1}) macroporous (porosity = 45 % and pore volume = 0.15 cm^3g^{-1}) sintered zirconia-hafnia (94.1 % ZrO_2-HfO_2) catalyst carrier (SZ-5564, obtained from M/s Norton Co., USA) by incipient wetness technique described in the earlier chapter (section 2.1.1.5 & 2.1.1.6). The high temperature (about 2000 ^{o}C) treatment and temperature shocks to the catalysts were given by putting directly an oxy-acetylene flame on the catalyst (0.3 g) kept in a zirconia boat once for 30 min or repeatedly for 30 s at an interval of 10 min.

The different catalytic reactions, as discussed in this chapter, over the catalysts were carried out at atmosphere pressure in a continuous flow quartz reactor (i.d. = 9 mm) packed with 0.2 g catalyst (22 – 30 mesh size) by the procedure described earlier chapter [sections 2.3.1 – 2.3.4]. Before use, in the reaction, the catalyst was reduced by 50 % H_2 in N_2 at 900^oC for 1 h. The gas hourly space velocity (GHSV) was measured at 0^oC and 1 atm pressure.

The TPR over the catalysts was carried out in a quartz reactor containing 0.15 g catalyst in a flow of 5 mol % H_2 in Ar (30 cm^3min^{-1}) from 50 to 1100 ^oC at a linear heating rate of 20 ^oC min^{-1} by the procedure described earlier in the earlier chapter [section 2.2.4]. The H_2 pulse reaction over the catalysts was carried out in a quartz pulse microreactor (containing 0.1g catalyst) connected to a gas chromatograph [13] (with a Porapak-Q column and thermal conductivity detector) by injecting a pulse of pure H_2 (0.2 cm^3) in the reactor, using Ar as the carrier gas, at different temperatures (200 – 900 ^oC) or injecting at 900 ^oC a number of H_2 pulses, one after another, at an interval of time of 10 min or 1 h and determining the conversion of H_2 in each pulse experiment.

5.3 Results and Discussion

5.3.1 Partial Oxidation of Methane to Syngas

A number of supported nickel, cobalt containing catalysts have been evaluated for their performance in the CPOM process and the results are presented in Table 5.1. The comparison of the catalysts supported on SZ-5564 commercial catalyst carrier (which is a low surface area macroporous highly sintered support consisting mainly of zirconia and haffnia) shows that the catalyst containing MgO with or without cerium oxide ($CoNiMgO_x$ / SZ-5564 and $CoNiMgCeO_x$ / SZ-5564) showed very high methane conversion activity (> 98 % methane conversion) and also high selectivity for both CO and H_2 (> 96 %) in the CPOM process at a low contact time (GHSV = 62,000 $cm^3g^{-1}h^{-1}$), even when the catalysts were precalcined at a very high temperature (1400 ^oC). Also, even when the two catalysts ($NiCoMgO_x$ / SZ-5564 and $NiCoMgCeO_x$ / SZ-5564) were subjected to still higher temperature (≥ 2000^oC) for 30 min or high temperature (≥ 2000^oC) shocks by directly exposing them to an oxy-acetylene flame, both the catalysts showed almost no change in their activity and selectivity in the CPOM process (Table 5.2). After the high temperature thermal treatments, there was no disintrigration of the catalyst particles and also no loss in their mechanical strength / attrition resistance was

observed. Thus, both the catalysts showed very high thermal stability for their use in the CPOM process and their performance in the CPOM process is quite comparable.

Table 5.1: Performance of the supported Ni-Co catalysts calcined at 1400 ^{o}C (for 4 h) in the partial oxidation of methane to syngas [feed: a mixture of 64.3 mol % CH_4 and 36.1 mol % O_2, GHSV = 62,000 cm^3 g^{-1} h^{-1}, temperature = 900 ^{o}C. All the catalysts reduced before the reaction in the presence of 50 vol % of H_2 in N_2 at 900 ^{o}C for 2 h]

Catalyst	Loading on support (Wt %)					CH_4 Conv. (%)	Selectivity (%)	
	Ni	Co	MgO	CeO_2	ZrO_2		H_2	CO
$NiCoO_x$ / SZ-5564	8.49	1.73	0.0	0.0	0.0	87.7	94.8	93.9
$NiCoCeO_x$ / SZ-5564	8.49	1.73	0.0	30.1	0.0	92.5	96.2	93.8
$NiCoMgO_x$ / SZ-5564	8.49	1.73	7.0	0.0	0.0	98.2	96.5	96.4
$NiCoO_x$ / MgO / SZ-5564	8.49	1.73	7.0	0.0	0.0	95.3	97.6	97.1
$NiCoMgCeO_x$ / SZ-5564	8.49	1.73	7.0	30.1	0.0	98.5	96.9	96.7
$NiCoZrO_x$ / SZ-5564	8.49	1.73	0.0	0.0	30.1	90.6	94.9	94.5
$NiCoO_x/ZrO_2$ / SZ-5564	8.49	1.73	0.0	0.0	30.1	70.5	82.7	87.8
$NiCoMgZrO_x$ / SZ-5564	8.49	1.73	7.0	0.0	30.1	92.6	97.5	95.4

Table 5.2: Performance of the $NiCoMgO_x$ / SZ-5564 and $NiCoMgCeO_x$ / SZ-5564 catalysts (precalcined at 900 or 1400 ^oC), subjected to high temperature shocks by directly exposing them to acetylene-oxygen flame, in the partial oxidation of methane to syngas at 850 ^oC (feed = a mixture of 64.3 mol % CH_4 and 35.7 mol % O_2).

Catalyst pre-calcination temperature (^oC)	Time for exposure to the flame (min)	GHSV ($cm^3g^{-1}h^{-1}$)	Conversion (%)		Selectivity (%)	
			CH_4	O_2	CO	H_2
Catalyst: $NiCoMgO_x$ / SZ – 5564						
900	None	120,000	95.7	100	97.4	98.4
900	30 (once)	120,000	95.6	100	96.1	98.0
1400	15 (once)	62,000	95.6	100	97.4	97.8
1400	30 (once)	62,000	95.5	100	98.5	98.4
1400	0.5(six times)[a]	62,000	95.8	100	97.6	98.6
Catalyst: $NiCoMgCeO_x$ / SZ – 5564						
900	None	62,000	97.5	100	97.1	97.1
900	15 (once)	120,000	98.3	100	96.9	96.7
900	30 (once)	120,000	98.2	100	96.7	98.2
900	0.5(six times)[a]	120,000	96.9	100	97.2	98.4
1400	30 (once)	62,000	97.2	100	96.9	97.6

[a] The catalyst was exposed to the oxy-acetylene flame repeatedly after an interval of 10 min, during which the flame-exposed catalyst is suddenly cooled in a flow of cool air. Thus the catalyst was subjected to high temperature shocks.

Results in Figure 5.1 showed the influence of reaction temperature and space velocity on the CH_4 conversion and CO and H_2 selectivity in the CPOM over both the catalysts (NiCoMgOx / SZ-5564 and CoNiMgCeOx / SZ-5564). As expected the conversion of CH_4 is increased by increasing the temperature and decreased exponantionally with increasing the space velocity. The selectivity of H_2 or CO is also increased with increasing the temperature, but decreased by increasing the space velocity. This indicates the water gas shift reaction ($CO + H_2O \rightarrow CO_2 + H_2$) occurring simultaneously to a larger extent at the lower temperature and also at the lower contact time (i.e. at the higher space velocity)

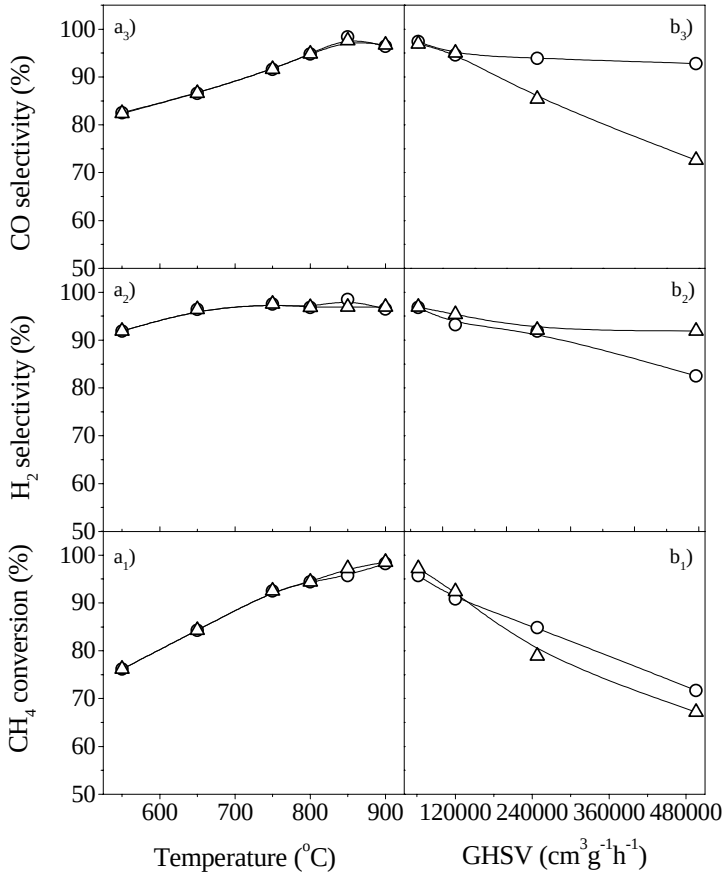

Figure 5.1: Effect of reaction temperature and space velocity over the $NiCoMgO_x$ / SZ-5564 (O) and $NiCoMgCeO_x$ / SZ-5564 (Δ) catalysts (calcined at 1400 ^oC) in the CPOM process [Reaction condition: for a_1, a_2 & a_3 GHSV = 62,000 $cm^3g^{-1}h^{-1}$, $CH_4/O_2 = 1.8$; for b_1, b_2 & b_3 Temperature = 850 ^oC, $CH_4/O_2 = 1.8$].

Results showing the influence of space velocity on the performance of the NiCoOx / SZ-5564, NiCoOx / ZrO_2 / SZ-5564 and NiCoZrOx / SZ-5564 catalysts are given in Table 5.3. Interestingly, both the conversion of CH_4 and selectivity for H_2 and CO are found to be increased with increasing space velocity for these catalysts. This is expected mostly because of the low selectivity of the catalysts, which results in a temperature increase at the catalyst surface with increasing the space velocity, causing the observed increase in the conversion and selectivity. When the reaction was carried out further at a much higher space velocity (500,000 $cm^3g^{-1}h^{-1}$), an unsteady or oscillating behavior of the reaction temperature was observed for the $NiCoO_x$ / SZ-5564 (precalcined at 1400 ^oC) catalyst (presented in Fig. 5.2). The unsteady / oscillating reaction behavior is expected due to the formation of hot spot at the catalyst surface with increasing the space velocity. Additional data for the supported Ni-Co catalysts, showing their performance in the CPOM process at different process conditions are presented in Appendix 5.1 – 5.14.

Table 5.3: Effect of space velocity in the performance of CPOM process over the supported catalysts (calcined at 1400 ^oC) containing Ni and Co with or without ZrO_2 at 850 ^oC [CH_4 / O_2 = 1.8 (all the catalysts were reduced before the reaction in the presence of 50 vol % of H_2 in N_2 at 900 ^oC for 2 h)]

GHSV ($cm^3g^{-1}h^{-1}$)	CH_4 conversion (%)	O_2 conversion (%)	H_2 selectivity (%)	CO selectivity (%)
Catalyst: $NiCoO_x$ / SZ-5564				
30000	73.9	100	85.6	84.2
62000	75.3	100	88.1	91.1
120000	78.3	100	88.6	93.9
Catalyst: $NiCoO_x$ / ZrO_2 / SZ-5564				
30000	53.6	100	64.9	70.8
62000	66.2	100	75.9	84.5
120000	67.9	99.7	78.8	91.2
Catalyst: $NiCoZrO_x$ / SZ-5564				
30000	75.4	99.7	87.7	85.8
62000	76.0	99.7	88.3	91.1
120000	79.2	99.7	94.1	94.1

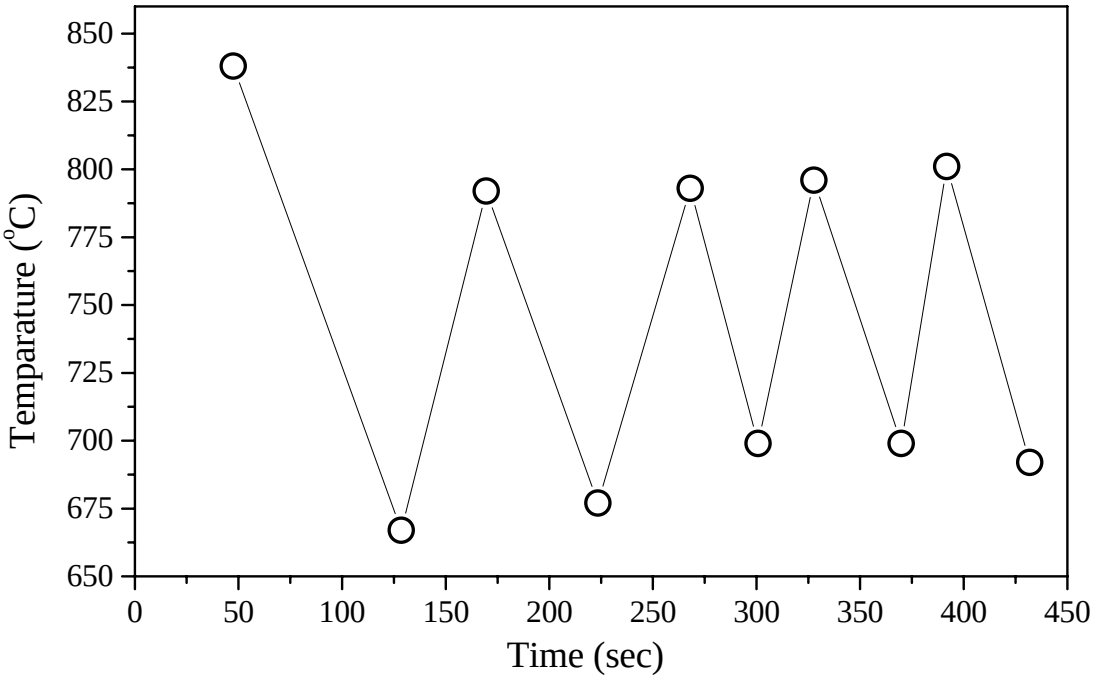

Figure 5.2 Temperature oscillations in the partial oxidation of methane over $NiCoO_x$ / SZ-5564 (precalcined at 1400 ^oC) catalyst [CH_4/O_2 = 1.8, GHSV = 500,000 $cm^3g^{-1}h^{-1}$ and temperature controller set temperature (T_s) = 750 ^oC]

Since the $NiCoMgO_x$/SZ-5564 and $NiCoMgCeO_x$/SZ-5564 catalysts showed highly promising and comparable performance, further work was carried out only on these two catalysts.

5.3.1.1 Effect of sulfur compound in the feed over $NiCoMgO_x$/SZ-5564 & $NiCoMgCeO_x$/SZ-5564 catalysts in the partial oxidation of methane to syngas.

For both the supported $NiCoMgO_x$ and $NiCoMgCeO_x$ catalysts (precalcined at 1400 ^oC), when thiophene at much higher concentration (7400 ppm) than that present in natural gas was introduced in the feed during the partial oxidation of methane at 850 ^oC (GHSV = 62,000 $cm^3g^{-1}h^{-1}$), the methane conversion, H_2 selectivity and CO selectivity were decreased continuously, as shown in Figs. 5.3 and 5.4, because of the catalyst poisoning by sulfur. However, after the oxidative treatment to the poisoned catalyst in a flow of 50 % O_2 in N_2 at 800 ^oC for 2 h, the original activity and selectivity of both the catalysts could be regained, indicating excellent regenerability of the catalysts, if poisoned by sulfur.

A comparison of the results (Fig. 5.3 and Fig. 5.4) reveals that the catalyst deactivation due to the sulfur poisoning is relatively slower for the $NiCoMgCeO_x$/SZ-5564 catalyst.

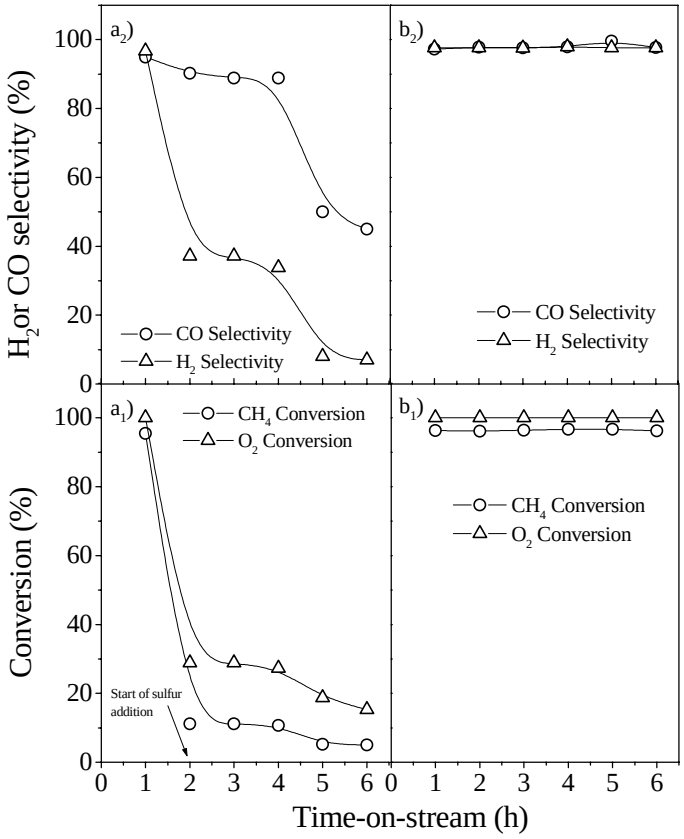

Figure 5.3 Time-on-stream activity on the performance of partial oxidation of methane at 850 ^oC over $NiCoMgO_x$/SZ-5564 catalyst (calcined at 1400 ^oC) in presence of thiophene (a_1, a_2) & after regeneration (b_1, b_2) the catalyst in presence of O_2+N_2 in 50:50 at 800 ^oC [Reaction condition: GHSV= 62000 $cm^3g^{-1}h^{-1}$, CH_4/O_2 = 1.8; catalyst reduced at 900 ^oC in presence of H_2+N_2 in 50:50 ratio for 2 h before start the reaction]

5.3.2 Steam and CO_2 Reforming of Methane to Syngas over $NiCoMgO_x$/SZ-5564 & $NiCoMgCeO_x$/SZ-5564 Catalysts

When the two catalysts (precalcined at 1400 ^oC) are compared for their performance in the methane steam and CO_2 reforming reactions (Table 5.4), the supported $NiCoMgO_x$ catalyst showed inferior performance than that showed by the supported $NiCoMgCeO_x$ catalyst. The later catalyst showed high activity in the steam reforming (94.2 % methane conversion) and also good CO_2 reforming activity (75 % methane conversion) at a higher space velocity (GHSV = 20,000 $cm^3g^{-1}h^{-1}$) than that normally used in the commercial steam reforming process. The

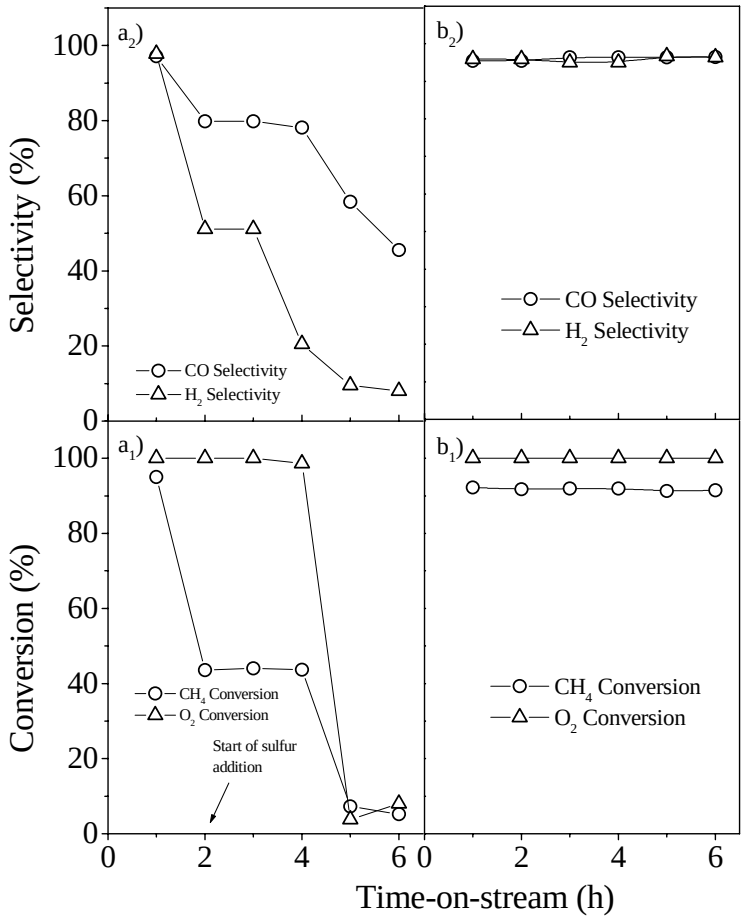

Figure 5.4 Time-on-stream activity on the performance of partial oxidation of methane at 850 ^{o}C over NiCoMgCeO$_x$/SZ-5564 catalyst (calcined at 1400 ^{o}C) in presence of thiophene (a_1, a_2) & after regeneration (b_1, b_2) the catalyst in presence of O_2+N_2 in 50:50 at 800 ^{o}C [Reaction condition: GHSV= 62000 cm^{3}g^{-1}h^{-1}, CH_4/O_2 = 1.8; catalyst reduced at 900 ^{o}C in presence of H_2+N_2 in 50:50 ratio for 1 h before start the reaction]

observed much higher activity in both the steam and CO_2 reforming reactions of the supported NiCoMgCeO$_x$ catalyst is attributed mostly to its higher oxygen storage capacity and / or oxygen mobility because of the presence of cerium oxide in the catalyst, as evidenced by the temperature programmed reduction (TPR) by H_2 and also by the H_2 pulse reaction over the two catalysts, discussed later.

Table 5.4: Performance of the $NiCoMgO_x$/SZ-5564 and $NiCoMgCeO_x$/SZ-5564 catalysts calcined at 1400 ^oC (for 4 h) in the methane steam and CO_2 reforming reactions at 850^oC [GHSV = 20,000 $cm^3g^{-1}h^{-1}$]

Catalyst	Methane conversion (%)	Selectivity (%)	
		H_2	CO
Steam reforming of methane (feed = 25 mol % CH_4 and 75 mol % steam)			
$NiCoMgO_x$ / SZ-5564	78.8	100	61.9
$NiCoMgCeO_x$ / SZ-5564	94.2	100	64.0
CO_2 reforming of methane (feed = 47.6 mol % CH_4 and 52.4 mol % CO_2)			
$NiCoMgO_x$ / SZ-5564	29.4	90.7	100
$NiCoMgCeO_x$ / SZ-5564	74.7	97.3	100

5.3.3 Oxy-Steam Reforming of Methane to Syngas over $NiCoMgO_x$/SZ-5564 & $NiCoMgCeO_x$/SZ-5564 Catalysts

In the oxy-steam reforming, following catalytic reactions are expected to occur simultaneously.

Partial oxidation of methane

$CH_4 + 0.5O_2 \rightarrow CO + 2H_2$ (ΔH_r = - 5.4 $kcal.mol^{-1}$) (1)

Methane steam reforming

$CH_4 + H_2O \rightarrow CO + 3H_2$ (ΔH_r = + 54.13 $kcal.mol^{-1}$) (2)

Water gas shift reaction

$CO + H_2O \rightarrow CO_2 + H_2$ (ΔH_r = - 8.08 $kcal.mol^{-1}$) (3)

5.3.3.1 Effect of H_2O/CH_4 ratio

Results showing the influence of H_2/CH_4 ratio in feed [when $CH_4/(O_2+0.5H_2O) = 1.82$] at 850 ^oC on the conversion, selectivity and net heat of reaction (ΔH_r) in the oxy-steam reforming of methane over both the catalysts at high space velocity (46,000 $cm^3g^{-1}h^{-1}$) are presented in Figs. 5.5 and 5.6. The net heat of reaction (ΔH_r) for the overall process is estimated by subtracting the heat of formation (at the process temperature) of the components in the feed from that of the components in the products stream. In oxy-steam reforming process, when the H_2O conversion is ≥ 0, the H_2 selectivity (based on methane) is 100 %.

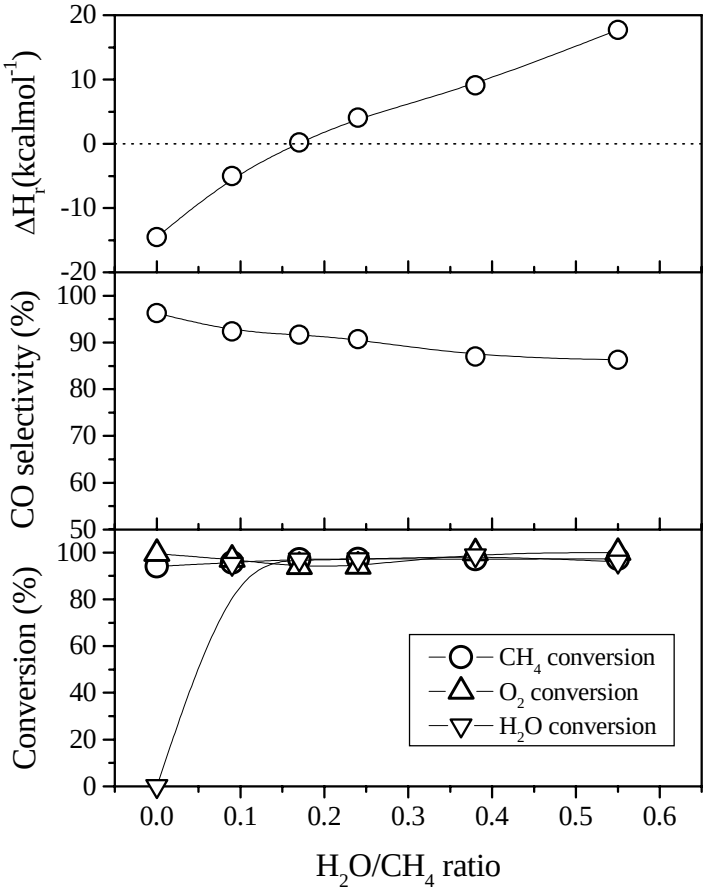

Figure 5.5 Effect of H_2O/CH_4 ratio in the performance of simultaneous oxy-steam reforming of methane over $NiCoMgO_x$/SZ-5564 (calcined at 1400 ^oC) at 850 ^oC [GHSV = 46,000 $cm^3.g^{-1}.h^{-1}$, CH_4/O_2=2.0, Catalyst reduced at 900^oC in presence of H_2+N_2 in 50:50 ratio for 1 h before start reaction]

When the H_2O/CH_4 ratio is increased while keeping the CH_4 / (O_2 + 0.5H_2O) ratio constant, the process performance is influenced as follows:

- The conversion of O_2 (which is nearly 100 %) or methane is almost not changed.
- The selectivity of CO is decreased significantly
- The net heat of reaction (ΔH_r) is increased, indicating a decrease in the process exothermicity or an increase in the process endothermicity.

The decrease in the CO selectivity shows that the rate of water gas shift reaction is increased with increasing the relative concentration of water in the feed.

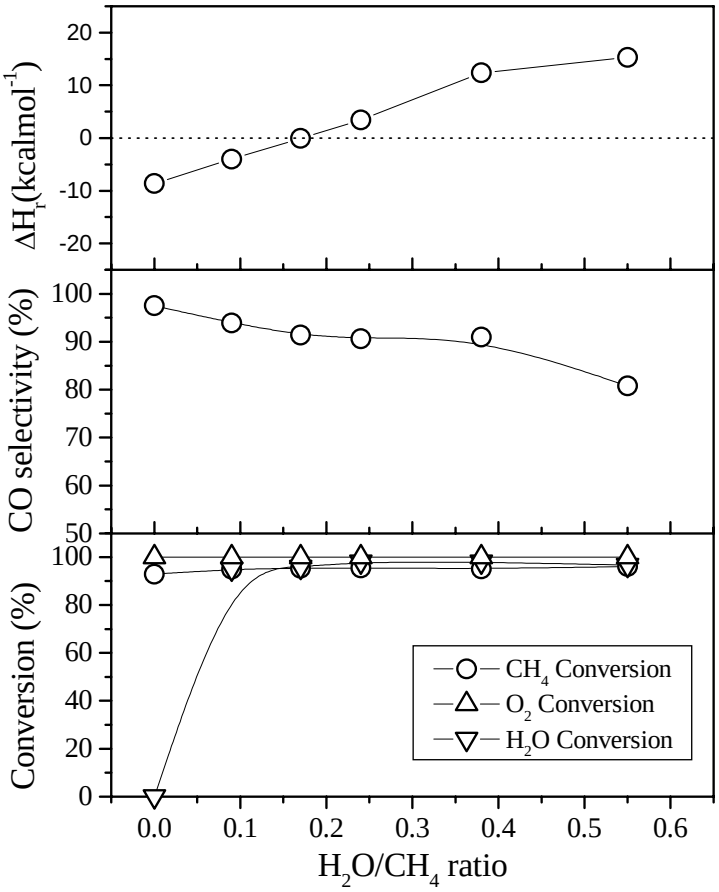

Figure 5.6 Effect of H_2O/CH_4 ratio on the performance of simultaneous oxy-steam reforming of methane over $NiCoMgCeO_x$/SZ-5564 (calcined at 1400 ^oC) at 850 ^oC [GHSV = 46,000 $cm^3g^{-1}h^{-1}$, CH_4/O_2=2.0. Catalyst was reduced at 900 ^oC in presence of H_2+N_2 in 50:50 ratio for 1 h before start reaction]

5.3.3.2. Effect of reaction temperature

The effect of temperature on the conversion, selectivity and net heat of reactions (ΔH_r) involved in the oxy-steam reforming process over $NiCoMgCeO_x$/SZ-5564 (calcined at 1400 ^oC) is shown in Fig. 5.7. The conversion of O_2 in all cases was 100%. The H_2 selectivity (based on methane) is 100 %, as the conversion of H_2O is positive.

The results (Fig. 5.7) show that, with the increase of temperature (750 – 900 ^oC) in the oxy-steam reforming of methane, (a) the conversion of methane and steam is increased, the increase being larger in the CH_4 conversion, (b) the selectivity for CO is increased markedly, and (c) the net heat of reaction (ΔH_r) is increased, indicating a decrease in the process exothermicity or an increase in the process endothermicity.

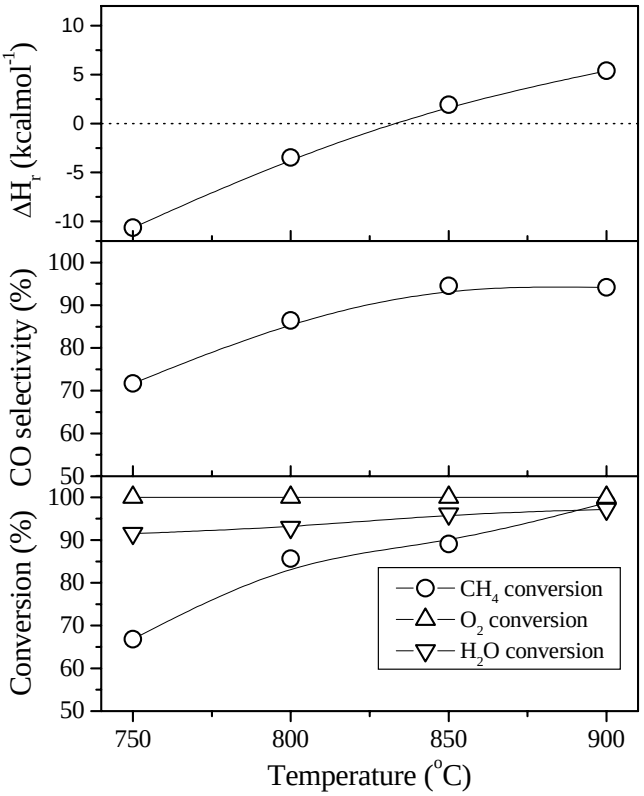

Figure 5.7 Effect of temperature on the performance of oxy-steam reforming of methane over $NiCoMgCeO_x$/SZ-5564 (calcined at 1400 ^oC [GHSV = 46,000 $cm^3g^{-1}h^{-1}$, O_2/CH_4 = 0.5, H_2O/CH_4 = 0.17. Catalyst was reduced at 900 ^oC in presence of H_2+N_2 in 50:50 ratio for 1 h before start reaction]

Thus by manipulating the temperature or water / CH_4 ratio in feed or both, the process can be made thermoneutral or mildly exothermic or endothermic, eliminating or drastically reducing the process hazards.

5.3.4 Oxy-CO_2 Reforming of Methane to Syngas over NiCoMgO$_x$/SZ-5564 & NiCoMgCeO$_x$/SZ-5564 Catalysts

Results showing the influence of temperature on the conversion and selectivity and also on the net heat of reaction (ΔH_r) in the oxy-CO_2 reforming of methane over both the catalysts at a high space velocity (46,000 $cm^3g^{-1}h^{-1}$) are presented in Figs. 5.8 and 5.9.

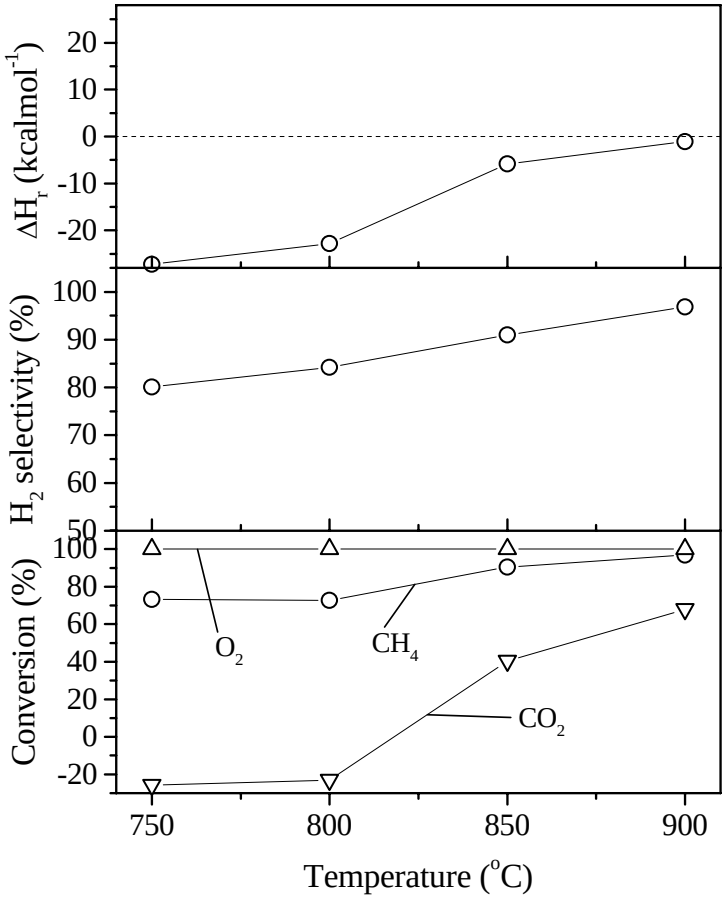

Figure 5.8 Effect of temperature on the performance of oxy-CO_2 reforming of methane over NiCoMgCeO$_x$/SZ-5564 catalyst (precalcined at 1400 ^oC) [CO_2/CH_4 = 0.14; O_2/CH_4 = 0.5; GHSV = 46,000 $cm^3g^{-1}h^{-1}$. Catalyst was reduced at 900 ^oC in presence of $H_2 + N_2$ in 50:50 ratio for 2 h before the reaction]

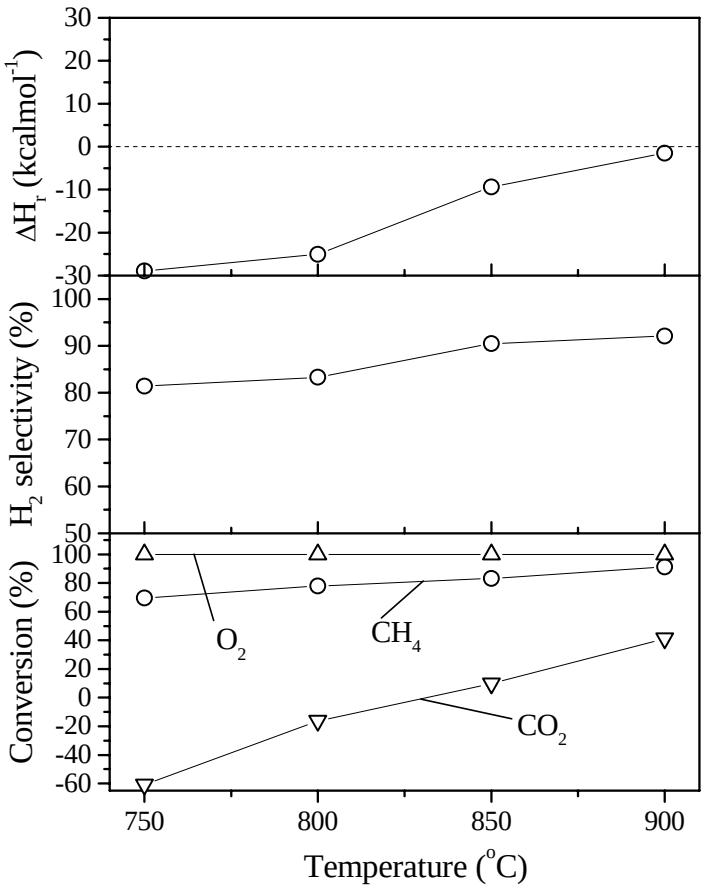

Figure 5.9 Effect of temperature on the performance of oxy-CO_2 reforming of methane over $NiCoMgO_x$/SZ-5564 catalyst (precalcined at 1400 ^oC) [CO_2/CH_4 = 0.14; O_2/CH_4 = 0.5; GHSV = 46,000 $cm^3g^{-1}h^{-1}$. Catalyst was reduced at 900 ^oC in presence of $H_2 + N_2$ in 50:50 ratio for 2 h before the reaction]

When reaction temperature is increased (Figs. 5.8 & 5.9), the conversion of CH_4 and CO_2, H_2 selectivity and net heat of reaction (ΔH_r) are increased markedly.

All the above results clearly indicate that both the supported $NiCoMgO_x$ and $NiCoMgCeO_x$ catalysts have very high thermal stability against the high temperature treatments / thermal shocks, and both show both high activity and selectivity in the CPOM process. Also, both the catalysts could be easily regenerated if poisoned by sulfur. Because of their high thermal stability, the formation of hot spots in the catalyst bed and / or high temperatures prevailing at the catalyst surface during the CPOM process would cause little or no effect on the catalytic activity and selectivity of the two catalysts making them suitable for the CPOM process, even operating under adiabatic condition. These results also indicate that

there is little or no formation of catalytically inactive mixed metal oxide phases during the high temperature treatments to both the catalysts. However, for the MATR (methane autothermal reforming) process, the supported $NiCoMgCeO_x$ catalyst is more suitable than the supported $NiCoMgO_x$ catalyst, because of the much higher performance of the former catalyst in both the steam and CO_2 reforming reactions. Also, the former catalyst showed very high activity in both the simultaneous oxy-steam and oxy-CO_2 reforming of methane.

The observed much higher activity of the supported $NiCoMgCeO_x$ catalyst is attributed mostly to its higher oxygen storage capacity and / or oxygen mobility because of the presence of cerium oxide in the catalyst, as evidenced by the temperature programmed reduction (TPR) by H_2 and also by the H_2 pulse reaction over the two catalysts as follows.

5.3.5 Catalyst Characterization

5.3.5.1. X-ray diffraction (XRD) spectroscopy

XRD spectra of the $NiCoMgO_x$ / SZ-5564 and $NiCoMgCeO_x$ / SZ-5564 catalysts, along with that of the support are presented in Figs. 5.10 and 5.11. The crystalline phases presented in the catalysts are as follows:

For $NiCoMgO_x$ / SZ-5564 catalyst : (Ni and Co-Mg) O solid solution, $MgCo_2O_4$

For $NiCoMgCeO_x$ / SZ-5564 catalyst : (Ni and Co-Mg) O solid solution, $MgCo_2O_4$, $MgCeO_3$ and CeO_2

5.3.5.2.Temperature programmed reduction (TPR)

The TPR curve for the supported $NiCoMgO_x$ catalyst (Fig. 5.12b) shows two TPR peaks (with peak maximum at 456 ^{o} and 1045 ^{o}C), whereas that for the supported $NiCoMgCeO_x$ catalyst (Fig. 12a) shows three peaks (with peak maximum at 413 ^{o}, 670 ^{o} and 1027 ^{o}C). For both the catalysts, the first low temperature peak (between 300 ^{o} and 500 ^{o}C) is due to the reduction of free nickel and / or cobalt oxides present in a very small amount in the catalyst and that at the high temperatures (above 800 ^{o}C) corresponds to the reduction of nickel-cobalt oxides dissolved in the MgO and also doped in the ZrO_2 (from the support). The peak between 500 ^{o} and 700 ^{o}C for the supported $NiCoMgCeO_x$ catalyst is expected mostly due to the reduction of cerium oxide ($2CeO_2 + H_2 \rightarrow Ce_2O_3 + H_2O$) present at the catalyst surface [11]. The degree of reduction of the nickel and cobalt oxides (estimated from the H_2 consumed

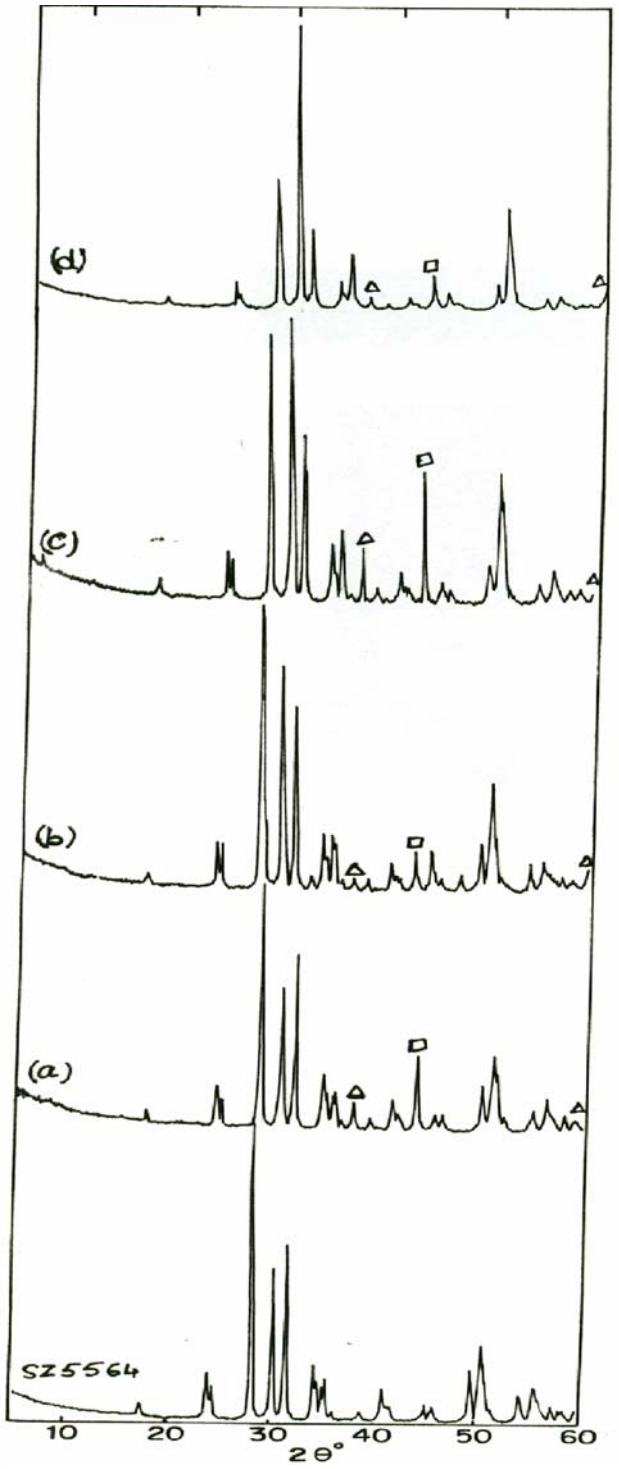

Figure 5.10 XRD spectra of the $NiCoMgO_x$ / SZ-5564 catalyst at different calcination temperatures: (a) 900 ^oC (fresh catalyst), (b) 900 ^oC (used catalyst), (c) 1400 ^oC (fresh catalyst), (d) 1400 ^oC (used catalyst) [Symbol for identifying different phases; $\Delta \rightarrow MgCo_2O_4$; □ $\rightarrow$ (Ni and Co-Mg) O solid solution].

Figure 5.11 XRD spectra of the $NiCoMgCeO_x$ / SZ-5564 catalyst at different calcination temperatures: (a) 900 ^oC (fresh catalyst), (b) 900 ^oC (used catalyst), (c) 1400 ^oC (fresh catalyst), (d) 1400 ^oC (used catalyst) [Symbol for identifying different phases; O $\rightarrow$ $MgCeO_3$; $\Delta \rightarrow MgCo_2O_4$; □ $\rightarrow$ (Ni and Co-Mg) O solid solution; $\ast \rightarrow$ Unidentified [$CeAlO_3$ (?); ◈ $\rightarrow$ CeO_2].

in the TPR) is found to be 32.8 and 55.2 %, for the supported $NiCoMgO_x$ and $NiCoMgCeO_x$ catalysts, respectively. The observed very significant shift in the TPR curve for the supported $NiCoMgCeO_x$ catalyst towards the lower temperature side and also its higher degree of reduction clearly show that the reduction of the nickel and cobalt oxides of the supported catalyst becomes easier because of the presence of cerium oxide in the catalyst. This is expected mostly because of an increase in the mobility of lattice oxygen in the catalyst in the presence of cerium oxide, particularly in the form of $MgCeO_3$ (observed by the XRD) and CeO_2-ZrO_2 solid solution.

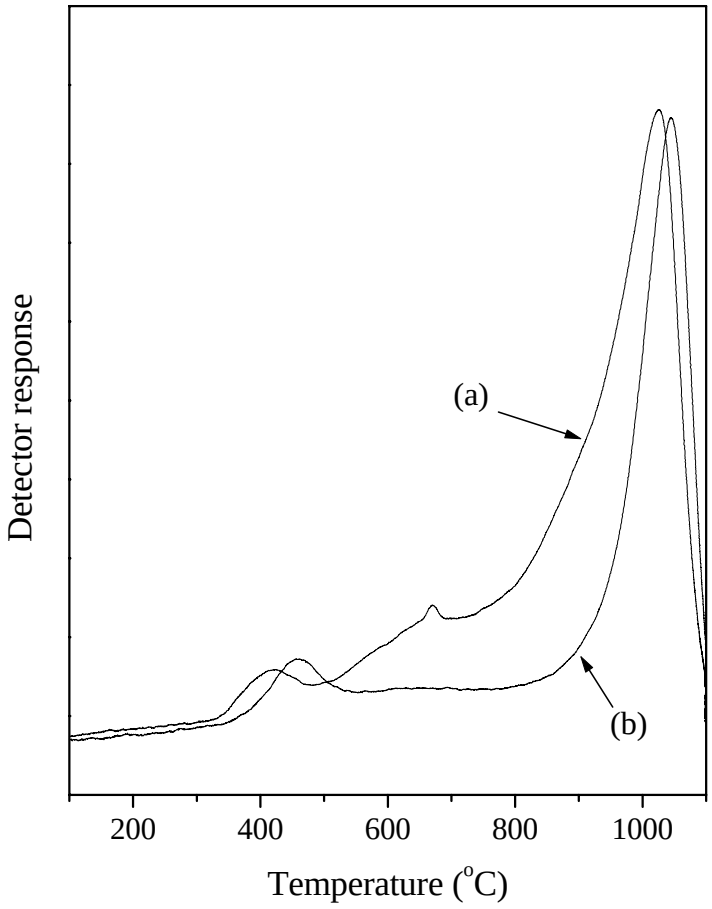

Figure 5.12 Temperature programmed reduction (TPR) by H_2 of (a) $NiCoMgCeO_x$/SZ – 5564 and (b) $NiCoMgO_x$/SZ – 5564

5.3.5.3 X-ray photoelectron spectroscopy (XPS)

Results showing the relative bulk and surface concentration of Co, Ni, Mg and Ce in both the catalysts are given in Table 5.5. The XPS spectra (general scan) for the catalysts are presented in Figs. 5.13 and 5.14.

For the $NiCoMgCeO_x$ / SZ-5564 catalyst, the surface concentration of cerium is much lower than that of the magnesium in the catalyst (at the surface, Ce/Mg = 0.02) (Table 5.5). This may be expected because of the formation of CeO_2-ZrO_2 (from the support) solid solution at the high calcination temperature.

Table 5.5: Relative bulk and surface concentrations of different metals in the supported $NiCoMgO_x$ and $NiCoMgCeO_x$ catalysts in their active form.

Catalyst	Co/Ni ratio		Ce/Mg ratio		Ni/Mg ratio		Co/Mg ratio	
	Bulk	Surface	Bulk	Surface	Bulk	Surface	Bulk	Surface
$NiCoMgO_x$/SZ-5564	0.2	1.09	0.0	0.0	1.2	0.04	0.17	0.04
$NiCoMgCeO_x$/SZ-5564	0.2	0.39	1.0	0.02	1.2	0.05	0.17	0.02

5.3.5.4 H_2 pulse reaction over the catalysts

Results of the H_2 pulse reaction over both the catalysts at different temperatures as a function of pulse number (at 900 ^oC) (Fig. 5.15) further confirm the above conclusion / prediction. In case of the supported $NiCoMgCeO_x$ catalyst, the H_2 conversion (at the same temperature) in the pulse reaction is much higher (Fig. 5.15a_1, b_1) and the observed increase in the H_2 conversion for the H_2 pulse injected after a much longer period (1 h) is also much higher (Fig. 5.15a_2, b_2). The increase in the H_2 conversion (by about 10 % and 20 % for the supported $NiCoMgO_x$ and $NiCoMgCeO_x$, respectively) due to the increase in the interval for the H_2 pulse injection (from 10 min to 1 h) is attributed to the migration of sub-surface oxygen to the catalyst surface. These results clearly showed that, the lattice oxygen in the catalyst in the

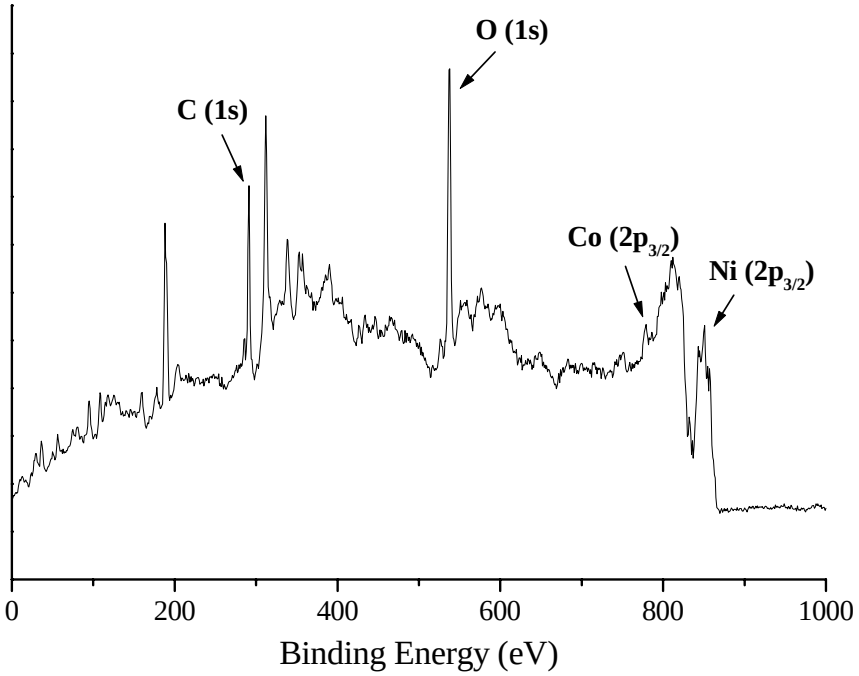

Figure 5.13 XPS general spectra of $NiCoMgO_x$/SZ-5564 (precalcined at 1400 ^oC) catalyst in its active form

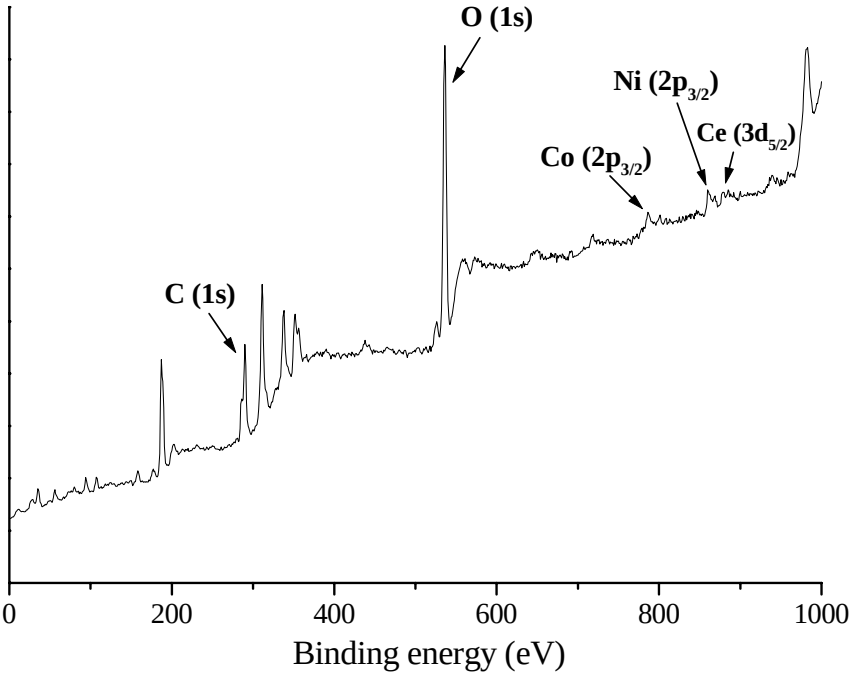

Figure 5.14 XPS general spectra of $NiCoMgCeO_x$/SZ-5564 (precalcined at 1400 ^oC) catalyst in its active form

presence of cerium oxide is more mobile. Thus the presence of cerium oxide in the catalyst not only provides an oxygen storage capacity but also greatly enhances the mobility of lattice oxygen in the catalyst. Hence, the supported $NiCoMgCeO_x$ catalyst, even when calcined at 1400 ^oC, shows excellent performance not only in the CPOM but also in the steam and CO_2 reforming reactions and also in the oxy-steam and oxy-CO_2 reforming reactions, with high stability against deactivation due to coking even in the CO_2 reforming. The observed appreciable oxygen mobility in the supported $NiCoMgO_x$ catalyst is, however, expected because of the doping of a part of the nickel and cobalt in the ZrO_2 [12].

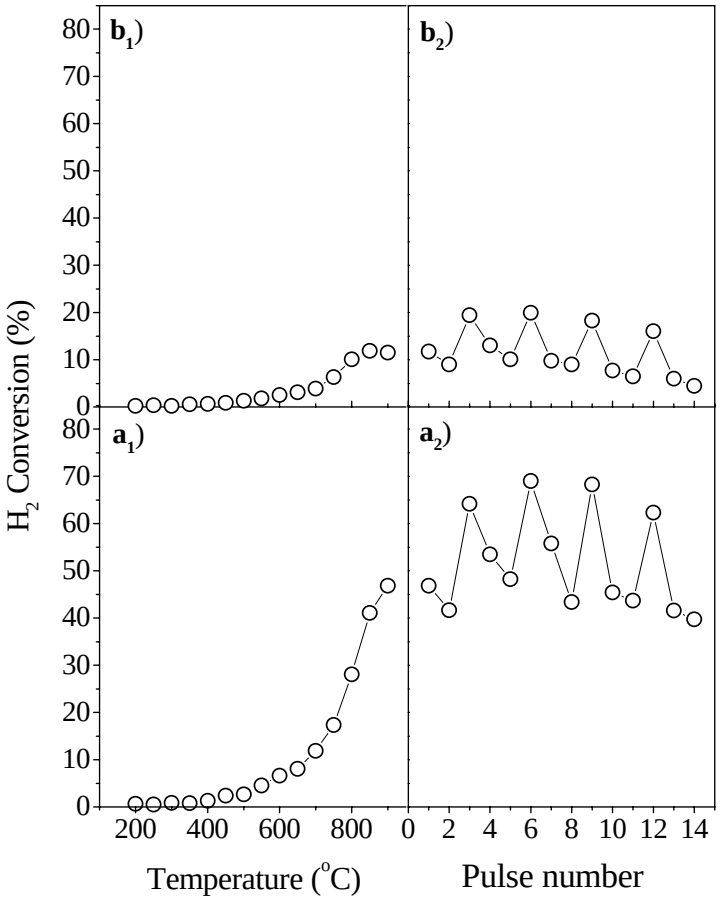

Figure 5.15 H_2 conversion (X_{H2}) in the pulse reaction of pure H_2 over the $NiCoMgCeO_x/SZ$ – 5564 (a_1, a_2) and $NiCoMgO_x/SZ$ – 5564 (b_1, b_2) catalysts (both precalcined at 1400 ^oC) as a function of reaction temperature and pulse number at 900 ^oC. For studying the influence of pulse number on the H_2 conversion, each of the H_2 pulses numbered 1, 2, 4, 5, 7, 8, 10, 11, 13 and 14 was injected in the reactor at 900 ^oC after an interval of 10 min, whereas each of the H_2 pulses numbered 3, 6, 9 and 12 was injected after an interval of 1.0 h.

3.3.6. Conclusions

From the studies on the catalytic partial oxidation, CO_2 reforming, steam reforming, oxy-steam reforming and oxy-CO_2 reforming reactions of methane for its conversion to syngas over the catalyst containing MgO with or without cerium oxide, following important conclusions have been drawn.

1. The catalyst containing MgO with or without cerium oxide ($NiCoMgO_x$/SZ-5564 and $NiCoMgCeO_x$/SZ-5564) showed very high methane conversion activity and also selectivity for both H_2 and CO in the CPOM process at a low contact time, even when the catalyst was precalcined at a very high temperature (1400 ^oC).
2. The catalysts show very high thermal stability even when subjected to an oxy-acetylene flame (very high temperature shocks).
3. For the MATR process, the supported $NiCoMgCeO_x$ catalyst is more suitable than the supported $NiCoMgO_x$ catalyst, because of the better performance of the former catalyst in both the steam and CO_2 reforming reactions.
4. The better performance of the supported $NiCoMgCeO_x$ catalyst is due to the presence of cerium oxide, which not only provides an oxygen storage capacity but also greatly enhances the mobility of lattice oxygen in the catalyst.

References

1. J. H. Lunsford, Catal. Today, 63 (2000) 165.
2. J. Haggin, Chem. Eng. News, (June 01 / 22) 22 (1987).
3. (a) Encyclopedia of Chemical Technology, Vol. 12 (Eds.: RE Kirk, D. F. Othmer), 3rd ed., Willy Interscience, New York; (b) Ulmann's Encyclopedia of Industrial Chemistry, Vol. A 12, 5th ed., VCH, Weinheim, (1989) p. 169.
4. (a) S. S. Bhardwaj and L. D. Schmidt, Fuel Processing Technol.,42 (1995) 109; (b) M. A. Pena, J. P. Gomez and J. L. G. Fierro, Appl. Catal., 144 (1996) 7; (c) S. C. Tsang, J. B. Claridge and M. L. H. Green, Catal. Today, 23 (1995) 3; (d) Y. H. Hu and E. Reckenstein, Catal. Reviews, 44 (2002) 423.
5. (a) V. R. Choudhary, A. S. Mamman and S. D. Sansare, Angew. Chem. Int. Ed. Engl., 31 (1992) 1189; (b) V. R. Choudhary, A. M. Rajput and V. H. Rane, J. Phys. Chem., 96

(1992) 8686; (c) V. R. Choudhary, A. M. Rajput and V. H. Rane, Catal. Lett., 16 (1992) 269; (d) V. R. Choudhary, V. H. Rane and A. M. Rajput, Catal. Lett., 22 (1993) 289.

6. (a) D. A. Hickman, L. D. Schmidt, Science 259 (1993) 343; (b) D. A. Hickman, E. A. Haupfear and L. D. Schmidt, J. Catal. , 138 (1992) 267.
7. V. R. Choudhary and A. S. Mamman, J. Catal., 172 (1997) 281.
8. (a) V. R. Choudhary, V. H. Rane and A. M. Rajput, Appl. Catal. A: Gen., 162 (1997) 235; (b) V. R. Choudhary, A. M. Rajput, B. Prabhakar and A. S. Mamman, Fuel, 77 (1998) 1803.
9. V. R. Choudhary, A. S. Mamman, J. Chem. Technol. Biotech., 73 (1998) 345.
10. V. R. Choudhary, A. S. Mamman, B. S. Uphade and R. E. Babcock, CO_2 Conversion and Utilization, Eds. C. Song, A. F. Gaffney and K. Fujimoto, ACS, Washington, DC, (2001) p. 224.
11. (a) R. de Souza Monteiro, F. B. Noronha, L. C. Dieguez, M. Schmal, Appl. Catal., 131 (1995) 89; (b) W-S. Dong, H-S. Roh, K-W. Jun, S-E. Park, Y-S. Oh, Appl. Catal. A: Gen., 226 (2002) 63.
12. V. R. Choudhary, S. Banerjee and S. G. Pataskar, Appl. Catal. A: Gen., 253 (2003) 65.
13. V. R. Choudhary and V. H. Rane, J. Catal., 135 (1992) 310.

Appendix 5.1: Effect of temperature in the performance of $NiCoO_x$/SZ-5564 catalyst precalcined at 1400 ^oC [Reaction condition: GHSV=62,000 $cm^3g^{-1}h^{-1}$; CH_4/O_2=1.8. The catalyst was reduced at 900 ^oC in presence of H_2+N_2 in 50:50 ratio for 2 h before start reaction]

Temperature (^oC)	CH_4 Conversion (%)	O_2 Conversion (%)	H_2 Selectivity (%)	CO Selectivity (%)
900	87.7	100	94.8	93.9
850	83.5	100	90.9	92.0
800	78.2	100	90.2	90.1
750	73.6	100	86.5	87.8
650	65.4	99.6	82.3	82.5
550	60.0	99.6	78.2	77.8

Appendix 5.2: Effect of temperature in the performance of $NiCoO_x$/SZ-5564 catalyst precalcined at 1400 ^oC [Reaction condition: GHSV=120,000 $cm^3g^{-1}h^{-1}$; CH_4/O_2=1.8. The catalyst was reduced at 900 ^oC in presence of H_2+N_2 in 50:50 ratio for 2 h before start reaction]

Temperature (^oC)	CH_4 Conversion (%)	O_2 Conversion (%)	H_2 Selectivity (%)	CO Selectivity (%)
900	87.4	100	91.4	94.5
850	83.4	100	88.6	92.7
800	81.5	100	88.4	90.9
750	77.2	100	86.6	90.0
650	68.7	100	79.3	87.3
550	61.6	100	79.4	84.7

Appendix 5.3: Effect of GHSV in the performance of partial oxidation of methane over $NiCoO_x$/SZ-5564 (precalcined at 900 ^oC) catalyst at temperature 850 ^oC. [CH_4/O_2 =1.8. The catalyst was reduced at 900 ^oC in presence of H_2+N_2 in 50:50 ratio for 2 h before start reaction]

GHSV ($cm^3g^{-1}h^{-1}$)	CH_4 Conversion (%)	O_2 Conversion (%)	H_2 Selectivity (%)	CO Selectivity (%)
60000	75.4	97.1	89.5	86.5
100000	74.2	99.7	81.5	87.0
300000	66.3	99.7	78.7	91.3
500000	63.6	99.6	68.9	91.8

Appendix 5.4: Effect of temperature in the performance of partial oxidation of methane over $NiCoZrO_x$/SZ-5564 (precalcined at 1400 ^oC) [GHSV = 62,000 $cm^3g^{-1}h^{-1}$; CH_4/O_2=1.8. The catalyst was reduced at 900 ^oC in presence of H_2+N_2 in 50:50 ratio for 2 h before start reaction]

Temperature (^oC)	CH_4 Conversion (%)	O_2 Conversion (%)	H_2 Selectivity (%)	CO Selectivity (%)
900	90.6	99.7	94.9	94.5
850	87.6	94.7	93.9	92.8
800	83.9	94.3	89.9	90.3
750	81.9	94.9	88.9	88.9
650	74.6	93.5	85.9	83.1
550	68.4	96.6	83.1	79.5

Appendix 5.5: Effect of temperature in the performance of partial oxidation of methane over $NiCoO_x/ZrO_2$/SZ-5564 (precalcined at 1400 ^oC) [GHSV = 62,000 $cm^3g^{-1}h^{-1}$; CH_4/O_2=1.8. The catalyst was reduced at 900 ^oC in presence of H_2+N_2 in 50:50 ratio for 2 h before start reaction]

Temperature (^oC)	CH_4 Conversion (%)	O_2 Conversion (%)	H_2 Selectivity (%)	CO Selectivity (%)
900	70.5	99.7	82.7	87.8
850	64.5	99.6	76.2	85.0
800	58.0	99.6	70.9	82.8
750	55.6	100	65.2	79.9
650	40.8	92.2	46.8	71.8

Appendix 5.6: Effect of temperature in the performance of partial oxidation of methane over $NiCoMgO_x$/SZ-5564 (precalcined at 1400 ^oC) [GHSV = 62,000 $cm^3g^{-1}h^{-1}$; CH_4/O_2=1.8. The catalyst was reduced at 900 ^oC in presence of H_2+N_2 in 50:50 ratio for 2 h before start reaction]

Temperature (^oC)	CH_4 Conversion (%)	O_2 Conversion (%)	H_2 Selectivity (%)	CO Selectivity (%)
900	98.4	100	96.9	96.7
850	95.7	100	96.8	97.4
800	94.4	100	96.8	94.8
750	92.5	100	97.5	91.6
650	84.3	100	96.4	86.6
550	76.2	100	91.9	82.5

Appendix 5.7: Effect of temperature in the performance of partial oxidation of methane over $NiCoMgO_x$/SZ-5564 (precalcined at 1400 ^oC) [GHSV = 120000 $cm^3g^{-1}h^{-1}$; CH_4/O_2=1.8. The catalyst was reduced at 900 ^oC in presence of H_2+N_2 in 50:50 ratio for 2 h before start reaction]

Temperature (^oC)	CH_4 Conversion (%)	O_2 Conversion (%)	H_2 Selectivity (%)	CO Selectivity (%)
900	94.3	100	93.5	95.9
850	92.4	100	95.0	95.4
800	90.8	100	94.2	94.0
750	88.1	100	93.0	92.6
650	82.8	100	91.1	89.2
550	77.0	100	94.0	85.5

Appendix 5.8: Effect of temperature in the performance of partial oxidation of methane over $NiCoMgO_x$/SZ-5564 (precalcined at 900 ^oC) [GHSV = 120,000 $cm^3g^{-1}h^{-1}$; CH_4/O_2=1.8. he catalyst was reduced at 900 ^oC in presence of H_2+N_2 in 50:50 ratio for 2 h before start reaction]

Temperature (^oC)	CH_4 Conversion (%)	O_2 Conversion (%)	H_2 Selectivity (%)	CO Selectivity (%)
900	96.1	100	98.6	98.2
850	94.0	100	98.8	97.4
800	91.0	100	97.4	96.7
750	85.5	100	97.3	95.6
650	78.8	100	97.0	92.5
550	70.2	100	88.9	87.7

Appendix 5.9: Effect of GHSV in the performance of partial oxidation of methane over $NiCoMgO_x$/SZ-5564 (precalcined at 900 ^oC) catalyst at temperature 850 ^oC. [Reaction condition: CH_4/O_2 =1.8. The catalyst was reduced at 900 ^oC in presence of H_2+N_2 in 50:50 ratio for 2 h before start reaction]

GHSV ($cm^3g^{-1}h^{-1}$)	CH_4 Conversion (%)	O_2 Conversion (%)	H_2 Selectivity (%)	CO Selectivity (%)
60000	88.1	99.6	95.5	97.2
120000	94.0	100	98.7	97.4
300000	88.1	93.4	92.0	95.1
500000	85.9	92.7	96.1	92.8

Appendix 5.10: Effect of temperature in the performance of partial oxidation of methane over $NiCoO_x$/MgO/SZ-5564 (precalcined at 1400 ^oC) [GHSV = 62,000 $cm^3g^{-1}h^{-1}$; CH_4/O_2=1.8. The catalyst was reduced at 900 ^oC in presence of H_2+N_2 in 50:50 ratio for 2 h before start reaction]

Temperature (^oC)	CH_4 Conversion (%)	O_2 Conversion (%)	H_2 Selectivity (%)	CO Selectivity (%)
900	95.3	100	97.6	97.1
850	91.9	100	95.0	95.3
800	87.9	100	94.8	93.9
750	83.2	100	91.2	90.2
650	74.1	100	91.7	85.2
550	67.6	100	90.9	80.9

Appendix 5.11: Effect of temperature in the performance of partial oxidation of methane over $NiCoMgCeO_x$/SZ-5564 (precalcined at 1400 ^oC) [GHSV = 62,000 $cm^3g^{-1}h^{-1}$; CH_4/O_2=1.8. The catalyst was reduced at 900 ^oC in presence of H_2+N_2 in 50:50 ratio for 2 h before start reaction]

Temperature (^oC)	CH_4 Conversion (%)	O_2 Conversion (%)	H_2 Selectivity (%)	CO Selectivity (%)
900	98.4	100	96.9	96.7
850	95.7	100	96.8	97.4
800	94.4	100	96.8	94.8
750	92.5	100	97.5	91.6
650	84.3	100	96.4	86.6
550	76.2	100	91.9	82.4

Appendix 5.12: Effect of temperature in the performance of partial oxidation of methane over $NiCoMgCeO_x$/SZ-5564 (precalcined at 1400 ^oC) [GHSV = 120000 $cm^3g^{-1}h^{-1}$; CH_4/O_2=1.8. The catalyst was reduced at 900 ^oC in presence of H_2+N_2 in 50:50 ratio for 2 h before start reaction]

Temperature (^oC)	CH_4 Conversion (%)	O_2 Conversion (%)	H_2 Selectivity (%)	CO Selectivity (%)
900	94.3	100	93.5	95.9
850	92.4	100	95.0	95.4
800	90.8	100	94.2	94.0
750	88.1	100	93.0	92.6
650	82.8	100	91.1	89.2
550	77.0	100	94.0	85.5

Appendix 5.13: Effect of temperature in the performance of partial oxidation of methane over $NiCoCeO_x$/SZ-5564 (precalcined at 900 ^oC) [GHSV = 120000 $cm^3g^{-1}h^{-1}$; CH_4/O_2=1.8. The catalyst was reduced at 900 ^oC in presence of H_2+N_2 in 50:50 ratio for 2 h before start reaction]

Temperature (^oC)	CH_4 Conversion (%)	O_2 Conversion (%)	H_2 Selectivity (%)	CO Selectivity (%)
900	98.1	100	98.4	98.1
850	96.2	100	97.2	97.3
800	92.9	100	98.3	96.0
750	90.4	100	95.7	94.4
650	83.9	100	92.5	90.8
550	77.4	100	90.9	87.7

Appendix 5.14: Effect of temperature in the performance of partial oxidation of methane over $NiCoCeO_x$/SZ-5564 (precalcined at 900 ^oC) [GHSV = 500000 $cm^3g^{-1}h^{-1}$; CH_4/O_2=1.8. The catalyst was reduced at 900 ^oC in presence of H_2+N_2 in 50:50 ratio for 2 h before start reaction]

Temperature (^oC)	CH_4 Conversion (%)	O_2 Conversion (%)	H_2 Selectivity (%)	CO Selectivity (%)
900	71.1	96.8	95.9	93.5
850	67.3	94.3	82.9	92.8
800	64.6	92.2	77.8	92.1
750	61.7	91.7	77.3	91.0
650	56.6	90.1	69.3	88.2
550	52.6	87.8	69.8	85.9

CHAPTER 6

LOW TEMPERATURE NON-OXIDATIVE ACTIVATION OF METHANE OVER BIFUNCTIONAL PENTASIL ZEOLITES IN PRESENCE OF METHANOL OR OTHER OXYGENATES: SIMULTANEOUS CONVERSION OF METHANE AND METHANOL OR OTHER OXYGENATES INTO HIGHER HYDROCARBONS / GASOLINE

CHAPTER 6

LOW TEMPERATURE NON-OXIDATIVE ACTIVATION OF METHANE OVER BIFUNCTIONAL PENTASIL ZEOLITES IN PRESENCE OF METHANOL OR OTHER OXYGENATES: SIMULTANEOUS CONVERSION OF METHANE AND METHANOL OR OTHER OXYGENATES INTO HIGHER HYDROCARBONS / GASOLINE

6.1. Earlier Work / Background and Objective of the Present Work

Methane is the main constituent of natural gas, coal–bed gas and bio–gas. The natural gas reserves are more than that of oil and more and more natural gas is being discovered than oil. There are also very huge untapped resources of methane, such as methane gas hydrate, lying deep on the sea beds. Methane is produced in huge quantities during oil production as associated gas and also in petroleum refining and petrochemical processes. Since methane is available and produced mostly in remote places, its transportation is very costly or even impossible. Both methane and carbon dioxide are greenhouse gases of very high potential, responsible for the global warming. Hence, presently practiced letting–out and/or flaring of the methane produced will not be allowed in the near future. Because of the increasing energy demands, worldwide efforts have been made since the last 2-3 decades for developing novel processes for the conversion of methane into value added products, such as ethylene (by oxidative coupling of methane) [1-3], syngas (by partial oxidation with or without simultaneous steam and/or CO_2 reforming of methane) [4-8] and gasoline/liquid hydrocarbon fuels [9-14] involving either oxidative [1-10] or non-oxidative [11-15] activation of methane. Since methane is the most inert hydrocarbon, a low temperature (below 600 ^oC) non-oxidative activation of methane is extremely challenging.

Even from the environmental consideration, for avoiding the methane flaring the methane produced in the remote places needs to be converted into easily transportable energy sources like liquid hydrocarbon fuels at the methane production sites. Most important approach to transform methane into liquid hydrocarbons is to follow the well-established and already commercially proven route [16]: methane $\rightarrow$ syngas $\rightarrow$ methanol $\rightarrow$ gasoline, based on Mobil's MTG (methanol–to–gasoline) process [16–18]. In 1985, Mobil had successfully operated a commercial plant in New Zealand for the methane-to-gasoline conversion. However, the commercial unit could not be operated economically due to

unfavourable process economics [19,20]. The cost of syngas production step (by steam reforming) is about twice the cost of methanol–to–gasoline production step [17]. The methane–to–gasoline process would get back its life and could be practiced economically provided an appreciable part of the methane is converted to gasoline without a need for its conversion to syngas and consequently to methanol. We have accomplished this very difficult goal by activating methane non–oxidatively and converting it simultaneously with methanol to gasoline range hydrocarbons over bifunctional Ga-, In-, Zn-, and/or Mo-modified ZSM–5 type zeolites having both the dehydrogenation and acid functions. We have shown here that the methane converted can be comparable to or even more than the methanol converted in this novel process, depending upon the process conditions. The methane-to-higher hydrocarbon conversion was confirmed by using ^{13}C- labeled methanol and analyzing the reaction products by GC-MS. This work has the potential to revolutionalize the methane-to-liquid hydrocarbons (MTL) conversion technology via the modified Mobil's MTG process.

6.2. Experimental

The preparation procedure of different Ga-, In-, Zn-, and/or Mo- modified ZSM-5 type zeolite catalysts used for this purpose has been discussed earlier (section 2.1.2.). In short H-GaAlMFI (Si/Al bulk composition = 49.6), ZSM-5 (Si/Al = 20), zeolites have been synthesized by their hydrothermal crystallization from a gel consisting of Na-trisilicate (Fluka), gallium nitrate (Aldrich) and/or aluminum nitrate (BDH), TPA-Br (Aldrich), sulfuric acid and demineralized water in a steel autoclave at 180 ^{o}C. The zeolite crystals were washed thoroughly with deionized water and dried at 120 ^{o}C for 10 h. The zeolites are calcined at 550 ^{o}C under static air for 15 h for removing occluded organic template from their channels. The calcined zeolites were exchanged with 1 M ammonium nitrate solution at 80 ^{o}C repeatedly (for four times) to convert them into their NH_4^+ form. After exchange, the zeolite crystals were washed with deionised water and dried at 120 ^{o}C for 10 h. The NH_4-ZSM-5 zeolite was impregnated with aqueous gallium, molybdenum, indium and/or zinc nitrate solution by incipient wetness technique and then dried as above. The NH_4-GaMFI (NH_4 form of gallosilicate with ZSM-5 type structure), NH_4-GaAlMFI (NH_4 form of galloaluminosilicate with ZSM-5 type structure), Ga/NH_4-ZSM-5 (Ga-impregnated NH_4-ZSM-5), In-Zn/NH_4-ZSM-5, Mo/NH_4-ZSM-5, Mo-Zn/NH_4-ZSM-5, Ga-Zn/NH_4-ZSM-5

zeolites were pressed binder-free and crushed to 22 – 30 mesh size particles and then calcined under static air at 600 ^{o}C for 1 h to convert the zeolites to their H-form. The Mo-containing catalysts were pretreated in a flow of hydrogen (6 %) and methane (1030 cm^3 g^{-1} h^{-1}) at 550 ^{o}C for a period of 4 h.

The experimental procedure for the simultaneous conversion of methane and oxygenates over the catalysts, have already been discussed in section 2.3.4 and Figs. 2.6 and 2.2.

6.3. Results and Discussions

6.3.1. Simultaneous Conversion of Methane and Methanol to Gasoline over Bifunctional Ga-, In-, Zn-, and / or Mo- Modified ZSM-5 Zeolites.

6.3.1.1. Thermodynamic consideration

Low temperature (≤ 600 ^{o}C) conversion of methane to aromatics is not thermodynamically feasible (free energy change > 8.0 kcal mol^{-1} of carbon) [Fig. 6.1].

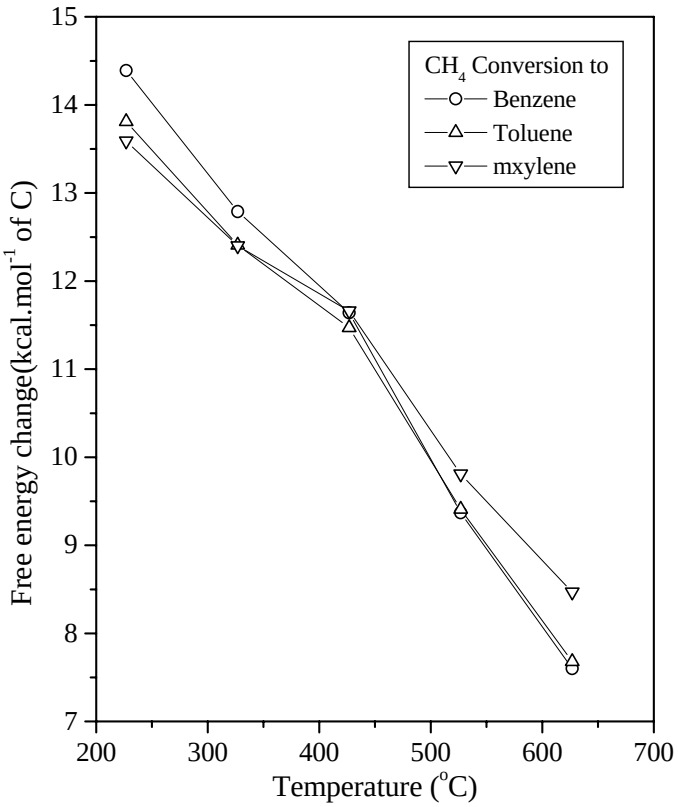

Figure 6.1: Free energy change in the conversion of methane to different aromatics

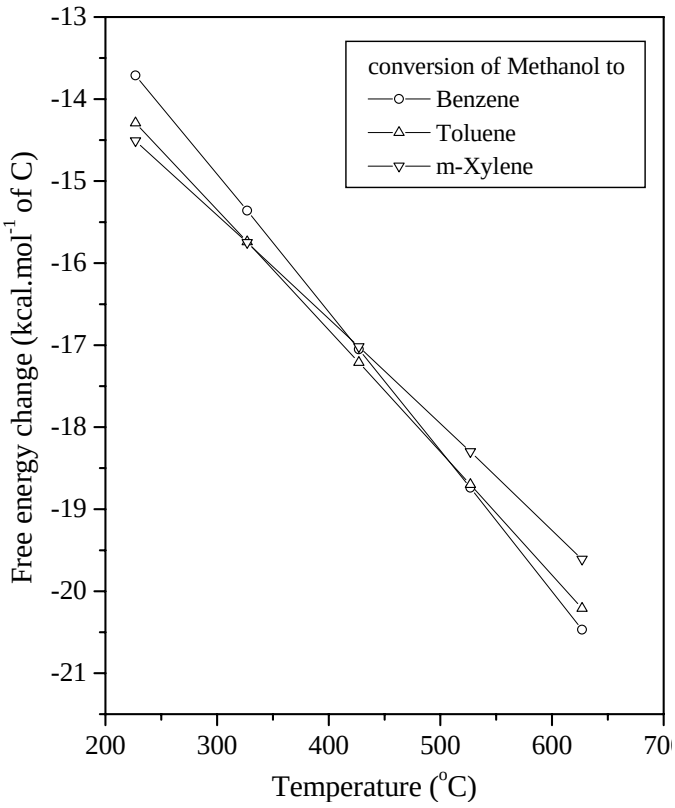

Figure 6.2: Free energy change in the conversion of methanol to different aromatic

In contrary methanol aromatization is highly exothermic [ΔH_r < -30 kcal mol^{-1} (aromatics)] and thermodymically favorable (ΔG is negative) [Fig. 6.2.] at low temperature (≤ 600 ^oC).

Table 6.1: Heat of overall reaction when methane is converted simultaneously with methanol to different aromatics with different ratios of moles of methane converted to the moles of methanol converted

Methane converted/ Methanol converted (mole ratio)	Heat of overall reaction (ΔH_r) [kcal mol^{-1} (aromatic hydrocarbon)]		
	Conversion to benzene	Conversion to toluene	Conversion to m–xylene
0.0 (i.e. for the conversion of methanol alone)	(–) 30.0	(–) 46.2	(–) 63.2
0.5	26.4	19.6	12.0

1.0	55.2	53.2	50.4
2.0	83.4	86.1	88.0
∞ (i.e. for the conversion of methane alone)	139.8	151.9	164.0

However, when methane is converted simultaneously with the methanol conversion over bifunctional zeolite catalysts, having strong protonic acid and dehydrogenation sites, the overall methanol and methane-to-aromatics conversion could be endothermic and thermodynamically favourable [Fig. 6.3.] because of a coupling of the exothermic methanol conversion reactions with the endothermic methane conversion reactions, depending upon the methane converted / methanol converted ratio [Table 6.1.].

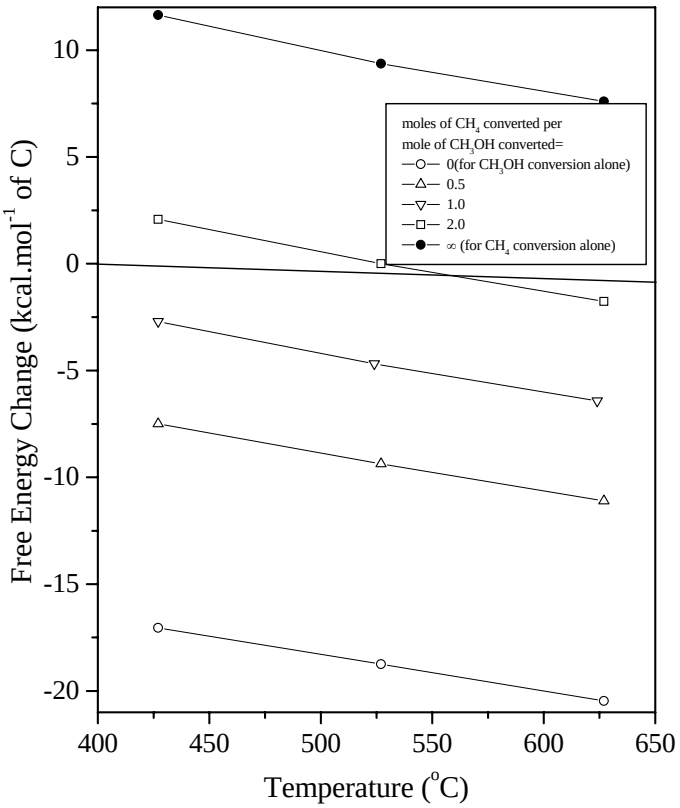

Figure 6.3: Free energy change for the simultaneous conversion of methane and methanol to benzene

6.3.1.2. Simultaneous aromatization of methane and methanol over Ga-, In-, Zn-, and/or Mo- modified bifunctional ZSM-5 zeolite catalysts

Results showing the influence of temperature on the moles of methane converted per mole of methanol over the bifunctional zeolite catalysts are presented in Fig. 6.4. The moles of methane converted per mole of methanol in the feed could be close to or even above 1.0, depending upon the process temperatures and the required methanol itself can be produced from methane by the well established technology ($CH_4 \rightarrow$ syngas $\rightarrow$ methanol).

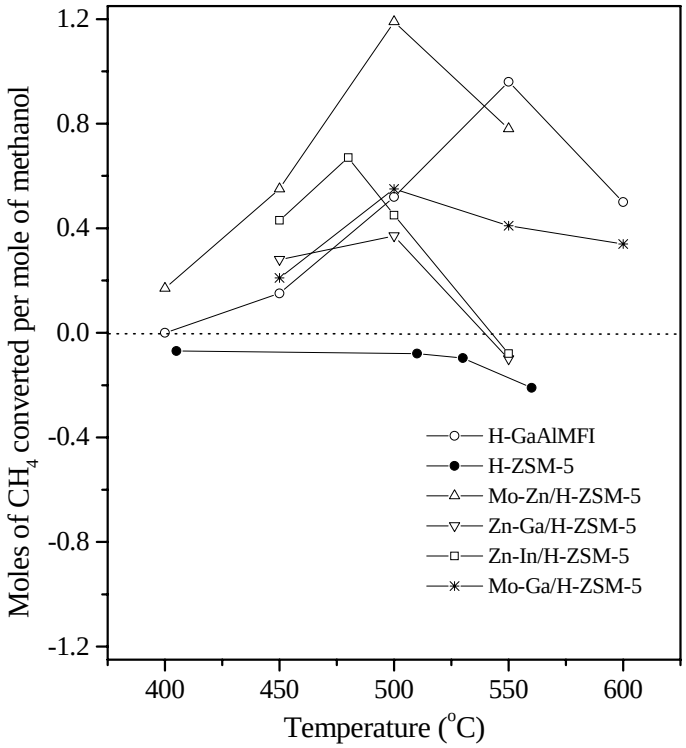

Figure 6.4. Moles of methane converted per mole of methanol in the simultaneous aromatization of methane and methanol over H-GaAlMFI and H-ZSM-5 zeolites (CH_4/CH_3OH = 15, CH_4/N_2 = 8.5, GHSV = 1050 $cm^3g^{-1}h^{-1}$); Mo-Zn/H-ZSM-5 zeolite (CH_4/CH_3OH = 14.1, CH_4/N_2 = 8.5, GHSV = 1050 $cm^3g^{-1}h^{-1}$); Zn-In/H-ZSM-5 zeolite (CH_4/CH_3OH = 12.72, CH_4/N_2 = 8.5, GHSV = 1200 $cm^3g^{-1}h^{-1}$); Mo-Ga/H-ZSM-5 zeolite (CH_4/CH_3OH = 13.75, CH_4/N_2 = 7.3, GHSV = 1200 $cm^3g^{-1}h^{-1}$) and Zn-Ga/H-ZSM-5 zeolite (CH_4/CH_3OH = 5.9, CH_4/N_2 = 7.2, GHSV = 1200 $cm^3g^{-1}h^{-1}$). The methanol conversion is 100%.

In the absence of methanol and/or bifunctional sites on the zeolites catalyst, there was no conversion of methane. The negative methane converted / methanol converted ratio for the H-ZSM-5 zeolite (Fig. 6.4) shows the net formation of methane. An optimum temperature is observed for achieving the highest ratio of methane converted to methanol converted in the process, depending upon the bifunctional zeolite used. This is expected because of a competition between the methane formation from methanol by cracking reactions, the rate of which is higher at higher temperature, and the activation / conversion of methane, the rate of which is lower at lower temperature.

Time-on-stream activity on moles of methane converted per mole of methanol over the H-GaAlMFI and Mo-Zn/H-ZSM-5 zeolite catalysts in the simultaneous conversion of methane and methanol is presented in Fig. 6.5. Both the catalysts showed good stability against the catalysts deactivation when tested for a time-on-stream of 7 h.

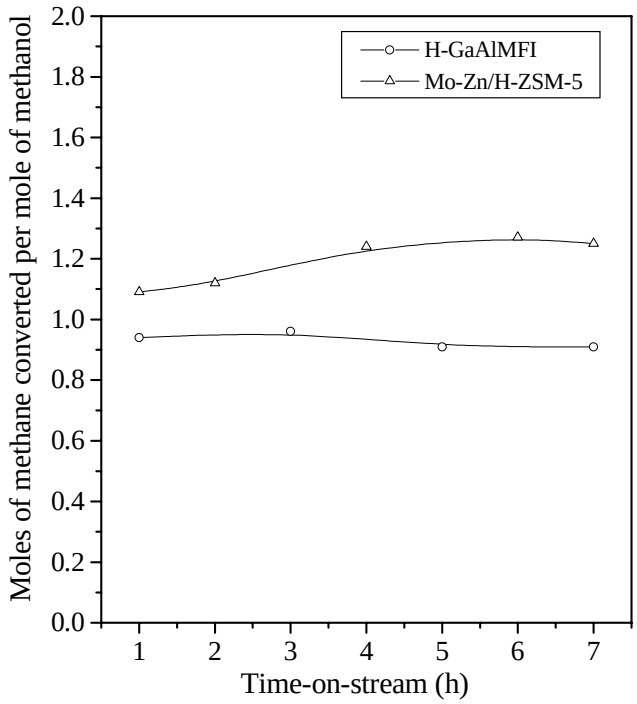

Figure 6.5. Time-on-stream data (moles of methane converted per mole of methanol) for the H-GaAlMFI and Mo-Zn/H-ZSM-5 zeolite catalysts in the simultaneous conversion of methane and methanol (For H-GaAlMFI catalyst: CH_4/CH_3OH = 15.0, GHSV = 1000 $cm^3g^{-1}h^{-1}$, CH_4/N_2 = 8.5 and Reaction temperature = 550 ^oC; For Mo-Zn/H-ZSM-5 catalyst: CH_4/CH_3OH = 14.1, GHSV = 1000 $cm^3g^{-1}h^{-1}$, CH_4/N_2 = 8.5 and Reaction temperature = 500 ^oC). Methanol conversion in both the cases was 100%.

6.3.1.3. Influence of temperature on the distribution of hydrocarbon products formed in the simultaneous conversion of methane and methanol over H-GaAlMFI and Mo-Zn/H-ZSM-5 zeolite catalysts.

Results in Fig. 6.6 show the influence of reaction temperature on the hydrocarbon ($C_2 - C_{10+}$) product distribution. For the H-GaAlMFI catalyst, the formation of C_2 and C_3 hydrocarbons is increased while that of C_{4+} aliphatic is decreased due to the increase in the temperature from 500 to 550 ^oC; the change in the formation of aromatics is, however, very small.

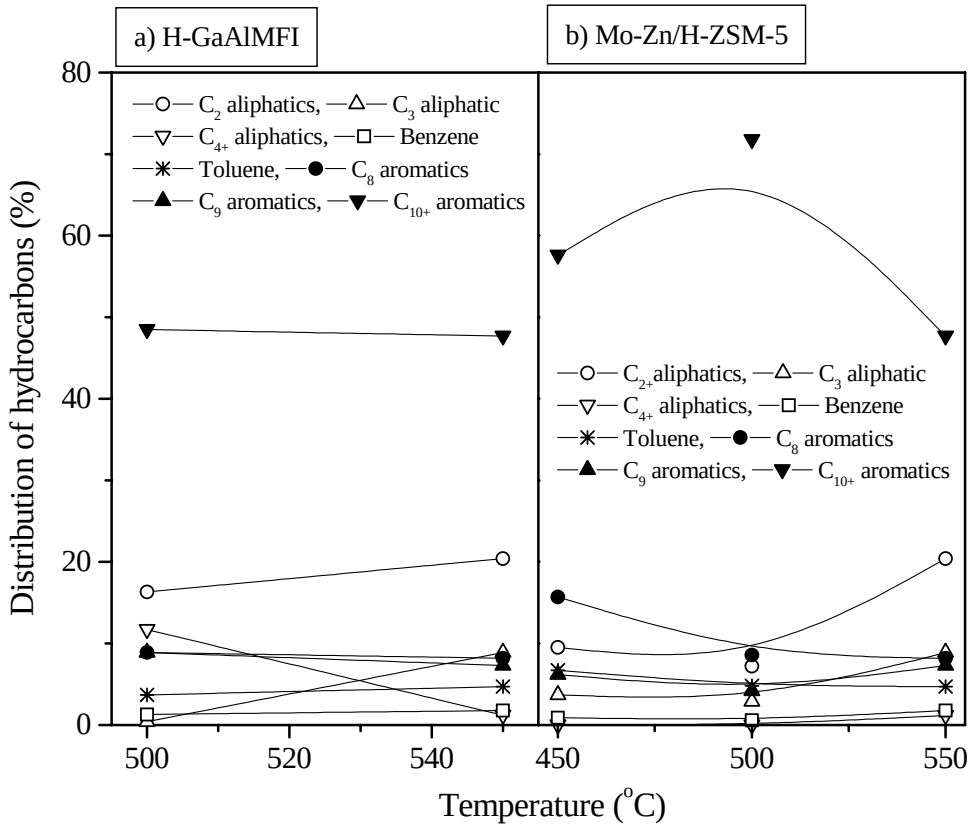

Figure 6.6: Effect of temperature on the distribution of aromatics in the simultaneous conversion of methane and methanol over a) H-GaAlMFI and b) Mo-Zn/H-ZSM-5 catalysts at a particular GHSV = 1000 $cm^3g^{-1}h^{-1}$

For the Mo-Zn / H-ZSM-5 catalyst, the increase in the temperature from 450 to 550 ^{o}C resulted in the following changes in the hydrocarbon product distribution:

- The formation of C_{10+} aromatics is passed through the maxima but there is almost no change in the formation of C_{10+} aromatics over H-GaAlMFI catalyst.
- The formation of C_9 aromatics is increased; the increase is, however, pronounced only at the higher temperature.
- The formation of C_8 aromatics is decreased continuously, mostly because of the increased dealkylation of C_8 with increasing the temperature.
- The formation of C_2 and C_3 aliphatic is increased exponentially.

6.3.1.4. Distribution of hydrocarbons formed in the aromatization of methanol over H-GaAlMFI and Mo-Zn/H-ZSM-5 zeolite in the presence and absence of methane.

Results showing a comparison of the distribution of hydrocarbons produced from methanol in the presence and absence of methane over the H-GaAlMFI and Mo-Zn / H-ZSM-5 catalysts are presented in Figs. 6.7 and 6.8 and Table 6.2. Results in Figs. 6.4, 6.7 and 6.8 and Table 6.2 clearly indicate that methane is non-oxidatively activated and converted at low temperature (below 600 ^{o}C) during the methanol conversion over the bifunctional zeolite catalysts. However, over the H-ZSM-5, methane is not at all activated / converted; it is rather produced in an appreciable amounts (Fig. 6.4). Because of the simultaneous conversion of methane, the hydrocarbon product distribution in the methanol-to-gasoline conversion is changed appreciably and also the formation of individual C_{2+} hydrocarbons is increased markedly, as shown in Fig. 6.7 and Fig. 6.8 and Table 6.2. The liquid hydrocarbons formed are mainly $C_7 - C_{12}$ aromatics. The formation of benzene (the presence of which is undesirable because of its toxicity) was very small. In the absence of methane, an appreciable amount of methane is produced in the aromatization of methanol. Hence, even a no net formation of methane in the methanol aromatization because of the presence of methane is beneficial.

The H-GaAlMFI, which is highly acidic (acidity = 0.41 mmolg^{-1}) and contains in its channels finely dispersed Ga-oxide species produced by degalliation of the frame work Ga, show much better performance than the catalyst prepared by externally impregnating either of the Ga-, Zn-, and Mo-oxide species on H-ZSM-5. However, the performance of the Mo-, Ga-oxide impregnated H-ZSM-5 was improved appreciably after the addition of Zn-oxide to

the catalyst. The catalytically active Mo-containing species may be Mo_2C and/or MoO_xC_y [22]. Many interactions, such as the interactions between the Mo species and the framework Al, and that between the Mo species and the acid sites of the zeolite, can be involved and would impose crucial influence on the catalytic performances.

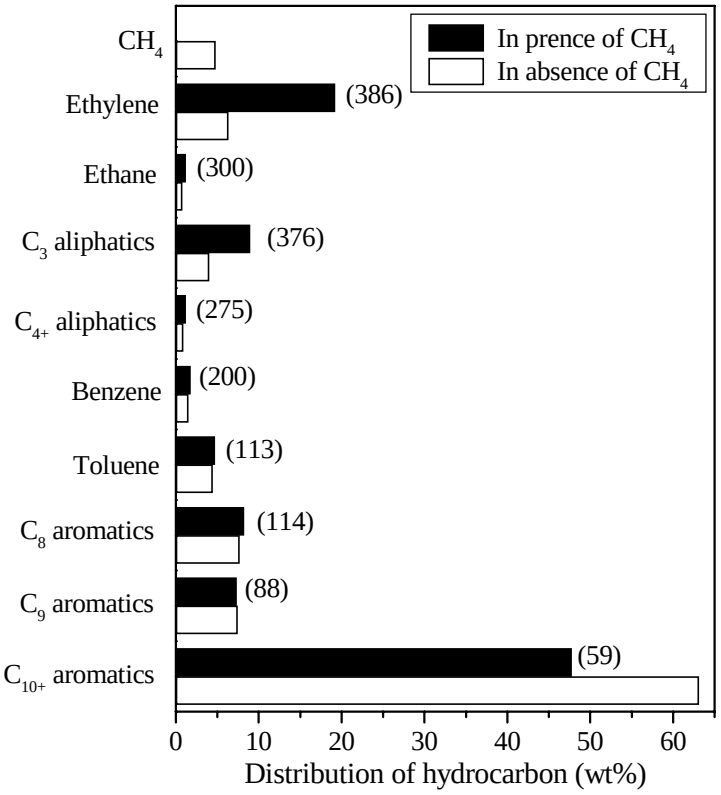

Figure 6.7: Distribution of hydrocarbons formed in the aromatization of methanol over H-GaAlMFI zeolite in the presence (solid bars) and absence (open bars) of methane at 550^oC (CH_4/CH_3OH = 15.0, CH_4/N_2 = 8.5 and GHSV (gas hourly space velocity, measured at 0 ^oC and 1 atm) = 1050 $cm^3g^{-1}h^{-1}$). The value given in the round brackets corresponds to the percentage increase in the formation of a particular hydrocarbon because of the presence of methane. The conversion of methanol in both the cases was 100%. In the presence of methane, the amount of methane converted was 0.96 moles per mole of methanol. In the continuous operation for 7 h, the catalysts showed no significant change in its catalytic activity for the methane conversion; there was carbon deposition only on the initial portion of the catalyst.

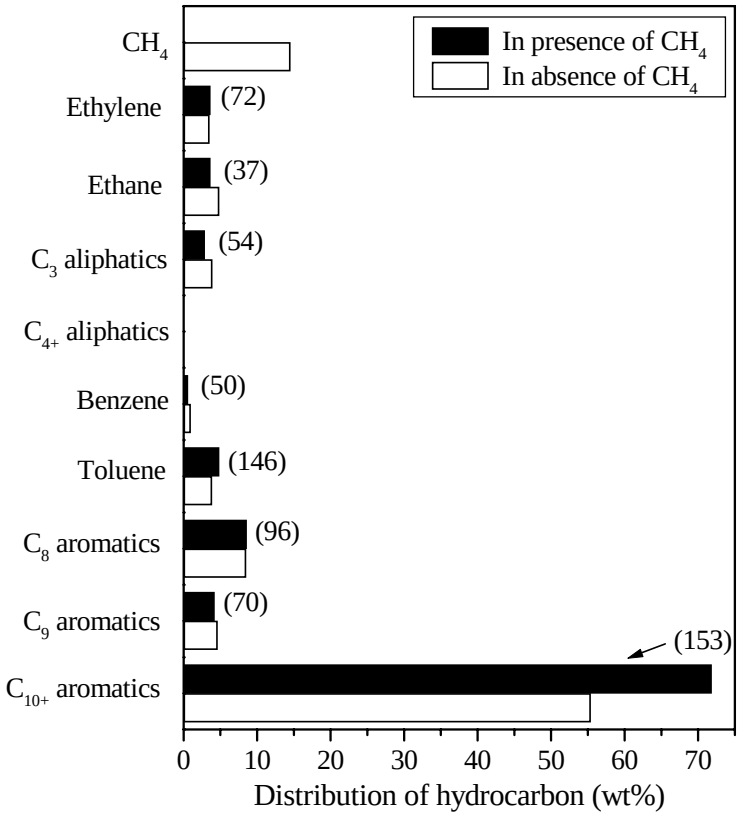

Figure 6.8: Distribution of hydrocarbons formed in the aromatization of methanol over Mo-Zn/H-ZSM-5 zeolite in the presence (solid bars) and absence (open bars) of methane at 500 ^{o}C (CH_4/CH_3OH = 14.1, CH_4/N_2 = 8.5 and GHSV = 1050 $cm^3g^{-1}h^{-1}$). The value given in the round brackets corresponds to the percentage increase in the formation of a particular hydrocarbon because of the presence of methane. The conversion of methanol in both the cases was 100%. In the presence of methane, the amount of methane converted was 1.19 mole per mole of methanol. In the continuous operation for 7 h, the catalyst showed no deactivation on its methane conversion activity. However, there was appreciable carbon deposition on the catalyst as compared to that for the H-GaAlMFI.

Table 6.2: Summary of the trends for the increase in the formation of C_2 – C_{12} hydrocarbons (in the process) due to the presence of methane over H-GaAlMFI and Mo-Zn / H-ZSM-5 zeolite catalysts at different process conditions.

Reaction conditions			Moles of CH_4 converted per mol of methanol	Increase in C_2 – C_{12} hydrocarbon, due to the presence of methane (%)
Temperatures (^oC)	CH_4/CH_3OH mol ratio	GHSV ($cm^3g^{-1}h^{-1}$)		
Catalyst: H-GaAlMFI				
500	15.0	1050	0.52	49
550	15.0	1050	0.96	108
550	7.0	1050	0.27	31.8
550	15.0	2100	0.79	83
Catalyst: Mo-Zn / H-ZSM-5				
450	14.1	1050	0.55	53
500	14.1	1050	1.19	126
550	14.1	1050	0.78	77
500	7.1	1050	0.29	30
500	14.1	2100	0.55	47

6.3.1.5. A ^{13}C Labelling Investigation

In order to confirm the methane activation / conversion in the presence of methanol, a mixture of labeled methanol [$^{13}CH_3OH$] vapours and premixed methane-N_2 (CH_4/N_2 mole ratio = 8.5) gas from a cylinder have passed over bifunctional Ga-, In-, and / or Zn- modified ZSM-5 catalyst at the reaction conditions. The liquid products were analyzed by GC-MS. The Mass spectra of toluene and xylene produced in the presence and absence of methane in the feed are compared in Fig. 6.9 and that of higher aromatics formed in the presence of methane are shown in Figs. 6.10 and 6.11. The mass spectra for toluene and xylene (in Fig. 6.9) and also for higher aromatics (Figs. 6.10 and 6.11, Appendix 6.2 – 6.6) clearly reveal the formation of unlabeled toluene and partially labled aromatics with or

without completely labeled aromatics in the aromatization of ^{13}C-labeled methanol over the H-GaAlMFI and Zn-In / H-ZSM-5 catalysts in the presence of methane.

In the formation of methylbenzenes and methylnaphthalenes, methane seems to act as an alkylating agent. Indeed, when a mixture of methane and benzene (CH_4/C_6H_6 = 12.5) was passed over the H-GaAlMFI zeolite at 550 ^oC, an alkylation of benzene with the formation of toluene and xylenes in significant amounts (1.0% conversion of benzene) was observed (Table 6.3). The results also shows the formation of C_9 – aromatics (Fig. 6.10) having different molecular weights (viz. 129, 127, 126, 125 and 124), indicating the incorporation of ^{12}C from methane in the aromatics formed during the aromatization of $^{13}CH_3OH$. The $I_{(m-1),}$ $I_{(m-2)}$ and $I_{(m-3)}$ to I_m intensity ratios for the aromatics formed in the simultaneous conversion of methane and ^{13}C labeled methanol ($^{13}CH_3OH$) differ very significantly / markedly from that for the unlabled aromatic compound, indicating the individual aromatic product with different mass numbers (Table 6.4).

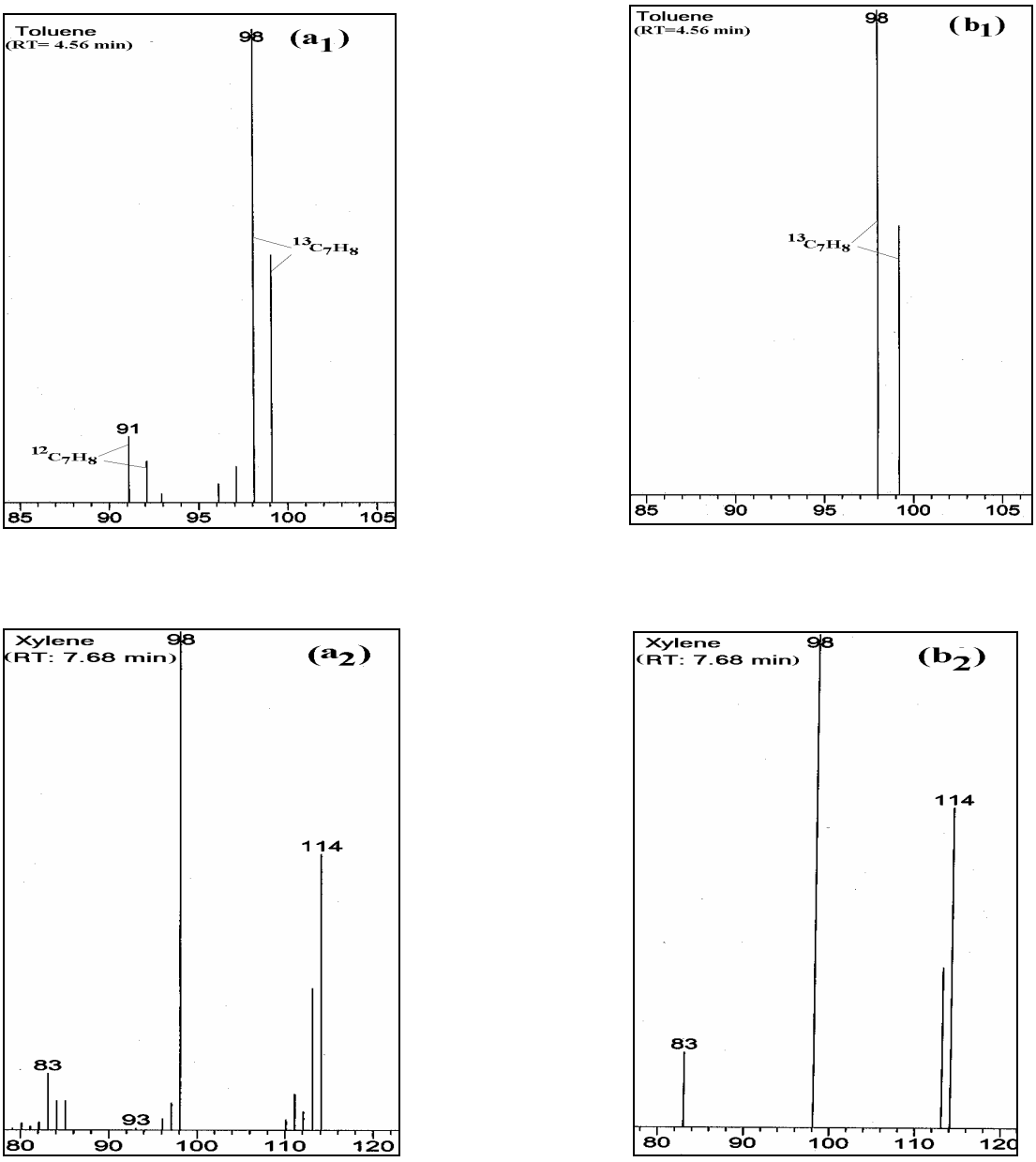

a) In presence of methane b) In absence of methane

Figure 6.9: GCMS spectra of toluene and xylene formed in the aromatization of ^{13}C labeled methanol ($^{13}CH_3OH$) over the H-GaAlMFI zeolite in the presence and absence of methane under identical conditions (at 550 ^oC and GHSV = 1050 $cm^3g^{-1}h^{-1}$) [Reaction condition: a) $CH_4/^{13}CH_3OH$ = 14.7 and CH_4/N_2 = 7.3, b) $CH_4/^{13}CH_3OH$ = Zero, $N_2/^{13}CH_3OH$ = 16.7]. RT = retention time for corresponding hydrocarbon.

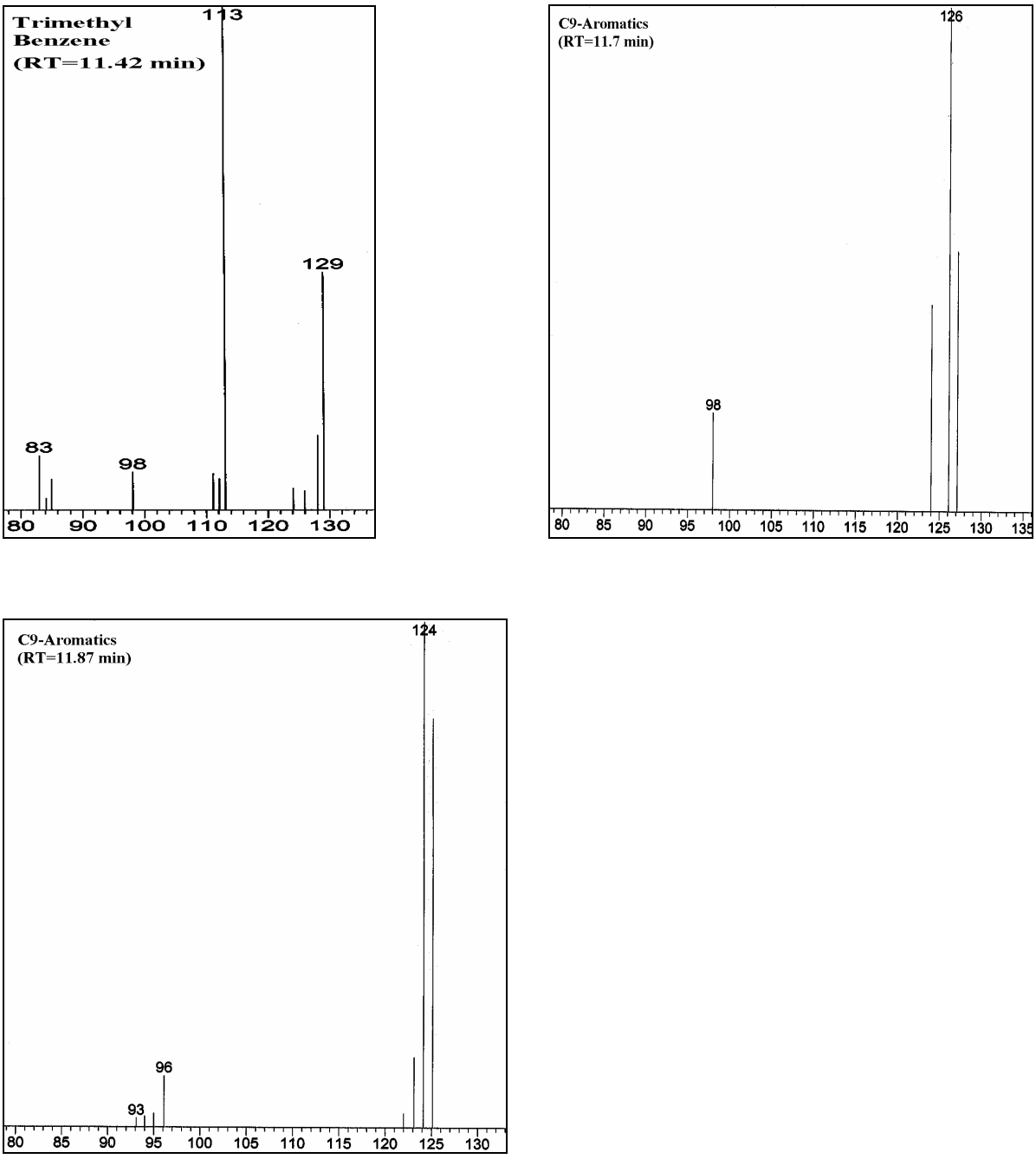

Figure 6.10. GCMS spectra of C_9 aromatics, having different retention times, formed in the aromatization of $^{13}CH_3OH$ in the presence of methane over the H-GaAlMFI zeolite catalyst at 550 ^oC [$^{12}CH_4$ / $^{13}CH_3OH$ = 14.7]

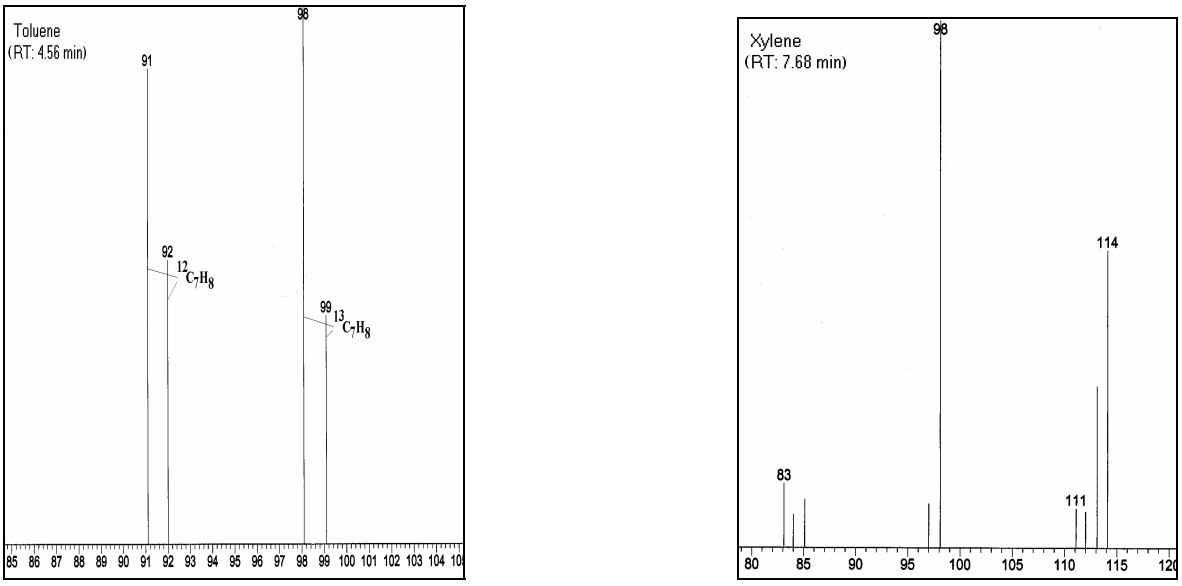

Figure 6.11. Mass spectra of toluene and xylene formed in the aromatization of ^{13}C labeled methanol ($^{13}CH_3OH$) over the Zn-In/H-ZSM-5 zeolite in the presence of methane at 480 ^oC [reaction conditions: $CH_4/^{13}CH_3OH$ = 14.7, CH_4/N_2 = 7.3, and GHSV = 1050 $cm^3g^{-1}h^{-1}$]. RT = GC retention time.

Table 6.3: Product distribution during the methane conversion in presence of benzene over the H-GaAlMFI catalyst at different temperatures.

Temp (^oC)	CH_4/CH_3OH Ratio in feed	GHSV ($cm^3g^{-1}h^{-1}$)	Aromatics distribution (%)		
			Benzene	Toluene	Xylene
535	12.48	1000	99.93	0.07	0.0
550	12.48	1000	99.76	0.16	0.08
602	12.48	1000	99.69	0.31	0
650	12.48	1000	99.0	0.90	0

Table 6.4: Intensity of MS peaks relative to that of the mass number (m) for the aromatics formed in the simultaneous aromatization of methane and $^{13}CH_3OH$ over the H-GaAlMFI and Zn-In / H-ZSM-5 zeolite catalysts.

Aromatic product	$I_{(m-1)}/I_m$		$I_{(m-2)}/I_m$		$I_{(m-3)}/I_m$	
	For the product	For unlabeled compound[a]	For the product	For unlabeled compound[a]	For the product	For unlabeled compound[a]
Catalyst: H-GaAlMFI						
Xylene	0.518	0.40	0.071	0.05	0.134	0.117
Trimethyl - benzene	0.34	0.26	0.04	0.07	0.07	0.11
C_{10} – Aromatics	0.25	0.19	-	-	-	-
Naphthalene	0.23	0.20	0.09	0.09	0.015	-
Methyl-naphthalene	0.099	0.65	0.134	0.029	0.02	0.087
Dimethyl-naphthalene	0.39	0.22	0.06	0.04	0.13	0.09
Catalyst: Zn-In / H-ZSM-5						
Xylene	0.54	0.40	0.12	0.05	0.14	0.11
Trimethyl - benzene	0.34	0.26	0.10	0.07	0.08	0.11
C_{10} – Aromatics	0.37	0.19	-	-	-	-
Naphthalene	0.29	0.20	0.12	0.09	0.02	-
Methyl-naphthalene	0.15	0.65	0.16	0.03	0.03	0.09
Dimethyl-naphthalene	0.47	0.22	0.1	0.04	0.15	0.09

[a] Data obtained from standard GCMS spectra of the corresponding aromatic compound.

6.3.1.6. Proposed mechanism

The following probable mechanism have been proposed for the activation and conversion of methane during the aromatization of methanol over the bifunctional zeolite catalysts, having strong Brönsted acid sites and non-framework Ga-, Zn-, and / or In- oxide species, with or without Mo_2C or MoO_xC_y species, as dehydrogenation sites in the zeolite channels.

Methanol Aromatization

$$Z^- H^+ + CH_3OH \rightleftharpoons Z^- [CH_3OH_2]^+ \longrightarrow$$

(I)

$$Z^- H^+ + \text{Water} + C_1 - C_{12} \text{ hydrocarbons} \qquad (1)$$

Methane Activation and Conversion

$$CH_4 + H^+ Z^- + M^{n+}— O^{2-} \longrightarrow \begin{matrix} H^+ & Z^- \\ \vdots & \vdots \\ H^{\delta-} & — CH_3^{\delta+} \\ \vdots & \vdots \\ M^{n+} & — O^{2-} \end{matrix} \longrightarrow$$

(where M= Ga, Zn or In)

$$Z^- [CH_5]^+ + M^{n+}O^{2-} \longrightarrow Z^- CH_3^+ + M^{n+}O^{2-} + H_2 \uparrow \qquad (2)$$

(II)

$$Z^- CH_3^+ \longrightarrow Z^- H^+ + CH_2 \qquad (3)$$

$$2\ CH_2 \longrightarrow C_2H_4 \xrightarrow[\text{Oligomerization \& aromatization}]{Z^- H^+ + M^{n+}— O^{2-}} \text{Aliphatics and Aromatics} \qquad (4)$$

$$Z^- CH_3^+ + Ar - H + M^{n+}— O^{2-} \longrightarrow \begin{matrix} CH_3^+ & Z^- \\ \vdots & \vdots \\ Ar^{\delta-} & — H^{\delta+} \\ \vdots & \vdots \\ M^{n+} & — O^{2-} \end{matrix} \longrightarrow$$

(Ar-H = aromatics)

$$Z^- [\ H_3C \diagup \begin{matrix} H \\ Ar \end{matrix}\ ]^+ + M^{n+}— O^{2-} \longrightarrow ArCH_3 + Z^- H^+ + M^{n+}— O^{2-} \qquad (5)$$

$$X + Z^- CH_3^+ \longrightarrow XCH_2 + Z^- H^+ \quad (6)$$

(Where X = Mo_2C or MoO_xC_y species)

$$2XCH_2 \longrightarrow 2X + C_2H_4 \quad (7)$$

Methane is mostly activated as a result of the combined action of the metal-oxide species and zeolitic protons, both present at the channel intersections in a close vicinity of each other. Our earlier studies on the alkane and alkene aromatization over Ga-modified ZSM-5 zeolites also revealed that the zeolitic protons and non-framework Ga-oxide species work in cooperation with each other [23]. Methyl cations are likely to be produced via the formation of penta coordinated carbocations (II), similar to that proposed earlier by Olah [24]. Since no methane conversion is observed in the absence of methanol and / or the bifunctional sites, the H-CH_3 bond activation and formation of the penta-coordinated carbocations (II) are expected to be facilitated by the non-framework metal oxide species in the presence of oxonium cations (I) and / or carbonium ions (II) formed from the olefins produced from methanol.

The highly unstable methyl cations are expected to be stabilized by the zeolytic framework negative charge (Z^-), as $Z^- CH_3^+$. The role of the metal oxide / carbide species (Ga-, In- and Zn-oxides, MoC_2 or MoO_xC_y species) present at the zeolite channels intersections in a close vicinity of the zeolite protons is not only to facilitate the methane activation but also to facilitate recombination of hydrogen adatoms [25] formed during the C-H activation (reaction-2). The mechanism explains the observed direct conversion of methane into toluene and incorporation of ^{12}C from methane into the aromatics produced from $^{13}CH_3OH$. The incorporation of ^{12}C from methane into aliphatics produced from $^{13}CH_3OH$ may also occur by a mechanism similar to that shown by reaction-5. There is also a possibility of the insertion of activated methane into carbonium ions produced from methanol, leading to the formation of penta-coordinated carbocations, in a similar way. For the formation of significant amount of methyl cations (by reaction 2) and / or penta-coordinated carbocations (II), higher concentration of methane relative to higher hydrocarbons, and consequently relative to methanol, is essential. This is consistent with the

observations; for lower methane / methanol feed ratios; the methane converted per mole of methanol converted was found to be smaller (Table 6.2).

6.3.2. Simultaneous Conversion of Methane and Ethanol over Bifunctional H-GaAlMFI Zeolite Catalyst

Results showing the hydrocarbon ($C_2 - C_{10+}$) product distribution and an appreciable increase in the hydrocarbons formed in presence of methane during the simultaneous conversion of methane and ethanol over H-GaAlMFI at 625 ^oC is presented in Fig. 6.12. These results clearly show that methane is non-oxidatively activated and converted during the ethanol conversion over the bifunctional zeolite catalyst. Because of the presence of methane, the hydrocarbon product distribution is changed very appreciably and also the formation of aromatics (except toluene) is increased markedly. The liquid hydrocarbons formed are mainly $C_6 - C_{12}$ aromatics. Interestingly the benzene formed was in an appreciable amount compared to that observed for methanol as an additive to methane. In the absence of methane, an appreciable amount of methane is produced in the aromatization of ethanol. Hence, even no net formation of methane in the ethanol aromatization because of the presence of methane is beneficial.

Results showing the influence of process conditions on the amount of methane converted per mole of ethanol converted in the process are presented in Table 6.5. It may be noted that in the presence of ethanol, the methane activation occurs at a higher temperature as compared to that required in the presence of methanol. Nevertheless, about 0.8 moles of methane per mole of ethanol are converted at 625 ^oC.

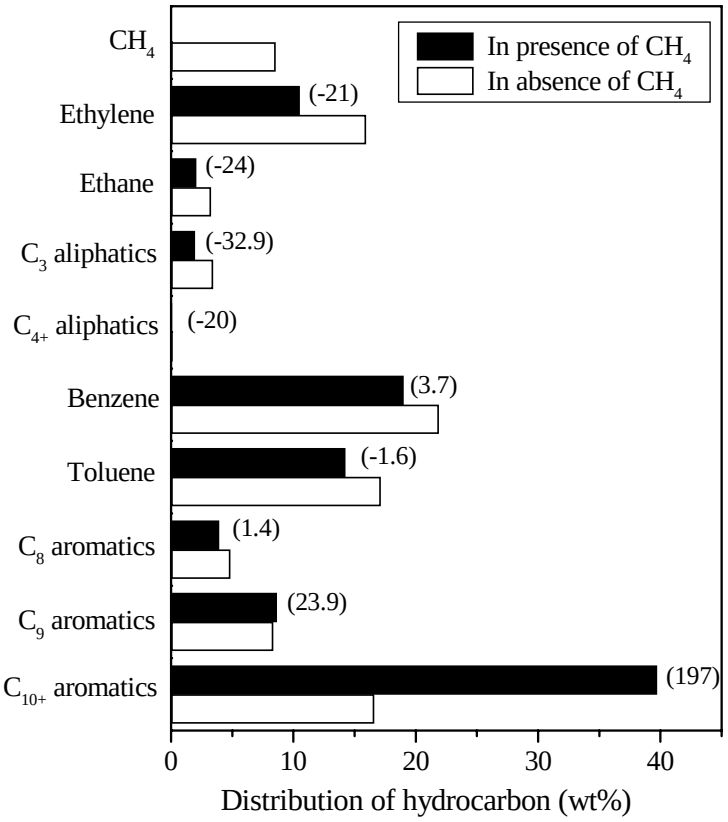

Figure 6.12: Distribution of hydrocarbons formed in the aromatization of ethanol over H-GaAlMFI zeolite in the presence (solid bars) and absence (open bars) of methane at 625 ^{o}C (CH_4/C_2H_5OH=10.3, GHSV=1050 $cm^3g^{-1}h^{-1}$). The value given in the brackets corresponds to the percentage increase in the formation of a particular hydrocarbon because of presence of methane. The ethanol was completely converted. In the presence of methane, the amount of methane converted was 0.80 moles per mole of ethanol.

Table 6.5. Results of the simultaneous conversion of methane and ethanol over H-GaAlMFI catalyst at different process conditions

Temperature (^oC)	GHSV ($cm^3g^{-1}h^{-1}$)	CH_4/C_2H_5OH mol ratio	Moles of methane converted per mole of ethanol
550	1050	10.3	0.0
600	1050	10.3	0.55
625	1050	10.3	0.80
550	2000	10.3	0.0
600	2000	10.3	0.37
625	2000	10.3	0.50
625	1050	14.92	0.64

6.3.3. Simultaneous Conversion of Methane and Dimethyl Ether (DME) over Bifunctional H-GaAlMFI Zeolite Catalyst

Results in Fig. 6.13 shows the product distribution and increase of the different hydrocarbons formed in the simultaneous conversion of methane and dimethyl ether over H-GaAlMFI at 550 ^oC**.** Results showing the influence of temperature and space velocity on the moles of methane converted per mole of DME in the process are given in Table 6.6. The results (Fig. 6.13 and Table 6.6) clearly indicate that methane is non-oxidatively activated and converted at low temperature (below 600 ^oC) during the dimethyl ether conversion over the bifunctional zeolite catalysts. Because of the presence of methane, the distribution of hydrocarbons produced is changed significantly, the formation of aromatics is increased appreciably and also the formation of individual C_{2+} hydrocarbons is increased markedly, as shown in Fig. 6.13. The liquid hydrocarbons formed are mainly $C_7 – C_{12}$ aromatics. Like in

the presence of methanol, the formation of benzene (the presence of which is undesirable because of its toxicity) was very small. In the absence of methane, an appreciable amount of methane is produced in the aromatization of dimethyl ether. Hence, even no net formation of methane in the dimethyl ether aromatization because of the presence of methane seems to be beneficial.

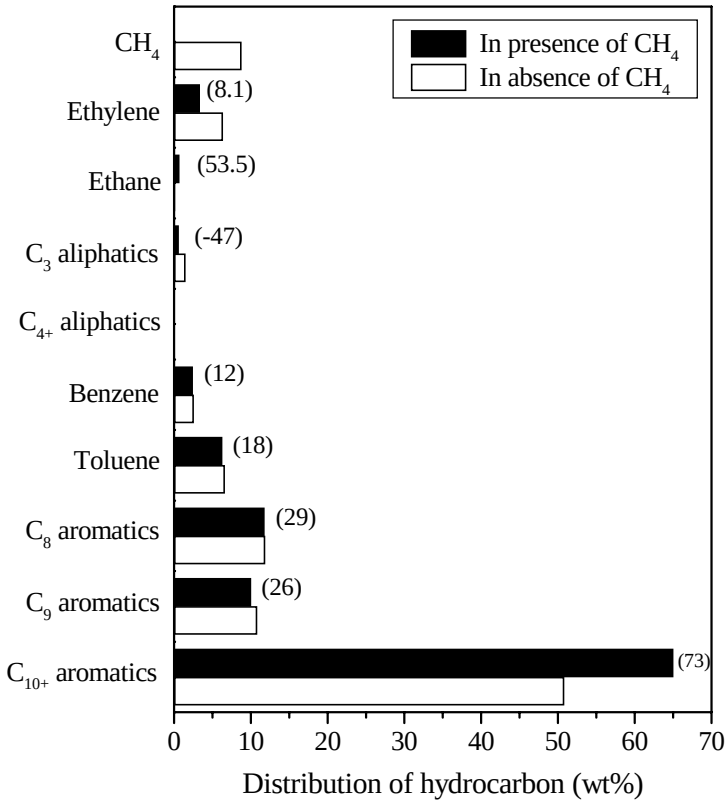

Figure 6.13. Distribution of hydrocarbons formed in the aromatization of dimethyl ether (DME**)** over H-GaAlMFI zeolite in the presence (solid bars) and absence (open bars) of methane at 550 ^{o}C (CH_4/DME=15.4, GHSV=1050 $cm^3g^{-1}h^{-1}$). The value given in the brackets corresponds to the percentage increase in the formation of a particular hydrocarbon because of presence of methane. The dimethyl ether was completely converted. In the presence of methane, the amount of methane converted was 0.94 moles per mole of dimethyl ether.

Table 6.6. Results of the simultaneous conversion of methane and dimethyl ether (DME) over H-GaAlMFI catalyst at different process conditions

Temperature (^oC)	GHSV ($cm^3g^{-1}h^{-1}$)	$CH_4/(CH_3)_2O$ mole ratio	Moles of methane converted per mole of dimethyl ether
500	1050	15.4	0.32
550	1050	15.4	0.94
550	1050	7.6	-0.17
550	2000	15.4	0.72

6.4. Advantages of the Simultaneous Conversion of Methane and Oxygenates to Gasoline / Liquid Hydrocarbons.

In the simultaneous methane and methanol–to–gasoline process, the amount of methane converted can be nearly the same as that of methanol converted. This would reduce very appreciably the cost of methane-to–methanol conversion for the Mobiles MTG (methanol–to–gasoline) process. In addition to, one more major limitation of the MTG process could be overcome as follows: Methanol aromatization is highly exothermic [ΔH_r < -30 kcal mol^{-1} (aromatics)] and this is one of the major concerns of the Mobil's MTG process. However, in the methane and methanol–to–gasoline conversion process, simultaneously occurring endothermic methane conversion and exothermic methanol aromatization reactions over the same catalyst are coupled, making the process highly energy efficient and also avoiding a possibility of process runway.

The other important advantages of this process over the earlier process based on the low temperature non-oxidative methane conversion in the presence of higher hydrocarbons are as follows:

i) The additive (methanol or dimethyl ether) in the methane feed can be produced from methane it self by well established technology (methane ⟶ syngas ⟶ methanol or dimethyl ether).

ii) The conversion of the additive is complete (100%).

iii) The moles of methane converted per mole of the additive can be close to 1.0 or even higher and hence the requirement of the additive is much smaller. Also the process based on high temperature (> 700 ^{o}C) methane aromatization over Mo / H-ZSM-5 catalyst [23] is technically not feasible because of very fast catalyst deactivation.

Because of its highly attractive features, the methane and methanol-to-gasoline conversion process is much more commercially feasible. A further work/development of the bifunctional zeolite catalyst and optimisation of the catalyst composition and process conditions would potentially lead to an economically feasible MTL technology to satisfy the increasing energy demands. It would also provide an immediate solution to avoid the flaring of the natural gas produced during the oil production at remote places.

References

1. T. Ito, J. H. Lunsford, Nature, 314 (1985) 721.
2. J. H. Lunsford, Angew. Chem. Int. Ed. Engl. 34 (1995) 970.
3. L. Mleczko, M. Baerns, Fuel Process. Technol. 42 (1995) 217.
4. A. T. Ashcroft, et al. Nature, 344 (1990) 319.
5. V. R. Choudhary, A. S. Mamman, S. D. Sansare, Angew. Chem. Int. Ed. Engl. 31 (1992) 1189.
6. D. A. Hickman, L. D. Schmidt, Science 259 (1993) 343.
7. V. R. Choudhary, A. M. Rajput, B. Prabhakar, Angew. Chem. Int. Ed. Engl. 33 (1994) 2104.
8. V. R. Choudhary, B. S. Uphade, A. S. Mamman, A. M. Rajput, US Patent 6, 293, 979 (2001).
9. V. R. Choudhary, S. D. Sansare, S. T. Chaudhari, US Patent 5, 336, 825 (1994)
10. V. R. Choudhary, S. D. Sansare, A. M. Rajput, US Patent 5, 306, 854 (1994).
11. V. R. Choudhary, A. K. Kinage, T. V. Choudhary, Science 275 (1997) 1286.
12. O. A. Anunziata, G. V. G. Mercado, L. B. Pierella, Catal. Lett. 87 (2003) 167.
13. T. Baba and H. Sawada, Phys. Chem. Chem. Phys. 4 (2003) 3919.
14. T. Baba and Y. Abe, Appl. Catal. A: Gen., 250 (2003) 265.
15. T. V. Choudhary, A. E. Aksoylu, D. W. Goodman, Catal. Rev., 45 (2003) 151.

16. S. L. Meisel, J. P. McCullough, C. H. Lechthaler, P. B. Weisz, Chemtech 89 (Feb. 1976).
17. C. D. Chang, et al. Ind. Eng. Chem. Process Des. Dev. 17 (1978) 255.
18. J. Haggin, Chem. Eng.News 22 (June 22, 1987).
19. J. Haggin, Chem. Eng. News. 22 (June 01, 1987).
20. J. H. Lunsford, Catal. Today 6 (1990) 235.
21. V. R. Choudhary, A. K. Kinage, T. V. Choudhary, Appl. Catal.A: Gen 162 (1997) 239.
22. Y. Xu, X. Bao, L. Lin, J. Catal., 216 (2003) 386.
23. V. R. Choudhary, S. A. R. Mulla, S. Banerjee, Micropor .Mesopor. Mater., 47 (2001) 253 and 57 (2003) 317.
24. G. A. Olah, Angew. Chem. Int. Ed. Engl. 34 (1995) 1393.
25. E. Iglesia, D. G. Burton, J. A. Biscardi, M. J. L. Gines and S. L. Soled, Catal. Today, 38 (1997) 339.
26. D. Liederman, S. M. Jacob, S. E. Voltz, J. J. Wise, Ind. Eng. Chem. Process Des. Dev. 17 (1978) 340.
27. C. D. Chang, S. M. Jacob, A. J. Silvestri, J. C. Zahner, US Patent 4,138,440 (1979).

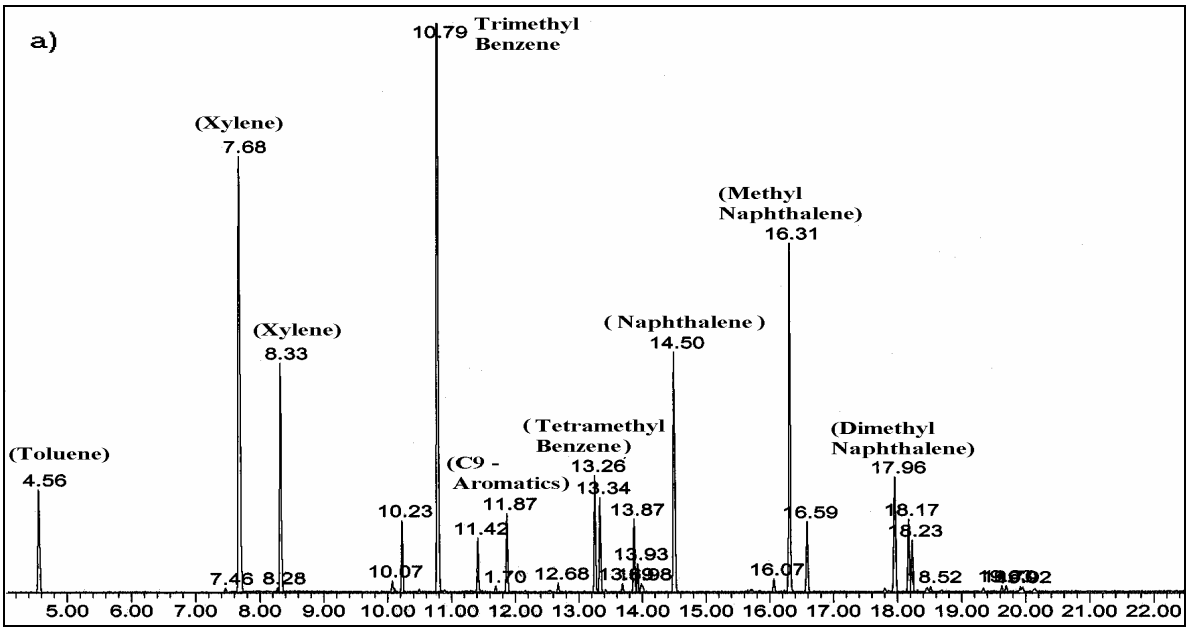

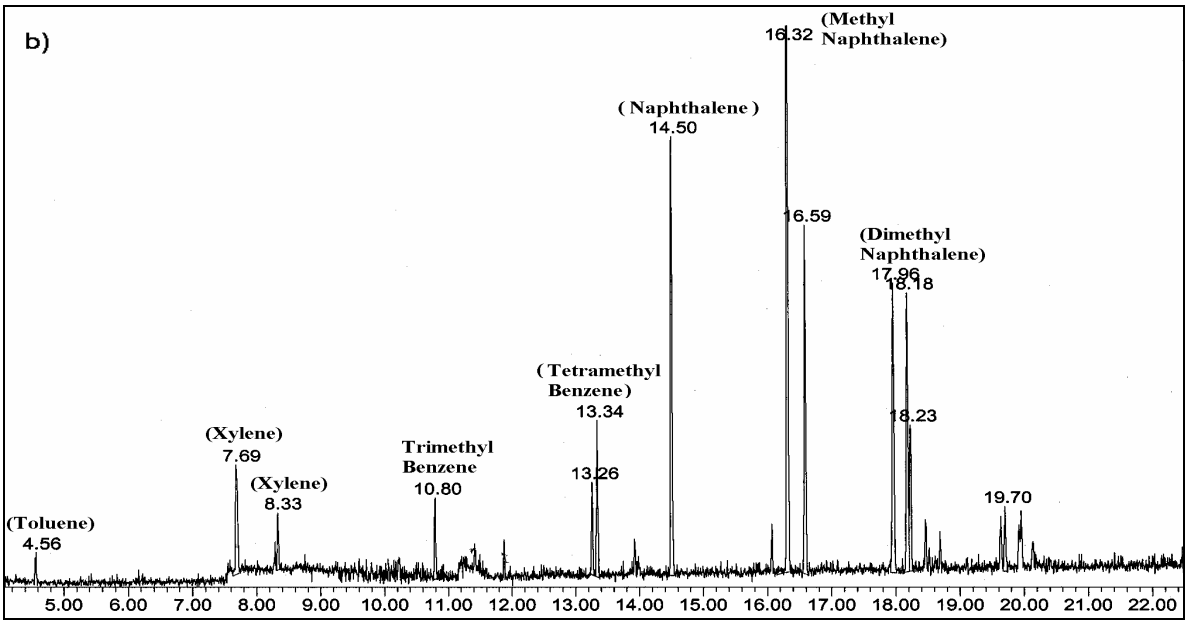

Appendix 6.1. GC peaks of GCMS analysis for the liquid hydrocarbon products formed in the aromatization of $^{13}CH_3OH$ over H-GaAlMFI zeolite (at 550^oC) (a) in presence of methane ($^{12}CH_4$ / $^{13}CH_3OH$ = 14.7) and (b) in absence of methane (N_2 / $^{13}CH_3OH$ = 14.7)

Discussion:

A comparison of the peaks in the two cases reveals a large change in the product distribution due to the presence of methane

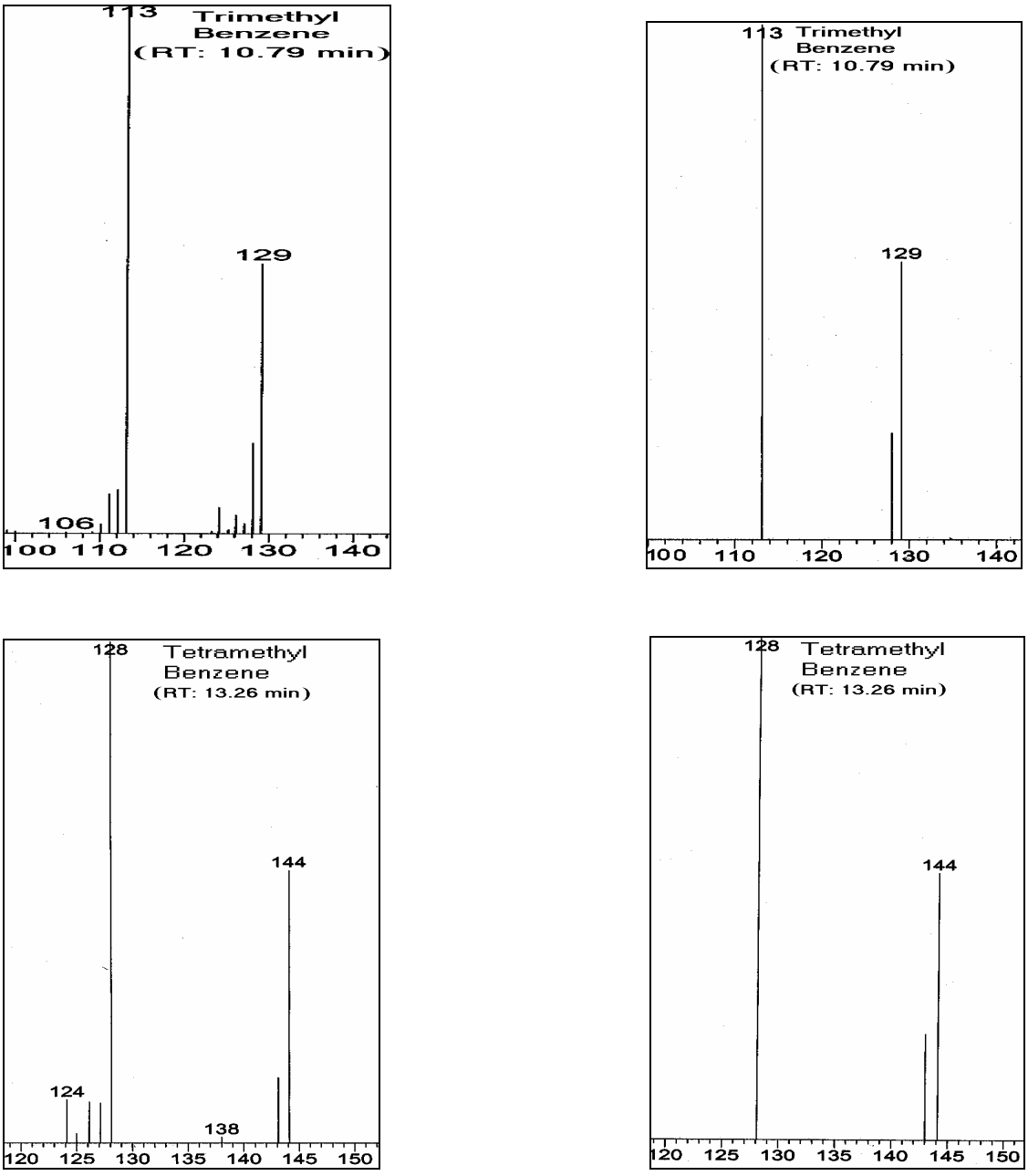

a) In presence of methane b) In absence of methane

Appendix 6.2. GCMS spectra of trimethyl and tetra methylbenzenes formed in the aromatization of ^{13}C labled methanol ($^{13}CH_3OH$) over the H-GaAlMFI zeolite in the presence and absence of methane under identical conditions, (550^oC and GHSV=1050 $cm^3g^{-1}h^{-1}$) by replacing methane by N_2 quantitatively. [reaction conditions: a) $CH_4/^{13}CH_3OH$=14.7 and CH_4/N_2=7.3, b) $CH_4/^{13}CH_3OH$= zero, $N_2/^{13}CH_3OH$=16.7]. RT= GC retention time.

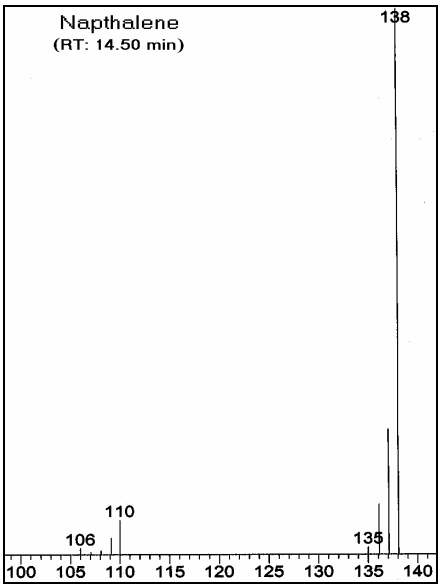

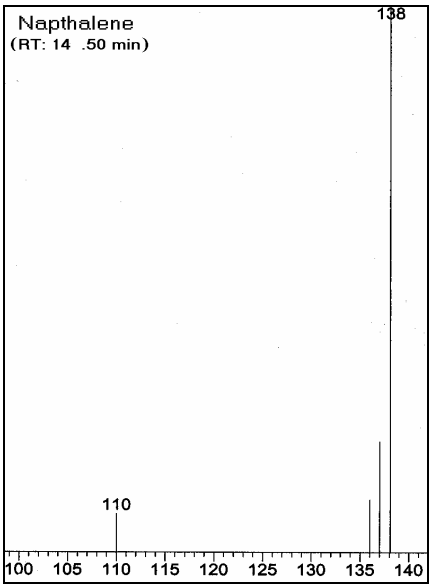

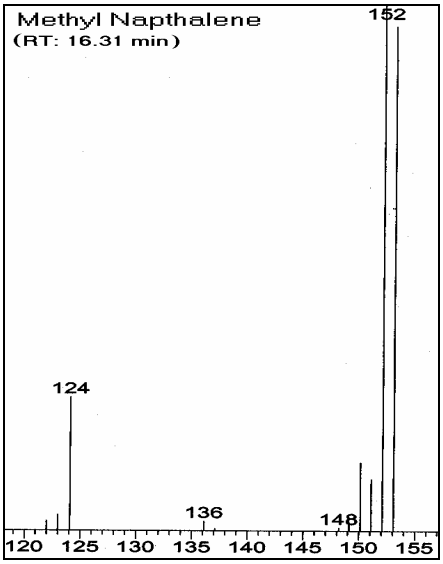

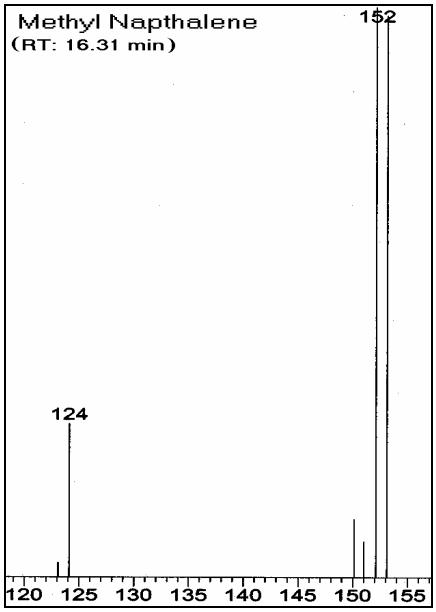

a) In presence of methane b) In absence of methane

Appendix 6.3. GCMS spectra of naphthalene and methylnaphthalene formed in the aromatization of ^{13}C labled methanol ($^{13}CH_3OH$) over the H-GaAlMFI zeolite in the presence and absence of methane under identical conditions.

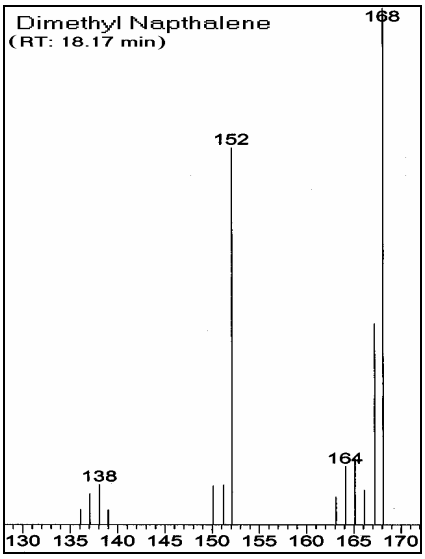

a) In presence of methane

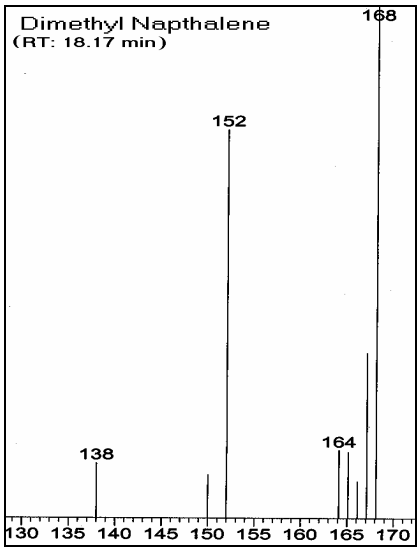

b) In absence of methane

Appendix 6.4. GCMS spectra of dimethylnaphthalene formed in the aromatization of ^{13}C labled methanol ($^{13}CH_3OH$) over the H-GaAlMFI zeolite in the presence and absence of methane under identical conditions.

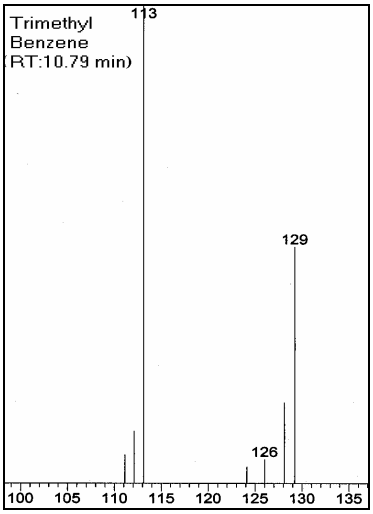

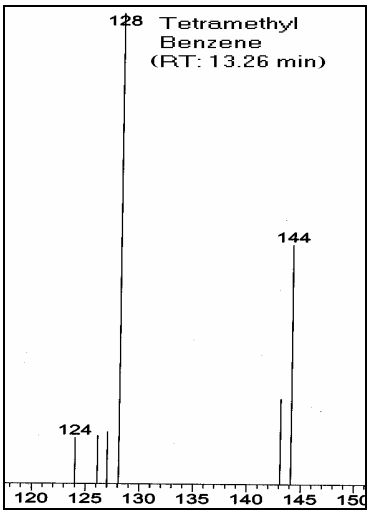

Appendix 6.5. Mass spectra of Trimethyl benzene and tetra methylbenzene formed in the aromatization of ^{13}C labled methanol ($^{13}CH_3OH$) over the Zn-In/H-ZSM-5 zeolite in the presence of methane at 480^oC [reaction conditions: $CH_4/^{13}CH_3OH$ = 14.7, CH_4/N_2 = 7.3, and GHSV = 1050 $cm^3g^{-1}h^{-1}$]. RT = GC retention time.

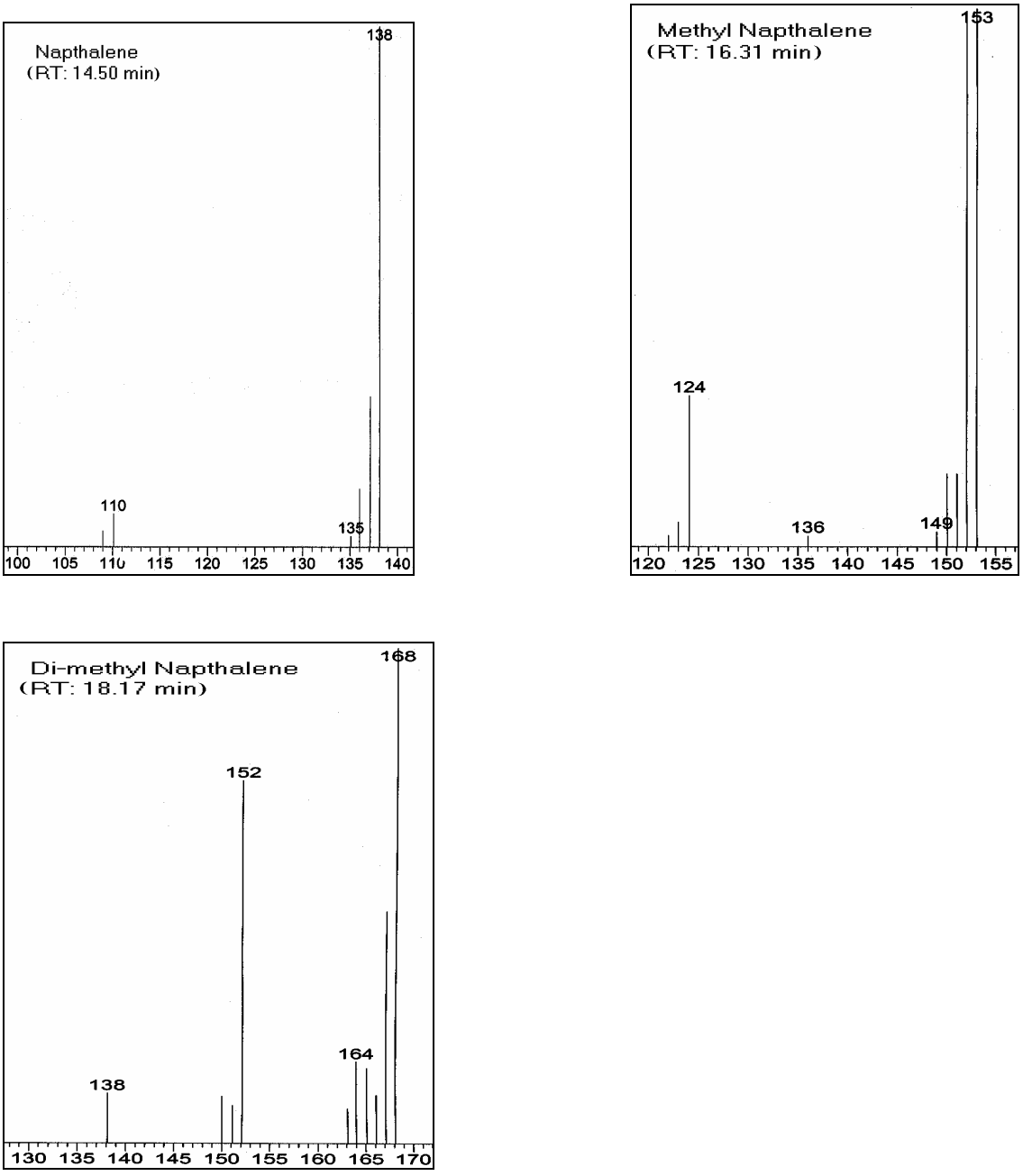

Appendix 6.6. Mass spectra of naphthalene, methylnaphthalene and dimethylnaphthalene formed in the aromatization of ^{13}C labled methanol ($^{13}CH_3OH$) over the Zn-In/H-ZSM-5 zeolite in the presence of methane at 480^{o}C. RT = GC retention time.

a) In the presence of methane

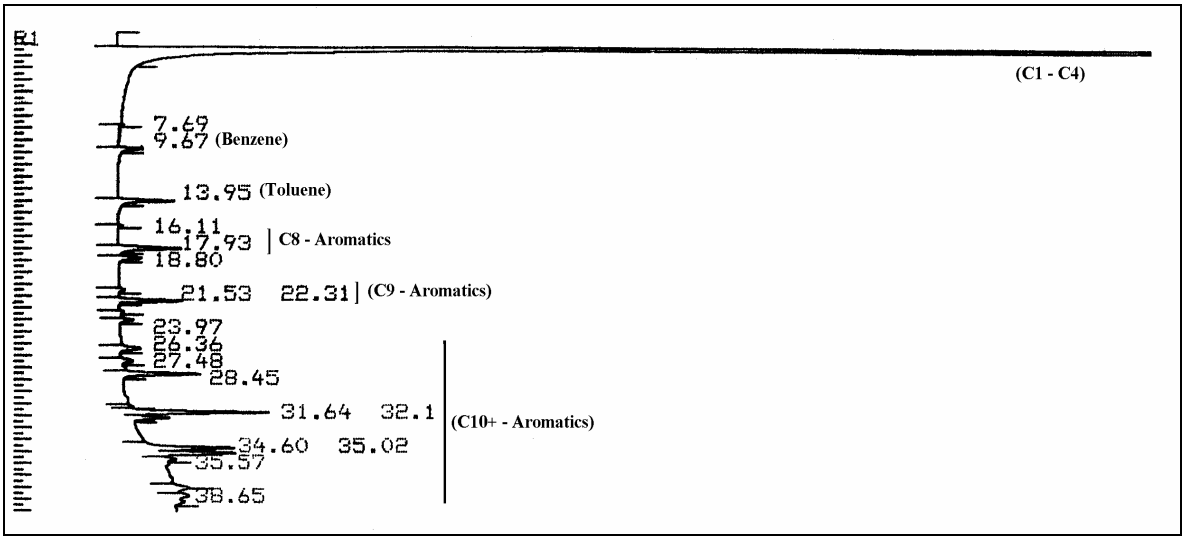

b) In the absence of methane [i.e. by replacing methane (80 cm^3/min) flow by N_2 flow (80 cm^3/min)

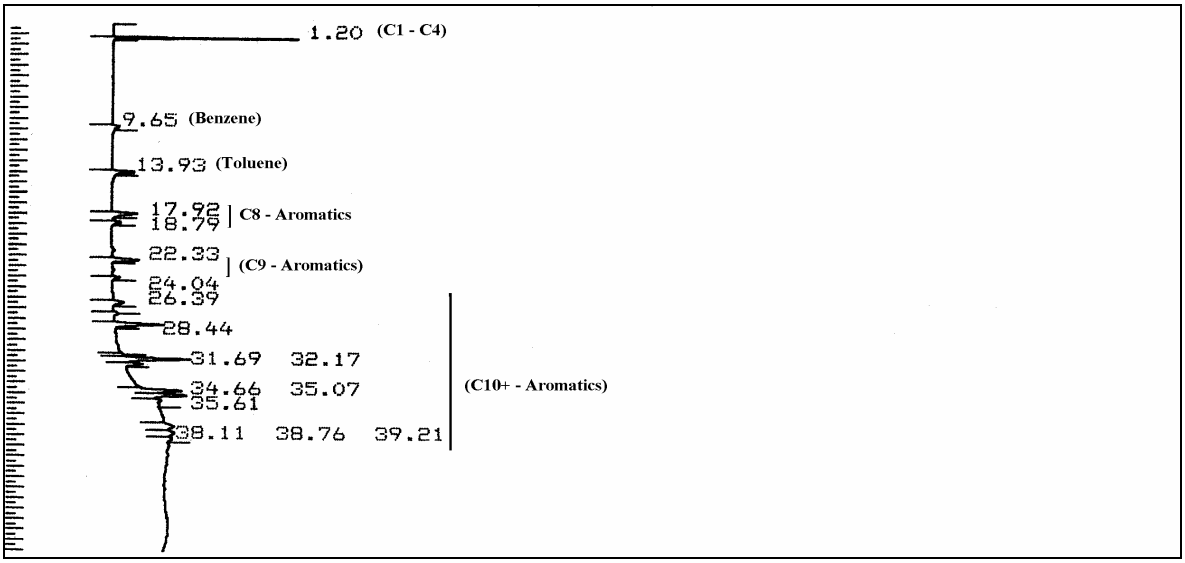

Appendix 6.7. GC analysis peaks for the hydrocarbon product stream of aromatization of methanol, in the presence or absence of methane over H-GaAlMFI zeolite at 550^oC under identical reaction and GC analysis conditions.

Discussion:

A comparison of the GC peaks for the two cases reveals a large increase in the formation of hydrocarbons due to the presence of methane.

a) In the presence of methane

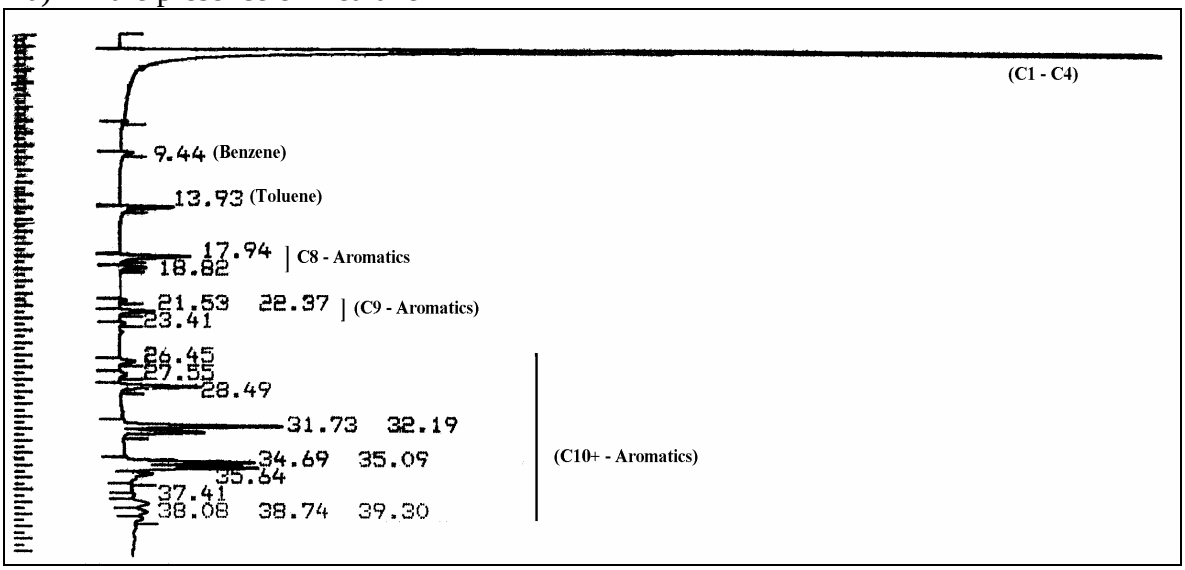

b) In absence of methane [i.e. by replacing methane (80 cm^3/min) flow by N_2 flow (80 cm^3/min)

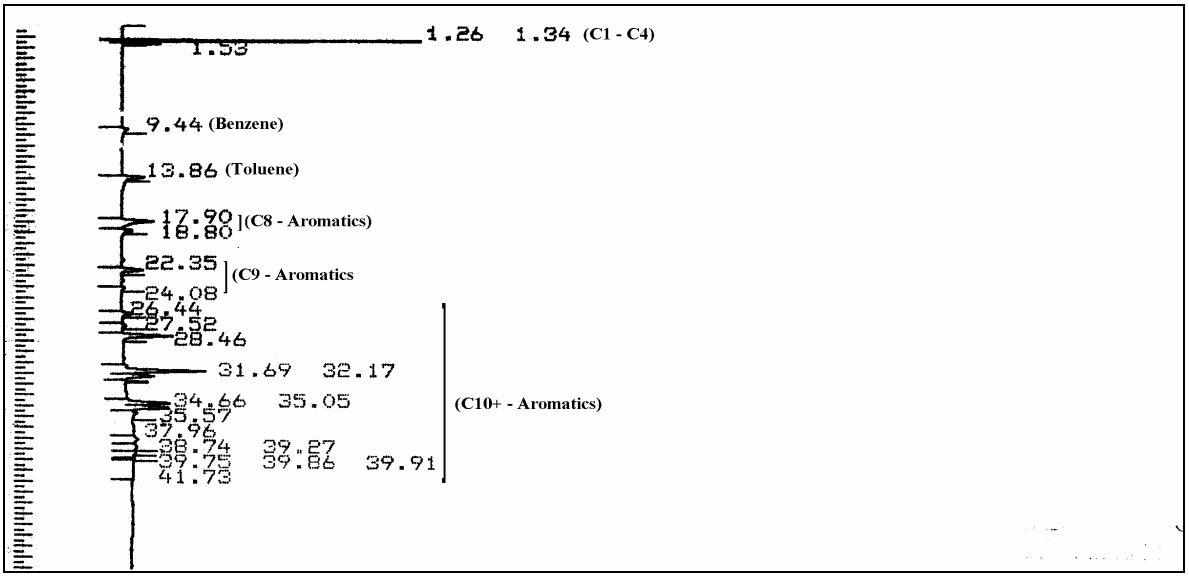

Appendix 6.8. GC analysis peaks for the hydrocarbon product stream of aromatization of methanol, in the presence or absence of methane over Mo-Zn/H-ZSM-5 zeolite at 500^oC under identical reaction and GC analysis conditions.

Discussion:

In this case also, a comparison of the GC peaks for the two cases reveals a large increase in the formation of hydrocarbons due to the presence of methane

CHAPTER 7

NON–CATALYTIC PYROLYSIS OF ETHANE TO ETHYLENE IN THE PRESENCE OF CO_2 WITH OR WITHOUT O_2

CHAPTER 7

NON–CATALYTIC PYROLYSIS OF ETHANE TO ETHYLENE IN THE PRESENCE OF CO_2 WITH OR WITHOUT O_2

7.1 Earlier Work / Background and Objective of the Present Work

The ethylene, which is keystone to petrochemical industry, is produced commercially by thermal cracking of ethane, ethane–propane mixture or naphtha in the presence of steam [1]. This process is highly endothermic, energy intensive and also involves extensive coke formation. The large amount of coke deposited on the inner walls of the tubular cracking reactor creates serious problems, such as reduction in the rate of heat transfer from reactor walls. This in turn requires higher wall temperature (upto 1100 ^{o}C) to achieve desirable ethane conversion, which increases the energy demand and also reduces the life of the reactor tubes. It also requires process shutdown for physically removing the coke. Moreover, the ethane conversion achieved is less than about 70 %, thus requiring a large recycle of the unconverted ethane. In order to overcome these problems Choudhary and coworkers [2 - 4] have suggested earlier to carry out ethane and propane thermal cracking reactions in the presence of limited oxygen. By carrying out the thermal cracking of ethane, propane or $C_2 – C_4$ hydrocarbons from natural gas in the presence of steam and limited oxygen, not only the energy requirement is drastically reduced but also the coke formation is eliminated or drastically reduced and also the hydrocarbon conversion much above 70 % could be obtained. Also in the presence of oxygen, the thermal cracking of ethane / propane is enhanced because of the change in the hydrocarbon activation mechanism and hence the oxy cracking process could be carried out at a much lower temperature and / or contact time than that required for achieving the same conversion in the thermal cracking process.

Carbon dioxide (a green house gas) can also act as a mild oxidant. Utilization of carbon dioxide in catalytic methane partial oxidation reactions, such as catalytic CO_2 reforming of methane [5] and oxidative coupling of methane [6], and also in the catalytic oxidative dehydrogenation of ethane [7 - 13] or propane [14] has been reported earlier. It is also interesting to use CO_2, as an oxidant, instead of oxygen or even in the presence of limited oxygen in the non-catalytic (thermal) hydrocarbon cracking processes for the production of ethylene and other olefins. The present investigation was undertaken for this purpose. The non-

catalytic cracking of ethane at atmospheric pressure in the presence of CO_2 at different CO_2 / ethane ratios (0 – 2.0) with or without oxygen (O_2 / ethane ratio = 0 to 0.3) has been thoroughly investigated at different temperatures (750 – 900 ^oC) and space velocities (1500 – 9000 h^{-1}) in the absence of steam in the feed.

7.2 Experimental Procedure

The non-catalytic ethane cracking reactions were carried out in a continuous-flow quartz reactor [2]. The reactor has a low dead volume. The reactor was kept in a tubular electric furnace such that the reaction zone was in the constant temperature zone of the furnace. The feed was a mixture of pure ethane and CO_2 with or without oxygen. The thermal cracking of ethane in the presence of CO_2 was carried out at different process conditions (viz. temperature = 750 – 900 ^oC; CO_2 / ethane = 0 – 2.0 and GHSV = 1500 – 9000 h^{-1}) with or without oxygen (O_2 / ethane = 0 – 0.3). All the ratios of feed components are mole ratios. GHSV is defined as the volume of gaseous feed (measured at 0 ^oC and 1 atm pressure) passed through a unit volume of the reactor per hour. The inlet and outlet temperatures of the reactor were measured by Chromel-Alumel thermocouples similar to that described earlier [4]. The maximum difference in the reactor inlet and outlet temperatures was 7 ^oC. The reactions were carried out by a procedure similar to that described earlier [15]. After the removal of water (formed particularly in the oxy-CO_2 ethane cracking) by condensation at 0 ^oC, the feed and products were analyzed by an on-line gas chromatograph with a thermal conductivity detector (TCD) and flame ionization detector (FID), using Poropak-Q and Spherocarb columns. The water condensed from the products was weighed.

The formation of O-containing products other than CO, CO_2 and H_2O was not observed. The experimental runs with the error in C, H and O mass balances less than 6 % were considered; the runs with higher errors were discarded. Product distribution data are provided for the product stream without CO_2 and water. Product selectivity reported in this investigation is based on the conversion of carbon from ethane to a particular product. It is described as follows:

Product selectivity = 100 × [Moles of the product formed per hour × number of C in the Product] ÷ [2 × Mole of ethane converted per hour]

7.3. Ethane Cracking in Presence of CO_2

Results showing influence of CO_2/C_2H_6 ratio in the feed, temperature and gas hourly space velocity (GHSV, measured at 0 ^oC and 1 atm pressure) on the ethane conversion and ethylene selectivity in the cracking of ethane are presented in Figs. 7.1 – 7.3. Influence of the process variables on the distribution (wt %) of various components (viz. H_2, CO, methane, ethylene, acetylene, ethane, propylene, propane, C_4 and C_{5+} hydrocarbon and benzene) present in the product stream, after the removal of water and CO_2 is shown in Fig. 7.4.

7.3.1. Influence of CO_2/C_2H_6 Ratio

The results (Fig. 7.1) show a strong influence of the presence of CO_2 on the ethane conversion; it is increased with increasing the CO_2/C_2H_6 ratio with little or no change in the ethylene selectivity with increasing the CO_2/C_2H_6 ratio. The concentration of ethane in the product stream is decreased whereas the concentration of most of the products is increased because of the increased ethane conversion. The formation of CO, acetylene, propane, propylene, C_{5+} aliphatic and benzene in the ethane cracking is however quite small. Since CO_2 is a very mild oxidant, the observed CO formation is expected by the reaction:

$$C_2H_6 + CO_2 \rightarrow C_2H_4 + CO + H_2O \qquad (1)$$

Results showing the strong influence of the CO_2/C_2H_6 ratio on the conversion of ethane by reaction 1 and purely by its thermal cracking are presented in Table 7.1. It is interesting to note that the ethane conversion by its oxidation by CO_2 (reaction 1) is very small (≤ 0.5 %); when compare to the total conversion of ethane. Thus the observed ethane conversion is mainly due to the thermal cracking of ethane even at very high CO_2 concentration in the feed (CO_2/C_2H_6 = 2.0). These observations reveal that the rate of ethane thermal cracking is enhanced markedly because of the presence of CO_2. These are quite similar to that reported earlier in case of the non-catalytic ethane or propane cracking in presence of limited O_2 [3, 4]. It seems that ethane is activated by CO_2 at the high reaction temperature (850 ^oC), enhancing the rate of C-C bond cleavage forming two methyl radicals, which are the primary products form in the thermal cracking of ethane.

The results in Fig. 7.4a show that the concentration of ethane in the product stream, after the removal of CO_2, is decreased while that of all the products is increased with increasing the CO_2/C_2H_6 ratio. This is expected because of the increase in the ethane conversion.

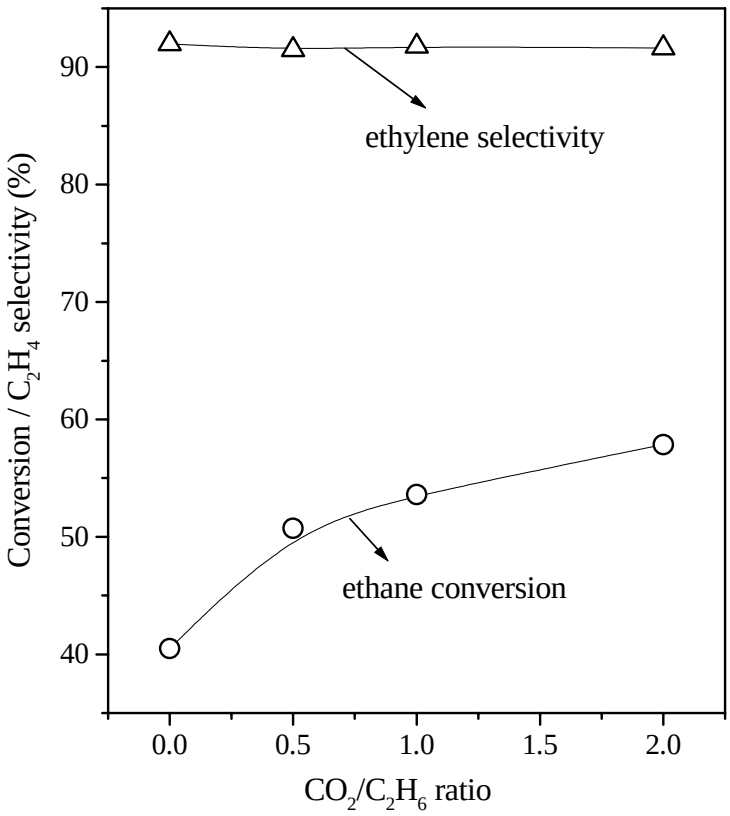

Figure 7.1 Effect of CO_2/C_2H_6 ratios on the conversion of ethane and selectivity of ethylene in the CO_2 cracking of ethane at 850 ^oC [GHSV = 6000 h^{-1}]

Table 7.1 Influence of the presence of CO_2 in feed on the thermal cracking of ethane at 850 ^oC (GHSV = 6000 h^{-1})

CO_2/C_2H_6 ratio in feed	Total ethane conversion (%)	Ethane conversion (%)	
		By reaction with CO_2	By ethane cracking
0.0	40.5	0.0	40.5
0.5	50.7	0.2	50.5
1.0	53.6	0.3	53.3
2.0	57.9	0.5	57.4

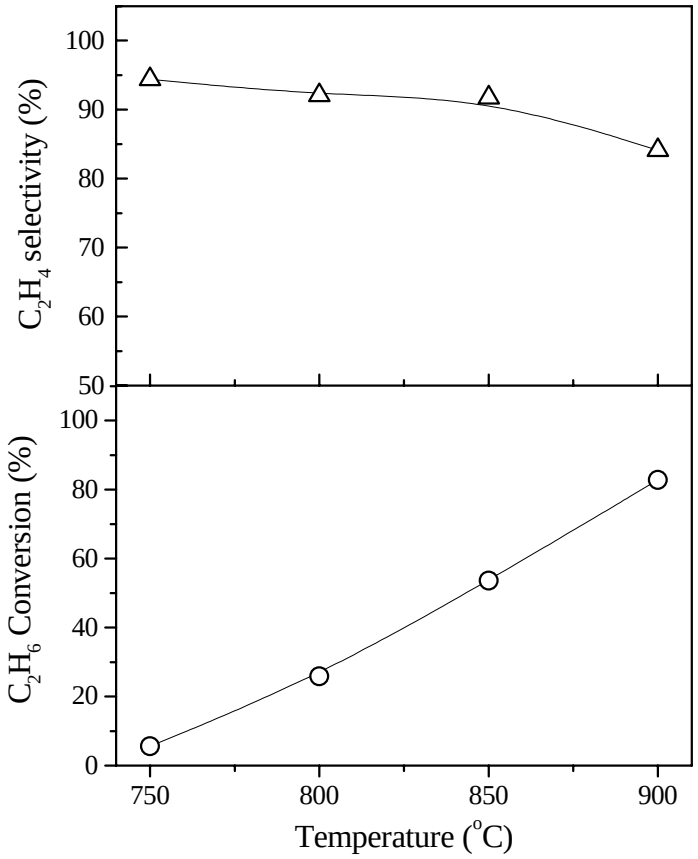

Figure 7.2 Effect of temperature on the conversion of ethane and selectivity of ethylene in the CO_2 cracking of ethane. [GHSV = 6000 h^{-1}; CO_2/C_2H_6 = 1.0]

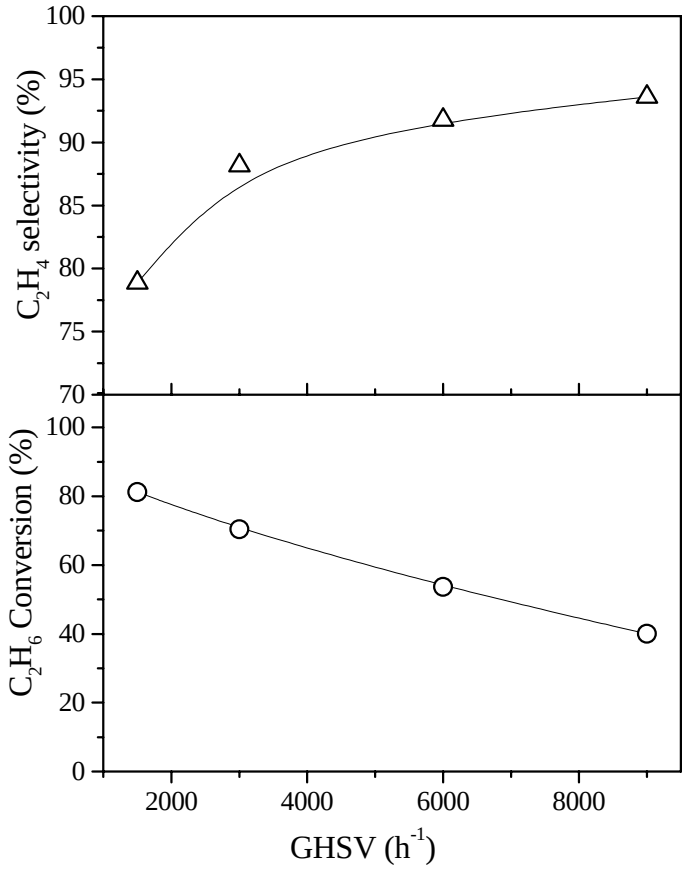

Figure 7.3 Effect of GHSV on the conversion of ethane and selectivity of ethylene in the CO_2 cracking of ethane at 850 ^oC [CO_2/C_2H_6 = 1.0]

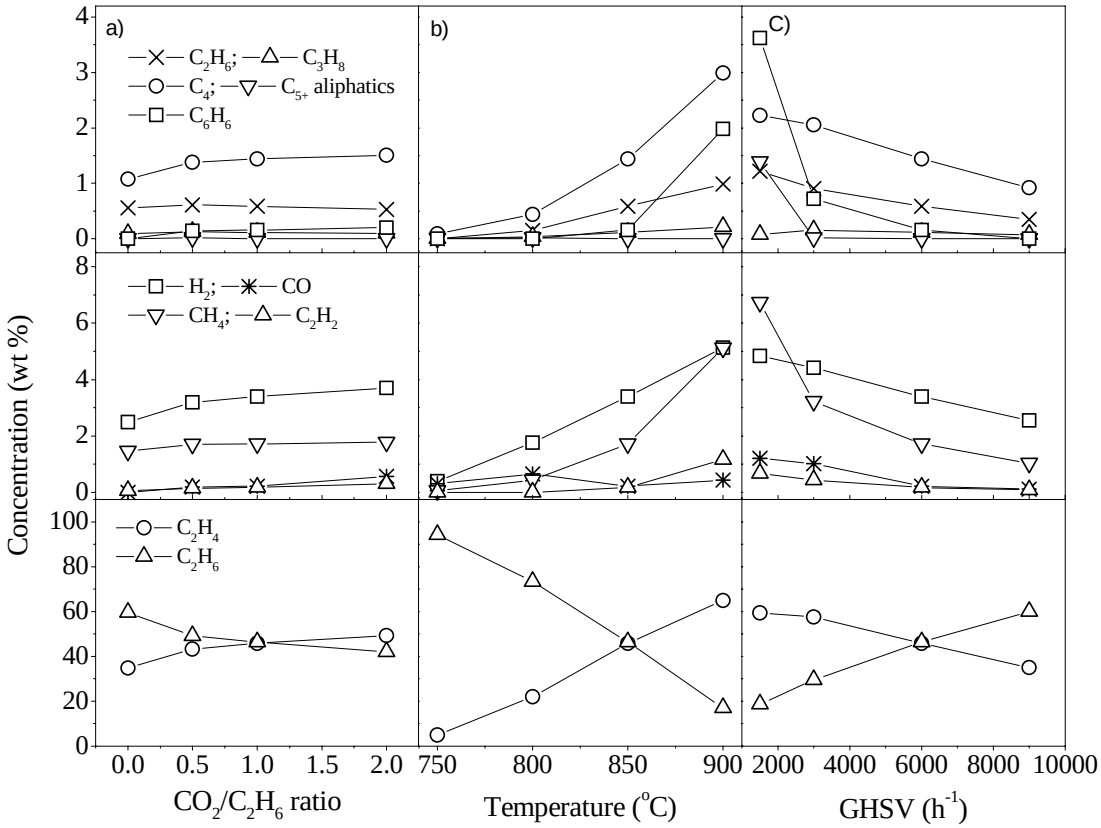

Figure 7.4 Influence of a) CO_2/C_2H_6 ratio (at 850 ^oC, GHSV = 6000 h^{-1}), b) reaction temperature (CO_2/C_2H_6 = 1.0 and GHSV = 6000 h^{-1}) and c) space velocity (at 850 ^oC, CO_2/C_2H_6 = 1.0) on the product distribution (without CO_2 and water) in the CO_2 cracking of ethane.

7.3.2. Influence of Temperature

With increasing the temperature (from 750 to 900 ^oC) the ethane conversion is increased (from about 5% to about 80%) almost exponentially. However, the ethylene selectivity is decreased. The selectivity of ethylene however, is decreased from about 95% to 85%; the decrease was more at the higher temperature (900 ^oC).

The decrease in the ethylene selectivity with increasing the temperature is because of the fact that the concentration in the product stream (without CO_2) is increased almost linearly with increasing the temperature but the increase in the concentration and consequently the formation of methane, C_4 hydrocarbon and benzene is exponential, as shown in Fig. 7.4b. The increase in the H_2 concentration was however, almost linear.

7.3.3. Influence of Space Velocity

The ethane conversion is decreased and the ethylene selectivity is increased with increasing the GHSV (Fig. 7.3).

The product distribution shown in Fig. 7.4c show that the concentration in product stream of methane, C_4 hydrocarbon and benzene is decreased exponentially while that of the other products is decreased almost linearly with increasing the space velocity.

7.4. Ethane Cracking in Presence of CO_2 and Limited O_2

Results on the conversion of ethane and O_2 and ethylene selectivity in the thermal cracking of ethane in the presence of CO_2 and limited O_2 (O_2/C_2H_6 = 0.25) at different CO_2/C_2H_6 ratios (0 – 2), temperatures (750 – 900 ^oC) and space velocities (GHSV from 3000 – 10,000 h^{-1}) are presented in Figs. 7.5 – 7.7. The product distribution and influence of the process parameters on the variation in the concentrations of different hydrocarbons, CO and H_2 in the product stream (without CO_2, O_2 and H_2O) have been given in Fig.7. 8.

A comparison of these results (Figs. 7.5 – 7.7) with those obtained in the absence of O_2 (Figs. 7.1 – 7.3) shows that, in the presence of both CO_2 and limited O_2, the ethane conversion is higher but the ethylene selectivity is lower as compared to the results obtained only in the presence of CO_2 (i.e. in the absence of limited O_2) due to the formation of CO from ethane partial combustion to an appreciable extent (Fig. 7.8). There is also a possibility of CO_2 formation, which, however, could not be measured because of the high CO_2 concentration in the feed. Earlier studies on the oxy cracking of ethane in the presence of limited O_2 have indicated that the formation of CO_2 as compared to CO in the process is very small [2].

7.4.1. Influence of CO_2/C_2H_6 Ratio

The results in Fig. 7.5 show that, like in the presence of CO_2 alone, the ethane conversion is increased with increasing the CO_2/C_2H_6 ratio. However, unlike in the presence of CO_2 alone, the ethylene selectivity is also increased significantly, the increase is almost linear. The O_2 conversion is however, passed through a maximum with increasing in the CO_2/C_2H_6 ratio.

7.4.2. Influence of Temperature

With increasing the temperature from 750 to 900 ^oC, the ethane conversion is increased linearly from 50% to 90%, but there is a small decrease in the O_2 conversion (from 98% to 94%) (Fig. 7.6). The ethylene selectivity is, however, first increase and passed through

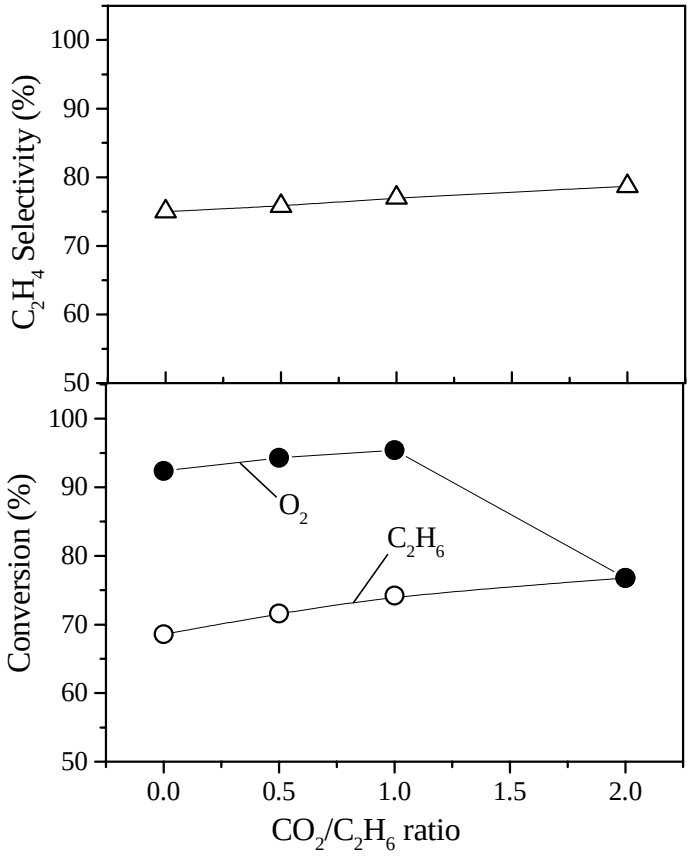

Figure 7.5. Effect of CO_2/C_2H_6 ratio on the conversion of ethane and selectivity of ethylene in the Pyrolysis of ethane in the presence of CO_2 and limited O_2 at 850 ^oC [O_2/C_2H_6 = 0.25; GHSV = 6000 h^{-1}]

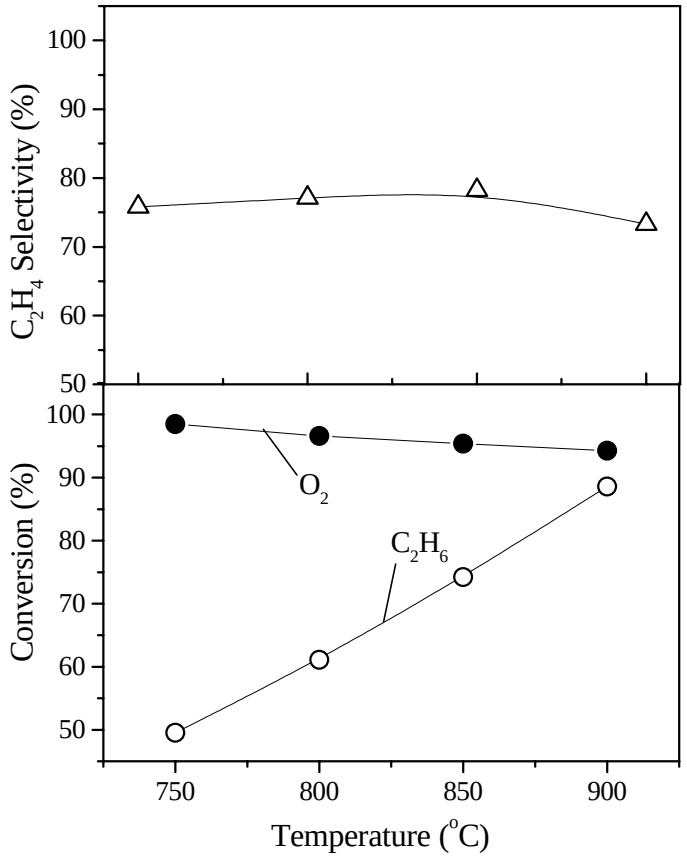

Figure 7.6. Effect of temperature on the conversion of ethane and selectivity of ethylene in the Pyrolysis of ethane in the presence of CO_2 and limited O_2 [O_2/C_2H_6=0.25; CO_2/C_2H_6=1.0; GHSV=6000 h^{-1}]

maximum at about 850 ^{o}C with increasing the temperature. The formation of the different products is also strongly influenced by the temperature, as shown in Fig. 7.8b.

7.4.3. Effect of Space Velocity

Unlike in the presence of CO_2 alone, the influence of GHSV on the conversion and selectivity in the ethane cracking in the presence of both the CO_2 and limited O_2 is small and consequently that on the product distribution is also small, as shown in Fig. 7.8c.

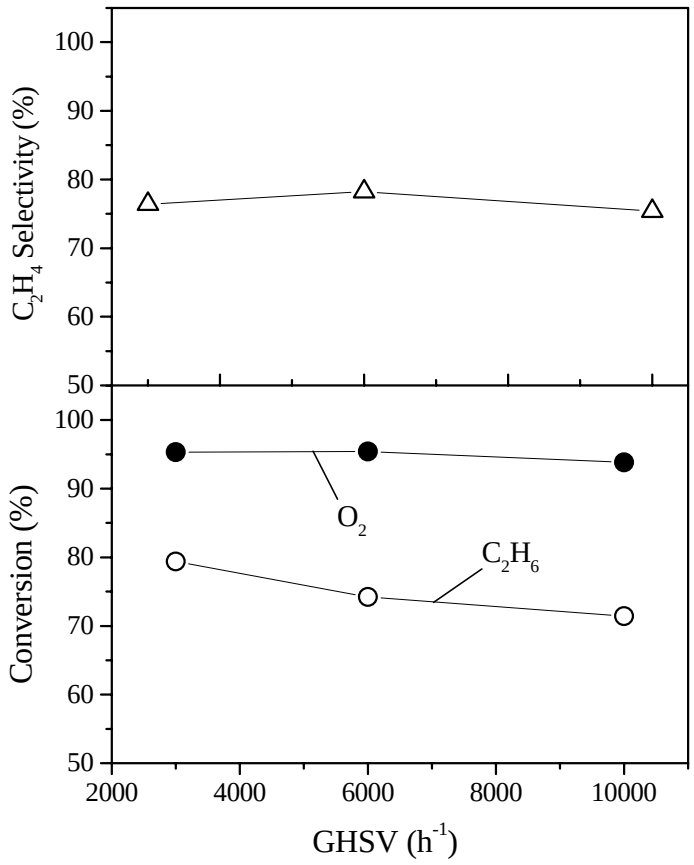

Figure 7.7. Effect of GHSV on the conversion of ethane and selectivity of ethylene in the Pyrolysis of ethane in presence of CO_2 and limited O_2 at 850 ^{o}C [O_2/C_2H_6 = 0.25; CO_2/C_2H_6 = 1.0]

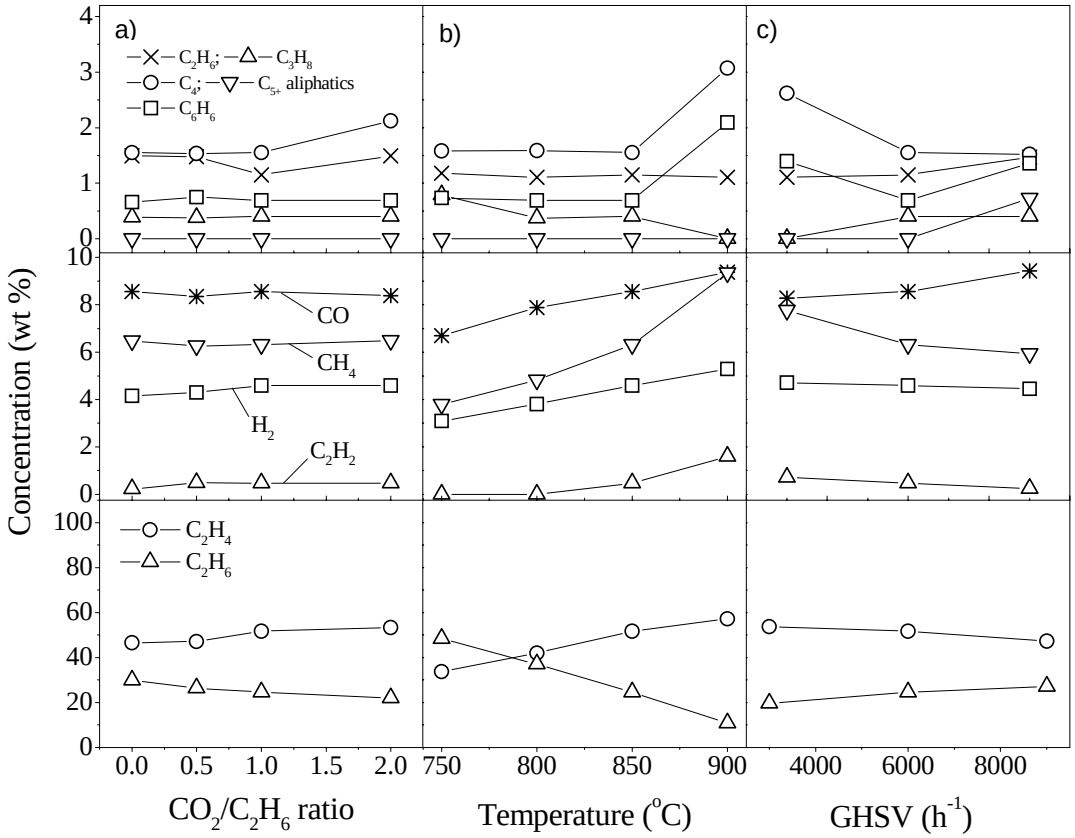

Figure 7.8. Influence of a) CO_2/C_2H_6 ratio (at 850 ^oC, GHSV = 6000 h^{-1}), b) reaction temperature (CO_2/C_2H_6 = 1.0, GHSV = 6000 h^{-1}), c) space velocity (at 850 ^oC, CO_2/C_2H_6 = 1.0) on the product distribution (without CO_2, water and O_2) in the oxy-CO_2 cracking of ethane (O_2/C_2H_6 = 0.25)

7.5. Reaction Involved in the Thermal Cracking of Ethane in the Presence of CO_2 with or without Limited O_2

In the presence of CO_2 alone, the reactions involved in the ethane cracking are expected to be similar to those involved in the conventional ethane cracking (ethane cracking is initiated by C-C bond cleavage, $C_2H_6 \rightarrow 2CH_3$) except the fact that ethane is activated in the presence of CO_2. However, in the presence of both the CO_2 and limited O_2, the mechanism and the reaction involves are expected to be similar to that involve in the oxy cracking of ethane (in the presence of O_2, the ethane cracking is initiated by the abstraction of H from ethane molecule by O_2 with the formation of ethyl radical, $C_2H_6 + O_2 \rightarrow C_2H_5 + HO_2$) [2].

The ethane cracking in the presence of CO_2 is highly endothermic process. However, the ethane cracking in the presence of both the CO_2 and limited O_2 can be mildly exothermic,

mildly endothermic or thermo neutral, depending upon the process conditions, as in case of the oxy cracking of ethane described earlier [2], because of coupling of the simultaneously occurring endothermic ethane cracking and exothermic ethane oxidation (mostly to CO and H_2O) reactions in the process, leading to an energy saving to a large extent.

7.6. Conclusions

From the above studies, following important conclusions can be made:

(1) The presence of CO_2 in both the conventional cracking of ethane and oxy cracking of ethane has beneficial effect.

(2) In both the cases, ethane conversion is increased with increasing the CO_2/C_2H_6 ratio in the feed; ethane seems to be activated in the presence of CO_2.

(3) At different process conditions, the ethane conversion is higher but ethylene selectivity is lower when the limited O_2 is added to the ethane-CO_2 feed, because of the formation of CO due to partial combustion of ethane. However, in the presence of both CO_2 and O_2, the process is expected to become highly energy efficient with a large energy saving for the ethylene production from ethane.

References

[1] I. Kniel, O. Winter, and K. Stork, In Ethylene: Keystone to the Petrochemical Industry, Dekker, New York (1980).

[2] V. R. Choudhary, S. A. R. Mulla, AIChE J., 43 (1997) 1545.

[3] V. R. Choudhary, S. A. R. Mulla, and A. M. Rajput, I & EC Res., 36 (1997) 2075.

[4] V. R. Choudhary, V. H. Rane, and A. M. Rajput, AIChE J., 44 (1998) 2293.

[5] M. C. J. Bradford and M. A. Vannice, Catal. Rev.-Sci. Eng., 41 (1999) 1.

[6] T. Nishiyama and K. Aika, J. Catal., 122 (1990) 346.

[7] K. Nakagawa, M. Okamura, N. Ikenaga, T. Suzuki and T. Kobayashi, Chem. Comm., (1998) 1025.

[8] S. Wang, K. Murata, T. Hayakawa, S. Hamakawa, and K. Suzuki, Chem. Lett., (1999) 569.

[9] S. Wang, K. Murata, T. Hayakawa, S. Hamakawa, and K. Suzuki, Catal. Lett., 63 (1999) 59.

[10] S. Wang, K. Murata, T. Hayakawa, S. Hamakawa, and K. Suzuki, React. Kinet. Catal. Lett., 68 (1999) 265.

[11] S. Wang, K. Murata, T. Hayakawa, S. Hamakawa, and K. Suzuki, Appl. Catal., 196 (2000) 1.

[12] X. Longya, L. Liwu, W. Qingxia, Y. Li, W. Debao, and L. Weichen, Natural Gas Conversion V, 119 (1998) 605.

[13] F. Solymosi and R. Nemeth, Catal. Lett., 62 (1999) 197.

[14] I. Takahara and M. Saito, Chem. Lett., (1996) 973.

[15] V. R. Choudhary, S. T. Choudhari, and A. M. Rajput, AIChE J., 37 (1991) 915.

SUGGESTION FOR FURTHER WORK

As an extension of the work reported in the thesis, following investigations may be carried out

- Testing life for a long period of the promising catalysts showing high activity/selectivity but little or no carbon carbon formation in the CO_2 reforming process.
- Partial oxidation of methane to syngas over the high temperature stable catalysts under adiabatic conditions on a much larger scale.
- Use of the high temperature stable catalysts for the autothermal reforming of methane to syngas.
- Development of better bifunctional zeolite catalyst and optimization of process conditions for the simultaneous methane and methanol conversion into liquid hydrocarbons.
- Detailed investigation for understanding the role of catalyst support in the carbon formation over the supported cobalt catalysts and also in controlling the catalytic activity/selectivity and thermal stability of the supported nickel and/or cobalt catalyst through their through characterization.

PUBLICATIONS AND PATENTS BASED ON THE WORK REPORTED IN THE THESIS

A. Papers (Accepted / Communicated / To be Communicated shortly)

1. *Carbon – free dry reforming of methane to syngas over $NdCoO_3$ perovskite-type mixed metal oxide catalyst*

   V. R. Choudhary, **K. C. Mondal**, A. S. Mamman and U. A. Joshi

   (revised manuscript communicated to Catalysis Letter)

2. *Simultaneous conversion of methane and methanol to gasoline over bifunctional Ga-, Zn-, In- and / or Mo- modified ZSM–5 zeolites*

   V. R. Choudhary, **K. C. Mondal** and S. A. R. Mulla (communicated to Angewandte Chemie)

3. *High temperature stable highly active / selective supported $NiCoMgCeO_x$ catalyst suitable for autothermal reforming or high temperature partial oxidation of methane to syngas*

   V. R. Choudhary, **K. C. Mondal** and A. S. Mamman (communicated to J. Catal.)

4. *Non–catalytic pyrolysis of ethane to ethylene in the presence of CO_2 with or without limited O_2*

   V. R. Choudhary, **K. C. Mondal** and S. A. R. Mulla (communicated to AIChE J)

5. *Dry reforming of methane to syngas different supported cobalt catalyst: Influence of support on the catalytic activity/selectivity and carbon deposition on the catalyst, CoO loading and process conditions.*

   V. R. Choudhary and **K. C. Mondal** (To be communicated)

6. *Dry reforming and oxy-CO_2 reforming of methane to syngas over cobalt supported on commercial low surface area macroporous silica-alumina (SA-5205) precoated with MgO.*

   V. R. Choudhary and **K. C. Mondal** (To be communicated)

7. *CO_2 reforming of methane to syngas over CoO_x/ZrO_2(or CeO_2)/SA-5205 catalyst in the presence and absence of oxygen.*

   V. R. Choudhary and **K. C. Mondal** (To be communicated)

8. Partial oxidation of methane to syngas in the presence and absence of steam and/or CO_2 over a high temperature stable catalyst $NiCoMgCeO_x$ supported on commercial low surface area macroporous zirconia-hafnia (SZ-5564) catalyst carriers.
   V. R. Choudhary and **K. C. Mondal** (To be communicated)
9. Simultaneous conversion of ethanol and methane to liquid hydrocarbons over bifunctional H-GaAlMFI zeolite.
   V. R. Choudhary and **K. C. Mondal** (To be communicated)
10. Partial oxidation of methane to syngas over high temperature (≥ 1400 ^oC) pretreated $NiCoMgO_x$/SZ-5564 catalyst in presence or absence of steam/CO_2.
    V. R. Choudhary and **K. C. Mondal** (To be communicated)

B. US and Indian Patent Application Filed

1. *Process for the simultaneous conversion of methane and organic oxygenate to $C_2 - C_{10}$ hydrocarbons and hydrogen using a bifunctional pentasil zeolite catalyst*
   Vasant R. Choudhary, **Kartick C. Mondal** and Shafeek A. R. Mulla
   (Filed both Indian and US patent application) (2002)
2. *A high temperature stable non-noble metal catalyst useful for catalytic autothermal reforming of hydrocarbon(s) to syngas and its use in syngas production from hydrocarbon(s)*
   Vasant R. Choudhary, **Kartick C. Mondal** and Ajit S. Mamman
   (Filed both Indian and US patent application) (2004)

Paper Presented in Symposium

1. *High temperature stable supported Ni-Co catalyst useful for autothermal reforming of methane to syngas,* **K. C. Mondal**, A. S. Mamman and V. R. Choudhary (Paper presented in the workshop on Advanced in Catalysis at Loyola College, Chennai, 6-7 January 2004.
2. *CO_2 Reforming of Methane Simultaneous with Steam Reforming or Partial Oxidation of Methane to Syngas over $NdCoO_3$ Perovskite derived Catalyst,* **K. C. Mondal** and V. R. Choudhary (Paper will be presented in the 17th National Symposium on Catalysis at CSMCRI, Bhavnagar, Gujrat, 18-20 January, 2005.